Book of Abstracts

Editors
Katrin Kahlen
Tsu-Wei Chen
Andreas Fricke
Hartmut Stützel

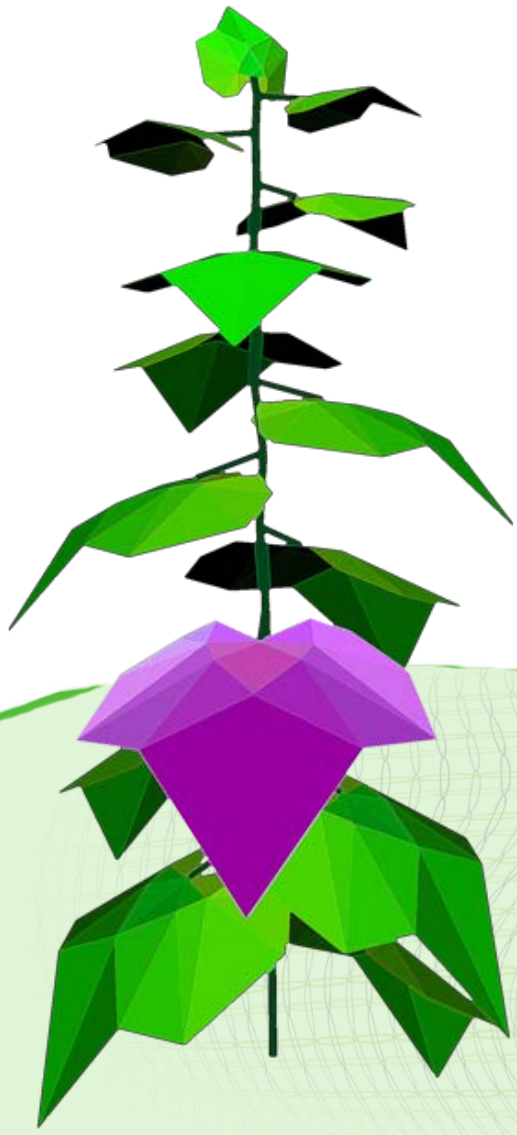

FSPM2020:

Towards Computable Plants

9th International Conference on
FUNCTIONAL-STRUCTURAL PLANT MODELS
5-9 October 2020

Book of Abstracts of the 9th International Conference on Functional-Structural Plant Models: FSPM2020, 5 - 9 October 2020. Eds. Katrin Kahlen, Tsu-Wei Chen, Andreas Fricke & Hartmut Stützel.

https://www.fspm2020.net

Editorial office:

Institute of Horticultural Production Systems
Herrenhäuser Strasse 2
30419 Hannover
Germany

tel.: +49-511 762 2638

e-mail: fspm2020@gem.uni-hannover.de

Foreword

This is the Book of Abstracts of the 9th Conference on Functional-Structural Plant Models (FSPM2020). For the first time in its almost 25-year history, FSPM2020 goes virtual! The pandemic gave us no other choice and since we have all gained some experience in virtual conferences we are confident that we will manage. Certainly, this will be challenging for all of us. Not only is our community scattered over different time zones around the globe, we also have to get used to different communication platforms and styles and (hopefully not too often) struggle with bandwidths. FSPM2020 will offer different formats of presentations and discussions in order to maximize interactions between participants. In a nutshell:

- FSPM2020 will take place on *StudIP* (https://studip.uni-hannover.de/), the e-learning tool of Hannover University. The instruction of using *StudIP* can be found on our website (https://www.fspm2020.net).
- Live-streams and live discussions (both real time) of the eight **keynotes** and the seven **software demonstrations** will be presented on *Meetings* in *StudIP*. Keynotes will also be recorded and made available on *Aufzeichnungen* in *StudIP.*
- On-demand videos for all 40 **oral presentations** and 38 **posters** will be available on *Aufzeichnungen* in *StudIP during October 2020.*
- In addition, **asynchronous discussions of all presentations** can take place on *Forum* in *StudIP*: Every presentation has a discussion area there. Presenters and co-authors are encouraged to subscribe to the area of their talk to get e-mail alerts when questions are posted in their own area. All participants can post questions and answers in an area and can subscribe to the areas they are interested in.
- Small talk and general comments are possible on *Blubber* in *StudIP*. #Hashtag can be used to ease the search of specific topics and talks.

Certainly, these new formats and new time lines will be challenging. In case you may need technical support, please contact us via e-mail (fspm2020@gem.uni-hannover.de).

A special issue on FSPM2020 will be published in ***in silico* Plants**. Submission deadline is scheduled on end of March 2021.

We are confident that the flexible and dynamic FSPM community will enjoy this new experience. Most importantly, we hope that we all stay healthy and enthusiastic until our next analogue meeting!

Katrin Kahlen[1], *Hartmut Stützel*[2], *Andreas Fricke*[2] and *Tsu-Wei Chen*[3]
Organizers FSPM2020

[1] Hochschule Geisenheim University
[2] Leibniz Universität Hannover
[3] Humboldt Universität zu Berlin

FSPM2020:
Towards Computable Plants

9th International Conference on FUNCTIONAL-STRUCTURAL PLANT MODELS 5-9 October 2020

Geisenheim University and Leibniz University Hannover jointly organise FSPM2020.

Organisers

Katrin Kahlen, Geisenheim University, katrin.kahlen@hs-gm.de
Hartmut Stützel, Leibniz University Hannover, stuetzel@gem.uni-hannover.de
Andreas Fricke, Leibniz University Hannover, fricke@gem.uni-hannover.de
Tsu-Wei Chen, Humboldt University of Berlin, tsu-wei.chen@hu-berlin.de

Local organising committee

Andreas Fricke (Chair), Leibniz University Hannover, fricke@gem.uni-hannover.de
Heike Bank (Secretary), Leibniz University Hannover
Ana Claudia Callau-Beyer, Leibniz University Hannover
Dany Moualeu Ngangue, Leibniz University Hannover
Magnus Adler, Leibniz University Hannover
Anni Romey, Leibniz University Hannover

Sponsor

Programme committee

Katrin Kahlen (Chair), Germany
Evelyne Costes (Co-Chair), France
Gerhard Buck-Sorlin, France
Mikolaj Cieslak, Canada
Jochem Evers, WUR, The Netherlands
M. Paulina Fernández, Chile
Yan Guo, China
Alla Selenzyova, New Zealand
Katarina Streit, The Netherlands

Scientific committee

Tsu-Wei Chen (Chair), Germany
Bruno Andrieu, France
Alexander Bucksch, USA
Gerhard Buck-Sorlin, France
Michaêl Chelle, France
Mikolaj Cieslak, Canada
Evelyne Costes, France
Paul-Henry Cournède, France
Jochem Evers, The Netherlands
M. Paulina Fernandez, Chile
Anja Geitmann, Canada
Christophe Godin, France
Yan Guo, China
Jim Hanan, Australia
Michael Henke, Germany
Katrin Kahlen, Germany
Winfried Kurth, Germany
Guillaume Lobet, Belgium
Johannes Postma, Germany
Christophe Pradal, France
Przemyslaw Prusinkiewicz, Canada
Anne-Lise Routier-Kierzkowska, Canada
Alla Seleznyova, New Zealand
Katarina Streit, The Netherlands
Hartmut Stützel, Germany

Publication committee

Tsu-Wei Chen (Chair), Germany
Jochem Evers (Co-Chair), The Netherlands
Katrin Kahlen, Germany
Andrea Schnepf, Germany
Kathy Steppe, Belgium

FSPM board

Gerhard Buck-Sorlin, France
Michaêl Chelle, France
Jochem Evers, The Netherlands
M. Paulina Fernández, Chile
Christophe Godin, France
Yan Guo, China
Jim Hanan, Australia
Katrin Kahlen, Germany
Przemyslaw Prusinkiewicz, Canada
Michael Renton, Australia
Alla Seleznyova, New Zealand

Time Schedule

Virtual Welcome Reception on Sunday, 4th of October from 18:00 to 20:00 CET

Time (CET)	Monday	Tuesday	Wednesday	Thursday	Friday
08:00			**Tim Oberländer 08:00**		
			A bidirectional interface between BwinPro and GroIMP		
09:00			**Xiao-Ren Zhuo 09:00**	**Marie Launay and Noémie Gaudio 09:00**	
			CPlantBox, a whole plant modelling framework	Exploring FSPM and crop models complementarities in up- and down-scaling from plant to field with a focus on modelling crop mixtures	
10:00			**Johannes Postma 10:00**	**Jochem Evers 10:00**	
			OpenSimRoot: Software for root architectural models	Teaching functional-structural plant modelling - perspectives from a plant scientist	
11:00			**Winfried Kurth 11:00**		**Evelyne Costes 11:00**
			Co-simulation with OpenAlea and GroIMP for cross-platform functional structural plant modelling		Considering genetic control of plant architecture in FSPM: a review of progresses and current challenges
12:00					**Tancrede Almeras 12:00**
					Multiscale modelling of tree and wood biomechanics
13:00					**Closing 13:00 - 14:00**
14:00	**Opening 14:30 - 15:00**				
15:00	**Kathy Steppe 15:00**		**Frédéric Boudon 15:00**		
	The power of 3D plant-microclimate interactions		Toward virtual modelling environments using notebooks for phenotyping and simulation of plant development		
16:00	**Andrea Schnepf 16:00**		**Dany Moualeu 16:00**		
	Functional-structural plant modelling with CPlantBox		Digitool: A tool for analyzing 3D plant architecture		
17:00					
18:00		**Dan Chitwood 18:00**	**Meagan Lang 18:00**		
		Topological Data Analysis (TDA) as a method to comprehensively measure the plant form	Yggdrasil - the crops in silico project's open-source Python package		
19:00		**Brian Bailey 19:00**			
		A new high-performance FSPM framework linking LiDAR-based canopy reconstructions with scalable biophysical models			
20:00					

Table of Contents

K01 The power of 3D plant-microclimate interaction 1
Kathy Steppe

K02 Functional-structural plant modelling with CPlantBox....2
Andrea Schnepf, Xiaoran Zhou, Daniel Leitner, Gernot Bodner, Deepanshu Khare, Jan Vanderborght, Harry Vereecken, Guillaume Lobet

K03 Topological Data Analysis (TDA) as a method to comprehensively measure the plant form 5
Daniel H. Chitwood

K04 A new high-performance FSPM framework linking LiDar-Based canopy reconstructions with scalable biophysiocal models 6
Brian N. Bailey

K05 Exploring FSPM and crop models complementarities in up- and down-scaling from plant to field....8
Marie Launay, Noémie Gaudio

K06 Teaching functional-structural plant modelling - perspectives from a plant scientist....10
Jochem B. Evers

K07 Genetics control of tree architecture 11
Evelyne Costes

K08 Multiscale modelling of tree and wood biomechanics....13
Tancrède Alméras

O01 Modelling and simulating tree growth dynamics including both shoot and root compartments. The RoCoCau+TOY model....14
Jean-Francois *Barczi, Yves Caraglio, Eric Nicolini, Herve Rey, Alexandre de Haldat*

O02 A modelling framework for the simulation of signal transport within 3D structure: application for the simulation of within-tree variability in floral induction in apple trees 16
Fares Belhassine, Damien Fumey, Christophe Pradal, Jérôme Chopard, Evelyne Costes, Benoît Pallas

O03 Testing leaf removal strategies and their effects on light absorption in virtual Riesling canopies (*Vitis vinifera* L.). 18
Christopher Bahr, Dominik Schmidt, Matthias Friedel, Katrin Kahlen

O04 Benchmarking root and soil interaction models exemplified with CPlantBox and DuMux 20
Daniel Leitner, Andrea Schnepf, Bernd Flemisch, Timo Koch, Jan Vanderborght, Harry Vereecken

O05 Simulating rhizodeposition as a function of shoot and root interactions within a new 3D functional-structural plant model 22
Frédéric Rees, Romain Barillot, Marion Gauthier, Loïc Pagès, Christophe Pradal, Bruno Andrieu

O06 Phenotypic traits extraction and plant type classification with 3D point clouds for field grown sugar beet through growth seasons 24
Honghong Chai, Ke Shao, Chao Yu, Jinwang Shao, Ruili Wang, Yang Sui, Yan Guo,Yuntao Ma

O07 A model for maize leaf elongation and ontogeny under drought stress 26
Jonas R. Coussement, Selwyn Villers, Hilde Nelissen, Dirk Inzé, Kathy Steppe

O08 Modelling the effect of traits related to plant architectural development on wind-dispersed crop disease development....28
Katarina Streit, Jochem B. Evers, Michael Henke, Michael Renton

O09 High-precision 3D segmentation of plants combining spectral clustering and quotient graph techniques: a multi-level approach 30
Katia Mirande, Franck Hétroy-Wheeler, Christophe Godin

O10 A 3D architectural model of grass shoot morphogenesis and plasticity, driven by organ metabolite concentrations and coordination rules 32
Marion Gauthier, Romain Barillot, Anne Schneider, Camille Chambon, Christian Fournier, Christophe Pradal, Bruno Andrieu

O11 Exploring the dual role of bent canopy in cut-rose production using a functional-structural plant model 34
Ningyi Zhang, Arian van Westreenen, Jochem B. Evers, Niels P.R. Anten, Leo F.M. Marcelis

O12 Toward a functional-structural model of oil palm accounting for architectural plasticity in response to planting density 36
Raphaël P.A. Perez, Rémi Vezy, Loïc Brancheriau, Frédéric Boudon, François Grand, Doni Artanto Raharjo, Jean-Pierre Caliman, Jean Dauzat

O13 Integrating the complex regulation of leaf growth by water and trophic dynamics in a functional-structural plant model of grass.....38
Romain Barillot, Marion Gauthier, Bruno Andrieu, Jean-Louis Durand, Isabel Roldan-Ruiz, Tom De Swaef

O14 Predicting function from structure - an analysis of the palisade mesophyll 40
Shiv Gangapersad, Bryn Jones, Andrew Fleming, Visakan Kadirkamanathan

O15 Modelling the contribution of plant traits to light partitioning in simultaneous maize/soybean intercropping 41
Shuangwei Li, Wopke van der Werf, Junqi Zhu, Yan Guo, Baoguo Li, Yuntao Ma, Jochem B. Evers

O16 Modelling the genetic diversity of perennial grass phenology in contrasted temperate climates 43
Simon Rouet, Jean-Louis Durand, Didier Combes, Abraham Escobar Gutiérrez, Romain Barillot

O17 A structural model of three poplar clones from short-rotation coppice 45
Christoph B. Stiehm, Andrea Plazas Cebrián, Winfried Kurth

O18 Machine and deep learning based identification of organs within LiDAR scans of tree canopies: application to the estimation of apple production.....47
Artzet Simon, Benoît Pallas, Evelyne Costes, Frederic Boudon

O19 Spectral and angle dependent reflection properties of leaves 49
Jens Balasus, Tim Hegemann, Tran Quoc Khanh

O20 Quantifying the effects of carbon status on berry growth using a mechanistic carbon transport model.....51
Junqi Zhu, Fareeda Begum, Gerhard Rossouw, Bruno Holzapfel, Michael Henke, Alla N Seleznyova

O21 High-efficient modelling of canopy structure of field-grown crops based on UAV images.....53
Binglin Zhu, Fusang Liu, Bangyou Zheng, Pengcheng Hu, Tao Duan, Yan Guo

O22 What structural plant modelling and image-based phenotyping can learn from each other? 55
Christian Fournier, Simon Artzet, François Tardieu, Christophe Pradal

O23 Improving interoperability between phenomics and modelling communities by designing a Plant Modelling Ontology (PMO).....57
Clément Saint Cast, Guillaume Lobet, Llorenç Cabrera-Bosquet, Valentin Couvreur, Christophe Pradal, Bertrand Muller, François Tardieu, Xavier Draye

O24 Modelling canola for image-based phenomics 59
Mikolaj Cieslak, Nazifa Khan, Raju Soolanayakanahally, Ian McQuillan, Pascal Ferraro, Steve Robinson, Isobel Parkin, Przemyslaw Prusinkiewicz

O25 Three-dimensional morphological model of water lilies *Nymphaea* spp. for breeding historical study.....61
Shiryu Kirié, Christophe Pradal, Hideo Iwasaki, Koji Noshita, Hiroyoshi Iwata

O26 UAV imagery and functional-structural plant modelling unravel distinct drought tolerance strategies in soybean genotypes....63
Tom De Swaef, Irene Borra-Serrano, Aamir Saleem, Jonas Aper, Isabel Roldán-Ruiz, Peter Lootens

O27 Puzzling shapes - modelling epidermal tissue morphogenesis....65
Amir J. Bidhendi, Bara Altartouri, Anja Geitmann

O28 Predicting the effect of environmental conditions on tomato fruit growth by a transpiration driven mechanistic model....66
Jakub Salagovic, Pieter Verboven, Bert Verlinden, Kristof Holsteens, Bram Van de Poel, Marlies Huysmans, Bart Nicolai

O29 A hydraulic model of leaf growth in grasses: reconciling old empirical evidence....68
Tom De Swaef, Romain Barillot, Jean-Louis Durand

O30 Virtual plants and artificial tropical forest scenes as training samples for deep learning plant classifiers. The case of Raphia hookeri....70
Marc Jaeger, Gaëlle Viennois, Mickaël Baril, Frédéric Borne, Hervé Rey, Yuichi Nagao, Philippe Borianne

O31 Hydraulic Viper, a virtual phenotyping pipeline for root hydraulic traits - multiscale approach....72
Adrien Heymans, Valentin Couvreur, Félicien Meunier, Guillaume Lobet

O32 In sillico prospections to define root system ideotypes for rapeseed adapted to low nitrogen environment....74
Christophe Lecarpentier, Céline Richard-Molard, Loïc Pagès

O33 In silico analysis of grapevine architectural response to elevated CO_2....76
Dominik Schmidt, Christopher Bahr, Matthias Friedel, Katrin Kahlen

O34 Axillary bud outgrowth regulation by light intensity: modelling hormone and sugar interactions....78
Jessica Bertheloot, Anne Schneider, L. Ledroit, M.-D. Perez-Garcia, F. Boudon, C. Godin, S. Sakr

O35 Using functional-structural plant modelling to simulate the eco-evolutionary dynamics that shape plant communities....80
Jorad de Vries, Simone Fior, Aksel Palsson, Alex Widmer, Jake M. Alexander

O36 A functional-structural model of tomato simulates increased fruit yields by far-red illumination through higher carbohydrate source and sinks....82
Pieter de Visser, Anja Dieleman

O37 Mechanistic simulation of competition for light and nitrogen in strip intercrops....84
Jochem B. Evers, Wopke van der Werf, Tjeerd J. Stomph, Jorad de Vries, Lammert Bastiaans, Niels P.R. Anten

O38 MTG as a standard representation of plants in FSPMs....86
Christophe Pradal, Christophe Godin

O39 Development of a quantitative comparison tool for plant models....88
Olivier Pieters, Tom De Swaef, Francis Wyffels

O40 The plant water pump: why water flows uphill of water potential gradients in a root hydraulic anatomy model....90
Valentin Couvreur, Xavier Draye

S01 A bidirectional interface between BwinPro and GroIMP....91
Tim Oberländer, Winfried Kurth

S02 CPlantBox, a whole plant modelling framework for the simulation of water and carbon related processes (flows and growth)....93
Xiao-Ran Zhou, Andrea Schnepf, Jan Vanderborght, Daniel Leitner, André Lacointe, Harry Vereecken, Guillaume Lobet

S03 OpenSimRoot: software for root architectural models....95
Johannes A. Postma, Ernst D. Schäfer, Christopher K. Black, Christian W. Kuppe

S04 Co-simulation with OpenAlea and GroIMP for cross-platform functional-structural plant modelling 97
Qinqin Long, Christophe Pradal, Winfried Kurth

S05 Toward virtual modelling environments using notebooks for phenotyping and simulation of plant development 99
Frédéric Boudon, Jan Vaillant, Christophe Pradal

S06 Digitool: a tool for analyzing 3D plant architecture 101
Dany Moualeu-Ngangué, Magnus Adler, Yi-Chen Pao, San Schwe Myint, Andreas Fricke, Tsu-Wei Chen, Hartmut Stützel

S07 Yggdrasil - the crops in silico project's open-source Python package for connecting computational models across programming languages 103
Meagan Lang

P01 A framework for modelling the transport of water and carbohydrates in apple trees - simulation of a coupled phloem/xylem system 105
Alex Tavkhelidze, Gerhard Buck-Sorlin, Winfried Kurth

P02 Developing a functional-structural plant model for cocoa to explore pruning-shade interactions 107
Ambra Tosto, Pieter A. Zuidema, Niels P.R. Anten, Jochem B. Evers

P03 A 3D model of *Rhizophora mangle* L. saplings based on digitization and reconstruction of foliage on the modelling platform GroIMP 109
Faustino Chi, Katarína Streit, Aleksi Tavkhelidze, Winfried Kurth

P04 The effect of tree architecture on photosynthetic production in tropical trees 111
Hannah O'Sullivan, Jari Perttunen, Risto Sievänen, James Rosindell, Tania Stathaki, Magna Soelma Bessera Moura, Jon Lloyd

P05 3D shape modelling of apple vasculature with a space colonization algorithm 113
Leroi Pols, Pieter Verboven, Bart Nicolai

P06 Modelling the Guayule plant growth and development with a functional structural plant model 115
Loic Brancheriau, Sylvie Sabatier, Marc Jaeger, Nicolas Hemery, Christ Mougani, Philippe de Reffye, Ali Abed Alsater, Serge Palu

P07 Use of process-based system dynamic models to generate biologically aware 3D trees 117
Mariano Crimaldi, Edoardo Pasolli, Francesco Giannino

P08 Comparison of the light interception of an order-based branching model of spruce by several simplified models 119
Marius Heidenreich, Winfried Kurth

P09 Development of a functional-structural plant model of cassava root system during early storage root formation 121
Nattharat Punyasu, Treenut Saithong, Jittrawan Thaiprasit, Saowalak Kalapanulak, Tobias Wojciechowski, Johannes A. Postma

P10 Improving the Brazilian silvopastoral system arrangement 123
Nilson Aparecido Vieira Junior, Jochem Evers, Murilo dos Santos Vianna, Bruno Carneiro e Pedreira, Fábio Ricardo Marin

P11 Modelling maize photosynthesis and light utilization based on 3D maize canopy model 125
Gu Shenghao, Wang Yongjian, Wen Weiliang, Lu Xianju, Yu Zetao, Guo Xinyu

P12 Functional-structural modelling of root water uptake based on measured MRI images of root systems 127
Tobias Selzner, Magdalena Landl, Andreas Pohlmeier, Jan Vanderborght, Daniel Leitner, Andrea Schnepf

P13 A functional-structural plant model of greenhouse-grown cucumber tailored for high-wire production 128
X. Cornilleau, G.H. Buck-Sorlin

P14 New high-throughput methods for leaf area index and height estimation are faster, more precise than and at least as accurate as current methods 130
Justin McGrath, Matthew Siebers, Stephen Long, Carl Bernacchi

P15 Topological skeleton models of complex jointed tree structures 131
Qiguan Shu, Wilfrid Middleton, Mohammad Asrafur Rahman, Ferdinand Ludwig

P16 Modelling shadow cast by trees using 3D models with artificial leaves 133
Rafael Bohn Reckziegel, Elena Larysch, Christopher Morhart, Hans-Peter Kahle, Thomas Seifert

P17 Detailed reconstruction of trees from TLS scans for radiative transfer modelling applications 135
Růžena Janoutová, Lucie Homolová, Zbyněk Malenovský, Jan Novotný, Barbora Navrátilová

P18 Characterization of light quantity and quality in agroforestry systems 137
Willem Coudron, Kris Verheyen, Pieter De Frenne, Bert Reubens, Kim Calders, Van Den Berge Sanne, Tom De Swaef

P19 Simulating the red:far-red ratio emitted by individual plants at a local and directional scale 139
Arthur Couturier, Elzbieta Frak, Didier Combes, Abraham Escobar-Gutierrez

P20 Bayesian statistical calibration of parameters in the APSIM-Maize crop model for improved yield prediction 141
Matteo G. Ziliani, Matthew F. McCabe

P21 An algorithm to measure root hair response to abiotic stresses in microscopy images 143
Peter Pietrzyk, Chartinun Chutoe, Patompong Saengwilai, Alexander Bucksch

P22 Digitizing plants: simultaneous capturing of plant structure and functioning for building a maize FSPM 144
Selwyn Villers, Jonas R. Coussement, Dirk Inzé, Kathy Steppe

P23 Simulating the spatial distribution of physiological processes using a reduced functional-structural plant model for wheat 146
Simon Lauwers, Jonas Coussement, Sarah Verbeke, Veerle De Schepper, Kathy Steppe

P24 Modelling the extension of silk and ear of summer maize 148
Zhiwei Wang, Weiwei Sun, Youhong Song

P25 A parameter-free system to measure morphological and physiological traits of Arabidopsis rosettes 150
Suxing Liu, Maria Ortega,, Chung-Jui Tsai, Alexander Bucksch

P26 DIRT/3D: 3D phenotyping system for maize architecture in the field 152
Suxing Liu, Carlos Sherard Barrow, Molly Hanlon, Jonathan P. Lynch, Alexander Bucksch

P27 Proteomics integrated with metabolomics reveals the systems reprograming in wheat inoculated with native bacteria and arbuscular mycorrhizal (AM) fungi 154
Radheshyam Yadav, Ramakrishna Wusirika

P28 Virtual pruning in cocoa: assessing the potential of a 3D cocoa model as communication tool for training purposes 155
Ambra Tosto, Faustina Obeng Adomaa, Urcil Kenfack Essougong, Pieter A. Zuidema, Jochem B. Evers, Niels P.R. Anten

P29 Exploratory analysis of bud fate frequency of Tonda di Giffoni cultivar (*Corylus avellana* L., 1753) in own-rooted and grafted plants 157
Francesca Grisafi, Daniela Farinelli, Sergio Tombesi

P30 Phenotypic spectrum: quantifying diversity of root architectures within genotypes on the example common bean (*Phaselous vulgaris*) 159
Limeng Xie, James Burridge, Nicolas Klepp, John Miller, Jonathan P. Lynch, Alexander Bucksch

P31 Estimation of extinction coefficients and light interception in 3D Arabic coffee trees under water deficit 160
Miroslava Rakocevic, Ricardo Antônio Almeida Pazianotto, Fabio Takeshi Matsunaga, Eliemar Campostrini, Rafael Vasconcelos Ribeiro, Romain Barillot, Didier Combes

P32 Structural acclimations of 3D coffee plants to water deficit....162
Miroslava Rakocevic, Ricardo Antônio Almeida Pazianotto, Fabio Takeshi Matsunaga, Eliemar Campostrini, Rafael Vasconcelos Ribeiro

P33 Understanding the impact of the aerial architecture on the performance of wheat cultivar mixtures....164
Emmanuelle Blanc, Jérôme Enjalbert, Christian Fournier, Christophe Pradal, Christophe Lecarpentier, Pierre Barbillon

P34 Impact of intraspecific trait variance on interspecific competition: a theoretical case study using the Virtual Grassland model 166
Béatrice Wolff, Bernadette Julier, Gaëtan Louarn

P35 WHEAMM: a functional-structural model to study plant growth and interactions with neighbors in wheat variety mixtures....167
Meije Gawinowski, Jérôme Enjalbert, Paul-Henry Cournède, Timothée Flutre

P36 Modelling shade cast by rows of trees using 3D models based on terrestrial laser scanning data 169
Rafael Bohn Reckziegel, Jonathan P. Sheppard, Christopher Morhart, Ben du Toit, Hans-Peter Kahle

P37 Efficient stochastic functional structural sympodial shrubs modelling based on structural hierarchy. Application to guayule 171
Marc Jaeger, Sylvie Sabatier, Philippe de Reffye, Ali Abed Alsater, Loic Brancheriau

P38 Light exchanges in discrete directions as an alternative to raytracing and radiosity 173
Rémi Vezy, Raphaël Perez, François Grand, Jean Dauzat

The power of 3D plant-microclimate interactions

Kathy Steppe[1]

[1] *Laboratory of Plant Ecology, Department of Plants and Crops, Faculty of Bioscience Engineering, Ghent University, Belgium*

For correspondence: kathy.steppe@UGent.be

Keywords: plant sensors, phylloclimate, turgor-driven growth, plant monitoring

Plant functioning and microclimate are tightly coupled. A change in one is instantly causing a change in the other. Both water and sugar flow, and hence turgor-driven growth, are affected by this interplay (Steppe et al., 2015; Coussement et al., 2018). In this keynote talk, new approaches will be presented that can advance our understanding of the dynamic interactions between plants and their microclimate. State-of the-art technology to measure dynamics in phylloclimate will be presented. The findings will be used as stepping-stone to highlight the importance and power of coupled plant monitoring-modelling approaches to aptly assess plant vitality and function, and steer plant production and quality.

Figure: Example of plant sensors to measure dynamic plant-microclimate interactions

References

Coussement et al., 2018, *Annals of Botany* 121: 849-861, doi: 10.1093/aob/mcx144
Steppe et al., 2015, *Trends in Plant Science* 20: 335-343, doi: 10.1016/j.tplants.2015.03.015

Functional-structural plant modelling with CPlantBox

Andrea Schnepf[1], Xiaoran Zhou[1], Daniel Leitner[2], Gernot Bodner[3], Deepanshu Khare[1], Jan Vanderborght[1], Harry Vereecken[1], Guillaume Lobet[1]

[1] *Forschungszentrum Juelich GmbH, Institute of Bio- and Geosciences, IBG-3: Agrosphere, Juelich, Germany*
[2] *Simulationswerkstatt, Ortmayrstrasse 20, 4060 Leonding, Austria*
[3] *University of Natural Resources and Life Sciences, Vienna, Institute of Agronomy, Konrad Lorenz-Straße 24, 3430 Tulln an der Donau, Austria*

For correspondence: a.schnepf@fz-juelich.de

Keywords: CPlantBox, functional-structural plant model, water flow, carbon flow

Introduction

Plants simultaneously experience and interact with different environmental compartments, i.e., the soil and the atmosphere, and they facilitate fluxes of water and carbon between those compartments. Yet, only few functional-structural plant models exist that have full 3D topology that is embedded in a 3D environment. There are whole-plant models that focus on light interception, water and carbon flow inside the plant. Detailed soil-plant interaction models resolve the spatially and temporally varying soil processes. In these models, there may be carbon allocation rules to the root, however the shoot is mostly treated in a simplified way.

We recently developed the whole-plant modelling framework CPlantBox as a further development of the 3D root architecture model CRootBox (Schnepf et al. 2018). CPlantBox is capable of simulating the growth and development of a variety of plant architectures. It can be used to grow individual organs (i.e. only the root system or only the shoot) or whole plants (i.e., root and shoot). In addition, the flexibility of CPlantBox enables its coupling with external modelling tools.

We demonstrate the use of the CPlantBox modelling framework by three examples. The first example illustrates the range of plant structures that can be simulated using CPlantBox. In the second example, we simulated diurnal carbon and water flows inside the plant, mimicking a laboratory experiment. Finally, we show a case study of a root architecture-only simulation, in which we simulate water flow in soil and root system of field-grown plants with contrasting mechanisms to cope with drought.

Materials and Methods

CPlantBox simulates plant growth by defining growth rules for each plant organ, including emergence, branching, elongation, senescence and death. It is written in C++ and has a Python binding that facilitates the creation of applications by simple scripting. It is available on a github repository, `github.com/Plant-Root-Soil-Interactions-Modelling/CPlantBox`.

To simulate carbon and water flow inside a plant created with CPlantBox, we coupled CPlantBox with a mechanistic model of water and carbon flow, PiafMuch (Lacointe and Minchin 2019). Root-soil interaction was simulated by coupling CPlantBox with DuMu^x, a free and open-source simulator for flow and transport processes in porous media (Flemisch et al. 2011). By using periodic boundary conditions on the sides, we simulated a field of soybean and a field of sunflower over the vegetation period. The coupling method in both cases was a light coupling via input- and output files.

Results and Discussion

Figure 1: Examples of plant structures simulated with CPlantBox.

Figure 1 shows examples of plant structures created with CPlantBox. The CPlantBox framework simulation results of water and carbon flow inside a plant could be corroborated with experimental data of a morning glory experiment (Knoblauch et al. 2016). In our third simulation example, two plants with contrasting drought coping mechanisms, sunflower (stomata controlled by leaf water potential) and soybean (hormonal regulation of stomata), are exposed to the same soil and climatic conditions. Results will compare the stress index, actual versus potential transpiration, for the two plant. Preliminary results are shown in Figure 2, a simulated sunflower root system and its root water uptake over the vegetation period, experiencing a dry summer.

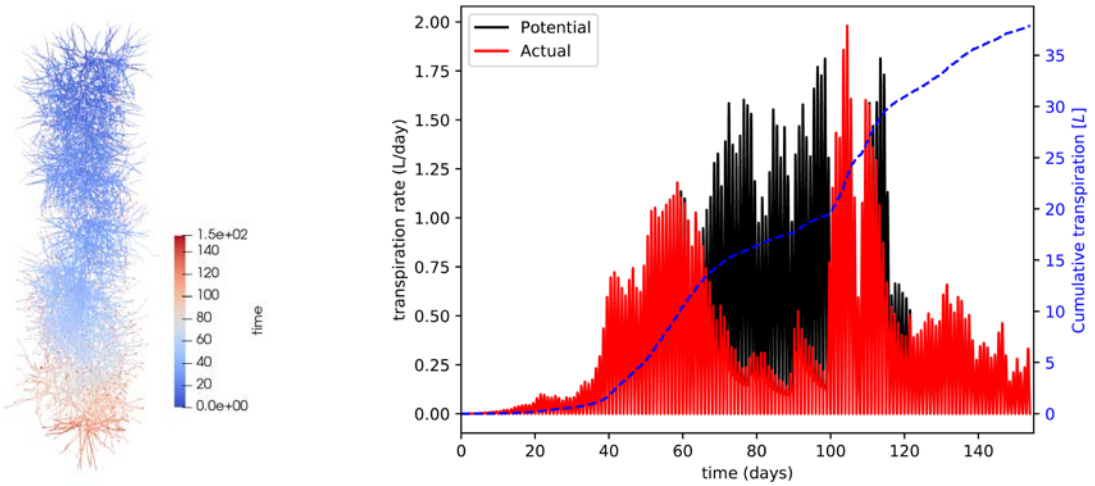

Figure 2: (a) Simulated sunflower root system. Colours denote the root segment creation time. (b) Potential and actual transpiration rates and cumulative transpiration by one plant in a sunflower field. Location: Hollabrunn, Austria; Climate data: year 2003; Soil type: loam.

Conclusion

CPlantBox is a generic tool to generate different types of plant structures. Its Python binding facilitates coupling to other models. The CPlantBox framework can be used to mimic laboratory experiments which can help to analyze and explain observed results and increase process understanding. It can also be used to perform field-scale simulations in order to predict expected stress conditions for different crops. Future work will combine photosynthesis with root exudation as affected by water and carbon flow inside the plant, and the effects of root exudation on local (rhizosphere) soil conditions.

References

Flemisch et al., 2011, Adv. Water Res. 34, doi: 10.1016/j.advwatres.2011.03.007
Knoblauch et al., 2016, eLife 5, doi: 10.7554/eLife.15341
Lacointe and Minchin, 2019, Phloem. Methods Mol Biol., doi: 10.1007/978-1-4939-9562-2_28.
Schnepf et al., 2018, Annals of Botany 121, doi:10.1093/aob/mcx221
Zhou et al., 2020, in silico Plants 2, doi:10.1093/insilicoplants/diaa001

Topological Data Analysis (TDA) as a method to comprehensively measure the plant form

Daniel H. Chitwood[1,2]

[1] *Department of Horticulture, Michigan State University, East Lansing, USA*
[2] *Department of Computational Mathematics, Science & Engineering, Michigan State University, East Lansing, USA*

For correspondence: dhchitwood@gmail.com

Keywords: Topological Data Analysis, morphometrics, X-ray Computed Tomography

Embedded in all shapes is information. For all lifeforms, morphology—at the cellular, tissue, organ, and organismal levels—arises from genetic and environmental influences, and their interaction. These influences on the organismal form can be statistically determined, and mathematical models derived to predict which forms will arise under certain genetic and environmental scenarios. The diversity of plant forms that have arisen through evolution, and the domesticated morphologies of plants that have been artificially selected to create the major crops of the world, have benefited humanity incalculably, and directly result from alterations to plant architecture and morphology. Despite morphology being intrinsically linked to the sizes of grains and fruits, the yields of branching inflorescences, the canopies of fields, and the economics of root architectures, and even with intense interest in developing sophisticated genetic technologies and statistics to model these traits, methods that adequately quantify plant morphology comprehensively and across scales remain underdeveloped.

In this talk, I will discuss the use of X-ray Computed Tomography (CT) to create 3D models of plants and time-lapses of plant growth. Topological Data Analysis (TDA) will be discussed as a framework to analyze the resulting volumetric image data from multiple plant species.

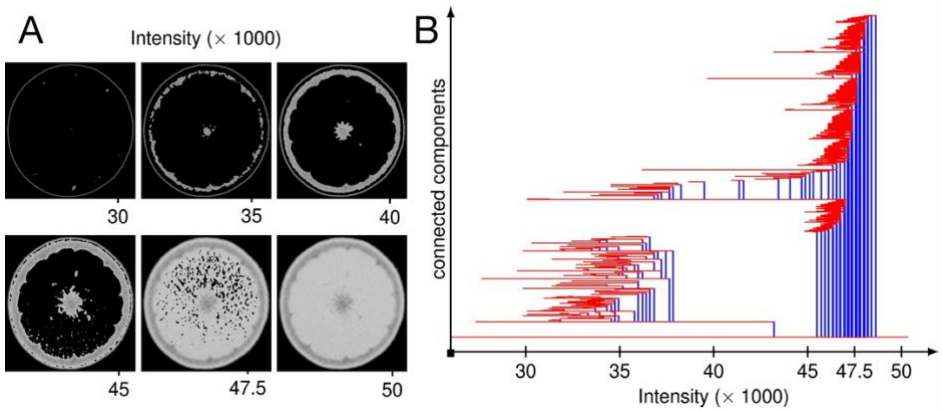

Figure 1: **An example of a persistence barcode.** A) Snapshots of an X-ray CT image of an orange. Only the pixels with intensity lower than indicated are displayed. B) Persistence barcode of connected components of such image.

References

Chitwood et al., 2019, *Mathematical Morphology and Its Applications to Signal and Image Processing. ISMM 2019. Lecture Notes in Computer Science.* 11564, doi: 10.1007/978-3-030-20867-7_7

A new high-performance FSPM framework linking LiDAR-based canopy reconstructions with scalable biophysical models

Brian N. Bailey[1]

[1] *Department of Plant Sciences, University of California, Davis, Davis, CA, U.S.A.*

For correspondence: bnbailey@ucdavis.edu

Keywords: Helios, heterogeneity, LiDAR reconstructions, phenotyping

Introduction

While functional-structural plant models (FSPMs) have successfully broadened our knowledge of how heterogeneity in vegetation structure at the plant-scale impacts a wide range of biophysical processes, current studies are most commonly limited to the scale of a few plants, or a relatively small number of plants that periodically repeat indefinitely across flat terrain. At the field scale, heterogeneity is often present across a number of scales due to factors including complex topography, soil texture variability, genotypic variability, and edge effects, among others. Representing such field-scale heterogeneity in FSPMs introduces a number of challenges. One is that this heterogeneity must first be quantified through high-throughput measurements in order to perform model calibration and validation. For large, dense plants, a large fraction of biomass is occluded from view of an external optically-based sensor, which prohibits direct measurement of the full plant structure. Additionally, models must be computationally efficient enough to resolve the full range of relevant scales in heterogeneity from sub-leaf through field scales if they are to be considered within the model.

Methods

A new 3D modelling framework, Helios, has been developed that is aimed at addressing these challenges in high-resolution measurement and modelling related to heterogeneity and scale (Bailey 2019). New phenotyping methods were developed to process terrestrial LiDAR point clouds into leaf-by-leaf canopy reconstructions that ensure that the overall distributions of leaf area and orientation within the reconstructions are consistent at sub-meter scales. This process begins by collecting ground-based or terrestrial LiDAR scanning data from multiple viewing directions of the plant(s) of interest (usually 3-4 viewing directions per plant is sufficient). This process yields millions of Cartesian (x,y,z) coordinates in space corresponding to LiDAR beam-object intersection points. The challenge is that Cartesian points in space are of little direct utility when it comes to providing inputs to an FSPM, and our task is to translate these points into surface-related information such as surface areas, normal vectors, and their respective variation in space.

The next step in the plant reconstruction process is to extract leaf normal vectors from the LiDAR point clouds. This is accomplished using a triangulation algorithm, and a filtering routine to remove erroneous triangles that connect adjacent surfaces that are disconnected in actuality (Bailey and Mahaffee 2017a). This process yields thousands of measurements of normal vectors and their distribution in space.

The triangles resulting from the above triangulation methodology are then connected to reconstruct the surfaces of leaves in direct view of the LiDAR scanner (Bailey and Ochoa 2018). A region-growing algorithm is used to connect contiguous groups of triangles, which are assumed to correspond to all or part of an individual leaf. While this approach is generally a robust means for reconstructing the visible leaf area, there is usually a significant fraction of leaves occluded from view that cannot be directly reconstructed.

Occluded leaf area is reconstructed using a statistical backfilling approach. Plant volumes are discretized into rectangular voxels, and a Beer's law inversion method is used to invert

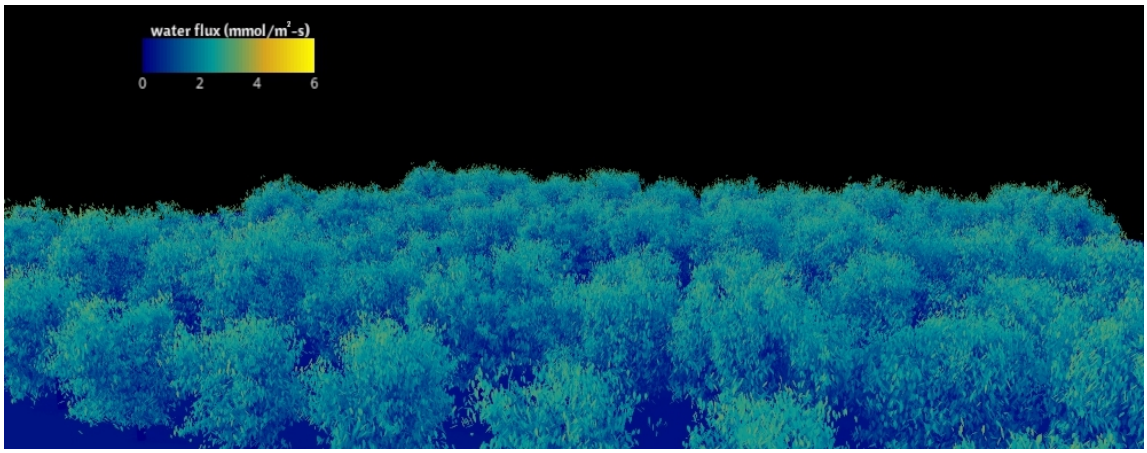

Figure 1. Example of LiDAR-based orchard reconstruction, combined with a 3D simulation of transpiration flux for every leaf in the canopy.

the LiDAR data to determine the total amount of leaf area (visible+occluded) in each voxel (Bailey and Mahaffee 2017b). Leaves are then backfilled into each voxel such that the correct amount of leaf area and leaf angle distribution are obtained (Bailey and Ochoa 2018).

This architectural data is assimilated into a new 3D plant modeling framework, Helios, that incorporates novel biophysical models with improved physical realism and efficiency. One such notable advance is the development of a new radiation transfer model for both shortwave and longwave radiation, which improves both efficiency and consistency of calculated absorbed radiation distributions (Bailey 2018).

The models and LiDAR data processing routines are accelerated by performing calculations on graphics processing units (GPUs), which allows for the simulation of hundreds of fully-resolved trees with ~100 million leaves on a desktop workstation.

Results

To date, Helios has been used in a number of different applications primarily focused on woody perennial crops. Examples include optimal design of vineyard systems to mitigate elevated berry temperatures due to climate instability, understanding the role of stomatal dynamics in canopy-scale gas exchange in crops, and optimizing irrigation practices in polyculture systems, among others.

Our group has also focused a significant amount of time on using Helios to better understand the assumptions and errors inherent in biophysical models of varying complexity. One important and somewhat surprising result from this work is that it is usually necessary for FSPMs to resolve vegetation at scales much smaller than individual leaves, otherwise large errors can arise that are significantly larger than that of a much simpler two-big-leaf or multilayer model. This is due to the fact that leaf-scale averaging inherently blurs the line between sunlit and shaded leaf area, whereas big-leaf-style models are statistical and probabilistically perform this separation independent of individual leaves. This further underscores the need for computational efficiency in FSPMs given these high requirements for resolving sub-leaf-scale heterogeneity.

References

Bailey, B.N. (2019). Frontiers in Plant Sciences 10:1185

Bailey, B.N. and Ochoa, M.H. (2018). Remote Sensing of Environment 208:133-144

Bailey, B.N. (2018). Ecological Modelling 368:233-245

Bailey, B.N. and Mahaffee, W.F. (2017). Measurement Science & Technology 28:064006

Bailey, B.N. and Mahaffee, W.F. (2017). Remote Sensing of Environment 193:63-67

Exploring FSPMs and crop models complementarities in up- and down-scaling from plant to field with a focus on modelling crop mixtures

Marie Launay[1], Noémie Gaudio[2]

[1] *US1116 AgroClim, F-84914, Avignon, France*
[2] *University of Toulouse, INRAE, UMR AGIR, F-31326, Castanet-Tolosan, France*

For correspondence: marie.launay@inrae.fr

Keywords: crop models, crop mixtures, upscaling in modelling

Crop mixtures for a sustainable agriculture

Increasing plant diversity in agriculture, in order to promote natural regulations, is suggested as a pathway towards more resilient and sustainable production systems. These natural regulations allow agroecosystems to provide ecosystem services that are broader than production alone, e.g. improvement of water quality (especially by reducing the use of chemical inputs) and soil fertility, or increasing biological pest control. At field scale, plant diversity can increase by using species mixtures such as in intercrops. Even if the agronomical advantages of these diversified systems were highlighted, several questions remain regarding their management and their integration in cropping systems to reach the ecosystem services targeted.

Modelling approaches to represent crop mixtures

Modelling their functioning is both a tool for understanding and a tool for testing hypotheses to support the agroecological transition. The main modelling approaches developed to study intercrops are process-based models at the plant scale (among which FSPMs) and at the crop scale (crop models) (Gaudio et al., 2019). Most of these models were adapted from models dedicated to isolated plants or sole crops. Modelling intercrops and ecosystem services they are designed for involves changes in the modelling approaches which are i) modelling plant-plant interactions (competition, complementarity, facilitation) and the impact of the environment and agricultural practices on these interactions, and ii) modelling the way these processes contribute to the functions and then to the ecosystem services targeted. Here we will focus on FSPMs and crop models complementarities.

Complementarity of the modelling approaches to understand crop mixtures functioning

From a strictly ecophysiological point of view, some processes are particularly determining in crop mixtures because they largely explain their functioning and performance, especially competition (for light, water and nutrients), complementarity (spatio-temporal and niche ones), phenotypic plasticity and facilitation. To represent these driving processes, different modelling approaches co-exist, from the most mechanistic and spatially explicit to the most empirical.
However, the environment, whether technical, pedoclimatic or biotic, also modifies the nature and intensity of these plant-plant interactions. Therefore, the capacity of models to take these plant-environment interactions into account appears to be crucial when it comes to building and thus evaluating the performance of mixtures to provide one or more ecosystem services.
Through various examples, we show how mobilizing the complementarity between crop models and FSPMs allows to better understand and simulate the functioning of crop mixtures.
In FSPMs, the result of plant-plant interactions is an emergent property of the models (Gaudio et al., 2019). Then, some FSPMs enable to quantify ecological processes (Zhu et al., 2015)

or given functional traits (Barillot et al., 2014) involved in intercrops performance or resource use efficiency (more often light). Then important processes highlighted by FSPMs can be summarized by functional relationships in order to be included in crop models (Barillot et al., 2011). In crop models, agricultural practices influence crop environment such as soil fertility and water availability, modifying the pedoclimatic context in which crop mixtures may adapt according to their complementarity and/or plasticity properties (Corre-Hellou et al., 2009). Thus, crop models are able to provide inputs to FSPMs, i.e. a quantified and dynamic description of the abiotic constraints within which crop mixture grows. In addition, when facing the question of crop mixtures and their skills, FSPMs and crop models face common issues, and sometimes share solutions. Other approaches such as qualitative hierarchical aggregative modelling may also be relevant when the goal is to qualify the factors that are involved in these complex ecosystems' functioning.

Towards ecosystem services assessment

It is even possible to use such modelling tools to co-construct agrosystems that are likely to meet the expectations of agricultural sectors, based on the fine interactions between plants, and between the plant and its biotic, abiotic and human environment. However, predicting how management activities and changing future conditions will alter services is made more complex by the interactions among multiple ecosystem services (trade-offs, synergies, etc.) (Agudelo et al., 2020); the more widespread use of biophysical models (FSPM, process-based models) for the estimation of ecosystem services could probably provide access to the physiological processes, or even the traits, behind the interactions between ecosystem services. Simulating ecosystem services provided by intercrops also requires taking into account their inclusion into crop rotation and the effect of the environment on the long term. This could be achieved by coupling knowledge brought by FSPMs and crop models, but also using more qualitative models based on farmers' expertise (e.g. Martin et al., 2019).

From a detailed understanding of the plant-plant processes within crop mixtures to the expression of the ecosystem services they can supply on different spatio-temporal scales, the complementarity between FSPMs and crop models is a relevant tool that should be better explored in the future.

References

Agudelo et al., 2020. *Ecol. Model.* 429, https://doi.org/10.1016/j.ecolmodel.2020.109103
Barillot et al., 2011, *Ann Bot.* 108, 1013–1024, https://doi.org/10.1093/aob/mcr199
Barillot et al., 2014, *Ann. Bot.* 108:1013-1024, doi: 10.1093/aob/mcr199
Corre-Hellou et al., 2009, *Field Crops Res*. 113:72-81, https://doi.org/10.1016/j.fcr.2009.04.007
Gaudio et al., 2019, *Agron. Sust. Dev.* 39:20, doi: 10.1007/s13593-019-0562-6
Martin et al., 2019, *European Conference on Crop Diversification*, pp. 34–35
Zhu et al., 2015, *New Phytol*. 207, 1213–1222, https://doi.org/10.1111/nph.13416

Teaching functional-structural plant modelling – perspectives from a plant scientist

Jochem B. Evers

Centre for Crop Systems Analysis, Wageningen University and Research, Wageningen, the Netherlands
For correspondence: jochem.evers@wur.nl

Keywords: abstraction, programming, didactics

Introduction

As our knowledge in the domain of plant science expands, we increasingly see the complexity of the biological systems we analyse. We discover ever more new mechanisms and processes at different scales, from molecular physiology to community ecology, as well as feedback relationships between these levels of biological integration. To make sense of this ever-increasing body of knowledge in plant science, simulation methods such as functional-structural plant (FSP) models are increasingly being developed and applied (Sievänen *et al.*, 2014; Evers *et al.*, 2018). As FSP models are becoming more widely accepted and used in research, and more and more play important societal roles (e.g. for decisions about regulation and management of biological systems), the need to include them in study programs has been increasing steadily.

Teaching FSP models can be divided into two broad categories: teaching the modelling itself, and teaching the application of such models in plant science. This distinction is important for the adoption of simulation models in plant research. If it is clear such models can be very useful in addressing questions in plant science without needing a degree in mathematics, programming or computer science, more students may be inclined to use models in research later. An added benefit for the acceptance and adoption by students of FSP models specifically, is the natural way in which plant growth and the effects of virtual treatment or (eco)physiological processes can be visualized convincingly in 3D.

A crucial step in teaching FPS modelling and its use, is separating the conceptual modelling from the actual implementation on a computer. In a conceptual model, the plant system is described in terms of its components and their relations. It is this first abstraction step that defines what the model looks like, and is important for teaching FSP models: designing and discussing a conceptual model first, leads to a good overview of the model structure to be implemented later. A lack of overview of what should be part of the model is one of the main reasons FSP modelling may come across as intimidating.

Another important aspect of teaching FSP modelling for plant science is discussing to which extent model development requires experimental data for model parameterization and for the evaluation of model performance. Even purely theoretical FSP models that are not meant to do numerical predictions, need to abstract from real plants at some level. Having the students do measurements on real plants, increases both the appreciation of the object to be modelled and the variation the model will need to be able to deal with.

In this keynote, I will provide some perspectives on teaching FSP modelling in postgraduate courses within the field of plant science. Based on experiences both as a student and as a teacher, I will discuss some ideas on how to efficiently teach the basics and biological relevance of FSP modelling to plant science students, aiming at a wider scale adoption of the approach within plant science in the years to come.

References

Evers et al., 2018, *Ann Bot* 121: 767–772, doi: 10.1093/aob/mcy050
Sievänen er al., 2014 *Ann Bot* 114: 599–603, doi: 10.1093/aob/mcu175

Considering genetic control of plant architecture in FSPM: a review of progresses and current challenges

Evelyne Costes[1]

[1] Univ. Montpellier, UMR AGAP CIRAD, INRAe, Institut Agro, Montpellier, France

For correspondence: evelyne.costes@inrae.fr

Keywords: quantitative genetics, allelic variation, QTLs, phenotyping, mutants, candidate genes

Many studies have emphasized the genetic inheritance of plant architectures, after this evidence has grounded founder studies, e.g. explorations of plant form evolution or architectural analyses by Hallé and co-authors. To study the genetic bases of plant architectures, two main approaches have been developed. The first approach is based on mutants, either with loss or gain of functions, whose phenotypes are linked to plant architecture. It has been proved efficient to decipher the physiological and molecular bases of several key processes of plant development, especially in plant models such as *Arabidopsis thaliana*. Such analyses of mutants have provided first comprehension of gene functions and their roles in regulatory pathways. For instance, the molecular bases of stem cell maintenance or growth cessation in apical meristems are largely deciphered or being deciphered. This approach has been enlarged to other species including perennials (e.g. Hollender and Dardick, 2018 for a review). Even though mutants are available for a limited number of species and traits, significant and fascinating progresses have been made. Moreover, comparisons among species currently suggest that some key genes and pathways acting on meristems could rely on ancient and well-conserved mechanisms across species. However, in many cases, the link with natural within-species genetic variability of plant architectures remains to be clarified.

This link could rely on the second approach that has been used to decipher the genetic control of plant architectures and which consists in the exploration of within-species variability of plant architectural traits by quantitative genetics. Such analyses are usually performed on specific traits screened over large population of plants that are specifically designed, i.e. segregating bi-parental or multi-parental progenies, panels of diversity. They aim to reveal the genetic part of traits variation and distinguish it from environmental effects. When plant architecture is decomposed into elementary traits or processes, numerous associations (i.e. Quantitative Trait Loci – QTLs) have been found (Costes and Gion, 2015 for a review on trees). For most traits, whatever the scale of observation, the existence of several associations, often with interactions between genomic regions, has suggested polygenetic and complex genetic controls. A step further has been rapidly reached when reference genomes have been sequenced, making possible to search for candidate genes within the associated genomic regions. However, linking QTL and positional candidate genes with physiological or molecular processes involved in the control of trait variation remains a laborious task.

As FSPM is a class of models that explicitly represents plant structures, the introduction of plant architecture control by genetic and physiologic mechanisms, despite still at its infancy, appears relevant to explore plant architecture diversity and the impact of genetic variations on the production and performances of plants of agronomic interest. From the acquired comprehension of molecular and physiological mechanisms controlling specific processes involved in plant development, mechanistic models have been developed. For instance, models of axillary bud outgrowth, initially statistical and probabilistic, have progressively introduced controls by hormone fluxes and interactions with sugars (Prusinkiewicz et al., 2009; Schneider et al., 2019). Floral induction of meristems at particular locations within plant structure is another key event of plant architectural development that has recently been

modelled, based on combinations of signal fluxes with probability determining meristem fates (Belhassine et al., 2020).

In parallel, allelic effects on elementary trait values, related to growth and branching, have been considered in FSPM, in cereals (Letort et al., 2008; Xu et al., 2011) and few perennial crops (e.g. Migault et al., 2017). However, simulating polycarpic plant architectures at coarse scales require accounting for interactions among traits while, in many cases, the genetic co-variances among traits remain unknown. At axis scale, allometry-based approach has been proposed for instance to simulate the variations of leaf form, accounting for the genetic and ontogenetic effects as well as morphogenetic gradients along the stem (Perez et al., 2016). At coarser scales, high throughput phenotyping tools based on imagery or scans are currently developed and could help to overcome the lack of knowledge on the dependencies and trade-off between traits during plant development. They could facilitate the consideration of genetic variability in FSPM and further support quantitative genetic studies (Mc Cormick et al., 2016; Coupel-Ledru et al., 2019).

In conclusion, both quantitative genetics and screening of mutants are currently providing new insights into the genetic and physiological control of plant architectures, at all scales i.e. from molecular, tissue and organ to whole plant scales. The considerable increase of genomic resources, the emergence of epi-genetics and multi-omics approaches is allowing exploring the natural variations of genes and mechanisms. New avenues will thus open for linking mechanistic models to the results of quantitative genetic analyses. Implementing such mechanistic models while accounting for the genetic variability due to allelic or epi-allelic variations in FSPM will certainly reinforce their contribution for designing genetic ideotypes and assist breeding programmes.

References

Belhassine et al., 2020, *Scientific reports*, 10: 1-14, doi : 10.1038/s41598-020-69861-8
Coupel-Ledru et al., 2019, *Horticultural Research*, 6: 52, doi: 10.1038/s41438-019-0137-3
Costes and Gion, 2015, doi: 10.1016/bs.abr.2015.05.001
Hollender and Dardick, 2015, *New Phytologist*, 206: 541-556, doi: 10.1111/nph.13204
Letort et al., 2008, *Annals of Botany*, 101:1243-1254, doi: 10.1093/aob/mcm197
McCormick et al., 2016, Plant physiology, 172: 823-834, doi:10.1104/pp.16.00948
Migault et al., 2017. *Frontiers in plant science*, 7, 2065. doi: 10.3389/fpls.2016.02065
Perez et al., 2016, *Journal of experimental botany*, 67: 4507-4521, doi: 10.1093/jxb/erw203
Prusinkiewicz et al. 2009, *PNAS* 106:17431-17436, doi: 10.1073/pnas.090669610
Schneider et al., 2019, *Frontiers in plant science*, 10, 1296, doi: 10.3389/fpls.2019.01296
Xu et al., 2011, *Annals of Botany*, 107: 817-828, doi: 10.1093/aob/mcq264

Multiscale modelling of tree and wood biomechanics

Tancrède Alméras[1]

[1] *Laboratory of mechanics and civil engineering, CNRS, Montpellier University, France*

For correspondence: tancrede.almeras@umontpellier.fr

Keywords: gravitropism, reaction wood, thigmomorphogenesis

Most of terrestrial biomass is made of wood, and most of wood biomass is made of fibres, whose function is mechanical. This massive investment of trees in support tissues aims at facing two kinds of major mechanical constraints: transient loads due to the external action of wind, snow or falling trees, and permanent loads due to gravity (self-weight of leaves and branches). The former directly impacts tree survival through the risk of breaking the stem, and the latter directly impacts tree growth and competition by controlling the amount of leaves and the height at which it can be supported.
The performance in these functions at the scale of the individual depends on both the quality of wood (mechanical properties) and its quantity (stem diameter), both of them being variable within an individual, between individuals and between species. Wood mechanical properties depend on it microstructure at the cell and cell wall levels. The amount and microstructure of wood produced by a tree are tuned to its needs, through two major regulatory processes: gravitropism (control of the orientation of woody axes in response to gravity), and thigmomorphogenesis (control of the balance between primary and secondary growth in response to external loads). These processes contribute to determine resource allocation and tree architecture.

Modeling and simulating tree growth dynamics including both shoot and root compartments. The RoCoCau+TOY model

JF Barczi[1], Yves Caraglio[1], Eric Nicolini[1], Herve Rey[1], Alexandre Haldat[1]

[1]*Amap, Cirad, France*

For correspondence: barczi@cirad.fr

Keywords : architecture, biomass, plasticity, whole plant, FSPM.

Introduction

Tree structural and biomass growth studies are mainly carried out on shoot compartment. Root compartment is usually taken apart due to the difficulties on measuring and observing it, especially when considering root growth. AMAP team is already leading experimental studies including both compartments through field experiments and observations. AMAP also provides shoot or root models and simulators of tree architecture and biomass production applied to many agronomic and forest species. It now becomes very critical to study tree structural plasticity according to global climate change. For this purpose, both shoot and root systems have to be considered at the same time since they play collaborative roles dedicated to climate traits (water availability for roots and light or carbon availability for shoots). We propose a whole-plant model and its simulator (RoCoCau) with a linkable external module (TOY) to represent shoot and root compartments dependencies and thus tree structural plasticity when facing various aerial and edaphic environments.

Literature shows this plasticity but generally at one moment of the tree life cycle. One of the main issue of such a tool is to understand how this balance is managed according to tree development (structure maintenance *vs* space exploration).

Materials and Methods

RoCoCau is made of the association of AmapSim (Barczi et al 2008) and DigR (Barczi et al 2018) to represent shoots and roots. The software simulation environment makes it possible to plug an external functional module to the core structure simulator. We propose the module (TOY) that roughly models the dependency between the two compartments. This dependency remains in (i) biomass production that needs water uptake through roots, carbon and light uptake through leaves and in (ii) biomass partitioning to control development and growth of both compartments in order to preserve a balanced uptake capacity on water, carbon and light.

Results and Discussion

We have been applying RoCoCau to *eucalyptus* root/shoot systems that were previously modeled to check its accuracy to mimic realistic whole tree growth dynamics (figure 1). We then plugged the TOY model to RoCoCau and tried some environmental stresses (water, carbon and light) applied on the same simple tree architecture with different responses capabilities (light-demanding, shade-tolerant, drought tolerant or not). Figure 2 shows optimal environment, water and light stresses applied on the same theoretical species. This situations result in different global plant sizes but also in different shoot/root balances. For each situation, we extracted data along simulations to show how much water,

light and carbon were collected and what was the consequence on growth rate change for both root and shoot compartments. It is then possible to monitor tree plasticity according to environmental change.

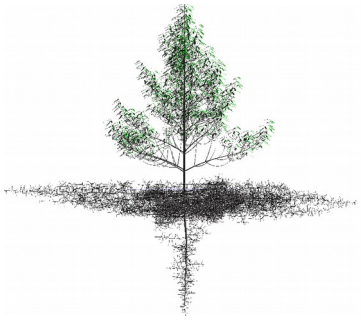

figure 1. « realistic» simulation(RoCoCau)

figure 2. same default plant species growing in optimal environment, with water stress and with light stress (RoCoCau+TOY)

The model has a good quantitative response in accordance to knowledge about tree plasticity. The proportion of root biomass is favored under drought conditions or more generally when trees grow on bad soil (Leuschner et al, 2001). In such stressed environment, stems show frequently a reduced leafy area (Kozlowsky & Pallardy 2002). In shade environment, trees invest more in leaf surface in order to increase light foraging capacity (Poorter & Nagel 2000). Simulations show a permanent balance of both root and shoot system with regulation of architecture and resource capture (leaves, fine roots) according to the species capabilities facing different environmental stresses.

For now, only an *in silico* study was carried out. It is now necessary to get field data to try TOY calibration. For this purpose some measurements are carried out into the FTC2 experimental device where 4 tropical species are grown in french Guyana. Tree individuals are regularly extracted and measured to feed a database used to train a neural network at TOY parameters calibration.

Conclusion

The simulation of the RoCoCau structural model linked with the TOY functional model allows to test hypothesis on tree plasticity facing environmental change. RoCoCau offers a good botanical accuracy at representing both shoot and root architectural dynamics. TOY includes main physiological processes to get water, light and carbon and to produce biomass that will be shared between the two compartments in a way that permanently controls the balance of their shoot and root foraging capabilities.

References

Barczi et al 2008, *Annals of Botany*, 101(8), 1125-1138, doi: 10.1093/aob/mcm194
Barczi et al 2018, *Annals of Botany,* 121(5), 1089-1104, doi: 10.0193/aob/mcy018
Kozlowsky & Pallardy 2002, *The Botanical Review*, 68(2):270-334, doi: 10.1663/0006-8101
Leuschner et al 2001, *Oecologia* volume 126, pages276–284, doi: 10.1007/s004420000507
Poorter & Nagel 2000, *Australian Journal of Plant Physiology*, 27, 595-607, doi: 10.1071/PP99173_CO

A modelling framework for the simulation of signal transport within 3D structure: application for the simulation of within-tree variability in floral induction in apple trees

Fares Belhassine[1,2], Damien Fumey[2], Christophe Pradal[1,3], Jérôme Chopard[2], Evelyne Costes[2], Benoît Pallas[1]

[1] *Université de Montpellier, UMR AGAP, INRA, CIRAD, Institut Agro, Montpellier, France*
[2] *ITK, Montpellier, France.*
[3] *CIRAD, Montpellier, France.*

For correspondence: benoit.pallas@inrae.fr

Keywords: flowering, architecture, signalling, fruit trees

Introduction

Organ development and meristem fate is partly determined by endogenous signals moving within plants. These signals (e.g. hormones, sugar…) originate from organs considered as sources (roots, leaves, seeds…) and act on meristems to trigger developmental processes such as transition toward flowering. Functional structural plant model (FSPM) are of major interest as they are based on an explicit description of plant architecture needed for simulating transports within plants. Transport or fluxes have been modeled in FSPM with a special consideration on carbon allocation (Génard et al., 2008). Approaches for simulating hormone fluxes are scarce, adapted to plant with simple architecture and usually associated with a comprehensive knowledge on the processes to be simulated (Prusinkiewicz et al., 2009); thus limiting their adaptability in various contexts. In this study, we present a generic model for simulating signal fluxes and their impact on meristem fates in complex 3D tree structure. We applied this model to the simulation of within tree variability of floral induction in the apple tree, as a first case of study. Previous experiments (Belhassine et al., 2019) showed that floral induction in meristems occurs less often in the presence of fruit whereas it is favoured by the presence of leaves. Furthermore, the influences of fruit and leaves on the floral induction of meristems depend on the distances of those organs within the tree structure. Fruit and leaves were thus assumed to be sources of inhibiting signals (possibly gibberellins from seeds) and activating signals (possibly FT protein), respectively. However, the distance at which these signals move within the structure and the relative sensitivity of the meristems to these signals are highly difficult to estimate from experimental studies, only.

Material and methods

The model uses libraries from the OpenAlea platform (Pradal et al., 2008). The model runs on 3D tree architectures coded in Multiscale Tree Graphs (MTG, Godin and Caraglio, 1999). It simulates transport of signals in both acropetal and basipetal directions and a decrease in signal quantity with the distances from the emitting sources. Making use of previous formalisms developed for carbon allocation models (Reyes et al., 2020), the decrease in signal quantity depends on the distance to the emitting source and an attenuation parameter (r) modulating the effect of distances. For r values close to 0, the signal is equally distributed among organs within the structure whereas it is transported at shorter distances when r increases. The amount of signal reaching each meristem then determines its probability to switch form a developmental stage to another This fate was determined with a sigmoidal function assuming two parameters, a transition parameter (t) and a shape parameter (v). t represents the amount of signal at which the probability of the meristem to switch to another developmental stage is equal to 50% and v represents the uncertainty in SAM fate for a given amount of signal.

The model was used for simulating within tree variability in floral induction in apple tree. Fruit were considered as sources of inhibiting signal and leaves as sources of activating signal. Both signals were combined to determine the occurrence of floral induction in each

shoot apical meristem of the tree. The model was calibrated on an original database of apple trees subjected to either leaf or fruit removal at different scales of plant organization (shoot, branch, tree) to modify the intensity of signals as well as the distances between the remaining leaves, fruit and meristems (Belhassine et al., 2019). 3D mock-ups built from digitizing data and measured floral induction in the different parts of the trees were confronted to model outputs for estimating the best combinations of parameter values. The model was validated on trees subjected both to leaf and fruit removal and to contrasted crop load conditions, testing two different functions to combine the impact of activating and inhibiting signals.

Results and Discussion

Simulations performed on simple hypothetical structures showed model consistency to simulate signal effects as well as the decrease in signal amount with distances and its distribution in branching systems. Calibrations performed on apple trees for simulating within tree variability were highly relevant (R^2>0.9 and RMSE <12%). Validations were consistent when simulations were compared to trees with contrasted crop load conditions but were of lower quality for trees subjected to both leaf and fruit removal. This is probably due to difficulties to combine the effects of inhibiting and activating signal. Analysis of parameter values give some clues about the physiological processes involved as the modelling approach allowed us to quantify the distances at which activating and inhibiting signals were transported as well as the sensitivity of the meristems to these signals when considered separately.

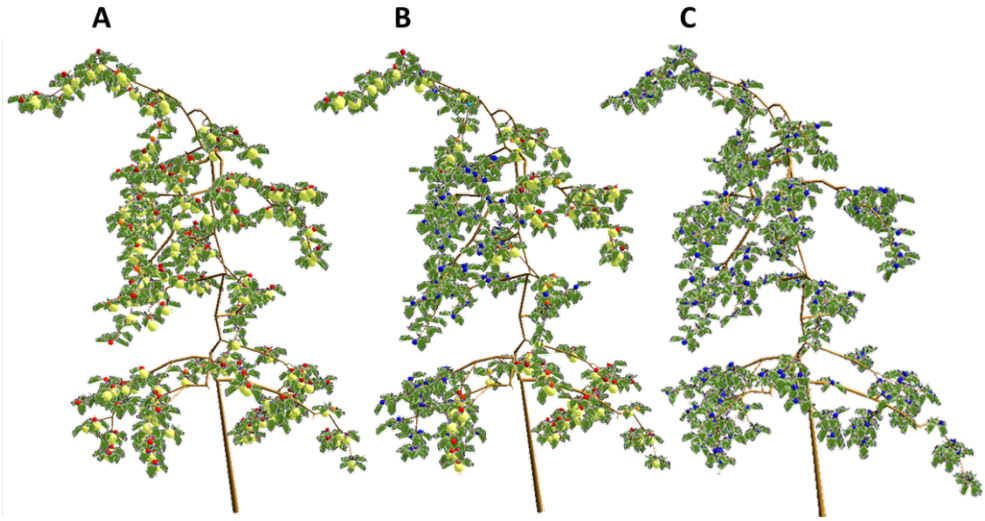

Figure: Simulation of floral induction variability in apple tree with different crop loads. A. High crop load, B. Fruit removal on half of the branches. C Low crop load (all fruit removed). Blue and red points are respectively induced and non-induced meristems.

Conclusion

The model uses MTG, a generic formalism adapted for representing all types of architectures, and simple assumptions that were compatible for simulating developmental switches such as floral induction in meristems in the apple tree case. It could be thus tested for exploring the consequences of tree architecture genetic variability on floral induction and fruiting behaviours. Experimental data are yet available and the model is currently used in this perspective.

References

Belhassine et al., 2019, *Front. Plant Sci.* 10:1233. doi: 10.3389/fpls.2019.01233
Génard et al., 2008, *Trees* 22: 269–282. doi: 10.1007/s00468-007-0176-5
Godin and Caraglio, 1999, *J. Theor. Biol.* 191: 1–46. doi:10.1006/jtbi.1997.0561
Pradal et al., 2008, *Funct. Plant Biol.* 35: 751–760. doi:10.1071/ FP08084
Reyes et al., 2020, *Ann. Bot. on press* doi: 10.1093/aob/mcz122

Testing leaf removal strategies and their effects on light absorption in virtual Riesling canopies (*Vitis vinifera* L.)

Christopher Bahr[1], Dominik Schmidt[1], Matthias Friedel[2], Katrin Kahlen[1]

[1] *Department of Modeling and Systems Analysis, Hochschule Geisenheim University, Geisenheim, Germany*
[2] *Department of General and Organic Viticulture, Hochschule Geisenheim University, Geisenheim, Germany*

For correspondence: christopher.bahr@hs-gm.de

Keywords: Virtual Riesling, leaf removal, FSPM, light interception, bunch zone

Introduction

Leaf removal is common practice in viticulture to control environmental and physiological conditions of grapevines. This management practice is applied to improve spray penetration, bunch compactness and fruit quality by changing the microclimate and light conditions. Depending on the desired outcome, approaches differ in timing, severity and location of leaf removal (e.g., VanderWeide et al. 2020) and there can be positive or negative effects on the berry's health status such as reducing disease infection or increasing berry sunburn (Chorti et al. 2010). The aim of this study was to use the model *Virtual Riesling* (*ViRi*) to show first steps towards testing different defoliation practices *in silico*. *ViRi* is a functional-structural plant model that simulates the growth of Riesling plants based on temperature and descriptive growth functions (Schmidt et al. 2019). Thus, we implemented a defoliation method and a light model in *ViRi* to compare light absorptions resulting from different defoliation strategies in virtual Riesling.

Materials and Methods

We run this study with *Virtual Riesling* with temperature data of the year 2018 in Geisenheim, Germany. Virtual vines were trained to a vertical shoot positioning (VSP-type) trellis system with four catch wires and the cane was trained 0.7 m above ground. Row orientation was north to south (Schmidt et al. 2019). For light simulations, we used a light model based on an approach from Evers and Bastiaans (2016), adjusted to the location. The light interacted in simulations with the virtual leaves according to their light properties taken from literature.
Here, we wanted to apply two different defoliation methods *in silico* and to compare their effects on light absorption in the virtual Riesling canopies. Therefore, we applied virtual leaf removal in two different vertical zones of the canopy. In scenario one (S1) leaf removal included the bunch zone. In scenario two (S2) we removed leaves above the bunch zone. Further, we applied defoliation only on the east side of the canopy as suggested by local experts.
In order to contrast light absorption in the two scenarios, we wanted to remove preferably the same potential light absorption in both zones. A preliminary analysis revealed that the first two leaves above the bunch zone intercepted nearly the same light as the first four leaves above the cane (at phenological stage of blooming). Thus, we implemented a method for defoliation, which removed on average four leaves in S1 and two leaves in S2 along the row and per shoot. In S1, the method removed leaves between 0.7 m (height of cane above ground) and 1.1 m and in S2 between 1.1 m and 1.4 m.
The application day of defoliation was the locally estimated phenological stage "end of blooming" in 2018 (5th of June). The current version of *ViRi* allows for canopy simulations until three weeks after this date. For the analysis, we run 25 simulations of a 70-plants-vineyard for each defoliation method and for one control without leaf removal. Analyzing the non-border plants resulted in 1000 plants per scenario.

Results and Conclusion

The graph shows that on application day both scenarios of leaf removal caused a decrease in light absorption on the east side of the canopies. However, canopies, where leaves were removed above the bunch zone (dotted green line), absorbed more light than the canopies, where leaf removal included the cane (dotted blue line). That is because below the cane there were only a minute number of leaves growing, which could have intercepted radiation at all (Schmidt et al. 2019).
A similar effect can be observed on the west part of the canopies in both defoliation scenarios (solid green and blue lines). Since leaves were removed only on the east side, leaves in the west intercepted slightly more light than the control (red lines). Moreover, the canopies treated above the bunch zone (S2, solid green line) absorbed more light than those of S1 (solid blue line) for the same period. As already discussed for the east side of the canopies, in scenario two there were more leaves growing below the treated zone and therefore more light was intercepted in this scenario.
In addition, both treatments tended to converge to the control. The reason is that secondary leaves evolve and grow over time, filling up the gaps in the canopies caused by leaf removal.
In summary, differences of light absorption between both scenarios depended mostly on the number of leaves intercepting light below the zones where leaves were removed. Only a small effect of east side leaf removal on west side light absorption was observed.
The simulations showed that the extended *Virtual Riesling* is capable to simulate leaf removal practices and their effects on light interception. We conclude that a further developed *ViRi* could be a powerful tool to test management practices *in silico* and therefore support elaborate field experiments.

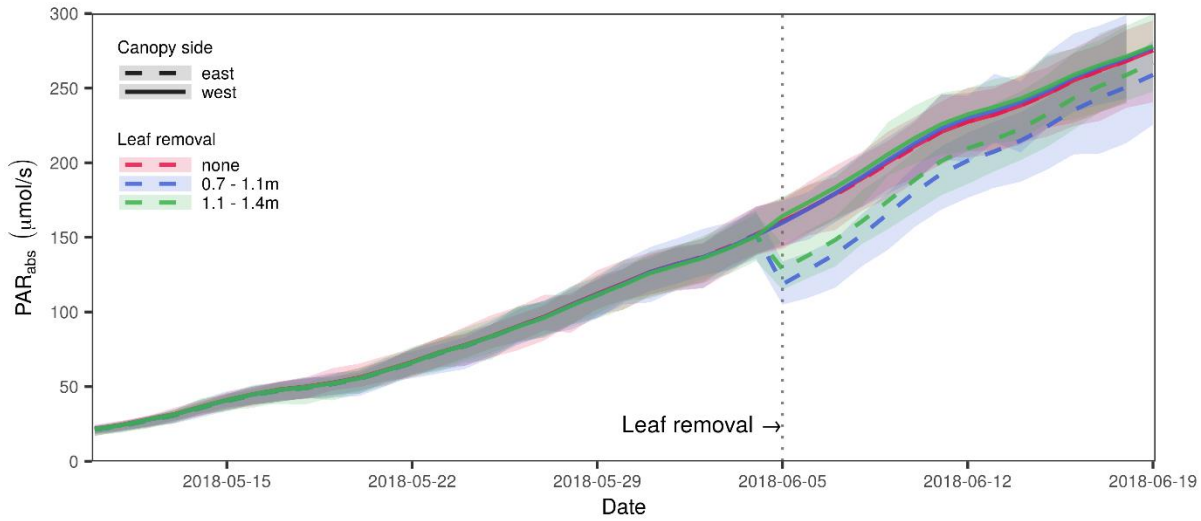

Figure: Average daily sum of PAR_{abs} of a vine and the 95% highest density interval for three east side treatments. Absorption curves are separated into east and west side of canopies: control (red) with no leaf removal; treatment including bunch zone (blue) with leaves removed between 0.7 m (cane) and 1.1 m; treatment excluding bunch zone (green) with leaves removed between 1.1 m and 1.4 m.

References

Chorti et al., 2010. *Am. J. Enol. Vitic.* 61(1), 23-30.
Evers and Bastiaans, 2016, *J. Plant Res.*, 129:339-351, doi: 10.1007/s10265-016-0807-2
Schmidt et al., 2019, *Agronomy* 1-29, doi: 10.3390/agronomy9080426
VanderWeide et al., 2020, *Am. J. Enol. Vitic.* 71(1): 70-79, doi: 10.5344/ajev.2019.19042

Benchmarking Root and Soil Interaction Models exemplified with CPlantBox and DuMu^x

Daniel Leitner[1], Andrea Schnepf[2], Bernd Flemisch[3], Timo Koch[3], Jan Vanderborght[2], Harry Vereecken[2]

[1] *SimWerk, Humboldtstrasse 40, Linz, Austria*
[2] *Institute of Bio- and Geosciences Agrosphere (IBG-3), FZ Jülich, Germany*
[3] *Institute for Modelling Hydraulic and Environmental Systems, University of Stuttgart, Germany*

For correspondence: daniel.leitner@simwerk.at

Keywords: mathematical modelling, water movement, sink term development, model testing

Introduction

Complex models of root architecture and function can increase our fundamental understanding of crop growth and function, and therefore will improve agricultural management strategies as well as root trait selection in plant breeding.

However, the analysis of such models is difficult. The variety of modelling approaches describing various processes lead to disagreement between the models. This discrepancy emerges from different root architecture development as well as different definitions of sink terms describing water and solute uptake.

In Schnepf et al. 2020 various research groups developed a systematic framework for benchmarking individual components of any root functional models. These components are root architecture, water flow and solute transport in soil and roots. For water movement and solute transport numerical aspects are of main interest, but also modelling aspects like the description of sink terms are analysed. Root architecture development is compared at a conceptual level as different models do not have a common process representation. Therefore, modelling results are compared to experimentally observed reference root systems.

Materials and Methods

Splitting root functional models into simpler sub components enables precise testing, quantitative inter-model comparisons as well as analysis of single common processes. We demonstrate the different benchmarks by applying them to the root growth model CPlantBox (formerly called CRootBox, Schnepf et al. 2018) for root architectural development and DuMu^x (Flemisch et al. 2011) as porous medium solver for water flow and solute transport in both soil and roots.

First, we benchmark the soil model using an infiltration and an evaporation benchmark as presented by Vanderborght et al. 2005. Next we benchmark water flow within roots assuming a static soil, for a single root and and root system using the exact analytical solution proposed by Meunier et al. 2017. Finally, we couple the soil model and root water movement model, and test it first for a small static root system, and then for a growing one.

Conclusions

Results of root architectural benchmarks help to interpret differences found in water and solute transport and uptake. Therefore, benchmarking will lead to greater confidence, and helps to avoid that future work is based on accidental results caused by bugs, numerical errors or conceptual misunderstandings. We encourage other plant functional modellers to join this benchmarking effort. Therefore, the benchmark scenarios are presented in Jupyter

Notebooks for easy accessibility and transparency (https://github.com/RSA-benchmarks/collaborative-comparison) and will set a standard for future model development.

References

Schnepf et al. 2020, *Front. Plant Sci.*, doi: 10.3389/fpls.2020.00316
Schnepf et al. 2018, *Annals of Botany 121*, doi: 10.1093/aob/mcx221
Flemisch et al. 2011, Advances in Water Resources 34, doi: 10.1016/j.advwatres.2011.03.007
Vanderborght et al. 2005, *Vadose Zone Journal 4,*doi: 10.2136/vzj2005.0206
Meunier et al. 2017, *Applied Mathematical Modelling* 52, doi: 10.1016/j.apm.2017.08.011

Simulating rhizodeposition as a function of shoot and root interactions within a new 3D Functional-Structural Plant Model

Frédéric Rees[1], Romain Barillot[2], Marion Gauthier[1,3], Loïc Pagès[4], Christophe Pradal[5,6], Bruno Andrieu[1]

[1] *Université Paris-Saclay, INRAE, AgroParisTech, UMR ECOSYS, F-78850 Thiverval-Grignon, France*
[2] *INRAE, UR P3F, F-86600, Lusignan, France*
[3] *ITK, avenue de l'Europe, F-34830 Clapiers, France*
[4] *UR 1115 PSH, INRAE, Site Agroparc, Avignon, France*
[5] *AGAP, CIRAD, INRAE, Montpellier Sup Agro, Univ Montpellier, France,*
[6] *CIRAD, AGAP and Inria, Zenith, Univ Montpellier, France*

For correspondence: frederic.rees@inrae.fr

Keywords: FSPM, wheat, exudation, carbon allocation, ArchiSimple, CN-Wheat

Introduction

Rhizodeposition, *i.e.* the release of organic materials by roots, represents a significant portion of plant's carbon (C) budget, ranging from 5% to 15% of net photosynthesized C (Pausch and Kuzyakov, 2018). Various rhizodeposits can be released by roots, *e.g.* soluble exudates, secreted mucilage, sloughed cells, or volatile organic compounds. Despite their short lifetime, some of these products have been shown to favor plant growth, *e.g.* by increasing water and nutrient uptake. Among rhizodeposition processes, exudation has been suggested to depend on the concentration of carbohydrates inside the roots (Personeni et al., 2007). However, rhizodeposition not only depends on the availability of C in the roots, but also on the architecture of the root system, and many have shown that rhizodeposits are more concentrated in specific areas, such as root tips. Consequently, a Functional-Structural Plant Model (FSPM) would theoretically represent the best framework for simulating the spatial and temporal dynamics of rhizodeposition, as it can describe the evolution of both the metabolism and the architecture of the plant. The objective of this work is to create such a framework by coupling a whole-plant FSPM, a 3D root architectural model, and a new model simulating rhizodeposition.

Modelling approach

Our strategy has been to combine the FSPM *CN-Wheat* (Barillot et al., 2016), which describes the main processes of C and nitrogen (N) acquisition and transformation by an individual wheat plant and the 3D growth and development of its aerial organs, with the model *ArchiSimple* (Pagès et al., 2014) that simulates the development of the 3D root architecture for a range of plant species, and the new model *RhizoDep*, which calculates a full C balance in each part of a root system in order to simulate local rhizodeposition fluxes. The complementarity of the three models is illustrated in Figure 1: i) *CN-Wheat* is used to calculate the amount of C allocated from the shoots to the roots, ii) *ArchiSimple* provides the 3D structure of the root system, and iii) *RhizoDep* distributes the C provided by the shoots within the 3D root system and simulates the actual growth, respiration and rhizodeposition of each root element based on C availability. The major link between the three models lies in the exchange of C between aboveground and belowground tissues, which is driven by gradients of sucrose concentration in the different compartments of the plant.

Preliminary results & short-term perspectives

The coupling of the three models has been started using the *OpenAlea* platform and its *Multiscale Tree Graph* formalism (Pradal et al., 2008). First simulations were done using the allocation of C to the roots simulated by *CN-Wheat* as an input to the root model based on the effective coupling of *ArchiSimple* and *RhizoDep*. These simulations show how rhizodeposition is intrinsically dependent on the architecture of the root system and on the total amount of available C. For completing the coupling, several issues still need to be

tackled, *e.g.* how N uptake and metabolism should be spatialized in a 3D root system, how it may be regulated by local C and N availability, and how rhizodeposition can modify soil N availability. However, this modelling approach has already led to a first prototype able to simulate rhizodeposition processes on a dynamic, 3D root system that is fully integrated within the functioning of the whole plant. Its refinement will offer unique opportunities to study the possible link between rhizodeposition and the environmental factors affecting plant growth, *e.g.* atmospheric CO_2 concentration or soil N availability.

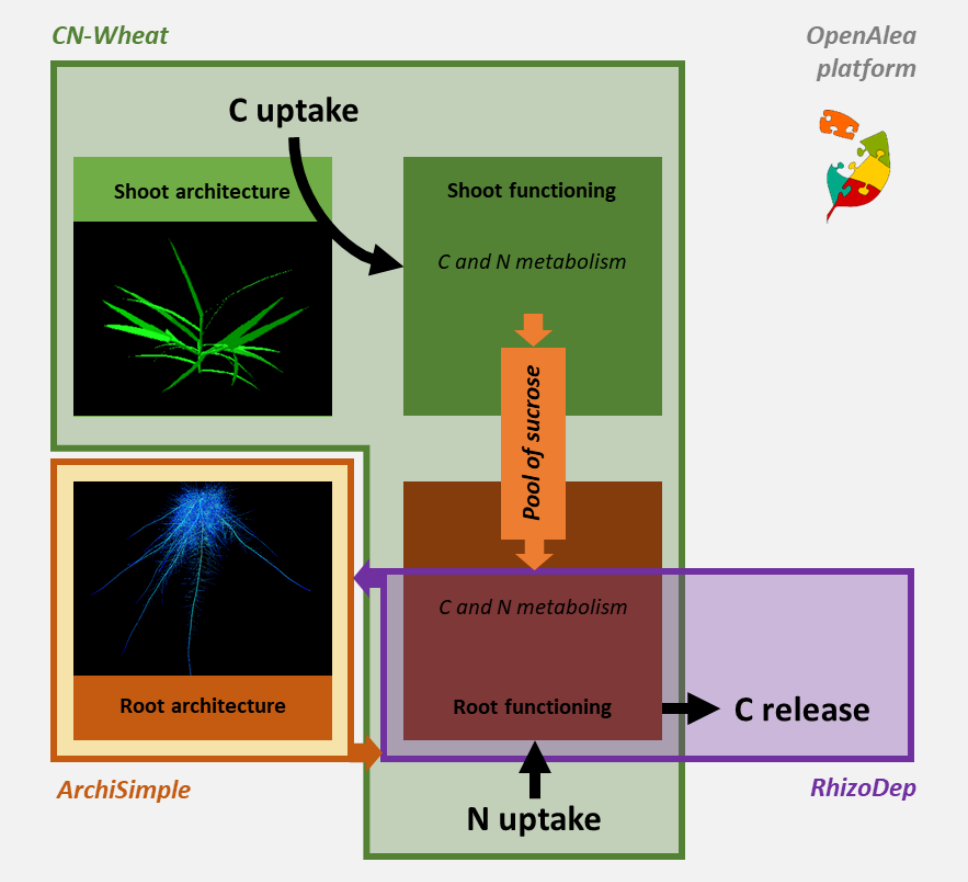

Figure 1: Modelling approach for simulating carbon rhizodeposition within a 3D plant model

References

Barillot et al., 2016, *Annals of botany* 118(5): 997-1013, doi: 10.1093/aob/mcw143
Pagès et al., 2014, *Ecological Modelling* 290: 76-84, doi: 10.1016/j.ecolmodel.2013.11.014
Pausch and Kuzyakov, 2018, *Global Change Biology* 24:1–12, doi: 10.1111/gcb.13850
Pradal et al., 2008, *Functional Plant Biology*, 35(10), 751-760. doi: 10.1071/FP08084
Personeni et al., 2007, *Journal of Experimental Botany* 58:2091–2099, doi: 10.1093/jxb/erm065

Phenotypic traits extraction and plant type classification with 3D point clouds for field grown sugar beet through growth seasons

Honghong Chai[1], Ke Shao[2], Chao Yu[2], Jinwang Shao[2], Ruili Wang[2], Yang Sui[2], Yan Guo,Yuntao Ma[1]*.

[1] North China Key Laboratory of Arable Land Conservation, Ministry of Agriculture, College of Land Science and Technology, China Agricultural University, Beijing 100193, China
[2] Inner Mongolia Key Laboratory of Molecular Biology of Characteristic Plants, Inner Mongolia Institute of Biotechnology, Huhhot 010070, China

**For correspondence. E-mail yuntao.ma@cau.edu.cn*

- Sugar beet is one of the main crops for sugar production in the world. With the increasing demand for sugar, more desirable sugar beet genotypes need to be cultivated through plant breeding programs. Sugar beet with different genotypes have great differences in the morphological traits both for root and shoot part. Morphological variations in shoot and root traits are key determinants in unraveling phenotypic diversity for sugar beet plant. In recent years, the development of image-based 3D reconstruction technology provides an opportunity for high-throughput phenotyping analysis. This study was designed to develop an automatic pipeline to quantify phenotypic traits of beet root and shoot. Sugar beet with 207 genotypes were selected as experimental materials. Multi-view images were obtained by moving mobile phone around root and shoot part separately. Three-dimensional point clouds were reconstructed from images using structure from motion method. An automatic data processing pipeline was developed to process point clouds of sugar beet.
- Based on the 3D point clouds of shoot part, data processing includes: preprocessing, coordinates correction, filtering and segmentation of point cloud of individual plant. Random Sample Consensus (RANSAC) algorithm was adopted to correct the coordinates of point cloud as z-axis perpendicular to the ground. We selected G minus R (G-R) as color filter to eliminate soil and shadows points from plant. In the processing of segmentation of individual plant, The region-growing algorithm was utilized to segment plant into individual leaves initially and then clustering based on Euclidean distance was used to improve the quality of segmented leaves. Phenotypic traits were automatically extracted regarding plant convex hull volume, concave hull volume, height, width in-row, width across-row, total leaf area and individual leaf length and maximum width. Total leaf area and convex hull volume were adopted to explore the relationship with biomass. The results showed that high correlations were found between measured and estimated plant height, and total leaf areas with $R^2 > 0.8$.
- Based on 3D point clouds of beetroot, ten phenotypic parameters describing the morphological characteristics of beetroots were extracted: maximum diameter, root length, convex hull volume, top projection area, compactness, convex index, convex angle, distal root end ratio, proximal root end ratio and root taper index. There was a good agreement between measured and calculated maximum diameter and root length with $R^2 > 0.95$. The K-medoids clustering algorithm with high stability was used to classified the beetroot into four categories. The better beetroot type was recommended with medium root length and moderate proportion, based on the combination of phenotypic traits and experts' knowledge. We took the categories adjusted by the experts as the true values and chose five prediction models to discriminate beetroot type. The five models include linear discrimination, random forest, support vector machine, decision tree, and naive Bayes. The results showed that the prediction accuracies of the five models were above 70%. Accuracy of random forest reached up to 82%.
- The pipeline proposed in this study can perform well for estimating plant phenotyping in the field, provide a basis for selection of high-quality beet varieties and help to find varieties suitable for mechanized production.

Keywords: shoot; root; image-based; machine learning

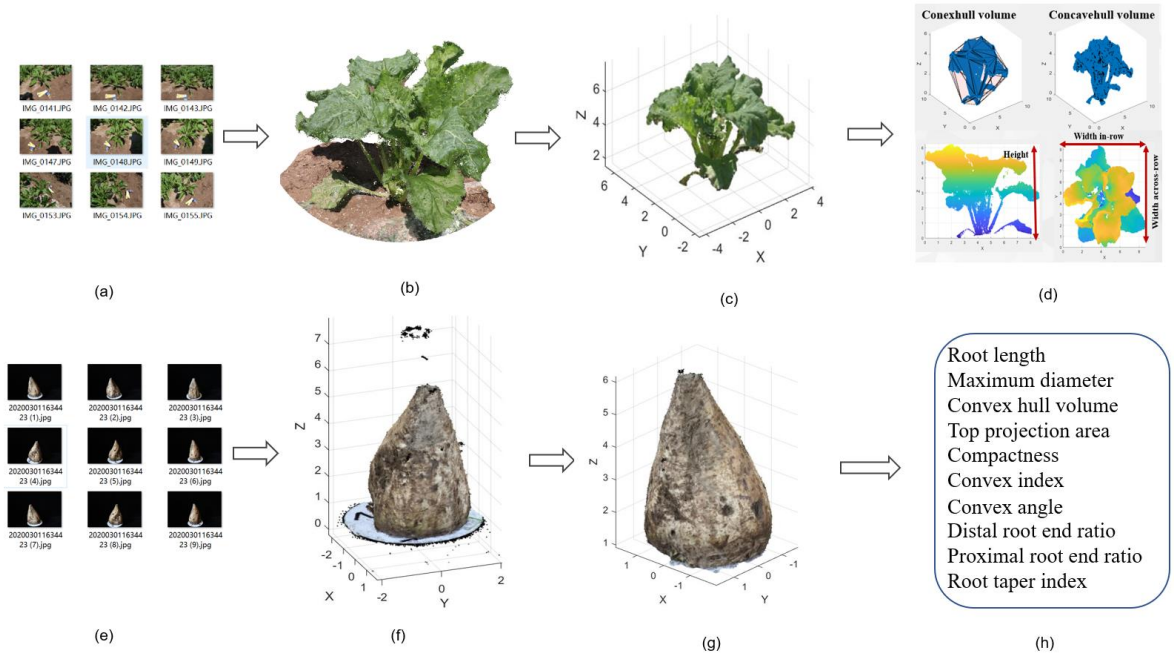

Fig. 1 Data process flow for shoot and root of sugar beet plant: (a) Multi-view image dataset of beet shoot in field; (b) Reconstructed point clouds of beet shoot; (c) Point clouds of beet shoot removed ground plane; (d) Phenotypic traits including conexhull volume, concavehull volume, height and width, invidiual leaf length and miaximum width etc; (e) Multi-view image dataset of beet root; (f) Reconstructed point clouds of beet root; (g) Denoised 3D point clouds of beet root; (h) Beetroot phenotypic traits.

References

Tsialtas J T, 2010, Maslaris N, Sugar Tech, 47-52. doi:10.1007/s12355-010-0009-5.
Stevanato P, Chiodi C, Broccanello C, et al., 2019, Sugar Tech, 1-14. doi:10.1007/s12355-019-00734-9.
Monteiro F, Frese L, Castro S, et al., 2018, Frontiers in plant science, 74-82. doi:10.3389/fpls.2018.00074.
Nankar A N, Tringovska I, Grozeva S, et al., 2020, Plants, 197-218.doi:10.3390/plants9020197.
Guan H, Liu M, Ma X, et al., 2018, Remote Sensing, 1206-1226. doi:10.3390/rs10081206.

A model for maize leaf elongation and ontogeny under drought stress

Jonas R. Coussement*[1], Selwyn Villers[1,2], Hilde Nelissen[2], Dirk Inzé[2], Kathy Steppe [1]

[1] *Ghent University, Faculty of Bioscience Engineering, Laboratory of Plant Ecology, 9000, Ghent, Belgium*

[2] *Flemish Institute for Biotechnology (VIB), Technologiepark 71, 9052 Zwijnaarde*

For correspondence: Jonas.Coussement@UGent.be

Keywords: FSPM, leaf elongation, ontogeny, drought, turgor, growth, stress

Introduction: One of the major limiting factors of maize yield worldwide is drought stress, a factor which is expected to only increase due to a changing climate. A correct understanding of the maize drought response is therefore crucial, as it affects many processes within the plant. One of the key processes impacting growth is maize leaf elongation, yet there is currently no available model which incorporates the effect of water limitations on the different expansion zones within the leaf. Hence, we propose to introduce turgor-driven limitations on growth and cell differentiation in the leaf elongation model by Durand *et al.* (1999) as a method to study the effect of drought during the different stages of leaf expansion. The leaf elongation model by Durand *et al.* (1999) describes the progression of three distinct cellular zones within a grass leaf, based on a combination of individual cell division, elongation, and cell differentiation from one zone onto the next. This behaviour is captured with fixed factors of relative elongation rate (RER) and time-dependent differentiation rates. In reality, however, data shows an impact of drought stress on the elongation rates, the differentiation rates and also the elongation and differentiation duration.

Materials and methods: A model was developed to represent a single developing leaf positioned at the top of a minimalistic representation of plant structure, which was necessary to realistically emulate plant hydraulics and the impact of whole-canopy transpiration. The developing leaf is initiated as a cluster of division zone cells. This zone expands and differentiates according to the rules established in Durand *et al.* (1999) and by extension Fournier *et al.* (2005). However, the dependency of leaf elongation and cell differentiation rates on drought stress was incorporated by introducing the Lockhart (1965) equation, which describes the cell growth in terms of turgor pressure, in each zone. Furthermore, the concept of turgor time was introduced in order to include a dependency of drought stress on the growth and differentiation durations of the different cell zones. The model was fitted on kinematic data of control and drought stressed maize plants to evaluate model performance.

Results and discussion: Theoretical simulations showed the models ability to simulate the diurnal patterns in maize leaf elongation rate which can be observed in the field. A reduction in water availability was shown to interfere with the ability of the leaf to establish sufficient turgor. Lower turgor pressure slower down the progression of the differentiation parameters in the model due to the introduced concept of turgor time, which allowed leaves of drought stressed plants to grow slower but longer with the same parameter set. This concept was shown to coincide with data of leaf elongation under a drought treatment. As a result, this is an important step towards expression leaf elongation with environmentally insensitive parameters which can still capture differences in drought treatments. The model is built in such a way that it simulates the progression of leaf turgor, and thus expansion rate, in terms of sap flow and transpiration. As a result, it is compatible for application in full plant models, such as functional-structural plant models, which aim at incorporating water limitations on plant growth.

Conclusion: A maize leaf expansion model is proposed which combines the contribution of water availability, cell wall kinetics, and leaf ontogeny. This model can aid in studying the fundamental effects on drought stress severity and timing on leaf expansion rate. Alternatively, the parameters within the model would allow insight in which plant characteristics are most associated with drought-stress mitigation in terms of leaf expansion rate.

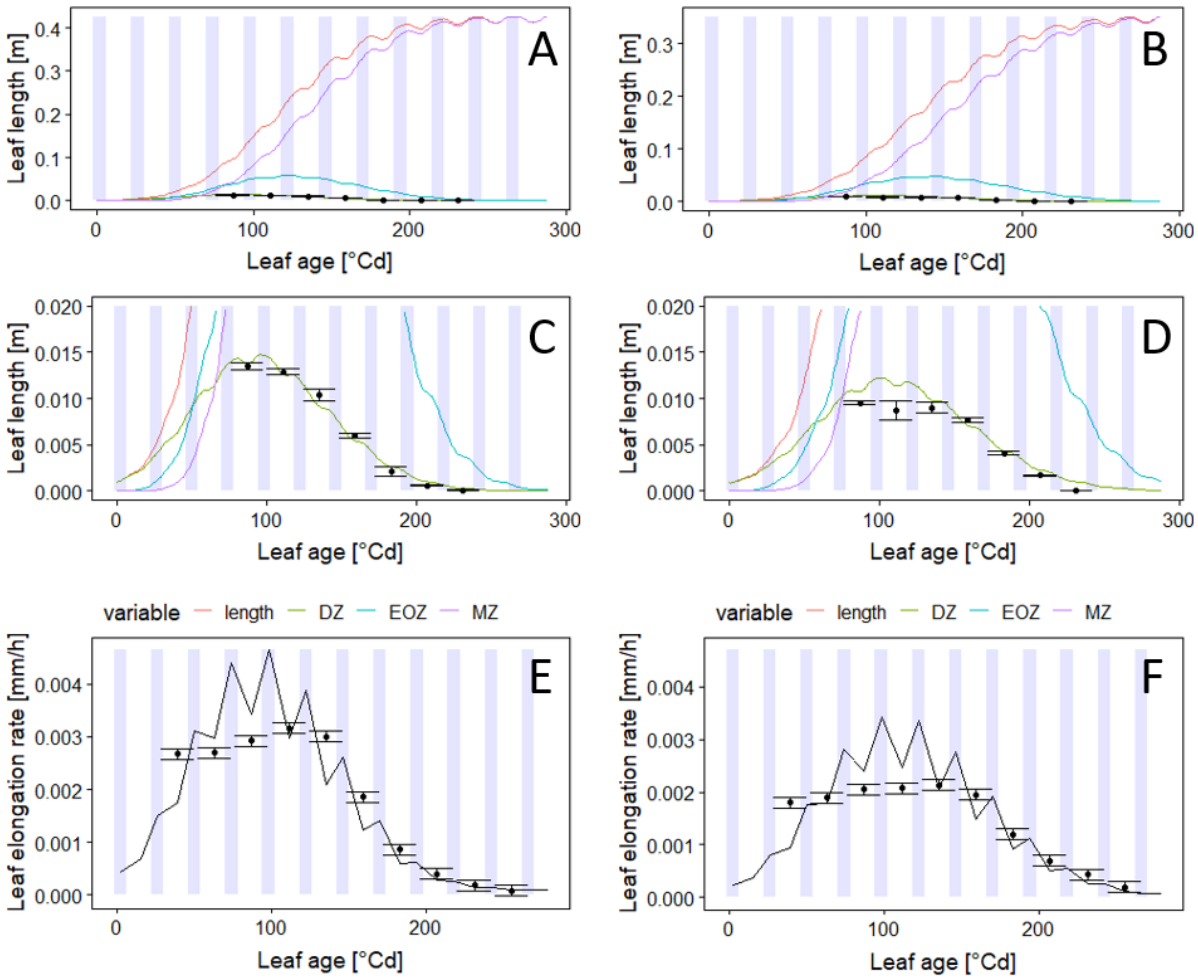

Figure: A and C) Progression of the leaf expansion model in terms of total leaf length and the respective length of the division zone (DZ), elongation-only zone (EOZ), and mature zone (MZ) in the leaf in a control treatment (lines), plotted alongside measurements of DZ length (points). B and D) Model simulation of the calibrated model parameters on the control treatment but under light drought stress (lines), plotted alongside measurements of DZ length (points). E and F) Differences in simulated leaf elongation rates, averaged for every day and night period (lines) alongside measurements (points) for both treatments. Diurnal patterns of shrinkage and expansion are the result of a daily transpiration patterns which correspond to water loss within the leaf, which, in turn, results in a loss of turgor pressure and consequently elastic shrinkage.

References:

Durand et al., 1999, *Annals of Botany* 577-588, doi: 10.1006/anbo.1999.0864

Fournier et al., 2005, *New Phytologist* 881-894, doi: 10.1111/j.1469-8137.2005.01371.x

Modelling the effect of traits related to plant architectural development on wind-dispersed crop disease development

Katarina Streit[1], Jochem B. Evers[2], Michael Henke[3], Michael Renton[1]

[1] *Schools of Biological Sciences, Agriculture & Environment, The University of Western Australia, Crawley, Australia*
[2] *Centre for Crop Systems Analysis, Wageningen University, Wageningen, The Netherlands*
[3] *Leibniz Institute of Plant Genetics and Crop Plant Research (IPK), OT Gatersleben, Stadt Seeland, Germany*

For correspondence: katarina.streit@gmail.com

Keywords: FSPM, wind dispersal, yellow spot, tan spot, wheat, host-pathogen interactions, GroIMP

Introduction

Manipulation of plant architecture plays a role in decreasing disease severity, by creating unfavourable conditions for disease development, and is often related to changes in canopy microclimate (Ando *et al*., 2007). Virtual plants or functional-structural plant (FSP) models, used in host-pathogen models have been suggested as the key approach to study the dynamics of plant-pathogen-environment interactions, as they include a detailed 3D representation of plant, and into various extend plant development and growth, as well as environmental factors. Recent modelling studies have shown that traits related to plant architecture and development, can help protect crops from rain-borne diseases (Vidal *et al*., 2018; Robert *et al*., 2018). The aim of this study was to use a modelling approach to analyse potential impact of plant architecture and development, further referred to as plant architectural development, for wind-dispersed diseases.

Materials and methods

To address the study aim, we developed a host-pathogen model for yellow spot (also known as tan spot) on wheat, an important foliar wheat disease in Australia, caused by a necrotrophic fungus *Pyrenophora tritici repentis*. The model combined 3 components, all driven by weather data: (i) a dynamic functional-structural plant (FSP) model for cereal crops (Evers and Bastiaans, 2016), adapted to wheat, (ii) a spatially-explicit wind dispersal model (acc. to Calonnec *et al*., 2008; Garin *et al*., 2014), and (iii) a disease model for yellow spot, with focus on the pathogenesis stage (infection by spores and latency period). Hourly weather data were obtained from a weather station in South Perth, Western Australia, for the growing season in 2016 (May 23 till October 25). To consider the difference in dynamics of host and pathogen processes, the time step for disease model was one hour while the time step for spore dispersal, as well as plant growth was one day. The reference canopy consisted of 60 plants, with plant population density of 160 plants m^{-2}. The disease model calculation started with the primary infection of a seedling. The secondary infection repeated multiple times during the simulated growing season. The continuous progression of secondary infection was calculated as a cumulated combined response to temperature and leaf wetness duration. For an infection to be successful, 6 hours of suitable conditions were required. Additionally, we computed infection efficiency (a proportion of deposited spores that will cause new infection) as a combined response to weather conditions and actual infection progression, i.e. the effect of weather on spore loss was higher directly after spore deposition. We considered spore loss by wash off (caused by rainfall) and by desiccation (caused by low humidity). On infected leaves, after fixed latency period, new spores were produced. Spores were dispersed in the direction of wind inside a virtual cone. Spore deposition on available green leaf segments was calculated, using an exponential model for dispersal gradient. Deposited spores that survived and caused new infection were the start of the next infection cycle. The model was implemented in the modelling platform GroIMP and parameterized using reasonable values from literature. We conducted virtual experiments for three parameters: phyllochron, leaf length-width ratio, and internode

elongation factor, which were reported to have effect on disease progression of rain-borne Septoria tritici blotch (STB) in wheat (Robert *et al*., 2018). For each experiment, we analysed the effect of varying one parameter on disease levels, while keeping others constant, with 10 replications for each combination to help account for stochasticity. We performed statistical analysis after day 80 and 110 of each simulation, using R.

Results and discussion

Simulations revealed that phyllochron (Fig. 1a) had more impact on changes in total diseased area, than the selected architectural traits. There was a negative effect of internode elongation factor on total diseased area (reduced disease with longer internodes; Fig. 1b). The impact of phyllochron and internode elongation was similar as reported for STB. However, modifications in leaf-width ratio had no significant effect on reduction in total diseased area (Fig. 1c). We observed variability in the impact of traits (results not shown), attributed to the stochastic behaviour of the model, parameterisation of the dispersal model, and feedbacks between plant architecture, development and growth. Further analysis of simulated outputs for plant development and growth will be necessary, to give more insights into the interactions between plant and disease development. Future modelling work should focus on 1) including additional traits related to plant architectural development, which are also known to have impact on photosynthesis and yield in wheat, into the simulation study, 2) analysing whether the impact of plant architectural development in wind-dispersed diseases depends on the choice of dispersal model, and 3) extrapolating our approach to the concept of 'infinite' canopies in FSP models.

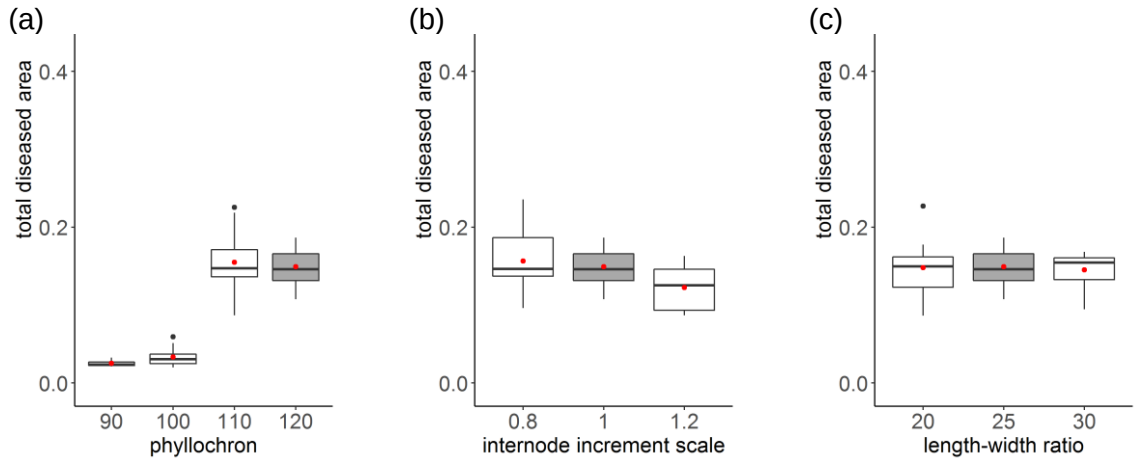

Figure 1: Total diseased area in the reference canopy after 80d (grey bar – control architecture, red dot – mean value): (a) for 4 values of phyllochron, (b) internode elongation factor (with +/- 20% of the control value), (c) length-width ratio (with +/- 20% of the control value).

References

Ando *et al*., 2007, *CAB Reviews: Perspectives in Agriculture, Veterinary Science, Nutrition and Natural Resources* 2: No. 026, doi: 10.1079/PAVSNNR20072026

Calonnec *et al*., 2008, *Plant Pathology* 57, doi: 10.1111/j.1365-3059.2007.01783.x

Evers and Bastiaans, 2016, *Journal of Plant Research* 129, doi: 10.1007/s10265-016-0807-2

Garin *et al*., 2014, *Annals of Botany* 114, doi: 10.1093/aob/mcu101

Robert *et al*., 2018, *Annals of Botany* 121, doi: 10.1093/aob/mcx192

Vidal *et al*., 2018, *Annals of Botany* 121, doi: 10.1093/aob/mcy024

High-precision 3D segmentation of plants combining spectral clustering and quotient graph techniques: a multi-level approach.

Katia Mirande[1,2], Franck Hétroy-Wheeler[2], Christophe Godin[1]

[1] *Laboratoire Reproduction et Développement des Plantes, University of Lyon, ENS de Lyon, UCB Lyon 1, CNRS, INRAE, Inria, F-69342 Lyon, France*
[2] *ICube CNRS, University of Strasbourg, Strasbourg, France*

katia.mirande@inria.fr, hetroywheeler@unistra.fr, christophe.godin@inria.fr

Keywords: Fiedler vector, phenotyping, energy minimization, prior knowledge

Context

Methods for phenotyping plant architectures have progressed rapidly in the recent years. Using digitizing techniques, like photogrammetry or Lidar, they aim to reconstruct the geometry and topology of plant organs from 3D point clouds. Depending on the agronomic or biological context, the plant species, and the acquisition system, various computer pipelines have been developed to achieve this task and produce segmentations identifying plant organs in the point clouds. While global geometric traits can be extracted successfully with these methods, and organ position and form can be estimated, extracting automatically and accurately local geometric traits of biological relevance, such as internode length, branch insertion angles, or angles between consecutive organs, is still largely an open issue (Paulus, 2019). Automatically measuring these complex traits first require high precision clustering to obtain results accurate enough to be relevant for botanical analysis.
Here we address this problem by using a combination of spectral clustering to find relevant clusters in the point cloud and quotient graph-based energy minimization approach to refine the clusters using *a priori* botanical knowledge.

Method

We assume that a dense 3D point cloud representing the observed plant geometry has been produced by some upstream algorithm (e.g. from a series of 2D photographs using space carving method for example Scharr et al., 2017). Our goal is to develop a robust classification strategy to identify the different organs in point cloud data and to derive faithful information about the plant topology and geometry.

Our approach proceeds in the following steps.
Step 1: Spectral analysis of the point cloud: from the 3D point cloud we first reconstruct a classical riemannian graph, representing 3D points as vertices and connecting them by edges to their nearest neighbors. Then, following Hétroy-Wheeler et al., 2016, we compute the eigen-decomposition of the Laplacian. We show that the gradient of the vertex values corresponding to the second eigen-vector (known as the Fiedler vector) provides a number of key features characterizing the different organs.

Step 2: Construction of a quotient graph: We then perform a first clustering using these gradient features. To do so, we use a standard unsupervised classification algorithm (e.g. agglomerative clustering or K-means). Connected components of the same classes are then extracted and used to build a quotient graph, where nodes represent connected components, and edges their adjacency relations inferred from the adjacency relation of their vertex components. This produces a much smaller graph which reflects the structure of the riemannian graph, at a macroscopic scale (Sanders and Schulz, 2011). This quotient graph provides a first rough representation of the plant structure.

Step 3: Refinement of the quotient graph by energy minimization: This first segmentation is then refined by local adjustments at point level. For this, following Pott's-based segmentation (Guinard and Landrieu, 2017) approaches, we define an energy on the quotiented riemannian graph. This energy is the sum of energy quanta associated with each vertex or with edges (reflecting an interaction energy between vertices). Interestingly, these energy quanta can be defined according to various criteria, topological, geometrical or botanical, and can be used to include high-level knowledge in our segmentation refinement algorithm. For instance, as the quotient graph ultimately represents the architecture of the plant, it should be a tree. As a consequence, the vertices represented by nodes that are part of a cycle or have more than one parent in the quotient graph will be of higher energy. This is a way to detect and correct cases in which two different leaves have been merged. We then use a stochastic procedure (in the family of simulated annealing algorithms) to progressively evolve the segmentation at point level in order to minimize the system's total energy.

Results, discussion & future works

Our study focuses a set of plant species (tomato plant, *Arabidopsis thaliana* and *Chenopodium album*). Figure 1 illustrates our segmentation method on *Chenopodium album*. As can be observed, the gradient norm alone allows to discriminate accurately leaves from the rest of the plant. The figure shows also the quotient graph constructed at a more macroscopic level from the segmentation resulting from step 2 and before energy optimization.
In the presentation, we will show how to exploit the quotient graph structure and its energy definition to inject a priori knowledge about the studied plant so as to obtain clusters with a relevant botanic meaning reflecting the plant branching structure.

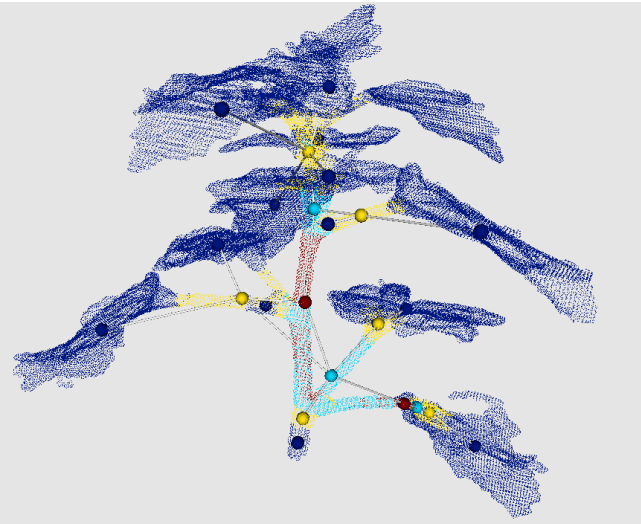

Figure 1: Output of step 2 on a Chenopodium album.

References

Guinard, S., Landrieu, L., 2017, *International Archives of the Photogrammetry, Remote Sensing & Spatial Information Sciences* 42, doi: 10.5194/isprs-archives-XLII-1-W1-151-2017
Hétroy-Wheeler, F., et al., 2016. *International Journal of Remote Sensing 37*, 2881–2907, doi: 10.1080/01431161.2016.1190988
Paulus, S., 2019. Measuring crops in 3D: using geometry for plant phenotyping. Plant Methods 15, doi: 10.1186/s13007-019-0490-0
Sanders, P., & Schulz, C., 2011, *European Symposium on Algorithms*, doi: 10.1007/978-3-642-23719-5_40
Scharr, H., et al, 2017. *Frontiers in Plant Science 8*. doi: 10.3389/fpls.2017.01680

A 3D architectural model of grass shoot morphogenesis and plasticity, driven by organ metabolite concentrations and coordination rules

Marion Gauthier[1,2], Romain Barillot[3], Anne Schneider[4], Camille Chambon[1], Christian Fournier[5], Christophe Pradal[6,7], Bruno Andrieu[1]

[1] *Université Paris-Saclay, INRAE, AgroParisTech, UMR ECOSYS, F-78850 Thiverval-Grignon, France*

[2] *ITK, avenue de l'Europe, F-34830 Clapiers, France*

[3] *INRAE, UR P3F, F-86600 Lusignan, France*

[4] *Université d'Angers, INRAE, Agrocampus-Ouest, SFR 4207 QUASAV, IRHS, F-49071 Angers, France*

[5] *Université de Montpellier, INRAE, Montpellier SupAgro, UMR LEPSE, F-34060 Montpellier, France*

[6] *CIRAD, UMR AGAP, and INRIA Montpellier, France*

[7] *AGAP, Université de Montpellier, CIRAD, INRAE, Montpellier SupAgro, Montpellier, France*

For correspondence: romain.barillot@inrae.fr

Keywords: carbon, nitrogen, metabolism, leaf growth, plasticity

Introduction

Phenotypic plasticity - the ability of one genotype to produce different phenotypes depending on growth conditions - is a core aspect of the interactions between plants and their environment. For instance, leaf traits define the ability of plants to capture light, as well as their exposition and responses to various signals and stresses. In turn, leaf traits such as dimensions, composition and mass are highly regulated by growth conditions. The explicit description of shoot architecture in functional-structural models (FSPM) open new possibilities to express these feedback loops, which regulate plant fitness and productivity. However, formalizing into models the processes that build the plastic responses of traits to growth conditions is a major bottleneck to date. Most FSPMs that address the coupling between resources availability and growth consider only carbon (C) and drive resource allocation by sink priorities defined from empirical relations. Besides, the determinism of traits such as the areal density, which links mass growth with dimension growth, are poorly understood, so that these traits are frequently approximated as constant, while they have been shown to vary widely with growth conditions. Finally, the lack of process-based formalisms of existing models impairs our ability to simulate morphogenesis under contrasting growth conditions. As a step toward more mechanistic approaches to simulate shoot morphogenesis, we propose a plant-scale FSPM of C and nitrogen (N) economy of the growing grass in which the morphogenesis is fully integrated with the plant metabolism.

Model description

The model represents the plant as a collection of tillers made of several growing and mature shoot phytomers (identifying lamina, sheath and internode mature tissues and growth zones), a single roots compartment and a shared pool mimicking the phloem. Each compartment has a structural mass and concentrations in mobile and storage metabolites. The plant is seen as a self-regulated system which relies on two processes: i) local C and N concentrations in the growth zones drive organ elongation rate, specific structural mass and width, ii) coordination rules link the timing of extension of the organs between successive phytomers. These processes were implemented into CN-Wheat (Barillot et al., 2016ab), a detailed FSPM of C and N metabolism previously developed for a culm with a static architecture. The new version of CN-Wheat presented here is the coupling of (i) a model of leaf, internode and root growth, (ii) a dynamic representation of the 3D geometry of plants which builds on the ADEL-Wheat

model (Fournier et al., 2003), (iii) a model of light distribution (Chelle and Andrieu, 1998), and finally (iv) a model simulating photosynthesis, N acquisition, synthesis and allocation of C and N metabolites, and senescence at the organ level, which extends the initial version of CN-Wheat. All above mentionned processes are regulated, at organ scale, by the environmental conditions and the concentrations in C and N metabolites.

Results and Discussion

The model was calibrated for wheat during the vegetative stages (from seedling emergence to the beginning of stem extension). First, the model was evaluated in field conditions representative of North-Western Europe, which resulted in realistic patterns of leaf dimensions, extension and senescence dynamics, organ mass and composition. A key result was the ability of the model to simulate, as emerging properties, key plant and agronomic traits *e.g.* the phyllochron, shoot/roots ratio dynamic, N dilution and radiation use efficiency. Then, we evaluated the model's ability to simulate plant plasticity under different scenarios of plant density, incoming light and soil nitrate concentration. The model simulated realistic responses of leaf traits such as dimensions, specific leaf area and specific leaf N; the figure illustrates the simulated variations of lamina dimensions and N vertical gradient with N resources.

Conclusion

Our model is innovative by the high level of explicitation of the processes underlying shoot morphogenesis, which provides new possibilities to link the phenotypic plasticity of plants to their C and N metabolic status at the place and time where traits are built. The approach could be extended to include other factors involved in plasticity, such as hormones or direct responses to the environment perceived. The genericity of the modelling frame makes it also applicable to explore shoot morphogenesis in other grass species.

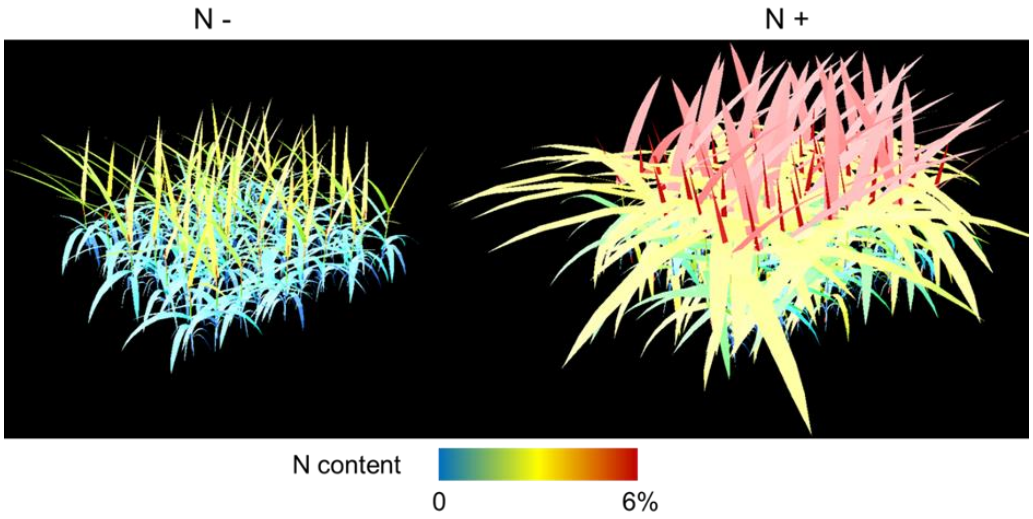

Figure: 3D-simulation of the growth of vegetative grass in contrasting N treatments. Seedlings initialised at stage 2.5 leaves with identical dimensions, mass and composition were grown under two N nutrition treatments for ~1200°C days.

References

Barillot et al., 2016a, *Annals of Botany* 118, 997-1013, doi: 10.1093/aob/mcw143
Barillot et al., 2016b, *Annals of Botany* 118, 1015-1031, doi: 10.1093/aob/mcw144
Chelle and Andrieu, 1998, *Ecological Modelling* 111, 75–91, doi: 10.1016/S0304-3800(98)00100-8
Fournier et al., 2003, Proceedings PMA03, 54–63, hal-00909184

Exploring the dual role of bent canopy in cut-rose production using a functional-structural plant model

Ningyi Zhang[1,2], Arian van Westreenen[1,2], Jochem B. Evers[2], Niels P.R. Anten[2], Leo F.M. Marcelis[1]

[1] *Horticulture and Product Physiology Group, Department of Plant Sciences, Wageningen University, PO Box 16, 6700 AA Wageningen, The Netherlands*
[2] *Centre for Crop Systems Analysis, Department of Plant Sciences, Wageningen University, P.O. Box 430, 6700 AK Wageningen, The Netherlands*

For correspondence: ningyi.zhang@wur.nl

Keywords: architectural traits, heterogeneous canopy, light absorption, photosynthesis, red to far-red ratio

Introduction In cut-rose production, weak and non-flowering shoots are usually bent downwards (the so-called bent canopy) to intercept light not captured by the upright flower shoots (Ohkawa and Suematsu, 1997). Bending part of the shoots in rose plants increases stem length, flower size and dry weight of upright shoots, resulting in high commercial quality of harvestable flower shoots (Kim and Lieth, 2004). The advantages of bent shoots in cut-rose production have been attributed to bent shoots capturing more light and thus providing more assimilates for flower shoot growth. However, far-red light can be scattered and reflected by bent shoots, which could lower the red to far-red ratio (R:FR) in light reflected upwards. Such a low R:FR signal may induce changes in upright shoot architecture and affect upright shoot light interception and photosynthesis. The objectives of this study are to (1) quantify the contribution of photosynthesis by bent shoots to upright flower shoot growth and (2) investigate the effect of far-red reflected by bent shoots on upright shoot architecture and photosynthesis.
Materials and Methods Two greenhouse experiments were conducted. In experiment 1, rose plants were grown with four upright flower shoots and with 0, 1 or 3 bent shoots per plant. In experiment 2, rose plants either with or without bent shoots were grown with neighbour rose plants either with or without bent shoots. In both experiments, plant architectural traits and organ dry weight were measured. Additionally, in exp.1, leaf photosynthetic parameters were measured, and in exp. 2, R:FR ratios at different heights and locations of the canopy were measured with spectrometer sensor facing up, down and sides. A functional-structural plant (FSP) model of rose was developed based on experimental data. The FSP model was used to calculate photosynthesis of upright shoots and bent shoots separately, and to estimate the effect of any upright shoot architectural changes induced by R:FR reflected by bent shoots on plant photosynthesis.
Results Bent shoots contributed to 43% to 53% of total assimilated CO_2 by the plant. Plant photosynthesis increased by 73% and 117% in plants with, respectively, 1 and 3 bent shoots compared to plants without bent shoots. Upright shoot dry weight increased by 35% and 59% in plants with, respectively, 1 and 3 bent shoots compared to plants without bent shoots. In addition, bent shoots reflected a substantial amount of far-red, which lowered R:FR in light reflected upwards. This induced an increase of leaf angle in upright shoots, regardless of the plant itself had bent shoots or not. Model simulations showed that the increased upright shoot dry weight in plants with bent shoots was entirely due to the contribution of extra photosynthesis by bent shoots. However, the steeper leaf angle in upright shoots, which was induced by low R:FR reflected off bent shoots, led to slightly decreases of upright shoot light absorption and photosynthesis. Plant photosynthesis was slightly increased (1-2%) when the low R:FR was reflected from bent shoots of the same plant, as the steeper leaf angle of upright shoots allowed more light to penetrate to bent shoots that were down in the canopy.
Conclusion Bent canopy has dual effects in cut-rose production system. On the one hand, additional assimilate supply from bent shoots enhanced flower shoot growth and quality. On the other hand, bent shoots lowered the R:FR in light reflected upwards, which induced a

steeper leaf angle in upright shoots and increased plant photosynthesis by improving light distribution in the canopy.

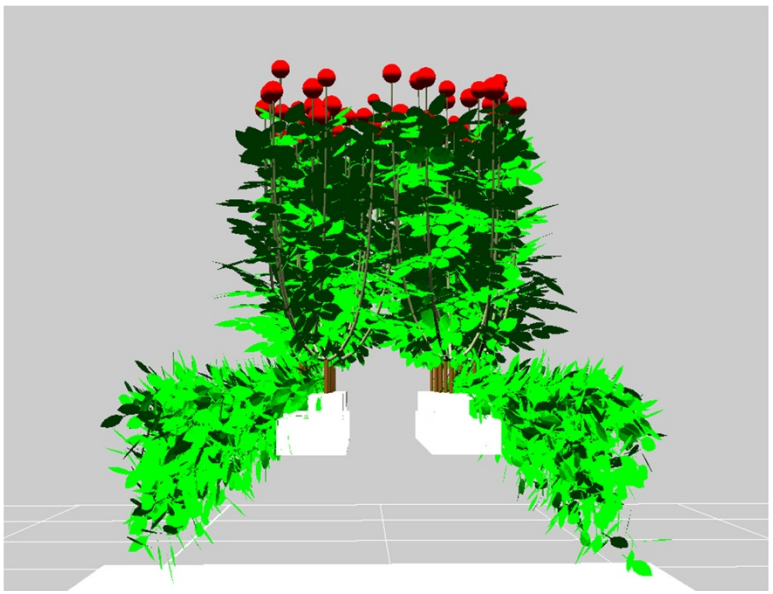

Figure: Three-dimensional representation of rose plants with three bent shoots per plant at flowering stage.

References

Ohkawa and Suematsu, 1997, *Acta Horti* 482: 47–52, doi: 10.17660/ActaHortic.1999.482.5
Kim and Lieth, 2004, *Sci Horti* 99: 331–343, doi: 10.1016/S0304-4238(03)00099-2

Toward a functional-structural model of oil palm accounting for architectural plasticity in response to planting density

Raphaël P.A Perez[1], Rémi Vezy[2], Loïc Brancheriau[3], Frédéric Boudon[1], François Grand[2], Doni Artanto Raharjo[4], Jean-Pierre Caliman[4] and Jean Dauzat[2]

[1]CIRAD, UMR AGAP, F-34398 Montpellier, France.
AGAP, Univ Montpellier, CIRAD, INRAE, Montpellier SupAgro, Montpellier, France.
[2]CIRAD, UMR AMAP, F-34398 Montpellier, France.
AMAP, Univ Montpellier, CIRAD, CNRS, INRAE, IRD, Montpellier, France
[3]CIRAD, UPR BioWooEB, F-34398 Montpellier, France.
BioWooEB, Univ Montpellier, CIRAD, CNRS, INRAE, IRD, Montpellier, France
[4]Sinar Mas Agro Resources Technology Research Institute (SMARTRI), Libo Estate, Kandis, Pekanbaru, Riau, Indonesia

For correspondence: raphael.perez@cirad.fr

Keywords: FSPM, Lidar, phenotypic plasticity, plant architecture, planting density

Abstract

Functional-structural plant modelling approaches (FSPM) open the way for exploring the relationships between the 3D structure and the physiological functioning of plants in relation to environmental conditions. FSPMs can be particularly interesting when dealing with perennial crops like oil palm, for which research on innovative management practices requires long and expensive agronomic trials. The present study is part of the PalmStudio project, which aims at developing a FSPM for oil palm capable of conducting virtual experiments to test the relevance of innovative management practiceds and/or design ideotypes.

We propose a methodological approach which integrates architectural responses to planting density in an existing oil palm FSPM (Perez *et al.* 2018a b). Combining standard field phenotyping with Lidar-based derived measurements, we manage to evaluate the phenotypic plasticity of the main parameters required for the calibration of the 3D plant model. LiDAR scans were processed using the PlantScan3D software (Boudon et al. 2014) to derive phenotypic traits of leaf geometry that were compared to labour-intensive measurements. Density-based allometries of leaf geometry and biomass are then derived from the observed variations in phenotypic traits and integrate into the FSPM.

Our results illustrate the accuracy and the efficiency of Lidar-based phenotyping of leaf geometrical traits. In average, we find less than 3% of difference in leaf dimensions (i.e. rachis length) in comparison with traditional hand-made field measurements. The fast and efficient measurements of usually labour-intensive traits such as leaf curvature allowed estimating the plasticity of leaf geometry in response to density. We find that the main traits affected by density were leaf dimensions (up to 15% and 25% of increase in rachis length and petiole length respectively) and curvature (15% of increase in leaf erectness-related parameter), whereas other structural traits like the number of leaflets per leaf remained unchanged. Simple density-based allometric relationships were then modelled and combined with the existing allometric-based 3D oil palm model VPalm (Perez *et al.* 2018a). These data also enable the development and the integration in VPalm of a biomechanical model simulating leaf curvature.

The methodology presented in this study paves the way for a rapid integration of phenotypic plasticity in FSPMs. Our FSPM is now able to estimate how planting density affect not only plant architecture but also functional processes such as carbon assimilation and transpiration. Ongoing research aims at coupling the current FSPM with a carbon allocation model (Pallas *et al.* 2013) to simulate the retroactions of functioning processes on plant architecture together with environmental and agronomic conditions.

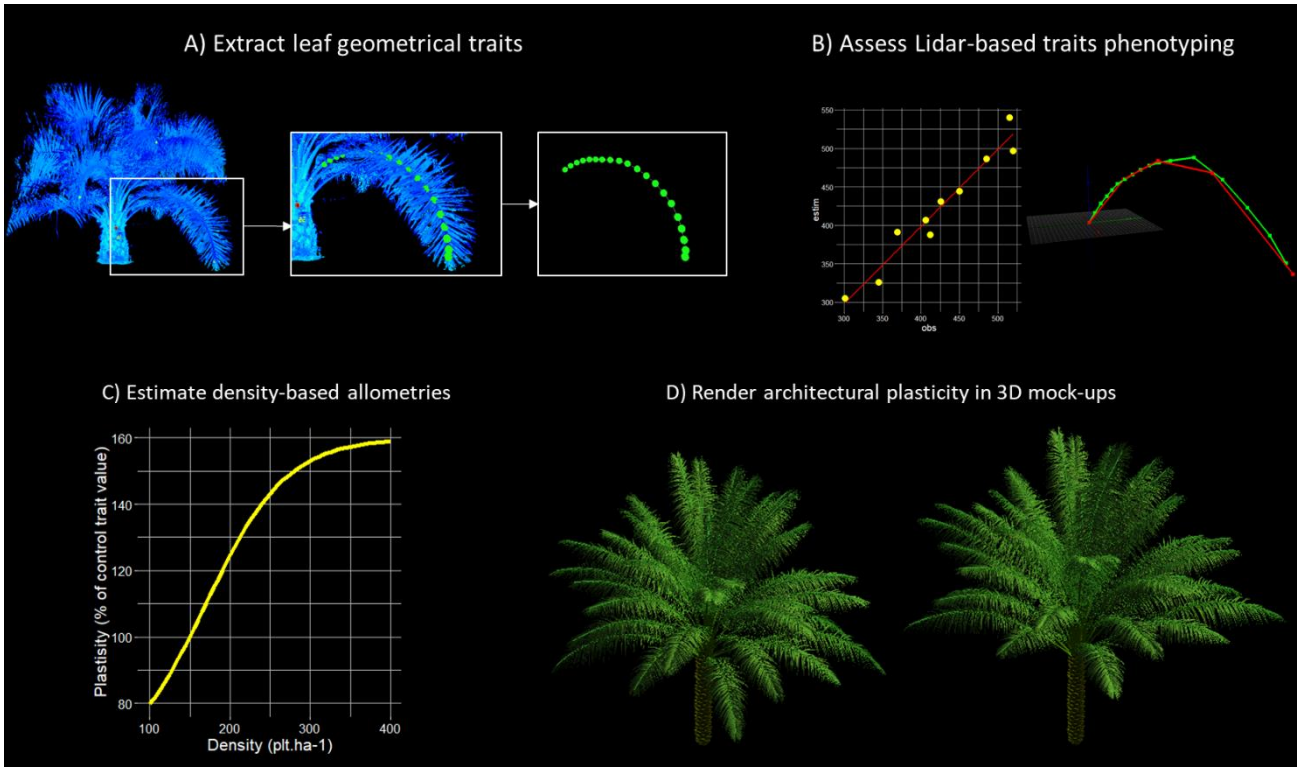

Figure: Overview of the methodological approach proposed to integrate in a 3D model the effect of planting density on plant architecture. A) Lidar point clouds with the extraction of leaf geometrical attributes (length and curvature). B) Comparison of Lidar-based vs hand-measured rachis length (left) and 3D positions for leaf curvature estimation (right). C) Example of density-based allometry. D) 3D model outputs for conventional (left) and double (right) density.

References

Boudon F., Preuksakarn C., Ferraro P., Diener J., Nacry P., Nikinmaa E., Godin C. (2014) Quantitative assessment of automatic reconstructions of branching systems obtained from laser scanning. *Annals of Botany*, **114** (4), 853-862.

Pallas B., Clément-Vidal A., Rebolledo M.-C., Soulié J.-C. & Luquet D. (2013) Using plant growth modeling to analyze C source-sink relations under drought: inter- and intraspecific comparison. *Frontiers in plant science* **4**, 437.

Perez R.P.A., Costes E., Théveny F., Griffon S., Caliman J.P. & Dauzat J. (2018a) 3D plant model assessed by terrestrial LiDAR and hemispherical photographs: A useful tool for comparing light interception among oil palm progenies. *Agricultural and Forest Meteorology* **249**, 250–263.

Perez R.P.A., Dauzat J., Pallas B., Lamour J., Verley P., Caliman J.P., … Faivre R. (2018b) Designing oil palm architectural ideotypes for optimal light interception and carbon assimilation through a sensitivity analysis of leaf traits. *Annals of Botany* **121**, 909–926.

Integrating the complex regulation of leaf growth by water and trophic dynamics in a functional-structural plant model of grass.

Romain Barillot[1], Marion Gauthier[2,3], Bruno Andrieu[2], Jean-Louis Durand[1], Isabel Roldan-Ruiz[4] and Tom De Swaef[4]

[1] *INRAE, UR P3F, F-86600, Lusignan, France*
[2] *Université Paris-Saclay, INRAE, AgroParisTech, UMR ECOSYS, F-78850, Thiverval-Grignon, France*
[3] *ITK, avenue de l'Europe, F-34830 Clapiers, France*
[4] *Plant Sciences Unit, Research Institute for Agriculture, Fisheries and Food (ILVO), Melle, Belgium*

For correspondence: romain.barillot@inrae.fr

Keywords: carbon, nitrogen, metabolism, water potential, turgor

Introduction

Climate change challenges agricultural production due to interacting effects of increased atmospheric CO_2 concentration ([CO_2]) and altered temperature and water availability. Anticipating climate change effects on agricultural systems and developing adaptation strategies is a major challenge for the next decades. Plant morphogenesis plays a crucial role in resource capture and is under a complex regulation which is mainly determined by the interplay between environmental factors. Climatic models for Western Europe show that climate change will probably affect water availability (through lower rainfalls) and demand (through increased evapotranspiration due to high temperatures), leading to more frequent water deficits and losses of biomass production (Durand *et al.*, 2010). On the other hand, higher [CO_2] will cause a decrease of the stomatal conductance which will improve water use efficiency. A major challenge therefore lies in our ability to anticipate the integrated response of plant morphogenesis. However, the complex feedback controls involved make it difficult to decipher plant response using only experimental approaches. Functional Structural Plant Models (FSPMs), which account for the interactions between biological processes and environmental factors are better suited to explore plant responses to climate change and possible adaptation mechanisms. Most of FSPMs available mainly focus on the competition for light and carbon acquisition, without considering water relations. In the present work, we describe a comprehensive FSPM, CNW-Grass, encompassing the regulation of leaf growth by water and trophic dynamics in grasses.

Model description

CNW-Grass is defined at individual tiller scale, composed of a series of interconnected laminae, sheaths, internodes and growth zones. Leaf elongation kinetics are split in two phases whose durations depend on coordination rules based on the emergence of successive leaves. During the early phase, which lasts until leaf $_{n-1}$ emergence, the growth of leaf *n* is assumed to be regulated by the carbon and nitrogen concentrations of the growth zone, considering water availability as non-limiting (as a first approximation for this initial version of the model). In the second phase, leaf growth is driven by turgor pressure, which is coupled to leaf water content variations and osmotic pressure (related to C content), thus resulting in elastic deformation and plastic irreversible growth (Coussement *et al.*, 2018). The water flow throughout the hydraulic architecture of the tiller is calculated from organ transpiration and water potential differences. Carbon and nitrogen concentrations, which affect leaf growth and osmotic pressure, are simulated at organ scale using CN-Wheat, a detailed model of the metabolic processes involved in CO_2 and nitrogen acquisition and allocation (Gauthier *et al.* 2020; Barillot *et al.*, 2016). The modelling framework was implemented in OpenAlea platform and uses the MTG formalism as a central data structure for model communication. The model was calibrated for wheat but the formalisms can be extended to many grass species.

Results and Discussion

To illustrate model behaviour, simulations are presented for a wheat plant grown for 800 hours and exposed to a mild drought period arbitrarily imposed at *t=400* hours by decreasing the roots' water potential from -0.1 to -0.2 MPa (Figure 1). Before 400 hours, the water potential of the emerged growing leaf was close to that of the roots and was slightly affected by the diurnal variations of transpiration. At *t=400* h, the water potential of the growing leaf in the 'drought treatment' immediately dropped to -0.2 MPa, which significantly reduced leaf elongation. As a consequence of the coupling between the water and trophic dynamics, CNW-Grass simulated an increase in carbon supply for roots, which positively affected nitrate uptake and the shoot: root ratio (data not shown).

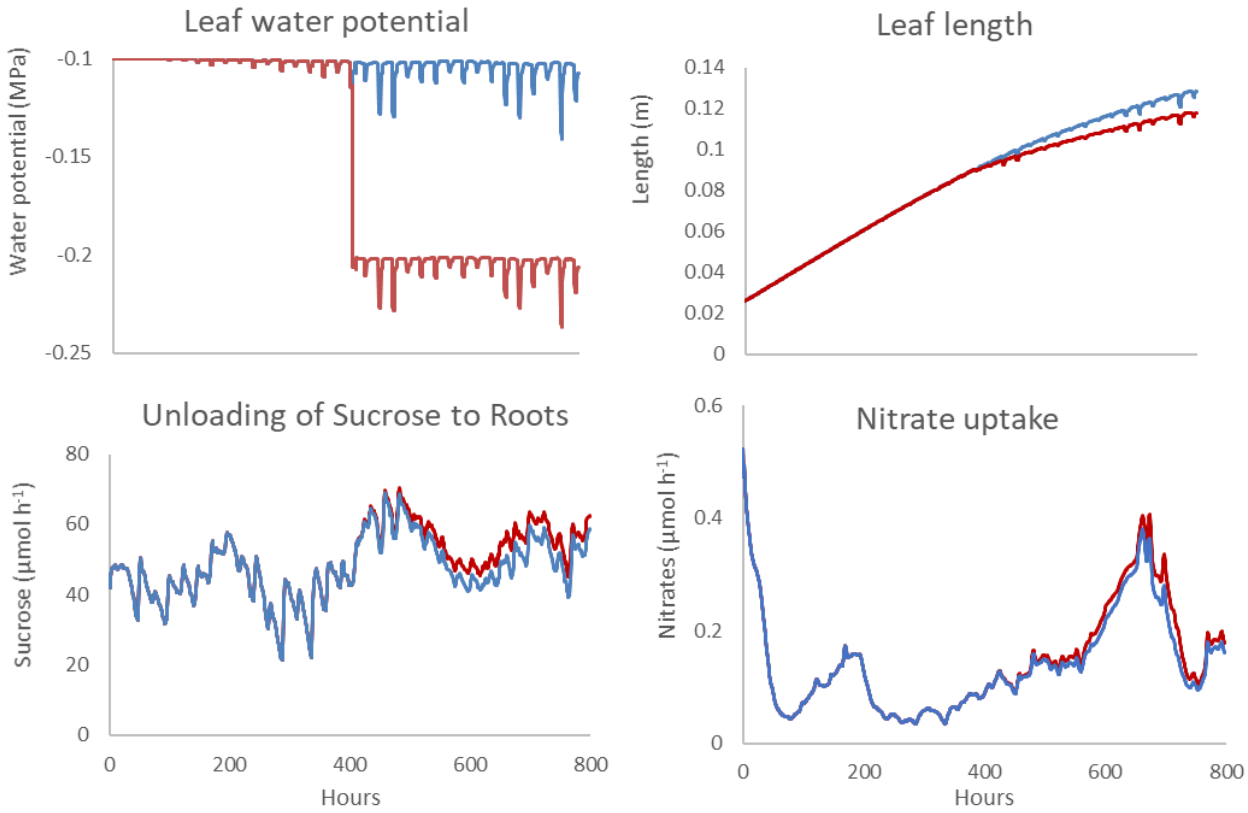

Figure 1: Dynamics of leaf water potential, leaf length, sucrose unloading in roots and nitrate uptake for control plants (blue) and water-stressed plants (red). The water stress was simulated by decreasing the water potential of roots from -0.1 to -0.2 MPa at 400 hours.

Conclusions

The complex feedbacks implemented in CNW-Grass between C, N and water dynamics allowed to account for the effects of drought on leaf growth but also the consequences on resource allocation between shoot organs and roots. CNW-Grass will be used to investigate the integrated response of plants to future climate conditions (*i.e.* combined variations of temperature, water and [CO_2]), which is a rather underexplored field of research. The model will also allow to explore the potential of the available natural variation in crops for improving plant production and resilience *e.g.* through the identification of plant traits useful for the adaptation of plants to climate change.

References

Barillot *et al.*, 2016, *Annals of Botany* 118: 997–1013, doi: https://doi.org/10.1093/aob/mcw143
Coussement *et al.*, 2018, *Annals of Botany* 121: 849–861, doi: https://doi.org/10.1093/aob/mcx144
Durand *et al.*, 2010, *The Green Book of the CLIMATOR project (2007–2010). ADEME.*
Gauthier *et al.*, 2010, *J Exp Bot, in press*, doi: https://doi.org/10.1093/jxb/eraa276

Predicting function from structure – An analysis of the palisade mesophyll

Shiv Gangapersad[1], Bryn Jones[1], Andrew Fleming[2], Visakan Kadirkamanathan[1]

[1] *Department of Automatic Control & Systems Engineering, University of Sheffield, United Kingdom*
[2] *Department of Animal & Plant Sciences, University of Sheffield, United Kingdom*

For correspondence: sjgangapersad1@sheffield.ac.uk

Keywords: palisade mesophyll, diffusion, modelling, carbon dioxide uptake

The photosynthetic pathway has been extensively researched at the subcellular level and for the whole leaf, with established biochemical and mechanistic models (Farquhar et al., 2001). While it is known that the balance of intercellular airspace and cellular material depends on patterns of cell division and growth, it is less well understood how different intercellular airspace arrangements impact photosynthesis (Lehmeier et al., 2017). What is the relationship between the amount of internal mesophyll surface area exposed to air, photosynthetic capacity and cell size? Is there an optimal airspace-tissue balance, and if so, how will it change under future levels of CO_2 (Pritchard et al., 1999)?

With recent advances in micro-computer tomography (micro-CT), it is possible to quantify the intercellular mesophyll airspace at a local scale and obtain paired datasets of global gas exchange measurements (Pajor et al., 2013; Lehmeier et al., 2017). Assuming steady-state photosynthesis, we can model pores in the palisade mesophyll as microscopic air channels by applying Fick's 1st law of diffusion (Parkhurst, 1994). By validating this mechanistic model with experimental observations of paired micro-CT/gas exchange data in a series of *Arabidopsis Thaliana* mutants, we can explore the trade-off between the amount of cellular material and airspaces in the palisade layer. More importantly, this structure-function modelling framework allows us to identify which of these structural properties are favoured by mutants with better photosynthetic performance, and quantify whether there is any consistent behaviour leading to an 'optimal' trade-off between cellular material and airspaces.

The analysis shows that the intercellular CO_2 uptake rate is a function of the palisade mesophyll air channel height. This observation implies a trend in which leaves with shorter intercellular diffusion pathways within the palisade mesophyll have a higher CO_2 assimilation rate, which could suggest an optimisation of the inner mesophyll cell structure. Hence, from a physical diffusion-based model supported by data-driven estimation, we are able to predict function from structure.

References

Farquhar et al., 2001, Plant Physiology 125(1):42, doi: 10.1104/pp.125.1.42
Lehmeier et al, 2017, The Plant Journal 92(6):981, doi: 10.1111/tpj.13727
Pritchard et al., 1999, Global Change Biology 5(7):807, doi: 10.1046/j.1365-2486.1999.00268.x
Pajor et al., 2013, Journal of Experimental Botany 64(2):385, doi: 10.1093/jxb/ers392
Parkhurst, 1994, New Phytologist 126(3):449, doi: 10.1111/j.1469-8137.1994.tb04244.x

Modelling the contribution of plant traits to light partitioning in simultaneous maize/soybean intercropping

Shuangwei Li[1,2], Wopke van der Werf[2], Junqi Zhu[3], Yan Guo[1], Baoguo Li[1], Yuntao Ma[1*], Jochem B. Evers[2]

[1] *College of Land Science and Technology, China Agricultural University, Beijing 100193, China*
[2] *Centre for Crop Systems Analysis, Wageningen University, 6700 AK Wageningen, The Netherlands*
[3] *The New Zealand Institute for Plant & Food Research Ltd, Blenheim 7201, New Zealand*

[*] *For correspondence: yuntao.ma@cau.edu.cn*

Keywords: intercropping, phenotypic plasticity, border effect, light partitioning

Introduction

Strip intercropping entails the cultivation of mixtures in narrow strips of each species whereby each strip comprises a few rows of a species. Strip intercropping is a system that can enhance resource capture and production, particularly if the species are sown as a relay strip intercrop with differences in sowing and harvest date between species (Zhu et al., 2015; Li et al., 2020). The canopy structure of a strip intercrop is spatially heterogeneous, which affects light distribution as well as light capture and productivity of each species (Gou et al., 2016; Liu et al., 2018). The spatial configuration of the intercrop in strips and the plasticity in plant traits were found to both affect the light capture in relay strip intercrops of wheat and maize (Zhu et al., 2015). There is limited knowledge on the effects of configuration and plant traits on light distribution in simultaneous intercropping systems, such as maize/soybean. In maize/soybean, maize captures most of the light, while soybean is shaded. It is not clear how plasticity in plant traits of maize and soybean in the mixed canopy modulates the partitioning of radiation between the two species and whether such plasticity in plant traits can contribute to yield increase. A key question in this respect is also whether soybean, as the shaded species, responds architecturally in ways that mitigate the negative consequences of shading by maize. We therefore study here the role of plant traits of soybean in driving light interception by component species in simultaneous maize/soybean intercropping.

Materials and Methods

We constructed a functional-structural plant (FSP) model that represents maize/soybean canopy development. Field data were used to derive model parameters for sole and intercrop phenotypes of both species. Independent field data were used for model validation. To quantify the effect of phenotype in different crop configurations (sole crop or intercrop), light interception of each species was simulated using plants traits measured either in the sole crop or intercrop. The intercrop consisted of alternate strips of two maize rows and three soybean rows, at 60 cm row distance for maize, 30 cm for soybean and 50 cm between the two species. In a given crop setting, we changed the individual soybean plant traits to identify their effect on light capture. The studied traits comprised final internode length, final leaf dimensions, leaf life span, petiole declination angle, final petiole length and phyllochron.

Results

Intercropping increased leaf width, internode diameter and leaf declination angle (angle with the vertical) in maize. Intercropped soybean had lower leaf appearance rate, smaller leaves and thinner stems, but longer internodes, than sole soybean. The intercrop maize phenotype increased the simulated light capture of a pure maize stand by 2%. Soybean intercrop phenotype, however, reduced the simulated light capture of a pure soybean stand by 5–10%. Overall, intercrop light of maize was 29% higher than expected based on the relative densities (556.5 MJ m^{-2} vs 431.6 MJ m^{-2}). For soybean, simulated light capture was 42% lower than expected (163.7 MJ m^{-2} vs 281.7 MJ m^{-2}). The difference in total system light capture was only 1% different from expectation (715.7 MJ m^{-2} vs 713.3 MJ m^{-2}). Leaf size had the greatest effect

of all traits tested on light interception by intercropped soybean. Longer internodes helped soybean intercept more light in intercropping, but not in the sole crop. Longer leaf life span increased light capture in both the sole crop and intercrop configuration.

Discussion

Increasing soybean leaf size, leaf life span and internode length under shade could help improve maize/soybean intercrop performance. Soybean performance in intercrops with maize could furthermore be improved by using short stature maize genotypes, by using wider gaps between maize rows, or by maize leaf stripping.

Conclusion

The results of this study illustrate a major shift of light capture from shorter species (soybean) to the taller component (maize) in a simultaneous strip intercrop. Plastic plant traits modulate this overall effect, but only marginally.

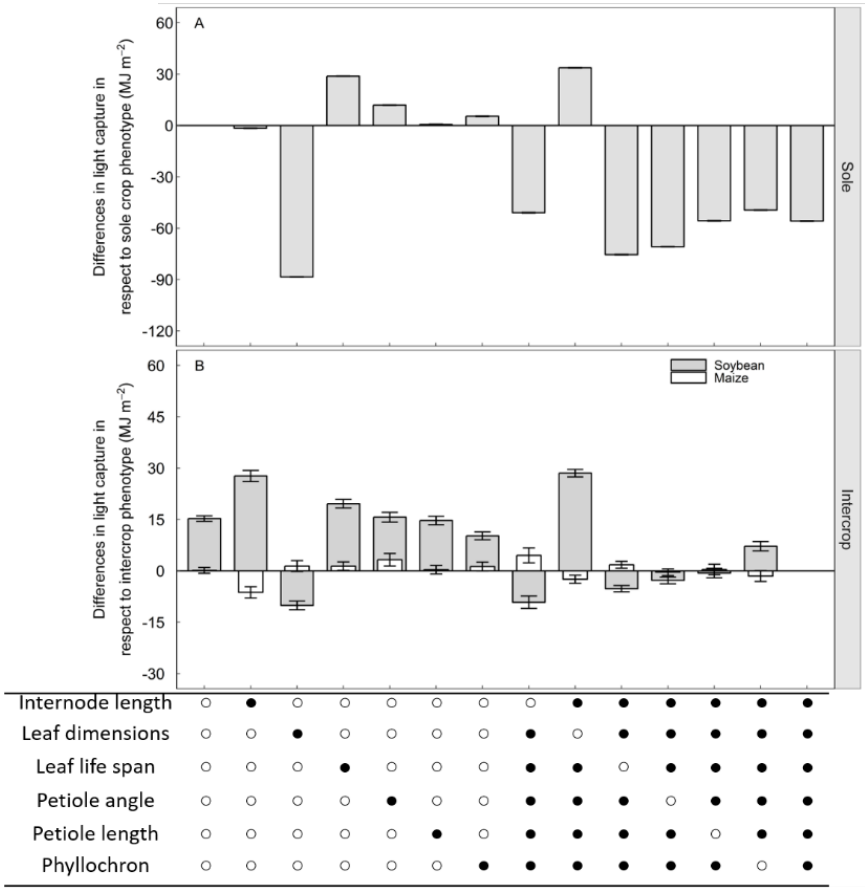

Figure: Differences in light capture in respect to sole crop phenotype in sole soybean (A) and intercrop phenotype in intercrop (B) when soybean with and without selected single plant trait. ○, the value in sole phenotype was used in the simulation. ●, the value in the intercrop phenotype, expressed as a weighted mean value (2/3 border row + 1/3 inner row). Further plant traits (growth duration of internode and leaf and internode diameter) came from sole crop (A) or intercrop (B). The combination of different symbols represents the integration of those plastic traits. The light capture of soybean with pure sole crop traits was 687.1±0.2 MJ m^{-2} in sole crop. The light capture of plants with pure intercrop traits were 575.5±1.9 MJ m^{-2} for maize and 140.2±1.5 MJ m^{-2} for soybean in intercrop. Error bars that not shown are within 1% of the averaged values. Values are means ± s.e. (*n* = 10).

References

Gou et al., 2016, *Eur. J. Agron*. 76, 17-27, doi: 10.1016/j.eja.2016.01.005
Li et al., 2020, *Nature Plants.* 6, 653–660. doi: 10.1038/s41477-020-0680-9
Liu et al., 2018, *Field Crop Res*. 224, 91-101, doi: 10.1016/j.fcr.2018.05.010
Zhu et al., 2015, *New Phytol.* 207, 1213-1222, doi: 10.1111/nph.13416

Modelling the genetic diversity of perennial grass phenology in contrasted temperate climates

Simon Rouet[1], Jean-Louis Durand[1], Didier Combes[1], Abraham Escobar Gutiérrez[1], Romain Barillot[1]

[1]*INRAE UR P3F, Lusignan, France*

For correspondence: simon.rouet@inrae.fr

Keywords: floral transition, grassland, temperature, photoperiod, individual-based model

Introduction

In perennial grasses, flowering is a periodical event that deeply affects plant morphogenesis and has consequences on biomass production, quality and tiller demography. Despite the importance of perennial grasses in continental ecosystems, we still lack accurate models predicting perennial grass flowering and its consequences on plant development. The available models often directly use the heading date (HD) as an input parameter or poorly account for the floral induction process in response to climate. In addition, the vegetative and reproductive developments are usually represented as two independent phases instead of a continuous process. In the present work, we developed an original Functional-Structural Plant Model (FSPM) of grasses, named L-grassF representing the floral development of individual tillers in interaction with the vegetative stages and considering the dynamic effect of environmental conditions on floral induction. Our objective was to simulate the genetic diversity of the response of floral induction and growth of individual tillers to environmental variations.

Materials and Methods

L-grassF describes the canopy as a set of individual plants, each being composed of one or more tillers. The dynamics of leaf growth and tillering are determined by self-regulation rules as described in the original version of the L-grass model (Verdenal et al. 2008). We added a phenological module integrating the effects of temperature and photoperiod on the functioning of each apex of the plant, assuming a dual induction requirement as established for *Lolium perenne* (Heide 1994). The model predicts the HD of tillers from the emergent process of heading which results from the simulation of floral transition (FT), final leaf number and 3D expansion of leaves, internodes and spikes. Parameters of vegetative growth and floral induction were calibrated on an experiment describing organ appearance and growth in three *Lolium perenne* cultivars grown under four inductive conditions in growth chambers. Three conditions consisted in a period of primary induction followed by an exposition to long days after 0, 3 or 6 weeks of short days. In the fourth condition, plants were not exposed to the conditions necessary for the primary induction. Finally, the model was evaluated against phenological records of the same cultivars grown in seven French field sites for several years.

Results and Discussion

The model was run in two contrasted environments for tillers initiated arbitrarily at four different dates in order to represent different cohorts, from main stems emerged after sowing in October, to tillers initiated in April (Figure 1). Simulations were performed at two locations (Fig.1a, c) with similar photoperiod but different thermic regimes. In particular, winter temperatures in Theix (Fig.1c) were significantly colder than in Ploudaniel (Fig.1a). The environmental conditions modified the proportion of flowering tillers (Fig.1b, d). Under a climate with a relatively warm winter (Fig.1a), young tillers (initiated on Feb. 1st and Apr. 1st) do not accumulate enough low temperatures to reach primary induction (blue arrows). As the secondary induction by photoperiod (green arrows) is constrained by the achievement of the primary induction, these tillers remained vegetative and produced leaves indefinitely. Lower temperatures in winter (Fig.1c) reduced the duration required for primary induction and allowed the flowering of one more tiller. The final leaf number of heading tillers globally increased with

higher winter temperatures (Fig.1b). It was also dependent on primary and secondary induction dates. The HD (red arrows) occurred at different time after the last leaf appearance depending on the spike morphology (spikelet number) and the temperature conditions during its growth. Nevertheless, whatever the climate context, the model simulates close HD in comparison with the repartition of the tiller initiation dates. Changing the values of the induction model parameters allowed the simulation of the genetic diversity of the HD in *Lolium perenne* in interaction with the environment (results not shown).

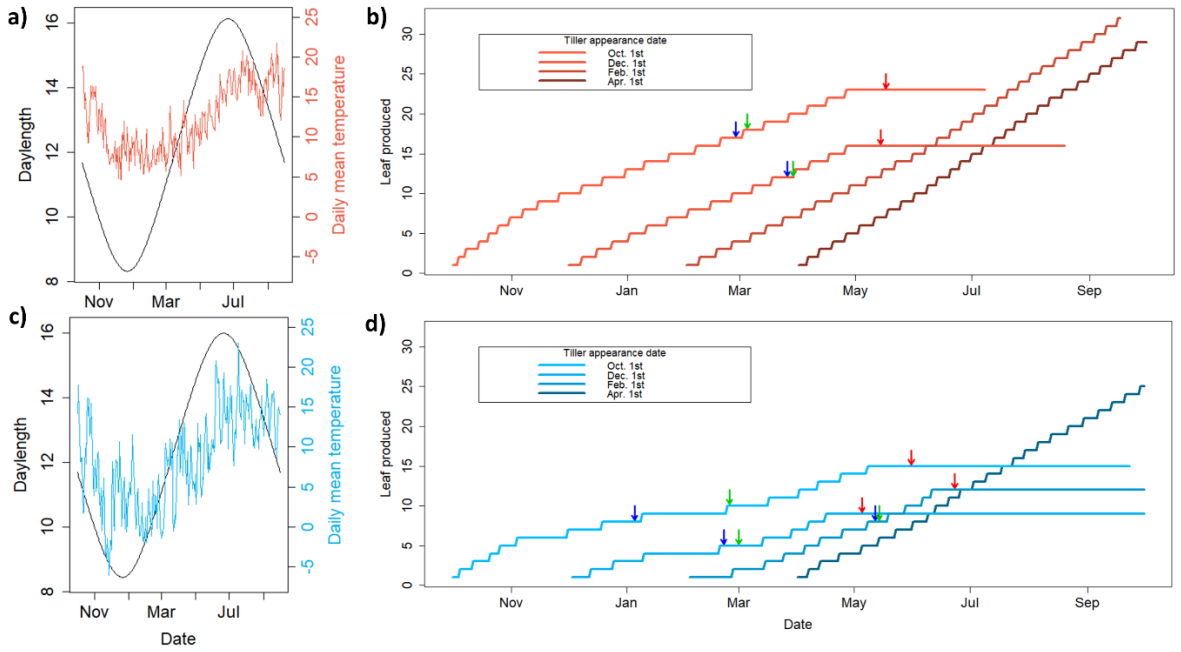

Figure: Cumulated number of leaves produced by tillers set on four different dates (Oct.1st, Dec.1st, Feb.1st and Apr.1st) in two French contrasted climates. Climates and simulations of the phenology: (a, b) in Ploudaniel (oceanic) and (c, d) in Theix (continental). Blue arrows: end of primary induction, green arrows: secondary induction, red arrows: HD

Conclusion

The present model is the first individual-based model of perennial grasses accounting for plant morphogenesis and FT in response to environmental factors. In the context of climate change, the model can allow the identification of perennial grass ideotypes for meadows adapted to future climate conditions and therefore help the breeding of new cultivars.

References

Heide, 1994, *New Phytol.*, 128:347-362, doi: 10.1111/j.1469-8137.1994.tb04019.x

Verdenal et al., 2008, *Functional Plant Biol*., 35:911-924, doi: 10.1071/FP08050

A Structural Model of Three Poplar Clones from Short-Rotation Coppice

Christoph B. Stiehm[1], Andrea Plazas Cebrián[2], Winfried Kurth[2]

[1] *Department Forest Genetic Resources, Northwest German Forest Research Institution, Hann.Münden, Germany*
[2] *Department Ecoinformatics, Biometrics and Forest Growth, Georg-August Universität Göttingen, Göttingen, Germany*

For correspondence: wk@informatik.uni-goettingen.de

Keywords: crown architecture, leaf shape, SRC, *Populus*, GroIMP

Introduction

On various experimental sites across Germany, short-rotation plantations were established with the aim to compare different poplar and willow clones in terms of site-specific yield (Stiehm and Hofmann, 2018). Apart from possible interactions with environmental factors, genotype is a strong determinant of morphology. Differences in tree structure between clones can in turn have a significant impact on yield, and structural traits have been, directly or indirectly, a target in tree breeding, especially for conditions in densely planted short rotation coppice plantations for biomass production (Ceulemans, 1990; Dickmann et al., 2002). We made an extensive analysis of data from the above-ground parts of individual plants of three poplar clones, called "Max1", "Hybride 275" and "AF2", from two 3-year rotation cycles. It is a characteristic feature of poplar in short-rotation coppice plantations that in the second and even later rotation cycles, several new stems emerge from the rootstock which remains after the above-ground part was completely harvested. Usually one of these stems becomes the dominant (strongest) one. Nevertheless the architecture of these young tree individuals differs considerably from poplars growing under undisturbed natural conditions. We intended to capture these specific features in a model. A further motivation for the project was to identify morphological differences between the clones.

The Models

Based on our statistical results, we implemented two models, working at different scales of spatial resolution: A single-tree based, position-independent yield model to predict height and dry mass from soil parameters and meteorological data (this model was then implemented as an extension to the BWINPro platform, Nagel and Schmidt, 2006) and a structural, 3-dimensional model of crown development and architecture, including survival rates, internode numbers per growth unit, growth unit lengths, branching frequencies, formation of sylleptic shoots, occurrence of short shoots, secondary growth, leaf shape and branch curvature. The latter model was implemented in the language XL on the platform GroIMP (Hemmerling et al. 2008). The model is purely empirically-based, with Linear Models (LMs) and Generalized Linear Models (GLMs) as the main statistical tool. Building on first results by Plazas Cebrián (2014), the detailed model was elaborated by Stiehm (2019). The Figure below shows the graphical output of the structural model for one of the three clones.
The yield did not differ significantly between the clones. However, there were morphological differences in the frequency of short shoots and sylleptic shoots, in the branch curvature and in some parameters influencing leaf shape, which could lead to differences in competition strength under certain conditions.

Model Interconnection and Perspectives

Finally, both models were linked in a way that soil and weather information can be used to automatically tune the survival and growth parameters of the structural model. The model primarily represents the knowledge gained from the empirical data in a condensed way. On the other hand, it could be extended in the future to a functional-structural model by including

light interception and carbon fixation. This could then allow some extrapolation of the model beyond the climate conditions under which our data were obtained.

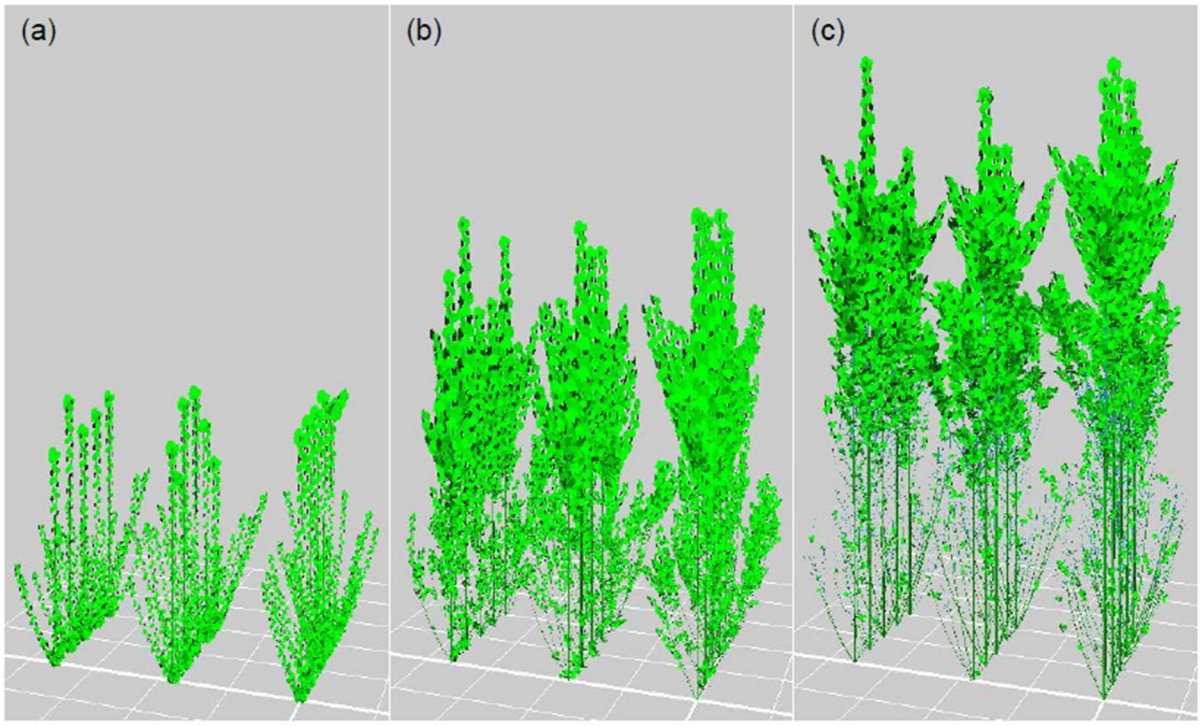

Figure: Graphical output of the structural model for a small plantation stand of 15 trees from clone "Max 1" in 3 rows. The panels show the stand at the end of each vegetation period from 1 (a) to 3 (c).

Acknowledgements

We thank Niels Lakämper, Stephan Rimmele, Marcel Schwarz and Christian Willems for measurements. Parts of this work were funded by FNR in the frame of the project "ProLoc – Clone-site interaction in SRC of poplar and willow on agricultural sites". All support is gratefully acknowledged.

References

Ceulemans, 1990, Genetic variation in functional and structural productivity determinants in poplar. Thesis, Amsterdam, ISBN 978-90-5170-044-2.

Dickmann, 2002, in: Poplar culture in North America, NRC Res. Press, Ottawa, Ont., http://nrcresearchpress.com/doi/book/10.1139/9780660181455, pp. 77-115.

Hemmerling et al., 2008, *Functional Plant Biology* 35:739-750, doi: 10.1071/FP08052.

Nagel and Schmidt, 2006, The silvicultural decision support system BWINPro. In *Sustainable Forest Management*, Springer, Berlin, 59-63.

Plazas Cebrián, 2014, Datenanalyse für Strukturmodelle dreier Pappelklone auf Kurzumtriebs-plantagen. B.Sc. thesis, University of Göttingen.

Stiehm, 2019, Interconnection of a Forest Growth Model and a Structural Model for Young Poplar Trees (*Populus* spp.), Dissertation, University of Göttingen.

Stiehm and Hofmann, 2018, *Landbauforschung – Appl. Agric. For. Res.* 68:67-82, doi: 10.3220/ LBF1542350476000.

Machine and deep learning based identification of organs within LiDAR scans of tree canopies: Application to the estimation of apple production.

Artzet Simon[1], Benoît Pallas[1], Evelyne Costes[1], Frederic Boudon[1,2]

[1] AGAP, Univ Montpellier, CIRAD, INRAE, Institut Agro, Montpellier, France
[2] CIRAD, UMR AGAP, F-34398 Montpellier, France.

For correspondence: frederic.boudon@cirad.fr

Keywords: Random Forest, PointNet, Yield evaluation, FSPM, High Throughput Phenotyping (5 max)

Introduction

Theoretically, 3D acquisition systems such as terrestrial LiDAR technology could allow capturing tree shapes at high throughput with a high precision. However, in practice, the quality of the canopy reconstruction from data acquired in the field largely depends on the weather conditions, shape of the trees and on the position and number of scans collected. In a previous study, a HT protocol using T-LIDAR technology was developed for characterising simple architectural traits at the tree scale (volume, light interception efficiency) on a large population of apple trees (Coupel-Ledru et al., 2019). Nevertheless, LIDAR point clouds generated with this HT protocol were highly noisy, limiting thus the ability to identify all individual organs within the canopy. Machine and deep learning methods seems an interesting solution as they are capable to adapt to various types of noise by learning directly from training data. As a first case of study, we aimed to automatically detect apples within apple tree point clouds. For this, we developed two automatic pipelines based on machine and deep learning methods that were applied to tree point clouds acquired from LiDAR technology or simulated from synthetic data.

Materials and Methods

Our study was carried out on 281, 3 and 4-years-old, apple trees scanned in 2018 and 2019 with terrestrial LiDAR using two specific acquisition protocols. The first one, called LowRes (described in Coupel-Ledru et al., 2019) consisted in taking a scan in the middle of the row every 5 trees, in the different rows of the orchard. With this protocol applied during 1 week, 250 trees with apples were scanned. A second protocol, called HiRes, consisted in scanning more precisely 31 trees: each being scanned from both sides. For the validation, mean and total weight of apple of each tree were measured allowing to estimate the number of apples. Additionally, synthetic data were generated by simulating LiDAR scans on 239 virtual apple trees from their 4 cardinal sides with the MAppleT model (Costes et al., 2008) and the PlantGL software (Pradal et al., 2009). Our training dataset was composed of 10 point clouds of apple trees, in which points were manually labeled into two classes (unknown or apple). It was complemented by a training dataset of 100 synthetic point clouds of simulated apple trees automatically labeled.

The first pipeline based on machine learning includes three steps. First, points are characterized with Fast Point Feature Histograms (FPFH) (Rusu et al., 2009). Second, based on the computed FPFH features and reflectance information from the LiDAR, a random forest model was trained to predict the class of each point. Third, points are clustered into individual apples using the DBSCAN algorithm. The second pipeline merge the two first steps by classifying points directly from their position and reflectance information using a deep learning model based on PointNet (Qi et al., 2017). Finally pipeline

performance was assessed by comparing the number of apple point clusters detected in each tree to the number of apples estimated during harvest.

Results and Discussion

The random forest model currently showed the best performance, with an accuracy of 0.76 at test stage. Using the same configuration, the PointNet based model performed worse with an accuracy of 0.60, certainly due to the limited size of the training data. Using the random forest model, the pipeline predicted the number of apples per tree on synthetic data with a high accuracy (linear regression coefficient c=1.03 and r^2=0.79). The accuracy was lower when applied on apple trees scanned with the HiRes protocol (c=2.18 and r^2=0.51) and even lower with the LowRes protocol (c=2.16 and r^2=0.23). A strong effect of the LIDAR position relative to the tree and consequently of the point cloud resolution was observed. Indeed, for the trees closest to the scan positions with LowRes protocol (i.e .for a distance tree-LIDAR nearly equivalent to HiRes protocol), the prediction was more reliable (c=2.16 and r^2=0.45) than for the farest trees from the scan positions (c=2.08 and r^2=0.07).

Conclusion

We compared two phenotyping pipelines based on machine and deep learning approaches and applied them to evaluate and virtually experience LiDAR acquisition protocols in order to improve the quality of canopy reconstruction and organ detection. Our results suggest that a tradeoff between scan resolution and accuracy of organ detection has to be considered in future protocols, depending on the objectives. This tradeoff may depend on the tree age and training systems. With limited ground truth data, our experience shows better results with machine learning approach. However, results of the deep learning model can certainly be improved with more realistic geometric models and scanning noise for the synthetic data and/or with a larger amount of annotated data from real scans.

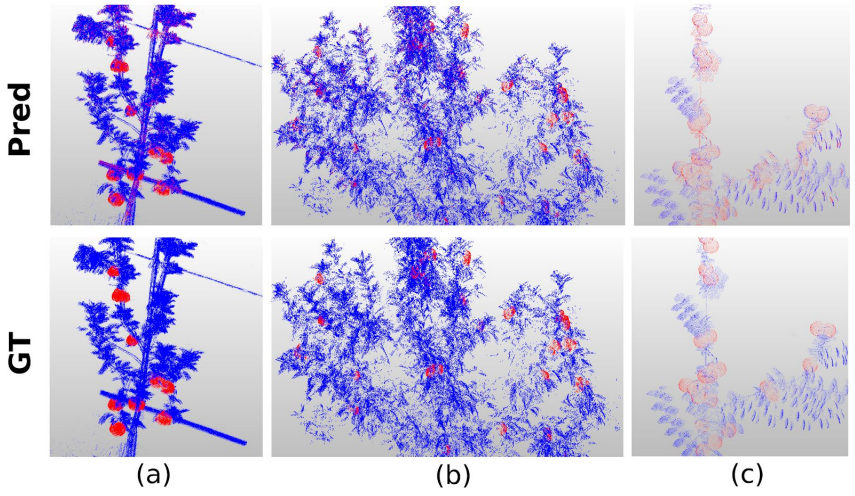

Figure1: Qualitative comparison of the results of our pipeline prediction (Pred) on ground truth (GT) validation dataset. (a) scan from HiRes protocol (b) scan from the LowRes protocol (c) simulated apple tree.

References (5 max)

Costes et al., 2008, Functional Plant Biology 35, 936-950, https://doi.org/10.1071/FP08081
Coupel-Ledru et al., 2019, Horticultural Research 6:52, https://doi.org/10.1038/s41438-019-0137-3
Pradal et al., 2009, Graphical Models, 71 : 1-21, https://doi.org/10.1016/j.gmod.2008.10.001
Qi et al., 2017, CVPR, The IEEE CVPR, 2017, pp. 652-660, arXiv:1612.00593
Rusu et al., 2009, IEEE International Conference on Robotics and Automation, 3212–3217

Spectral and angle dependent reflection properties of leaves

Jens Balasus[1], Tim Hegemann[1], Tran Quoc Khanh[1]

[1] *Laboratory of Lighting Technology, Technische Universität Darmstadt, Germany*

For correspondence: balasus@lichttechnik.tu-darmstadt.de

Keywords: optical leaf properties, led lighting, reflection

Introduction and Motivation

With the introduction of multi-channel LED plant luminaires in horticulture, a previously unavailable variety of spectral adjustment options is now available. Virtual plant models could be used to optimize their spectral composition and are already used today to gain information about light-plant interactions. Knowledge about the reflectance and transmission of leaves is essential for these kinds of studies. GroIMP offers the possibility to adjust the reflectance of surfaces through parameters (diffuse, specular, shininess) by using the Phong-shader (Henke and Buck-Sorlin, 2018). For a precise simulation of the spectral light distribution within canopies, information about the spectral and angle-dependent reflection properties of leaves are needed. Bousquet et al. (Bousquet et al., 2015) clearly showed, that there is a wavelength-dependent diffuse and specular component in reflection. In this work, a method to find suitable parameters for light simulation based on a measured spectral bidirectional reflectance distribution function (BRDF) is presented and discussed.

Materials and Methods

To measure the spectral leaf BRDF a gonioreflectometer (GRM) as described in (Li et al., 2006) is used. Measurement on a cucumber leaf is performed to get sample data. During this, the light angles of incidence (AOI) are varied between -60° and 60° in steps of 15°. The spectral reflectance is measured in angles ranging from -55° to 55° in steps of 5°. Relative spectral reflectance is calculated from the measured reflectance and the incident light. Reflectance and incident light are measured in the same layer, so the leaf is assumed to be isotropic.

On the digital side, a setup of a plane surface in GroIMP surrounded by a circular array of sensors is used. The surface shader is set as Phong. In the experiment, Phong-parameters are varied using Bayesian optimization. The root-mean-square error (RMSE) between the simulation data and the measured one is minimized within 100 iterations. Parameters are determined for wavelengths between 440 and 740 nm in 5 nm steps. The Phong-parameters are used to perform a simulation with other light incident angles to compare the results with the measured ones by calculating the RMSE.

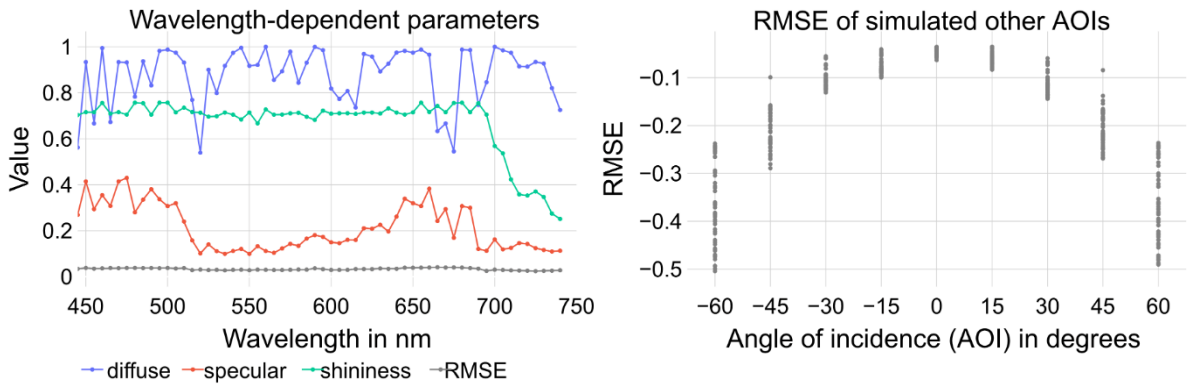

Figure 1 One possible combination of wavelength-dependent Phong-parameters with RMSE between simulation and measurement for one measured leaf (left). RMSE of simulated and measured values in dependency of AOI (right).

Results and Discussion

Figure 1 (left) shows the difference within spectral ranges. The specular component is highest in the blue and the red region. The shininess is rather constant with lower values in the far-red region. Particularly interesting is the variation between red and far-red light. This could be especially important for the simulation of the red to far-red ration. The diffuse part shows no systematic wavelength dependence, this could be because only relative distributions were calculated, and the diffuse part has no significant impact on these.

Figure 1 (right) shows the RMSE between simulations with the given parameters and the measured data with different AOIs. With larger AOIs the error increases, especially for those over 45°.

The focus in this work is on the process of getting parameters for the simulation with Phong-shader. First results seem promising that fitting parameters can be found in this way. A few things need to be considered or improved in future studies: (1) More measurements, also with different leaf ages and different plants are going to be performed. (2) Found parameters were only evaluated in a simple geometric setting, more complex scenarios are going to be evaluated to investigate the error made by using Phong-shader. (3) Measurements were only performed in one layer, assuming an isotropic reflection type. (4) Only relative distributions were considered; simulation parameters for absolute distribution need to be found. (5) Parameters for transmission need to be evaluated.

References

Henke, M., & Buck-Sorlin, G. H., 2018, Using a full spectral raytracer for calculating light microclimate in functional-structural plant modelling. *Computing and Informatics*, 36(6): 1492-1522.

Bousquet, Laurent, et al., 2005, *Remote Sensing of Environment* 98: 201-211, doi: 10.1016/j.rse.2005.07.005

Li, H., Foo, S. C., Torrance, K. E., & Westin, S. H., 2006, *Optical Engineering, 45*(4), doi: 10.1117/12.617589

Quantifying the effects of carbon status on berry growth using a mechanistic carbon transport model

Junqi Zhu[1], Fareeda Begum[2] , Gerhard Rossouw[3], Bruno Holzapfel[3], Michael Henke[4], Alla N Seleznyova[5]

[1] *The New Zealand Institute for Plant & Food Research Limited (PFR), Blenheim 7201, New Zealand*
[2] *Department of Mathematics and Statistics, University of Canterbury, Christchurch 8041, New Zealand*
[3] *National Wine and Grape Industry Centre, Charles Sturt University, Wagga Wagga, NSW, 2678, Australia;*
[4] *Leibniz Institute of Plant Genetics and Crop Plant Research (IPK), OT Gatersleben, Corrensstrasse 3, D-06466 Stadt Seeland, Germany*
[5] *The New Zealand Institute for Plant & Food Research Limited, Palmerston North 4442, New Zealand*
For correspondence: Junqi.zhu@plantandfood.co.nz

Keywords: carbon transport, GrapevineXL, phloem sucrose concentration, xylem water potential, berry growth

Introduction

The dynamics of the fruit population is affected by multiple factors changing during the course of fruit development including canopy structure, light distribution, carbohydrate accumulation and transport, location of individual fruits within the canopy and their proximity to sources and other sinks. Quantitative methods are essential for disentangling these factors and evaluating their respective roles. Previously developed GroIMP-based whole-plant grapevine model GrapevineXL (Zhu et al., 2019) simulates the effects of variations in environmental conditions (e.g., soil water potential and radiation etc.), plant water status (e.g., xylem and leaf water potential) and carbon status (e.g., phloem sucrose concentration) on post-véraison grape berry growth with a static canopy architecture. However, this model assumes uniform xylem water potential and phloem sucrose concentration (C_p) throughout the shoot. Therefore the GrapevineXL model was extended with a mechanistic carbon transport model (Seleznyova et al, 2018) to allow further investigations of the effects of canopy structure, C_p and distribution of C_p along shoot on fruit growth.

Model development

We included the hydraulic properties of the shoot (Albasha et al., 2019) and adopted a mechanistic phytomer-level model of coupled phloem/xylem transport (Seleznyova et al, 2018) developed in L-Studio to improve the capacity of the GrapevineXL model to simulate intra-vine competition. The carbon transport in the model is driven by carbon-concentration-dependent sink/source activities. At each time step, the model finds steady-state solutions for carbon concentration distribution and fluxes within the plant. Although GroIMP has built-in numerical methods for solving ordinary differential equations (Hemmerling et al., 2013), which in principle could be applied for solving mechanistic Munch-based equations for coupled phloem/xylem transport in systems with dynamical structure, so far these methods were implemented mainly for diffusion-driven transport. Solving for Munch-based equations would add additional complexity due to non-linearity of the problem. Hence we used alternative methods specifically developed for mechanistic modelling of quasi-stationary phloem/xylem transport in systems with dynamical structure (Seleznyova et al., 2018). For this purpose, a special procedure was developed in GroIMP to enforce it to perform the same calculation sequences as it was in L-Studio version.

Model calibration and simulations

The carbon allocation between different components was calibrated using field-grown potted vines (Rossouw et al., 2017). The experiments had three leaf treatments nine days after the start of véraison: 0, 25, 100 leaves per vine. Three vines from each treatment were destructively harvested every 9–10 days after the start of the experiment. The fresh and dry weight of the whole root systems, leaf blades, trunk, shoot and all berries were determined for each vine. Total non-structural carbohydrates were determined for root, leaf and berries.

Potential growth rates were determined either based on the pot experiment (Rossouw et al., 2017) or our previous studies. Parameters related to the carbon transport, e.g. Michaelis-constant were first taken from the GrapevineXL and L-Kiwi (Cieslak et al., 2011) and then explored by trial and error to ensure the simulated trends were in agreement with experimental data. Five key parameters which determine the carbon unloading responses of berry, root, internode and trunk to C_p and the rate of starch hydrolysis in root, internode and trunk were selected for fine optimization. Two hundred parameter combinations were generated using the function of parameterSets in the R Sensitivity package. The simulation results of GrapevineXL based on those parameter sets were inputted into a Gaussian process emulator for developing statistical models between the parameter values and the model output. The derived statistical model was further used for optimizing the parameter values given the observed data. The optimized parameter values were then used GrapevineXL for further validation and optimization.

Results and Discussion

The model confirmed the gradient of carbon concentration in phloem transport pathways, and showed that the shoot has the highest carbon concentration under 100 leaves per vine while the root the highest carbon concentration under 0 leaves per vine. The model reproduced the dynamics of berry dry matter with 100 leaves per vine and captured the effects of carbon stress on berry growth under the treatment of 0 leaves per vine (Figure 1). Further investigations are being conducted on the effects of position (relative distance to the sources), different trellis systems, and the effect of the relationship between leaf area and fruit load on berry ripening. We aim to determine the minimum leaf area to fruit load ratio in different trellis systems that would ensure berry ripening and sufficient carbon reserve in root and trunk for next season's bunch and shoot growth.

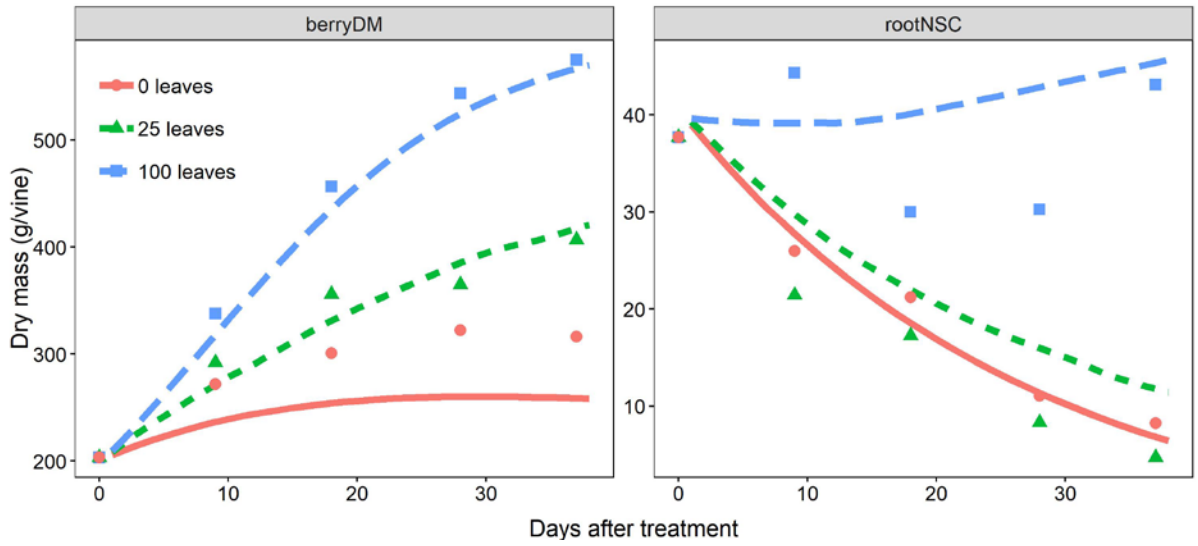

Figure 1: Model verification of the simulated dynamics of berry dry mass and total root non-structural carbon per vine under different leaf treatment.

References

Albasha et al., 2019. In silico Plants, 1(1). doi:10.1093/insilicoplants/diz007
Cieslak et al., 2011. Annals of Botany, 107(5), 747-764. doi:10.1093/aob/mcq180
Hemmerling et al.,2013. Computers and Electronics in Agriculture, 92(0), 1-8. doi: 10.1016/j.compag.2012.12.007
Rossouw et al., 2017. Physiol Plant, 161(4), 434-450. doi:10.1111/ppl.12604
Seleznyova et al., 2018. Annals of Botany, 121(5), 991-1003. doi:10.1093/aob/mcx204
Zhu et al., 2019. Journal of Experimental Botany, 70(9), 2505-2521. doi:10.1093/jxb/ery367

High-Efficient Modeling of Canopy Structure of Field-Grown Crops based on UAV Images

ZHU Binglin[1], LIU Fusang[1], ZHENG Bangyou[2], HU Pengcheng[2], DUAN Tao[3], GUO Yan[1]

1 College of land science and technology, China Agricultural University, Beijing, China

2 CSIRO Agriculture and Food, Queensland Biosciences Precinct, Queensland, Australia

3 Institute of Microelectronics of Chinese Academy of Sciences, Beijing, China

For correspondence: yan.guo@cau.edu.cn

Abstract

Introduction Rapid and high-throughput crop phenotyping has been proposed recently to significantly improve plant breeding efficiency (Sankaran et al., 2015). Different phenotypic platforms have been developed for indoor and outdoor applications. However, they are usually expensive and large with poor flexibility and portability (Virletet al.,2017). With the miniaturization of unmanned aerial vehicles (UAVs) and the performance enhancement of mounted sensors, it is now feasible to use UAVs to collect high-resolution images in the field to quickly obtain accurate canopy structure and estimate phenotypic parameters of field-grown crops.

Materials and Methods We employed a Mavic 2 Pro micro UAV (DJI, China) to capture image sequences of field-grown maize canopy at different growth stages (i.e. seedling and mature). The three-dimensional (3D) canopy point clouds were reconstructed using the image sequences. The support vector machine (SVM) classifier was then used to classify the point clouds into vegetation and non-vegetation (e.g. soil surface). For vegetation point clouds at the late growth stages, we used maximum likelihood estimation sample consensus (MLESAC) algorithm (Terr and Zisserman, 2000) to remove the noisy vegetation points of the leaf residues on the ground. The remaining noisy points were identified and removed by the *k*-nearest neighboring algorithm.

Based on the preprocessed point clouds, pseudo pole-Crust algorithm (Amenta and Bern, 1999) was applied to reconstruct the canopy structure models which were represented by facets. Abnormal facets (i.e. the individual facets with abnormally long side length) were filtered and eliminated. The leaf edges were smoothed by adjusting the normal direction. Finally, the reconstructed models were evaluated through the comparision with the field measurements of plant height, blade length, blade maximum width and blade area.

Results and discussion A good agreement was obtained between the measured and estimated plant height, blade length and blade maximum width with R^2 higher than 0.90 and the RMSE, rRMSE, ME achieved superior performance for different growth stages. Consistent with previous research, these results demonstrated that agreement on early growth stages conformably outperformed late growth stage with R^2 varying from over 0.90 to 0.70 for blade area. As RMSE, rRMSE, ME increased, the accuracy of the calculation dropped slightly at the mature stage.

Conclusion Using the multi-view images collected by UAV in the field, the point clouds of maize canopy were reconstructed for canopy structure modeling. The results indicated that we can efficiently reconstruct the canopy structure of maize and extract the phenotypic values related to leaf shape and area at the organ scale. Considering

that existing methods (e.g. 3D digitalization) are time-consuming and invasive in term of data collection of canopy structure, our method has the substantial advantage as the multi-view images of a canopy can be quickly and noninvasively collected in the field. The proposed method provides a promising prospect for high-throughput 3D modeling and phenotyping of plant structure of field-grown crops.

Key words: unmanned aerial vehicles, maize, multi-view images, functional-structural plant modelling, phenotyping

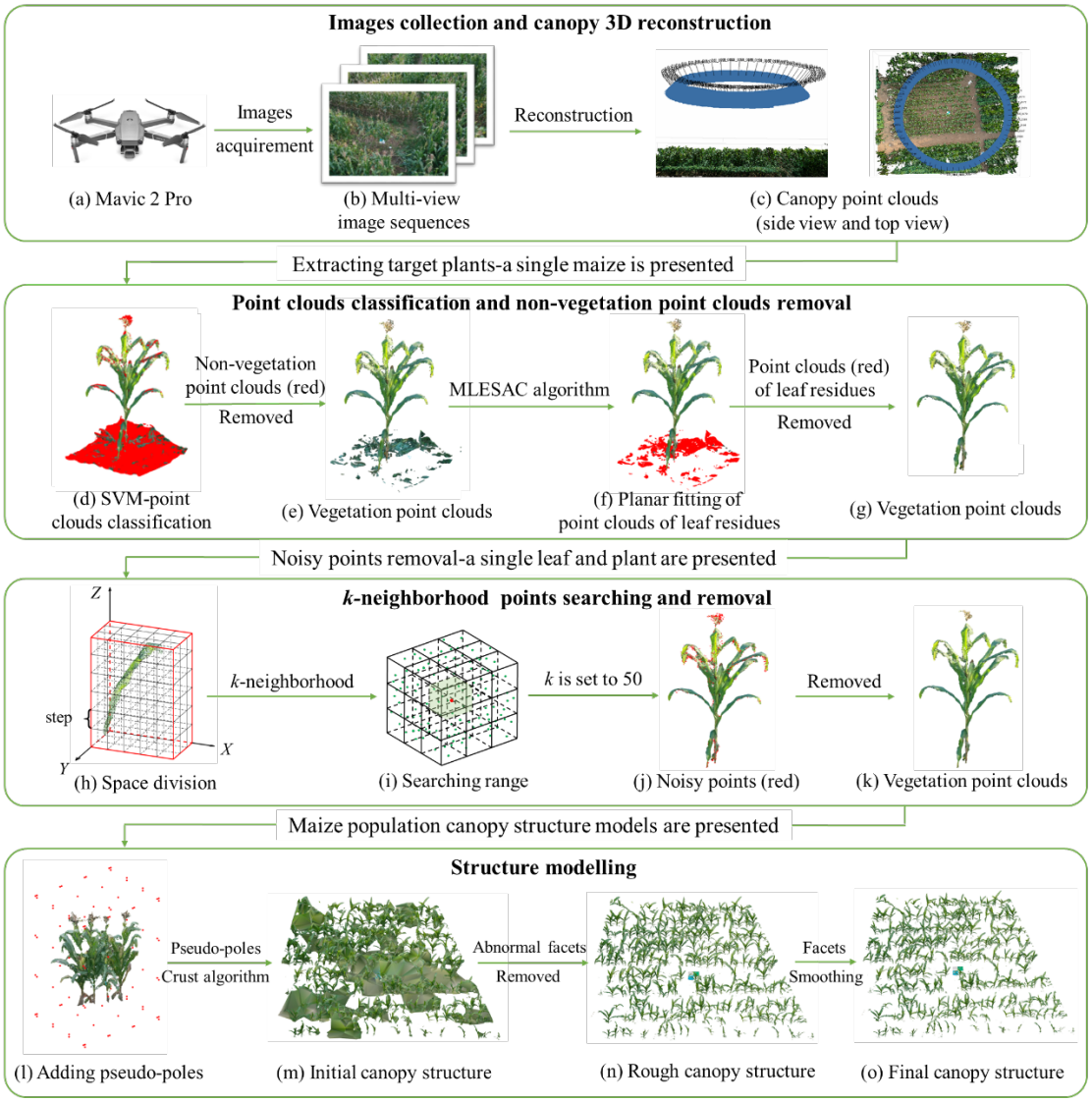

Figure: Pipeline of image acquirement, canopy point cloud reconstruction, data preprocessing and canopy structure modelling

References

Sankaran S et al., 2015, *European Journal of Agronomy* 112–123, doi: 10.1016/j.eja.2015.07.004

Virlet N et al., 2017, *Functional Plant Biology* 143–153, doi: 10.1071/FP16163

Torr P H S and Zisserman A, 2000, *Computer Vision and Image Understanding* 138–156, doi: 10.1006/cviu.1999.0832

Amenta N and Bern M, 1999, *Discrete & Computational Geometry* 481-504, 10.1007/PL00009475

What structural plant modelling and image-based phenotyping can learn from each other?

Christian Fournier[1], Simon Artzet[1], François Tardieu[1], Christophe Pradal [2,3]

[1] *LEPSE, INRA, Univ. Montpellier, Institut Agro, Montpellier, France*.
[2] *CIRAD, UMR AGAP & inria, Zenith team, Montpellier, France*
[3] *AGAP, Univ. Montpellier, CIRAD, INRA, Institut Agro, Montpellier, France*

For correspondence: christian.fournier@inrae.fr

Keywords: model-oriented phenotyping, high throughput phenotyping, maize, architecture, development

Introduction

High throughput phenotyping technologies have spread rapidly in the recent years to meet the demand for phenotyping of large panels of plants, covering a large genetic diversity and a large range of environmental conditions. Image-based technology, which allows following the architectural development of plant over time, is among the most popular, due to its simplicity, to a high degree of automation of the acquisition process, and to the richness of the information acquired. The automation of the analysis process is also actively developing (Ubbens et al., 2020), which offers unprecedentedly large and detailed dataset for plant modelling and for the development of new applications. Linking phenomics and crop modelling allows for example already to integrate the genetic variability of responses of plants to the environment, and to reason which combination of alleles is desirable for different pedo-climatic conditions, for present and future climate (Tardieu et al, 2017). By design, crop models however do not capture in details the architectural development of plants, that is the core data produced by image based phenomics. Using and adapting structural (functional) plant models for the analysis of such data will potentially minimise the loss of information, improve the modelling at fine scale and provide simulation tools that can be used as new source of information for crop modelling. Our objective is to experiment such a coupling for maize architectural development, and discuss how it may affect modelling and phenotyping.

Materials and Methods

Multi-view images from a large phenotyping experiment (1600 plants, 40 days) performed on the PhenoArch platform (https://www6.montpellier.inra.fr/lepse/M3P/PHENOARCH) are analysed with the Phenomenal image analysis pipeline (Artzet et al., 2019), which generates, for each plant, a sequence of 3D reconstructions at different stages of development (Figure 1A). Phenomenal also allow to segment the plant into smaller components (stem and individual leaves), and extract phenotypic feature such as leaf length, leaf width and leaf angles. We first use these data to parameterise, one-time point at a time, a static structural model of maize (Fournier et al., 2012) (Figure 1B). The different time points are then used together to estimate a dynamic model of plant development as a function of temperature (ADEL-maize, Fournier et al., 1998) (Figure 1C). To evaluate the quality of the representation of these two nested levels of simplification, virtual plants are illuminated with a light model and compared for their interception efficiency in several conditions (isolated plants and self-similar canopies, under clear sky and overcast conditions). We also assess how the raw phenotypic features extracted by Phenomenal compare to those simulated by the dynamic model.

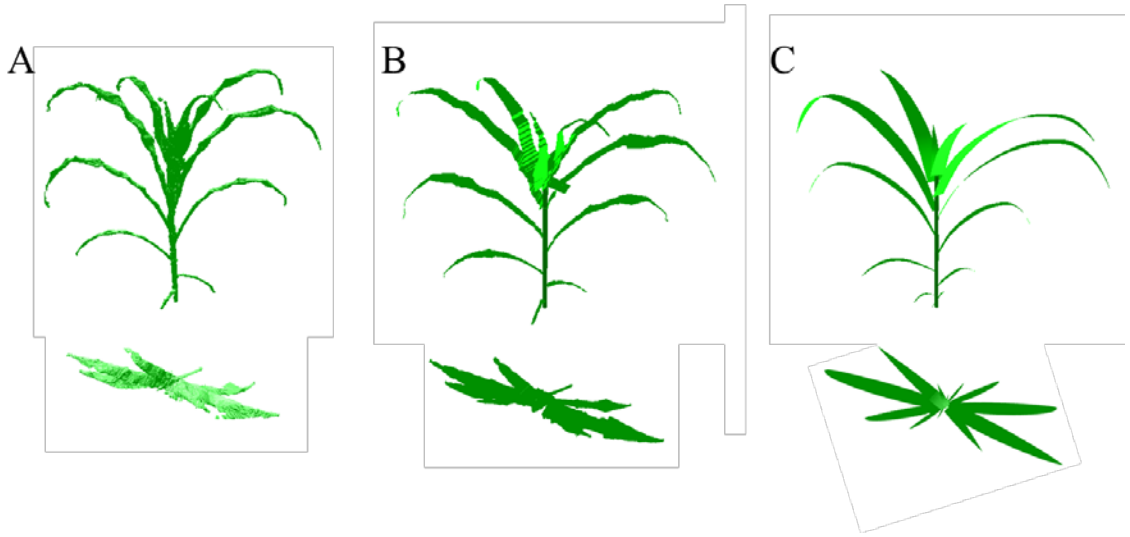

Figure 1: 3 Perspective and top view of maize plants, at different stages of the analysis pipeline. A : Raw 3D plant reconstructed as a set of voxels, with the Phenomenal pipeline. B: 3D virtual plant simulated by a static plant model fitted to the data. C: 3D virtual plant simulated by a dynamic plant model fitted to the entire developmental sequence.

Result and discussion

Each modeling step results in a high level of compression of the data, the highest level being between the raw plant and the static model (from 1A to 1B). The first compression is essentially linked to the simplification of the specification of the geometry (from voxels to meshes) and to the use of construction rules. The second compression is linked to the use of parametric models that capture the evolution of the objects with time, but with simplifications. In terms of light interception, all models yield similar value for self-similar canopy simulation. For isolated plants, the static model produces interception values similar to raw data, but the dynamic model can have up to 50% difference on interception in zenithal direction. This is explained by an over simplification of the leaf reorientation patterns. Fitting the dynamic model allows to improve the different measurements of plant organs (lengths, width, ..). This is explained by the compilation of the repetition of the measurements over time. The dynamic model allows to get temporal leaf tracking and to identify artifacts in the segmentations. Combining raw data and leaf tracking finally allows to extract dynamics patterns of development, including the sequence of leaf reorientation, that could be used for modelling.

Conclusions

Fitting a structural plant model to elaborated phenotyping data acquired in a platform was beneficial both for model improvement and data analysis. The improved model more closely matches the interception efficiency of observations and has more robust parameterisations. Data analysis was enriched with dynamical features and benefits from averaging of repeated measurements. As a result, we obtain a fully parameterised structural model for hundreds of genotypes. Foreseen application of such a model range from multi-genotype analysis of plant development, use in interpretation of phenotyping data in the field and ideotyping.

References

Artzet et al. 2019, https://doi.org/10.1101/805739
Fournier et al. 1998, *Ann. Bot.*, 81 233.https://doi.org/10.1006/anbo.1997.0549
Fournier et al. 2012, *IEEE,* 125 10.1109/PMA.2012.6524823
Tardieu et al., 2017, *Current Biology*, 770, https://doi.org/10.1016/j.cub.2017.05.055
Ubbens et al., 2020, *Plant Phenomics*, 2020,5801869, 10.34133/2020/5801869

Improving interoperability between phenomics and modelling communities by designing a Plant Modelling Ontology (PMO)

Clément Saint Cast[1], Guillaume Lobet[1,2], Llorenç Cabrera-Bosquet[3], Valentin Couvreur[1], Christophe Pradal[4,5], Bertrand Muller[3], François Tardieu[3], Xavier Draye[1]

[1] Earth and Life Institute, Université catholique de Louvain, 1348, Louvain-la-Neuve, Belgium
[2] Agrosphere, IBG3, Forschungszentrum Jülich, 52428, Jülich, Germany
[3] INRAE, LEPSE, Montpellier SupAgro, Université de Montpellier, 34060, Montpellier, France
[4] CIRAD, AGAP, 34398, Montpellier, France
[5] AGAP, Université de Montpellier, CIRAD, INRAE, SupAgro, Montpellier, France

For correspondence: clement.saintcast@uclouvain.be

Keywords: ontology, interoperability, modelling, phenomics, collaborative standard design

In recent years, plant phenomics has produced massive datasets involving millions of images in experiments performed in the field and in controlled conditions, concerning hundreds of genotypes at different phenological stages and scales (Tardieu et al., 2017). In the future, information extracted from these datasets will be used increasingly as variables or parameters of mathematical and computational models, thereby broadening the scope of information extracted from phenomics data (Muller and Martre, 2019). Feeding such data to structural plant models (SPMs), functional plant models (FPMs), functional-structural plant models (FSPMs) and process-based crop simulation models (CSMs) in ad hoc pipelines has the potential to derive high-throughput predictions of integrated (e.g. yield) or functional traits (e.g. root system architecture) across a wide range of target environments or management practices (Chen et al., 2019). Unfortunately, the connectivity between these two communities is greatly limited by the absence of a common semantic framework and harmonized vocabulary.

Currently, the terminology (e.g. objects, variables) used by these communities can be quite heterogeneous depending on the research discipline, scale and objective and even can differ between research groups. This limits the ability to accurately relate information within and across communities. A solution to facilitate the connection and the exchange of information is the use of a controlled and standardized vocabulary of common and internationally recognized descriptive terminology that can be connected and shared uniformly among the communities. The phenomics community has tackled these issues by reusing existing ontologies (e.g. Plant Ontology – PO or Plant Trait Ontology – TO), developing new standards (e.g. MIAPPE) as well as ontology-driven information systems (e.g. PHIS). Similarly, some initiatives have been developed within the crop modelling community such as the ICASA Master Variables List (ICASA-MVL) and the AgMIP data standards and data translator tools, the recent functional-structural root architecture modelling community or some open software platforms (e.g. OpenAlea). However, despite these recent developments no ontology describing the variable inputs, the variable outputs and the parameters of the plant models exists and can be used to facilitate exchange in and across communities. One solution to this problem involves the development of structured controlled vocabularies for the plant modelling community arranged in a new ontology (Plant Modelling Ontology – PMO).

The goal of the PMO is to produce structured controlled vocabularies of the variables and parameters used by mathematical and computational models (SPMs, FPMs, FSPMs and CPMs) with clear definitions and relations with the existing phenomics ontologies (e.g. description of the phenomics variables used in the parameter estimations). In addition of the benefit to find compatibilities between phenomics datasets and plant models using ontologies (Figure 1), the PMO facilitates the connexion between the models themselves, promoting the design of multiscale models (Christensen et al., 2018) or the intercomparisons of models (Athanasiadis et al., 2009). This new project, initiated and supported by the European infrastructure EMPHASIS, involves an interdisciplinary collaboration in order to:

1) **Inventory and define the vocabulary used by the plant models.** We compile a list of the variable inputs, variable outputs and parameters used by the plant models.

2) **Formalise terms and their relationships in a common ontology.** We formalise the terms and establish relations and properties within and between the different terms used in modelling and plant phenomics by using semantic web technologies (e.g. OWL).

3) **Develop a web application.** We design an interactive web companion for model developers and users to identify possible connections between plant models' variables and parameters and phenomics datasets. This application helps to design model-based data analysis pipelines.

Following the recent development of quantitative-plant.org (a website referencing plant and crop simulation models), we take advantage of this new network to engage the interest of the plant modelers in the development of a Plant Modelling Ontology. The design of this ontology aims to be a collaborative effort by defining the terms used by any group or researcher using or developing a plant model. One important aim of this activity is a joint publication and web services that show the proposed Plant Modelling Ontology as well as an overview of connections with the phenomics community. In the future, a long-term cooperation between the phenomics and modeling communities towards the development of common platforms could be designed to enable transparent data exchange from models to experiments and vice-versa.

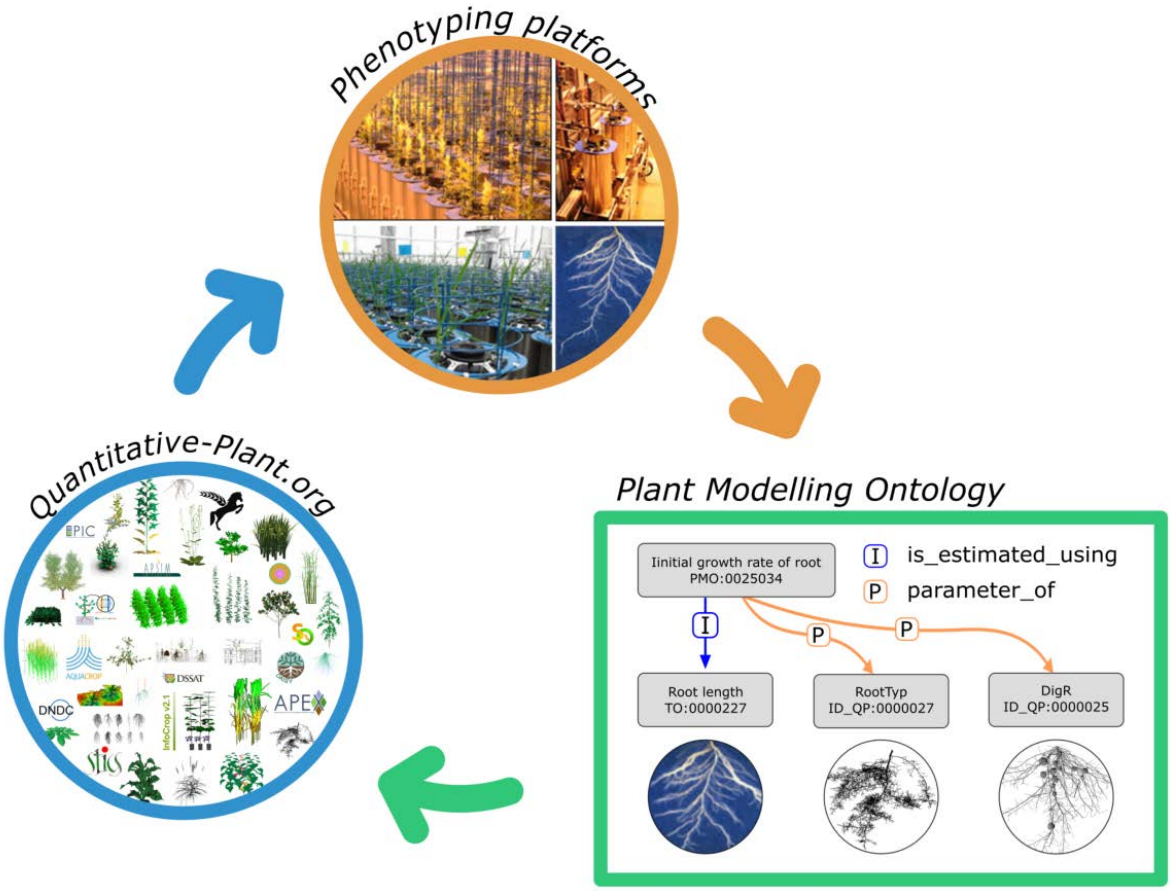

Figure 1: Schematic representation of the connexion between the phenomics and the modelling communities using a Plant Modelling Ontology (PMO)

References

Athanasiadis et al., 2009, *Metadata and Semantic Research*, doi: 10.1007/978-3-642-04590-5_27
Chen et al., 2019, *Journal of Experimental Botany* 70: 2523–2534, doi: 10.1093/jxb/ery309
Christensen et al., 2018, *Nutrition Reviews* 76: 332–347, doi: 10.1093/nutrit/nux076
Muller and Martre, 2019, *Journal of Experimental Botany* 70: 2339–2344, doi: 10.1093/jxb/erz175
Tardieu et al., 2017, *Current Biology*, doi: 10.1016/j.cub.2017.05.055

Modelling canola for image-based phenomics

Mikolaj Cieslak[1], Nazifa Khan[2], Raju Soolanayakanahally[3], Ian McQuillan[2], Pascal Ferraro[1], Steve Robinson[3], Isobel Parkin[3], Przemyslaw Prusinkiewicz[1]

[1] *Department of Computer Science, University of Calgary, Calgary, Canada*
[2] *Department of Computer Science, University of Saskatchewan, Saskatoon, Canada*
[3] *Agriculture and Agri-Food Canada, Saskatoon, Canada*

For correspondence: mscieslа@ucalgary.ca, pwp@ucalgary.ca

Keywords: *Brassica napus* L., model calibration, L-system

Forward phenomics relies on screening collections of plants to identify those with desirable traits (Furbank and Tester 2011). As traditional plant-measurement techniques are impractical for screening large numbers of plants, computer vision (image-based phenotyping) has been proposed as an alternative. Vision algorithms employing artificial neural networks and deep learning show particular promise (Singh et al., 2018), but their training requires large sets of annotated images, which are themselves difficult to obtain. Plant models that can be used to automatically generate large sets of realistic annotated images alleviate this problem (Ubbens et al., 2018). The question is how to create and calibrate these models accurately and quickly.

We describe a parametrized procedural model of canola (*Brassica napus* L.), which we designed to generate large sets of images representing different canola phenotypes. The model is specified in the L-system-based L+C modeling language, and implemented within the Virtual Laboratory (vlab) plant modeling environment (Prusinkiewicz 2004). It specifies the general architecture of canola plants as an L-system simulating plant development. Quantitative aspects including the size and density of plant components (higher-order branches and plant organs: leaves, flowers and siliques) are defined as functions of their position on the supporting branches (Prusinkiewicz et al., 2001). This use of positional information is a crucial aspect of the model, resulting in an intuitive relation between the functions and the plant attributes they control.

During model calibration, the functions are interactively manipulated by the modeler to match images representing sample plants and their development over time. To facilitate interactive specifications of functions and comparisons of models with reality, we extended the vlab plant simulator (lpfg) and interactive function and shape editors with the capability of showing images of real plants in the background. Changes of any function are immediately reflected in the model, providing crucially important instantaneous visual feedback to the modeler.

We developed the model using time series images of a single canola plant grown in a greenhouse (Fig.1 A,B). We further calibrated it using a large collection of canola plants images representing approximately 300 individuals from 90 diverse genotypes grown under controlled and water-stressed conditions. These images were captured daily for 40 days using the LemnaTec indoor plant imaging system. Every day, the data set for each plant consisted of 10 side views, rotated by 36° with respect to each other, and a top view. The calibration process relied on visual comparisons of the reference plant images with the parametrized model (Fig.1 C,D). This reliance on the human vision system is acceptable, as the objective is to use the model to automatize the visual inspection of plants as opposed to measuring them.

We found that the model can reproduce diverse sample phenotypes and is likely capable of generating the entire range of canola phenotypes. The interactive manipulation of model parameters (positional functions) is straightforward. The diverse representatives of the same

phenotype needed as training data for deep learning can be obtained by modifying model parameters using normally distributed random variables. Our implementation also allows for many plants to be arranged into fields, with simulated interactions between individual plants including mechanical responses to crowding (Fig. 1 E-H).

In addition to image-based phenotyping, the model can be used to explore novel phenotypes *in silico*, by varying parameters associated with biological factors and estimating the fitness of the resulting plants via simulation ('virtual profiling'; Génard et al., 2010). Principal component analysis or T-distributed Stochastic Neighbor Embedding can be used to identify key phenotypical variables that capture the differences between distinct canola plants. Finally, the canola model can be extended to link genotypes with phenotypes, accelerating crop development via simulated virtual breeding.

References

Furbank and Tester, 2011, *Trends in Plant Science* 16(1): 635-644, doi: 10.1016/j.tplants.2011.09.005
Singh et al., 2018, *Trends in Plant Science* 23(10): 883-898, doi: 10.1016/j.tplants.2018.07.004
Ubbens et al., 2018, *Plant Methods* 14(6), doi: 10.1186/s13007-018-0273-z
Prusinkiewicz et al., 2001, *Proc. of SIGGRAPH*, pp. 289-300.
Prusinkiewicz, 2004, *Acta Hort*. 630, pp. 15-28
Génard et al., 2010, *The Plant Journal* 62:344-355, doi: 10.1111/j.1365-313X.2010.04152.x

Figure 1: Visual comparison of photographs of real canola plants (A,C,E,F) to images generated by the model (B, D,G,H). (A,B) Five stages of the development of an individual plant. (C,D) Three diverse canola phenotypes at approximately 40 days after sowing. (E-H) Two stages of canola growing in the field. Photographs (E,F) courtesy of the Plant Phenotyping and Imaging Research Centre, University of Saskatchewan).

Three-dimensional morphological model of water lilies *Nymphaea spp.* for breeding historical study

Shiryu Kirié[1], Christophe Pradal[2], Hideo Iwasaki[3], Koji Noshita[4], Hiroyoshi Iwata[1]*

1. Graduate School of Agricultural and Life Sciences, The University of Tokyo, Tokyo
2. CIRAD, UMR AGAP & Inria, Univ Montpellier, Montpellier, France
3. School of Advanced Science and Engineering, Waseda University, Tokyo
4. Graduate School of Science, Kyushu University, Fukuoka

For correspondence: iwata@ut-biomet.org

Keywords: Theoretical morphology, *Nymphaea*, Horticultural study, Flower morphology

Introduction

The water lilies *Nymphaea* spp. show a wide range of morphological features obtained through the horticultural breeding performed over 100 years, and diverse cultivars were created in the breeding history, such as those drawn by Claude Monet. We aim to understand how the floral morphologies have evolved to enhance their ornamental value. We propose a 3D morphological theoretical model to represent the floral structure of water lily. We will present a model to enable realistic representations from real data, such as the shape of the contour of a floral organ, and applications for our goal.

Model overview

The theoretical morphological model of the water lily is an algebraic operator that allows composing morphological models of floral organs using a model of phyllotaxis to generate a 3D flower architecture. Each floral organ is generated from a function that computes a three-dimensional C-spline surface from the size and lateral and longitudinal curvature. The ovary was represented by a curved surface obtained by rotating a two-dimensional C-spline curve around the vertical axis. The spiral phyllotaxis operator was designed for the arrangement of floral organs on the ovary surface. Here, as the expression of the spiral phyllotaxis, intervals between adjacent organs are assigned based on the ratio of those sizes, and each floral organ is arranged with rotation by the golden angle (137.5°). These settings on the phyllotactic pattern is based on previous studies (eg. Prusinkiewicz et al. 2001 [1]). We adopted linear interpolation between angles of the outermost floral organ and the innermost floral organ for the expression of the series of elevation angles. A 3D morphological model is obtained by combining all these parametric operators.

Result

Spline surfaces enabled flexible control of the theoretical morphological model. By extracting and applying parameters from image data of the floral organs, we were able to represent the morphology of water lilies as a three-dimensional form on a computer. Thus, even if it is challenging to acquire a three-dimensional morphology directly, it is possible to reproduce a morphology of the flower from the scanned two-dimensional image of each organ. The morphological model of the water lily flower can also be used to evaluate the three-dimensional morphological characteristics with geometrical indices, for example, using the convex hull, and these indices can be used to define an ideotype quantitatively. This information provides us the structural and qualitative understanding of morphological changes under the breeder‘s perspective.

Discussion and conclusion

Diverse horticultural varieties of water lilies are commercially distributed, and they display a wide range of morphological characteristics to enhance ornamental values. In horticultural catalogs of water lily, There are some types of qualitative descriptions of flower shape, like the “stellate“ or the “cup-like“. The relationship between geometrical indices and qualitative descriptions can display occupation patterns indicating quantitative correspondence in the morphospace. This model can be applied to evaluate the characteristics of existing varieties and facilitating the breeding process of new cultivars by linking genotypic information and developmental mechanism. The *Nymphaea* spp. are expected to be used as "model clades" in recent years (Chanderbali et al. 2016 [2]), and this study, which enables comparison of morphological characteristics between different varieties, may be applicable to the study of flower evolution and development, and for ideotype design.

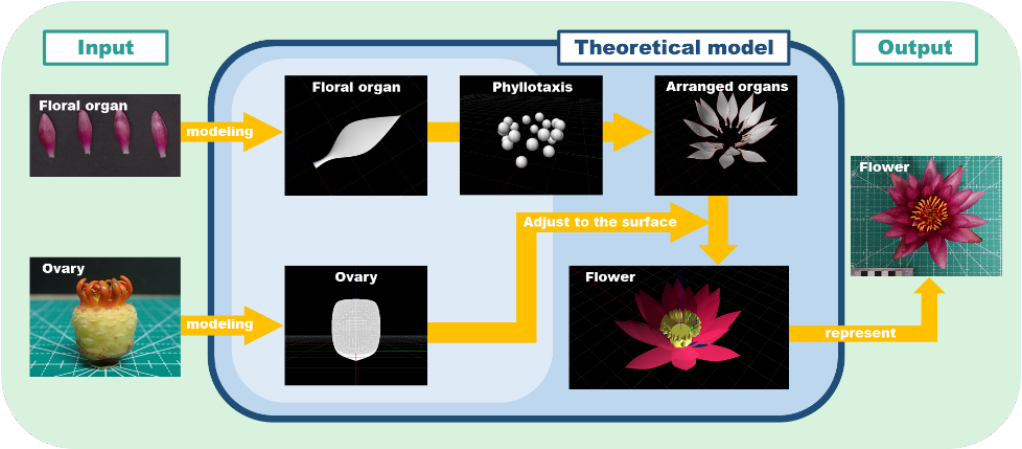

Figure: The overview of the modeling of flower morphology of *Nymphaea spp.*

Reference

[1] Prusinkiewicz et al. 2001, Proceedings of the 28th Annual Conference on Computer Graphics and Interactive Techniques, SIGGRAPH 2001, 289-300
[2] Chanderbali et al., 2016, *Genetics,* 202:1255-65.

UAV imagery and Functional-Structural Plant Modelling unravel distinct drought tolerance strategies in soybean genotypes

Tom De Swaef[1], Irene Borra-Serrano[1], Aamir Saleem[1], Jonas Aper[1], Isabel Roldán-Ruiz[1], Peter Lootens[1]

[1] Plant *Sciences Unit, Institute for Agricultural and Fisheries Research (ILVO), Melle, Belgium*

For correspondence: tom.deswaef@ilvo.vlaanderen.be

Keywords: Thermal camera, RGB camera, plant water potential, plant height, stomatal conductance

Introduction

Drought stress affects multiple physiological mechanisms in soybean, among others phenology, nitrogen fixation, flower abortion and organ growth. Each of these mechanisms is affected differently and the impact varies with the growth stage of the crop, but overall, drought stress can invoke yield reductions exceeding 40%. Given the fact that dry spells are expected to become more intense and more frequent in North Western Europe, breeding drought tolerant varieties is an important climate change adaptation strategy. Consequently, phenotypic traits promoting drought tolerance are under great attention. A major challenge in phenotyping remains in the interpretation and transferability of observations, as the drought response is very complex and to a large extent influenced by the environment and management. Moreover, measurement of some variables like the plant water potential, which is generally considered as one of the best plant water status indicators, currently relies on destructive sampling and is not fit for high throughput phenotyping. Nonetheless, it is crucial to identify genotypes with complementary drought tolerance strategies to design improved crossing strategies, and ultimately improve drought stress tolerance.

Therefore, we present an approach that uses UAV based plant height (Borra-Serrano et al., 2019) and canopy temperature observations in combination with a simplified soybean functional structural model. This model is based on the model of Tuzet et al. (2003), which provides a whole plant water transport description including drought induced stomatal closure. Moreover, this model enables continuous simulation of the plant water potential. We further extended this model with a model of plant growth driven by turgor pressure, to enable linkage between plant water status and plant growth in variable growth conditions (Coussement et al. 2018) (Fig. 1 Left).

Materials and Methods

In the framework of the EU project EUCLEG (www.eucleg.eu), an experiment with 360 accessions of 4 early maturity groups (MGI, MG0, MG00, MG000) was installed in Melle, Belgium, in the growing seasons of 2018 and 2019 according to a randomized row-column-block augmented design in two neighbouring fields. On one of the fields a mild drought treatment was imposed at flowering (R2 stage) using rain-out shelters (Fig. 1 Right), while in the other field irrigation was applied to keep the soil up to field capacity (control). Soil moisture was monitored using TDR sensors and weather information was recorded by a mobile weather station. The growth and development of the plots were monitored from germination to harvest on a weekly basis using UAV based imagery. More specifically, a time series of plant height and canopy cover was developed from RGB images and canopy temperature was measured with a thermal camera at five times during the experiment (Fig 1. Right).

The model was implemented as a system of ordinary differential equations in R using the RxODE package, and parameters related to whole-plant hydraulic resistance, tissue extensibility and stomatal conductance sensitivity to drought were estimated specifically for each genotype via calibration on the UAV based measurements of the control and drought

stress treatments. As such, continuous simulations of plant water potential and turgor pressure enabled estimation of plant height under both control and drought stress conditions.

Results and Discussion

This approach enabled to unravel different water use strategies among the different genotypes. More specifically, some genotypes displayed isohydric behavior, by closing their stomata around noon and consequently allowing higher leaf temperature, while maintaining an unaltered plant growth rate. Others showed anisohydric behavior by being rather insensitive in terms of stomatal conductance, and thus keeping canopy temperature low, while substantially reducing plant growth rate. Our model provides the mechanistic link between this diverse behavior through simulation of water potential and turgor pressure, and coupling to stomatal conductance. These results are extremely useful for future crossing schemes, as genotypes with complementary strategies can be identified as potential cross mates. Furthermore, our approach provided genotypic-specific model parameters that can serve as selection criteria in the breeding process. Finally, these genotype specific parameters can then be used as more environmentally independent phenotypes, and will be linked to the genotypic information to improve marker development.

Conclusions

Our approach using time series of RGB and thermal images from UAV flights, in combination with a plant model that includes plant water potential and turgor driven growth concepts allowed to disentangle complementary mechanisms of drought stress responses. As such, a range of iso-/anisohydric behavior was apparent in soybean genotype panel.

References

Borra-Serrano et al., 2019, *Grass and Forage Sci.* 74:356–369, doi: 10.1111/gfs.12439
Coussement et al., 2018, *Ann. Bot.* 121: 849–861, doi: 10.1093/aob/mcx144
Tuzet et al., 2003, *Plant Cell Environ.* 26: 1097-1116, doi:10.1046/j.1365-3040.2003.01035.x

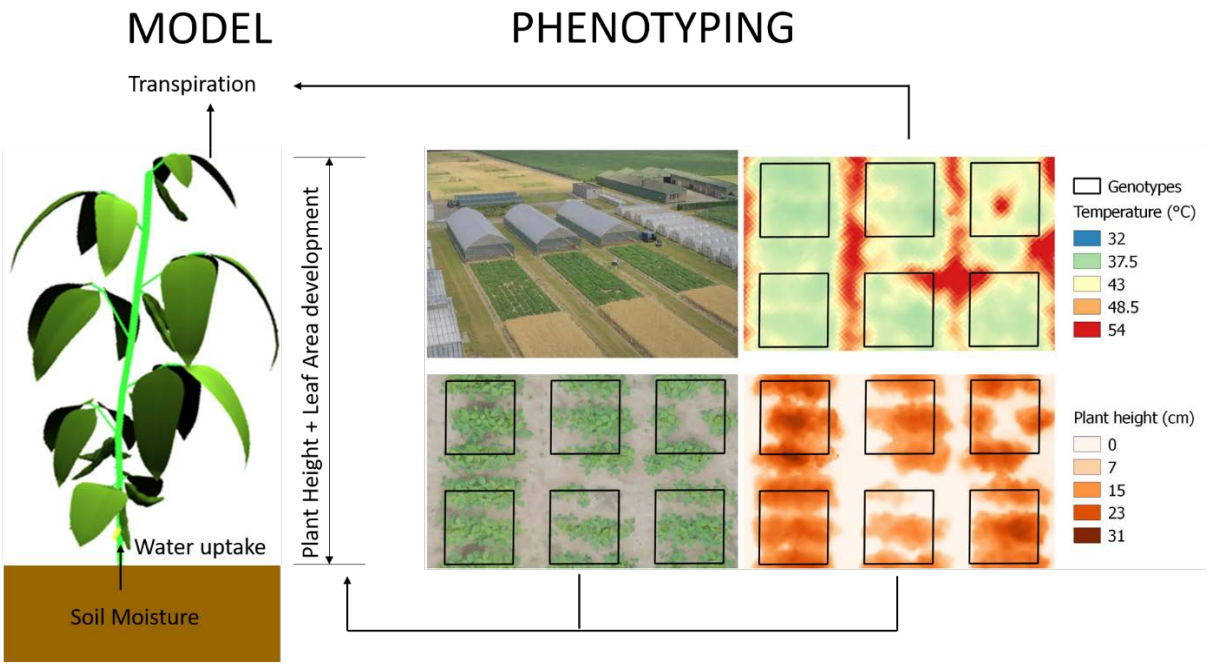

Fig. 1 – Schematic overview of the approach combining UAV phenotyping and Functional-Structural Plant Modelling

Puzzling shapes - Modeling epidermal tissue morphogenesis

Amir J Bidhendi[1,2], Bara Altartouri[2], Anja Geitmann[1]

[1] *Department of Plant Science, McGill University, Sainte-Anne-de-Bellevue, QC H9X3V9, Canada*
[2] *Département de sciences biologiques, Université de Montréal, Montréal, QC H1X2B2, Canada*

For correspondence: geitmann.aes@mcgill.ca

Keywords: leaf, epidermis, cell wall, cell shape, finite element modeling

The generation of simple plant cell geometries such as cylindrical shoot epidermal cells is known to be regulated by the extensibility pattern of the primary cell wall, which in turn is thought to be largely determined by cellulose microfibrils. However, the mechanism leading to more complex shapes such as the interdigitated, jigsaw puzzle-like patterns in the epidermis of eudicotyledon leaves (Fig. 1A) is poorly understood. Using mechanical modeling combined with 4D imaging, we investigated how the cell wall regulates the morphogenetic process in these cells and which initial steps lead to the characteristic undulations in the cell circumference. Live dyes for cell wall polymers (Bidhendi et al. 2020), Brillouin microscopy, and polarized fluorescence imaging (Altartouri et al. 2019) allowed us to untangle the respective roles of cellulose (Fig. 1B) and homogalacturonan pectin during lobe formation in the epidermal pavement cells of the cotyledons of *Arabidopsis thaliana*. We show that non-uniform distribution of cellulose microfibrils and demethylated pectin correlate with spatial differences in cell wall stiffness but intervene at different developmental stages. Challenging the widely accepted paradigm of cellulose as a crucial morphogenetic agent, we discovered that lobe initiation involves a modulation of cell wall stiffness through the local enrichment in demethylated pectin, whereas only the subsequent increase in lobe amplitude is mediated by the stress-induced deposition of aligned cellulose microfibrils. Finite element simulations (Fig. 1C) lead us to propose that both steps are preceded by a turgor-driven mechanical buckling event that serves as the initial trigger for the multi-step morphogenetic process (Bidhendi and Geitmann 2019, Bidhendi et al. 2019).

References

Altartouri et al. 2019, *Plant Physiology* 181: 127-141, doi: 10.1104/pp.19.00303
Bidhendi et al. 2019, *Cell Reports* 28: 1237-1250, doi: 10.1016/j.celrep.2019.07.006
Bidhendi et al. 2020, *Journal of Microscopy* 278: 164-181, doi: 10.1111/jmi.12895
Bidhendi and Geitmann A, 2019, *Developmental Cell* 50: 117-125, doi: 10.1016/j.devcel.2019.05.001

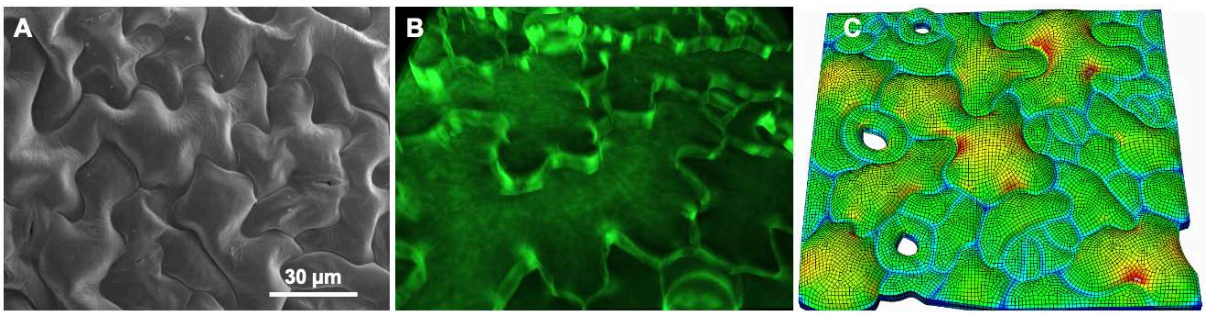

Figure 1: Epidermis of Arabidopsis thaliana cotyledon. A. Scanning electron micrograph of epidermal pavement cells. B. Oblique view of 3D reconstruction of confocal laser scanning z-stack showing pavement cells labeled for cellulose. C. Finite element model of leaf epidermal layer showing pavement cells and stomates.

Predicting the effect of environmental conditions on tomato fruit growth by a transpiration driven mechanistic model

Jakub Salagovic[1], Pieter Verboven[1], Bert Verlinden[2], Kristof Holsteens[3], Bram Van de Poel[3], Marlies Huysmans[4], Bart Nicolai[1,2]

[1] *Division of Mechatronics, Biostatistics and Sensors (MeBioS), KU Leuven, Leuven, Belgium*
[2] *Flanders Centre of Postharvest Technology, Leuven, Belgium*
[3] *Division of Crop Biotechnics, KU Leuven, Leuven, Belgium*
[4] *Research group Fruit Vegetables, Proefcentrum Hoogstraten, Meerle, Belgium*

For correspondence: jakub.salagovic@kuleuven.be

Keywords: horticulture, transpiration, compartment model, microclimate

Tomato fruit production and quality (*Solanum lycopersicum* L.) are largely affected by physiological processes related to whole-plant carbon and water relations (De Swaef et al. 2010). In order to enhance the understanding of dry matter and water accumulation in the tomato fruit, it is crucial to determine the link between fruit growth and plant carbon and water status. De Swaef and colleagues proposed a mechanistic flow model of water and carbon connected to a tomato fruit growth model (De Swaef et al., 2010; Liu et al., 2007). However, this approach requires direct plant measurements as input for the model, such as sap flow at different positions on the plant stem. Although this approach could explain some flow properties variations in the main stem, it requires monitoring of each plant and is not applicable for making long-term predictions of tomato fruit growth in practice. Furthermore, such models usually do not fully include growers' management practices, such as pruning. Microclimate effects throughout the canopy are often neglected.

We propose to use a transpiration driven plant growth model to estimate carbon and water flows towards the fruit. The model's inputs are environmental variables (e.g., temperature) and cultivation parameters (e.g., plant density). Monitoring of specific plant parameters is only necessary for implementation, calibration, and validation of the model.

A subpart of the reduced TOMGRO model (Jones et al. 1999) was used to model node production and leaf area of the plant. The model was adapted to common pruning practices to attain a fixed leaf area index (LAI) throughout the season, while still modelling new leaf biomass production. This model was coupled to the model proposed as a virtual sensor for transpiration by Sánchez et al. (2012). The tomato fruit growth model was adapted and parameterized for a selected cultivar and certain conditions (Liu et al., 2007). Leaves and fruit were interconnected through stem segments, for which we model vascular water flow according to the van den Honert concept of an analogue electric current (De Swaef et al., 2010). The plant model was adapted to the dynamic compartment model structure (De Reffye et al. 2009) where the compartment is a population of individual organs of the same age and type. Water flows driven by transpiration ($J_{tr,i}$) and water biomass fixation ($J_{gr,i}$) are calculated for each compartment *i* for both fruit and leaves in order to calculate water potential (Ψ_i) – Fig. 1. The water potential of the compartment 0 is equal to the water potential of the substrate (Ψ_0). In the next step, a simulated sucrose loading to the phloem, based on photosynthesis and sugar metabolism kinetics, is going to be coupled to existing microclimate measurements (T, RH, PAR), based on the leaf area, in order to compute osmotic potential turgor pressure of phloem.

Experiments were conducted in an experimental research station, following industry-standard growing practices. Plants of the cultivar Merlice grown on rockwool substrate were monitored from anthesis of the first truss until the harvest of the fourth truss (number of nodes, stem length, stem diameter, leaf area). Trusses were pruned to five fruits per truss. Growers'

treatments are important factors, especially in commercial greenhouse production. Once tomatoes reach the crop wire, plants are managed to maintain a specified height (rehanging) and leaf area index (pruning) throughout the season. Temperature (T), relative humidity (RH), and photosynthetic active radiation (PAR) of the different compartments through the canopy together with water potential of the substrate were monitored and used as inputs to the model – Fig. 1. Sap flow, substrate water potential, and fruit diameter were continuously monitored by the attached sensors. The water potential of the stem was measured using a pressure chamber. For fruit, we measured soluble solids content, osmotic potential, and water potential of the fruit pedicel (by pressure chamber). These measurements were destructive, fruits were thus sampled from different plants. Fruits were harvested weekly through their whole development from the third week after flowering till their harvest when ripe.

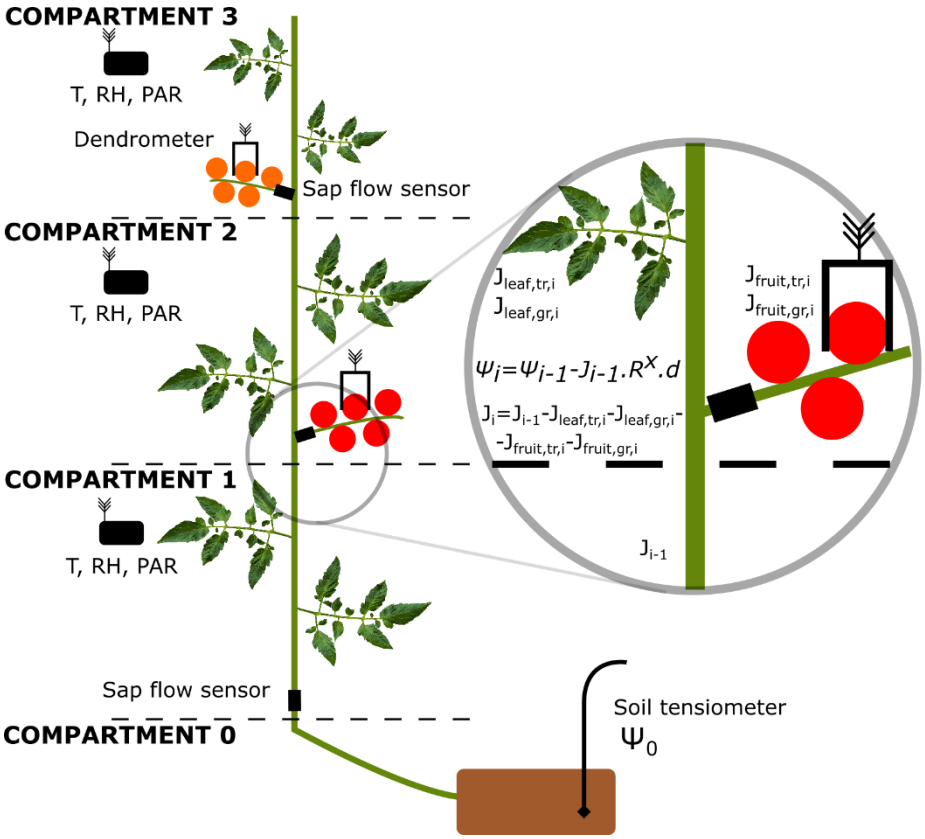

Fig. 1 – Schematic overview of the sensor installation and flows ($J_{organ,process,compartment}$) with *tr* – transpiration, *gr* – growth) of the plant. In this example, the plant is divided into four compartments, but the number of compartments is variable.

The presented approach incorporates models for water and carbon flows to predict values of water and osmotic potential of xylem and phloem, crucial for precise modelling of the fruit growth. This concept does not require online monitoring of specific plant parameters and implements climate variables currently monitored in greenhouses. Our model incorporates growers' practices and plant microclimate.

References

De Reffye et al., 2009, *Crop modeling and decision support* 130-147, doi:10.1007/978-3-642-01132-0_15
De Swaef et al., 2010, *Functional Plant Biology* 429-438, doi: 10.1071/FP09233
Jones et al., 1999, *Transactions of the ASAE* 255, doi: 10.13031/2013.13203
Liu et al., 2007, *Journal of Experimental Botany* 3567-3580, doi 10.1093/jxb/erm202
Sánchez et al., 2012, *Sensors* 15244-15266, doi: 10.3390/s121115244

A hydraulic model of leaf growth in grasses: reconciling old empirical evidence

Tom De Swaef[1], Romain Barillot[2], Jean-Louis Durand[2]

[1] *Plant Sciences Unit, Institute for Agricultural and Fisheries Research (ILVO), Melle, Belgium*
[2] *INRAE, UR P3F, Lusignan, France*

For correspondence: tom.deswaef@ilvo.vlaanderen.be

Keywords: water potential, turgor pressure, leaf elongation, hydraulic model

Introduction

Evidence in grasses, among which tall fescue and maize, has demonstrated a clear link between leaf water potential and leaf elongation rates. More specifically, it has been evidenced that leaf growth results from water deposition in the elongation zone, originating from a quite substantial water potential gradient between xylem and the living cells. Martre et al. (2001) showed that the night-time growth-induced water potential gradient exceeded the gradient during light conditions, suggesting a larger driving force for water deposition and hence growth rate, during the night.

Despite this clear link with water potential, the actual mechanism behind plant cell growth, and by extension organ growth, is turgor pressure (Boyer and Silk, 2004). However, an extensive body of research shows that stem and leaf elongation rates can vary substantially, while concomitant turgor in elongation zones can remain constant (Boyer and Silk; 2004). On the other hand, in mature tissues, substantial variations in turgor have been observed, while these tissues are no longer elongating. Martre et al. (1999) show even that turgor pressure in the elongation zone is lower than in the mature zone of tall fescue leaves under night-time conditions.

Although the mechanism of turgor driven cell enlargement is widely accepted, the link between turgor and growth of grass leaves could not yet be demonstrated explicitly, whereas links with water potential are more prominent.

Therefore, we propose a hydraulic based model for grass leaf growth that reconciles insights collected in former studies in such a way that turgor is indeed the driving force for leaf elongation rate, while accommodating different apparent contradictions and empirical findings: (1) night-time turgor in the mature zone is higher than in the elongating zone; (2) variations in turgor in the elongation zone are smaller than in the mature zone; (3) the growth-induced water potential gradient is larger during the night than during the day.

Materials and Methods

The grass leaf was conceptualised as presented in Durand et al. (1999), with differentiation between division zone (DZ), an elongation only zone (EOZ) and a mature zone (MZ). Within each of these zones, further differentiation was made between the xylem (X) and the mesophyll (M). The leaf was connected to a root compartment, on which older leaves were already present.

Water flow was modelled based on water potential gradients and hydraulic resistances from the soil through the root and leaf xylem towards the mesophyll. Once the leaf emerged from the sheath, transpiration was modelled from the mesophyll in the MZ, *via* a simple rectangular function with zero transpiration during the night and a fixed value during the day, proportional to the exposed blade tissue.

Leaf hydraulic resistance architecture was designed following Martre et al. (2001), while assuming that root hydraulic conductance was proportional to the total leaf area on the tiller.

The link between water potential, turgor pressure and leaf growth was implemented following the concepts of Coussement et al. (2018), in which variations in water content result in reversible and irreversible variations in organ size.

Results and Discussion

Fig. 1A shows the simulated complete leaf elongation from the initiation until the final size. Using the model three hypotheses were evaluated. Firstly, Fig. 1B shows that night-time turgor in the mature zone is higher than in the elongating zone. Secondly, Fig. 1B shows that variations in turgor in the elongation zone are smaller than in the mature zone. Finally, results presented in Fig. 1C demonstrate that the growth-induced water potential gradient is larger during the night than during the day.

Conclusions

The model successfully described short-term variations of leaf elongation rate as a function of turgor pressure, while reconciling apparent contradictory empirical evidence. Furthermore, the model included the division zone of a grass leaf, which allowed to simulate realistic long-term leaf growth, primarily based on leaf hydraulics. These insights are crucial for better understanding of the factors that determine grass leaf growth, both in well-watered and in water-limited conditions.

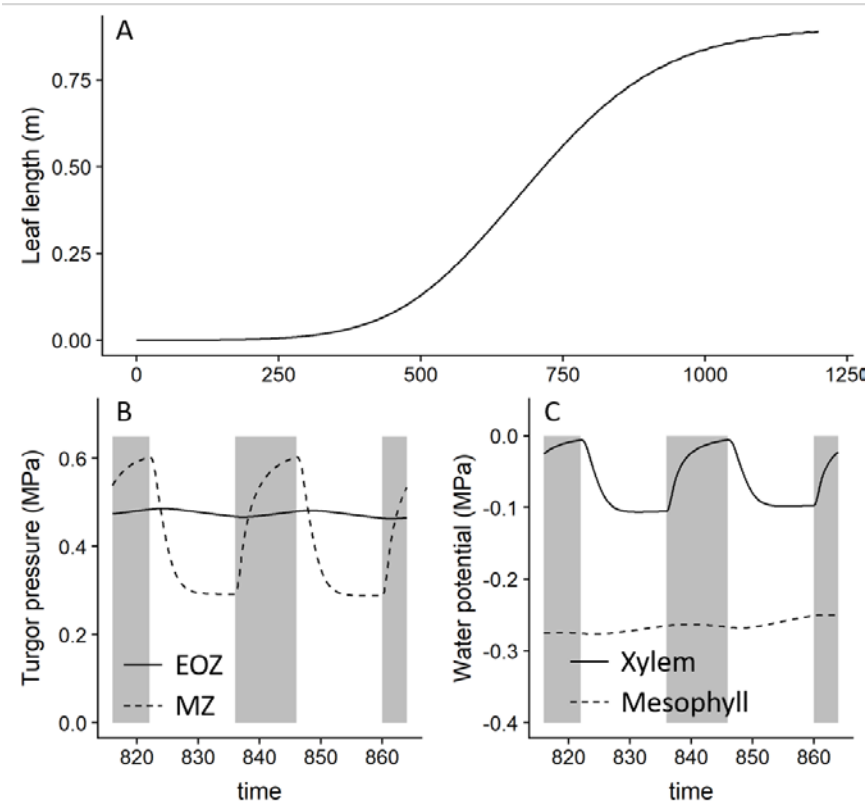

Fig 1: Simulation of (A) Leaf length from initiation to final leaf length as a function of time, in hours, under well-watered conditions; (B) turgor pressure over the 2 days in the elongation zone (EOZ) and the mature zone (MZ); and (C) the water potential in the elongation zone of the xylem and the mesophyll. Grey boxes indicate the night time. Time is expressed in hours.

References

Boyer and Silk, 2004, *Funct. Plant Biol.* 31:61-773, doi: 10.1071/FP04062

Coussement et al., 2018, *Ann. Bot.* 121:849–861, doi: 10.1093/aob/mcx144

Durand et al., 1999, *Ann. Bot.* 83:577-588, doi: 10.1006/anbo.1999.0864

Martre et al., 1999, *New Phytol.* 142:435-439, doi: 10.1046/j.1469-8137.1999.00405.x

Martre et al., 2001, *Plant Cell Environ.* 24:65-76, doi: 10.1046/j.1365-3040.2001.00657.x

Virtual plants and artificial tropical forest scenes as training samples for deep learning plant classifiers. The case of *Raphia hookeri*

Marc Jaeger[1,2], Gaëlle Viennois[1], Mickaël Baril[1,2], Frédéric Borne[1,2], Hervé Rey[1,2], Yuichi Nagao[1,3], Ecole Centrale de Lyon - Université de Keio (Japon),Philippe Borianne[1,2]

[1]AMAP, Univ Montpellier, CIRAD, CNRS, INRAE, IRD, Montpellier, France
[2]CIRAD, UMR AMAP, F-34398 Montpellier, France
[3]CEcole Centrale de Lyon, France & Keio University, Japan

For correspondence: marc.jaeger@cirad.fr

Keywords: Palm Tree Model, Raphia hookeri, Virtual Forest, Computer Graphics, Convolution Networks

Introduction

Among the palms, the species *Raphia hookeri* is the most used and most important in Africa, bringing economic, ecological and societal benefits (Obahiagbon, 2009), but faced with increasing anthropogenic pressure, which we want to estimate. Under natural conditions, raphia palm trees congregate in swampy forests called Raphiales where the crowns intertwine, making it difficult to individualize the trees and estimate their biomass. Recently, we obtained minor results on UAV images using deep learning techniques; we found that the low reliability of the learning images set was the critical path for improvement. We therefore propose here to use synthetic images to learn identification of raphia individuals in real images. This requires building a realistic 3D model of the raffia, building artificial plant communities adding other 3D species models, rendering the scene with a very realistic appearance, and computing the scene as a labelled image to feed and test the convolution networks for raphia identification.

Materials and methods

The definition of *Raphia hookeri*'s geometric model mobilizes the Principes palm generator, derived from studies on *Elaeis guineensis* (Jourdan and Rey, 1997). The parameters describing the spear, fronds and pinnaes are issued from the literature, supplemented by distributions of angle measurements (torsions and torques in particular) from two Lidar acquisitions. Photographs and gonio-spectrometer measurements allowed us to evaluate the colour and reflectance of the organs. We generate and visualize the simulated 3D mock-ups in the AmapStudio software suite (Griffon and de Coligny, 2014). The same suite is mobilized to build square scenes from ¼ to 1 km^2 from individuals of various ages and other 3D mock-ups of tropical species, including other palms. Finally, we render the scenes in high resolution (0.1 m per pixel) from the top view. We update our in house rendering engine (Zhang et al, 2017) to generate two images per view: a pseudo-realistic image and a labelled image from which we retrieve a bounding box for each plant. At last, the realistic image and the bounding boxes are sent to a convolution network for learning and identification tests.

Results and Discussion

We designed a stochastic model of *Raphia hookeri* and generated 3D models at different stages (fig A) with geometric stochastic variations. We generated a dozen of aerial views and their rendering, changing especially the plant density, from no occlusion to strong occlusions between plants.

We first tried to build scenes as close to real natural scenes as possible, based on descriptions of the natural biome according to the literature and maps of plant species available to us. It turns out that this strategy was not effective: on the one hand, we did not have access to many 3D mockups of species; on the other hand, the environments around the Raphias in the created images do not show a great diversity. We finally adopted a simpler method to generate

artificial scenes. We simply involve all the 3D species models available in the laboratory (nearly 800), calculated at various ages, resulting in scenes of more than 5000 different trees, offering a wide range of local conditions in the learning process, thus increasing the identification capabilities of the network.

The deep-learning training on the synthetic scene images is currently in process. We are currently carrying out a study on the reflectance properties of plants: for example, we are carrying out tests using the same reflectance properties on all palms (20 model species are used), in order to assess the network's ability to distinguish the species of a family according to morphological criteria only. We also study the effect of plant density (occlusion) on identification performances. At the plant level, we plan refining the Raphia model, particularly with regard to the conservation of old, dry and wilted fronds, including the degradation of their respective reflectance properties.

Acknowledgement

The authors thank the French National Research Agency under the Investments for the Future Program, referred as ANR-16-CONV-0004 (#DigitAg), and the KIM Data & Life Sciences (Key Initiative of Montpellier University of Excellence) for their master supports; and also N. Barbier (IRD, Amap) for the UAV images and T-Lidar acquisitions.

Figure: A: *Raphia hookeri* mockups generated by PRINCIPES at age 18, 29, 40, 50, 60 and 70. B: Realistic virtual forest scene rendering; C: close-up of the realistic view; D: close-up of the labelled view.

References

Obahiagbon, F.I., 2009, A review of the origin, morphology, cultivation, economic products, health and physiological implications of raphia palm, *African journal of food science*, 3, 13, 447–453

Jourdan, C., and Rey, H., 1997. Modelling and simulation of the architecture and development of the oil-palm (Elaeis guineensis Jacq.). *Plant and soil*, 190(2), 217-233.

Griffon, S., and De Coligny, F., 2014. AMAPstudio: an editing and simulation software suite for plants architecture modelling, *Ecological Modelling*, 290, 3–10

Zhang, X.P., Bao, G.B., Meng, W.L., Jaeger, M., Li, H.J., Deussen, O., and Chen B.Q., 2017. Tree branch level of detail models for forest navigation. *Computer Graphics Forum*, 36, 8, 402-417

Hydraulic Viper, a virtual phenotyping pipeline for root hydraulic traits – multiscale approach.

Adrien Heymans[1], Valentin Couvreur[1], Félicien Meunier [2], Guillaume Lobet [1, 3]

[1] *Earth and Life Insitute, UCLouvain, Louvain-la-Neuve, Belgium*
[2] *CAVElab-Computational and Applied Vegetation Ecology, Ghent University, Ghent, Belgium*
[3] Agrosphere IBG3, Forschungszentrum Jülich, Jülich, Germany

For correspondence: Adrien.heymans@uclouvain.be

Keywords: root anatomy, hydraulic conductivity, hydraulic architecture,

Under water limitation, selecting the adequate root architectural features for a specific environment could increase plant performance (Comas et al., 2013). In this respect, optimizing the location of roots in space and time can help but it is the root hydraulic conductivity and the water potential being applied on all points of the root system that determine the amount of water transpirable by the plant. Moreover, root hydraulic conductivity can be a limiting factor along the water pathways between the soil and the leaf. Cell-scale hydraulic properties and anatomical features define the root hydraulic conductivities. Hydraulic properties are usually assumed to be controlled on the short- or medium-term by the plant while structural features are assumed to be long term (Vetterlein and Doussan, 2016). As such, root anatomy defines the baseline for the root radial and axial hydraulic properties. However, quantifying the influence of anatomical features on the hydraulic conductivity remains challenging due to complex and time-consuming experimental procedures. In addition, assessing their impact globally on a root system conductance is even more complicated.

We present here a virtual phenotyping pipeline for root hydraulic traits that will help better understand how cell-scale hydraulic properties and root anatomy could influence plant-scale hydraulic properties such as the whole root system conductance, the transpiration rate and the standard sink fraction. We used a model of water flow in root system hydraulic architecture to combine a generated root system architecture with specific hydraulic conductivities function: MARSHAL (Meunier et al., 2020). The hydraulic conductivities along the root axis were derived from the MECHA-GRANAR coupling (Heymans et al., 2020). This allows us to generate realistic root cross section anatomies and add the cell-scale hydraulic properties to the system to estimate radial and axial hydraulic conductivity. Finally, these evolving root system hydraulic architectures were placed in a set of environmental conditions to create the soil and atmospheric boundary conditions and estimate realistic root water uptake scenarios. Thus, the pipeline enables us to identify of the best combinations of traits for the tested scenarios.

In this case, we simulated 9 000 of root systems in total for three contrasted architecture types. We generated root cross sections for those root systems from a large sample of anatomical features and a broad range of cell-scale hydraulic properties and applied it accordingly to each root type. Per root system, we simulate five root cross sections, representing five root types (Tap-, Basal-, Shoot born-, Short lateral-, and Long lateral-root). This approach allowed us to highlight which combination of traits at the cell and organ level could potentially have the most impact on the global water uptake strategy for the selected environmental scenario and architectural types.

References

Comas et al., 2013, Frontiers in Plant Science, doi: 10.3389/fpls.2013.00442
Heymans et al., 2020, Plant Physiology, doi: 10.1104/pp.19.00617
Meunier et al., 2020, in silico Plants, doi: 10.1093/insilicoplants/diz012
Vetterlein et al., 2016, Plant Soil 407: 145–160, doi: 10.1007/s11104-016-2849-6

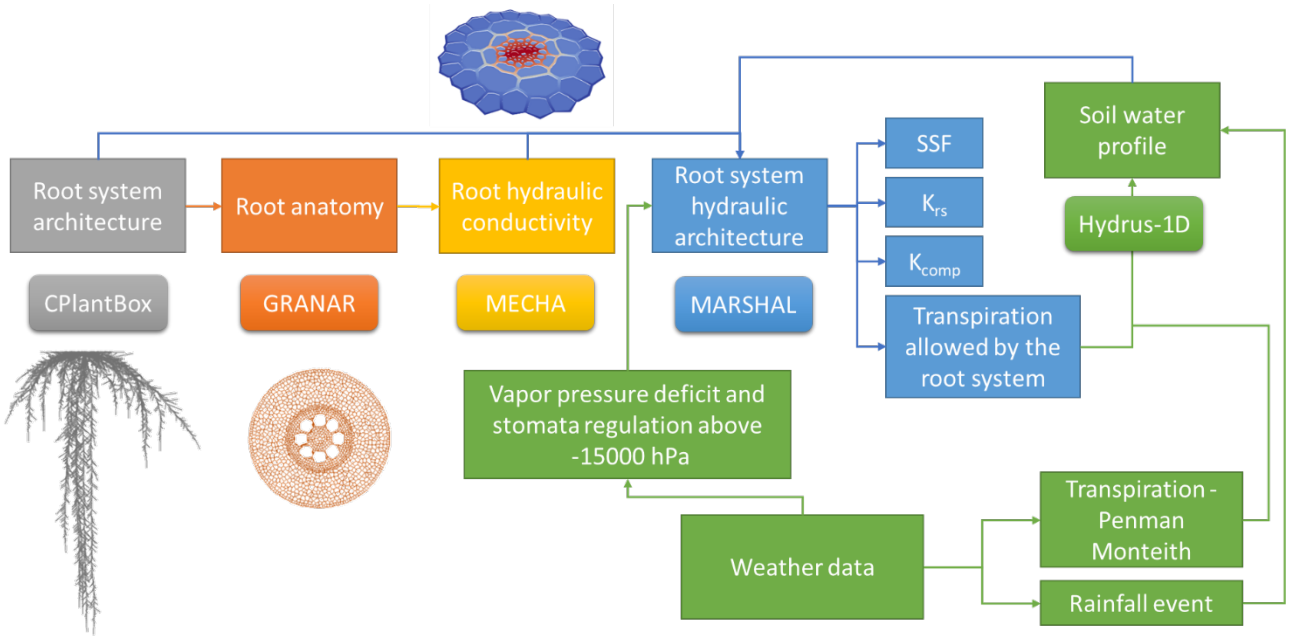

Overview of the pipeline work flow: 1. generation of a root system architecture; 2. creation of 10 root cross sections that represent the 5 different root types; 3. estimate the hydraulic conductivities: K_r and K_x; 4. resolve the hydraulic architecture and get the standard sink fraction, the root system conductance, the compensatory conductance, and the transpiration rate; 5. loop around the soil water flow and the root system hydraulic architecture

In sillico prospections to define rapeseed root system ideotypes for adapted to low nitrogen environment

Christophe Lecarpentier[1,2], Céline Richard-Molard[2], Loïc Pagès[1]

[1] *INRAE, UR1115, Plantes et Systèmes de culture Horticoles, CS40509, 84914 Avignon Cedex 9, France*
[2] *UMR ECOSYS, INRAE, AgroParisTech, Université Paris-Saclay, Thiverval-Grignon, France*

For correspondence: christophe.lecarpentier@inrae.fr

Keywords: Root system architecture, genotypic diversity, ArchiSimple, soil exploration, root branching

Introduction

In the new emerging agricultural context, a drastic reduction in fertilizer usage is required. A promising way to preserve high yields while reducing fertilizer inputs is to improve nutrient use efficiency, especially for winter oilseed rape (WOSR), known to have high nitrogen requirements. To reach this aim, one key lever relies on the optimization of the root system architecture (RSA). Plasticity of rapeseed RSA architecture to nitrogen limitation was previously characterized experimentally using ArchiSimple model (Pagès et al., 2014) as a screening tool, where model parameters were considered as phenotyping traits (Lecarpentier et al. submitted). This experimentation highlighted that nitrogen limitation induced mainly a decrease of root branching and in a lesser extent an increase of root hierarchy and root diameter variability. Despite this characterization, little is known on which are the major traits in root system development. Due to the difficulty to access the root system, soil exploration strategies of root systems are not commonly related to its architecture. Thus, to override experimental constraints, we propose to use modelling and to perform *in sillico* investigations. Therefore, we hereby aimed at (i) evaluating the ability of ArchiSimple to simulate genetic diversity of rapeseed root system architecture in response to nitrogen availability, (ii) identifying the major root architecture traits involved in root biomass elaboration and soil exploration and (iii) identifying root system ideotypes adapted to low nitrogen environment through *in sillico* investigations.

Material and Methods

Based on a previous experimentation where 10 genotypes of rapeseed were grown under two contrasting nitrogen levels, seven ArchiSimple parameters (root system architecture traits relative to root diameter, root branching and root elongation) were estimated for all the 20 modalities (G x N). However, four other parameters were considered as constant due to the lack of information concerning their genetic variability. Thus, so one value for each of these four parameters was set for all the modalities. The ability of ArchiSimple to predict root biomass was evaluated for each modality by a comparison between simulated and experimental root dry biomass at 30 days after sowing (800 degree days). Then, a sensitivity analysis was performed to evaluate the impact of genotypic architectural parameter on two major outputs of the model: the root biomass and the volume of soil colonized by the roots. Besides root system biomass and volume of colonized soil, we also have implemented the proportion of thin roots length in the whole system and the efficiency of colonization (*ie.* ratio between volume of explored soil root system biomass) to further characterize soil exploration strategies. Finally, four-dimensional Latin Hypercubes (one dimension for each of the most influent RSA

parameters) were set up to perform *in sillico* investigations to explore how root system architecture shapes soil exploration strategies.

Result

Our brief calibration of the four constant parameters led to a good prediction of the root biomass for most of the genotypes. Except for CHINE 25 and DARMOR BZH whose biomass were highly overestimated, the biomass of other genotypes was predicted with an average RMSE of 0.13g. Moreover, average error of biomass prediction was smaller for nitrogen-limited plants than for non-limited plants. The sensitivity analysis highlighted that the interbranch distance (IBD) was one of the most influent trait in the prediction of root total biomass and ELT (Elongation rate divided by apical diameter) was the most influent trait in the prediction of total volume of colonized soil. This difference may highlight that RSA traits could be indicators of various soil-exploration strategies. Results also confirmed those previously obtained through the previous experimental approach, highlighting IBD as the most plastic RSA trait in response to nitrogen availability (Lecarpentier et al. submitted). This underlies even more the interest of root branching properties to optimize nutrient acquisition efficiency. Finally, *in sillico* investigations pointed out different strategies of root development for all genotypes. Therefore, we identified the genotypes having the best ability to explore the soil and those colonizing soil the most efficiently.

References

Pagès et al., 2014, *Ecological Modelling* 76-84, doi: 10.1016/j.ecolmodel.2013.11.014
Lecarpentier et al., submitted to *Front. Plant Sci.*

In silico analysis of grapevine architectural response to elevated CO_2

Dominik Schmidt[1], Christopher Bahr[1], Matthias Friedel[2], Katrin Kahlen[1]

[1] *Department of Modeling and Systems Analysis, Hochschule Geisenheim University, Geisenheim, Germany*
[2] *Department of General and Organic Viticulture, Hochschule Geisenheim University, Geisenheim, Germany*

For correspondence: dominik.schmidt@hs-gm.de

Keywords: Virtual Riesling, FSPM, climate change, light interception, canopy

Introduction

Climate change associated with a notable increase in temperature is driven by rising atmospheric CO_2 levels. To study the effect of elevated CO_2 (eCO_2) compared to current ambient CO_2 (aCO_2) concentrations in field trials Free Air Carbon Dioxide Enrichment (FACE) facilities are used. While first FACE facilities focused on crops and forest settings, a few sites were also established for specialty crops, such as vegetables and grapevine. First results from the VineyardFACE at Geisenheim University already revealed some architectural differences in lateral shoot growth and bunch structure (Wohlfahrt et al., 2018). Hence, one might expect different light conditions in canopies grown under eCO_2 compared to aCO_2. Canopy light distribution affects various aspects of grapevine growth, for instance photosynthesis and related biochemical processes, grape composition and aroma development, but also detrimental effects, such as berry sunburn (Friedel et al., 2015).

Field studies on light interception are laborious and hence usually limited to a small section of a vineyard and hence possibly compromised by a high variability in plant architecture. Virtual plant simulations offer the chance to study an entire vineyard, overcoming the problem of local effects (Louarn et al., 2007). For example, Louarn et al. (2007) used a simple 3D statistical model parameterized with end-of-season digitization data to reconstruct a virtual vineyard for studying light interception. While such an approach offers a static *in silico* analysis, dynamic Functional-Structural Plant Models (FSPM) are required to study transient effects during the growth season. *Virtual Riesling* is such a dynamic FSPM focusing on a realistic and hence variable architectural growth of Riesling plants in a vertical shoot positioning trellis system (Schmidt et al., 2019). It is based on the concept of thermal time dependence of growth functions estimated from digitized plants grown under aCO_2 within the Geisenheim VineyardFACE. The aim of this study was to recalibrate the model with data from eCO_2 conditions for an *in silico* comparison of light interception in virtual canopies grown under aCO_2 and eCO_2.

Materials and Methods

Recently, the original *Virtual Riesling* model was extended to include a radiation model with daily time steps following an approach of Evers and Bastiaans (2016). This model, calibrated with measurements from aCO_2 conditions, is used as the reference model (aViRi) (for more details on calibration parameters, see Schmidt et al., 2019). Similar data from three Riesling plants grown under eCO_2 in the VineyardFACE were used for model calibration to create an elevated *Virtual Riesling* FSPM (eViRi). The dataset from 2018 covers four measurement dates between bud burst and first pruning. Plants have grown under elevated CO_2 since 2014. Both models were subjected to an *in silico* experiment simulating a virtual vineyard of 70 vines. Simulations were repeated 25 times to gather data on 1000 non-border plants per model. The radiation model uses 20×10^6 rays that interact with plant organs based on absorption and reflection coefficients extracted from literature. To optimize simulation execution times, multiple instances of *GroIMP* were run in parallel with the light model being executed on the graphical processing unit. For comparing aViRi and eViRi light interception we extracted data on absorbed photosynthetically active radiation (PAR_{abs}) estimated at leaf level.

Results and Discussion

Calibration results indicated a difference in mean bud burst (BB) date, as well as minor variations in the plant growth parameters, e.g. maximum internode length. However, results on light absorption at plant level show a very similar pattern in cumulative sum of PAR_{abs} per vine (s. Figure). Most differences can be explained by the on average earlier bud burst of aViRi compared to eViRi. High plant-to-plant variability was present in both cases supporting the hypothesis that comparing single vines in a field could lead to biased results due to a large architectural plasticity. This natural variability was not suppressed by the trellis system used in the model, although it ensured a more compact canopy. However, the trellis system might be a reason for only minor differences between aViRi and eViRi regarding light interception. In addition, this first calibration of eViRi focused on phenological (bud burst) and growth responses, while possible leaf shape responses to eCO_2, also affecting canopy light regime, were not yet implemented.

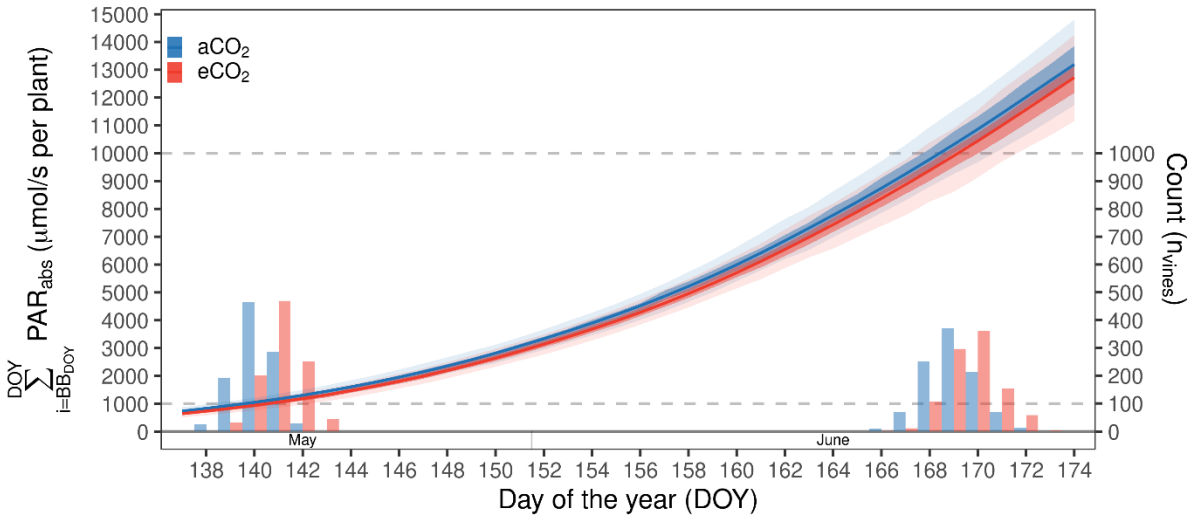

Figure: Cumulative sum of average daily sum of PAR_{abs} of a vine and the 50% and 95% highest density interval from ambient (aCO_2) and elevated (eCO_2) simulations with *Virtual Riesling*. Counts indicate the number of vines that for the first time reached a cumulative sum of 1000 µmol/s or 10000 µmol/s at this day. These thresholds also determine the presented timeframe (first and last crossing).

Conclusion

This preliminary study on introducing effects of elevated CO_2 in *Virtual Riesling* indicates that canopy light interception is stronger affected by plant-to-plant variability and applied management practices than by architectural responses due to differences in atmospheric CO_2 concentrations. To confirm this, we will collect additional data covering multiple seasons allowing for a more robust model calibration.

References

Bindi et al., 2001, Eur. J. Agron., 14(2):145-155, doi:10.1016/s1161-0301(00)00093-9
Evers and Bastiaans, 2016, J. Plant Res., 129:339-351, doi: 10.1007/s10265-016-0807-2
Friedel et al., 2015, Vitis, 54(3):107-116
Louarn et al., 2007, Ann. Bot. 101(8):1167–1184, doi: 10.1093/aob/mcm170
Schmidt et al., 2019, *Agronomy* 1-29, doi: 10.3390/agronomy9080426
Wohlfahrt et al., 2018, Eur. J. Agron. 101:149-162, doi: 10.1016/j.eja.2018.09.005

Axillary bud outgrowth regulation by light intensity: modelling hormone and sugar interactions

Jessica Bertheloot[1], Anne Schneider[1], L. Ledroit[1], M.-D. Perez-Garcia[1], F. Boudon[2,3], C. Godin[4], S. Sakr[1]

[1] *IRHS UMR1345, INRAE, AGROCAMPUS-Ouest, Université d'Angers, SFR 4207 QUASAV, 42 rue Georges Morel, 49071 Beaucouzé cedex, France*

[2] *CIRAD, UMR AGAP, F-34398 Montpellier, France.*

[3] *AGAP, Univ Montpellier, CIRAD, INRAE, Institut Agro, Montpellier, France*

[4] *Laboratoire Reproduction et Développement des Plantes, University of Lyon, ENS de Lyon, UCB Lyon 1, CNRS, INRAe, Inria, F-69342, Lyon, France*

For correspondence: jessica.bertheloot@inrae.fr

Keywords: Bud outgrowth, Light, Sugar, Hormones

Introduction

Branching is a key trait of plant adaptation to growth conditions. It involves a regulation of the outgrowth of axillary buds. These are inhibited by the fast-growing apical zone, a phenomenon called apical dominance. The extent of this inhibition depends on plant growth conditions. In this work, we investigate the ability of light intensity to modulate apical dominance and seek to identify the underlying mechanisms.

Apical dominance is mediated by hormonal and sugar competition mechanisms (Rameau et al., 2015; Schneider et al., 2019). The fast-growing apical zone is, on the one hand, a source of auxin, that is transported downwards in the stem and indirectly inhibits bud outgrowth. Auxin rapidly controls the production of two other hormones, the cytokinins (CK) and strigolactones (SL) in bud neighborhood, that are the direct regulators of bud outgrowth. On the other hand, the fast-growing apical zone is a highly important sink organ that deprives axillary buds from sugar (Mason et al. 2014). Such deprivation inhibits bud outgrowth in an unknown manner (Barbier et al., 2015).

Plant incident light intensity dampened apical dominance through increasing CK production in the stem in rose (Corot et al., 2017). The sugar involvement in light effect is unclear, despite light-induced changes in photosynthesis and plant sugar level. Here, we hypothesize that both CK and sugar are involved in incident light-related stimulation of bud outgrowth and antagonize dose-dependently auxin inhibiting effect. Moreover, CK production is supposed to be related to light perceived locally by the bud-bearing stem. Our objective was to test, by a combination of experiments and simulations, whether this hypothesis accounts for bud outgrowth differences observed between three light intensity regimes experienced by rose plants. First, we developed and calibrated a model at the scale of the bud-bearing stem using experiments *in vitro*. It assumes an effect of light on CK production, and an antagonistic and dose-dependent effect between CK-sugar module and auxin on bud outgrowth (see figure, left). Then, we used this model with, as inputs, the values of sugar, light, and auxin measured on intact plants, and tested model ability to simulate the observations of CK and bud outgrowth for the three light regimes.

Material and Methods

To develop and calibrate the model at the bud-bearing stem scale, single bud-bearing stem segments of rose were grown *in vitro* under different sucrose and hormone concentrations, and light intensities. Bud length was scored each day, so as to estimate the time at which bud outgrowth started (denoted T). Moreover, stem CK content was monitored for two auxin and sucrose levels. From all these data, a model was built and calibrated by minimizing the relative errors between measured and simulated values of CK contents and T. An absence of bud outgrowth was considered as an infinite T.

To test our light regulation hypothesis, young rose plants were grown under three different light intensity regimes: continuous low light (LL), continuous high light (HH), or temporary light limitation before the expected bud outgrowth period (LH). For each regime, the time at which bud outgrowth started was scored along the primary axis, while physiological variables (sugar, CK, auxin, and light levels in the axis median zone) was recorded before bud outgrowth started. The observed values in auxin, sugar, and absolute light level, were set as inputs of the *in vitro*-established model, and CK contents and the start of bud outgrowth were simulated.

Results

A first set of *in vitro* experiments was dedicated to model sugar and auxin antagonistic effect on bud outgrowth. They indicated that sucrose availability did not antagonize auxin effect on CK levels but repressed bud response to SL (Bertheloot et al., 2020). Assembling these observations into a computational model was able to reproduce a diversity of observed dose-dependent sucrose-hormones effects on bud outgrowth for bud-bearing stems *in vitro*. A second set of *in vitro* experiments was dedicated to integrate light effect in this model. Adding a light intensity effect on CK production in the stem was able to capture observed bud outgrowth responses to light intensity, in interaction with sucrose and auxin levels. All these experiments led to a quantitative model simulating local light intensity, auxin, and sugar effect on bud outgrowth (see figure, left).

Our experiments in intact plants under different light regimes showed strong differences in bud outgrowth between LL, LH, and HH. This was correlated to differences in starch, CK, and local light levels. Introducing these differences in starch and light as inputs of the above-described model captured the observed differences in CK levels and bud outgrowth between LL, LH, and HH (see figure, right). This supports our initial hypothesis that plant light regimes modulates auxin-mediated apical dominance through changes in both (i) bud light environment that impacts stem CK production, and (ii) sugar availability.

Conclusion

We have developed a model of bud outgrowth regulation accounting for the effect of local levels of hormone, sugar, and light intensity. The use of this model in intact plants made it possible to explain light intensity impact on the outgrowth of axillary buds by local variations in sugar and hormones in bud vicinity.

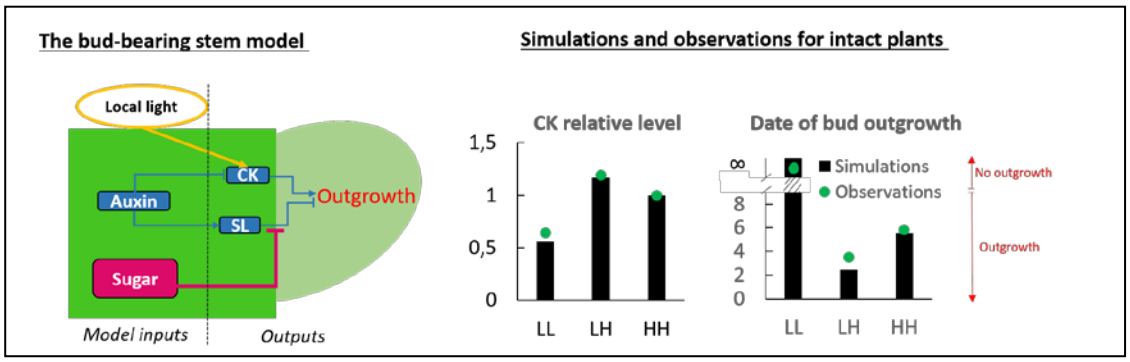

Figure: Bud outgrowth regulation by three different plant light regimes (LL, LH, HH): a model in which sugar and light-driven CK in bud neighborhood antagonizes dose-dependently auxin effect.

References

Barbier et al., 2015, *Journal of Experimental Botany*, 2569-2582, doi: 10.1093/jxb/erv047
Bertheloot et al., 2020, *New Phytologist*, 866-879, doi: 10.1111/nph.16201
Corot et al., 2017, *Frontiers in Plant Science*, 8, doi: 10.3389/fpls.2017.01724
Mason et al., 2014, *PNAS* 6092-6097, doi: 10.1073/pnas.1322045111
Rameau et al., 2015, *Frontiers in Plant Science*, 5, doi: 10.3389/fpls.2014.00741

Using functional-structural plant modelling to simulate the eco-evolutionary dynamics that shape plant communities

Jorad de Vries[1], Simone Fior[1], Aksel Palsson[1], Alex Widmer[1], Jake M. Alexander[1]

[1] *Institute of Integrative Biology, ETH Zürich, Switzerland*

For correspondence: jorad.devries@usys.ethz.ch

Keywords: elevation, functional traits, natural selection, range limits.

A fundamental goal of evolutionary ecology is understanding the mechanisms that shape species' distributions, but unravelling the physiological basis of range limits and how these are shaped by biotic and abiotic selection pressures is a formidable challenge (Alexander *et al.*, 2016). This calls for the development of new mechanistic approaches that can integrate data and hypotheses about the physiological constraints and interacting selection pressures that shape plant phenotypes across their range. To simulate the eco-evolutionary dynamics that shape plant communities, I propose combining a functional-structural plant (FSP) modelling approach that is based on resource competition between plants with a model of natural selection. Analytical models of evolutionary game theory and highly detailed three-dimensional models of plant growth and development have existed for decades, and despite facing significant challenges, models that combine the two methodologies have become increasingly complex and dynamic (Bornhofen *et al.*, 2011; Yoshinaka *et al.*, 2018).

Here, we present an evolutionary FSP model whose novelty lies in further advancing the complexity of the simulated plant's form and function, and in the use of empirical data for model parameterisation and validation. The model combines physiological, ecological and evolutionary mechanisms to simulate population dynamics and natural selection in a plant community. The genotype of the virtual plants is represented by a set of heritable traits that describe an individual's morphology, phenology and physiology. These traits interact with the biotic and abiotic factors in the environment to shape the plant's phenotype and subsequent fitness. This measure of fitness then determines the likelihood that the plant's offspring will be present in the next generation of plants, taking recombination and genetic variation in the population into consideration. The model has been parameterised and validated using field data collected from low and high elevation populations of a perennial plant, *Dianthus carthusianorum*, from the Swiss alps (Figure 1). Populations of *D. carthusianorum* growing in low and high elevation habitats are characterised by significant differences in several morphological and phenological traits (Figure 1), which is indicative of selection acting on divergent ecotypes adapted to contrasting environments (Halbritter *et al.*, 2018). With the model, we aim to disentangle what biotic and abiotic drivers selected for the traits that characterize these low and high elevation ecotypes; flowering time, base temperature, lignin content (affecting frost resistance and stalk length:biomass ratio), stalk length and the number of stalks. We selected four environmental drivers that could be associated with the changing biotic and abiotic conditions along an elevation gradient: temperature, plant density, pollinator density and pollinator behaviour.

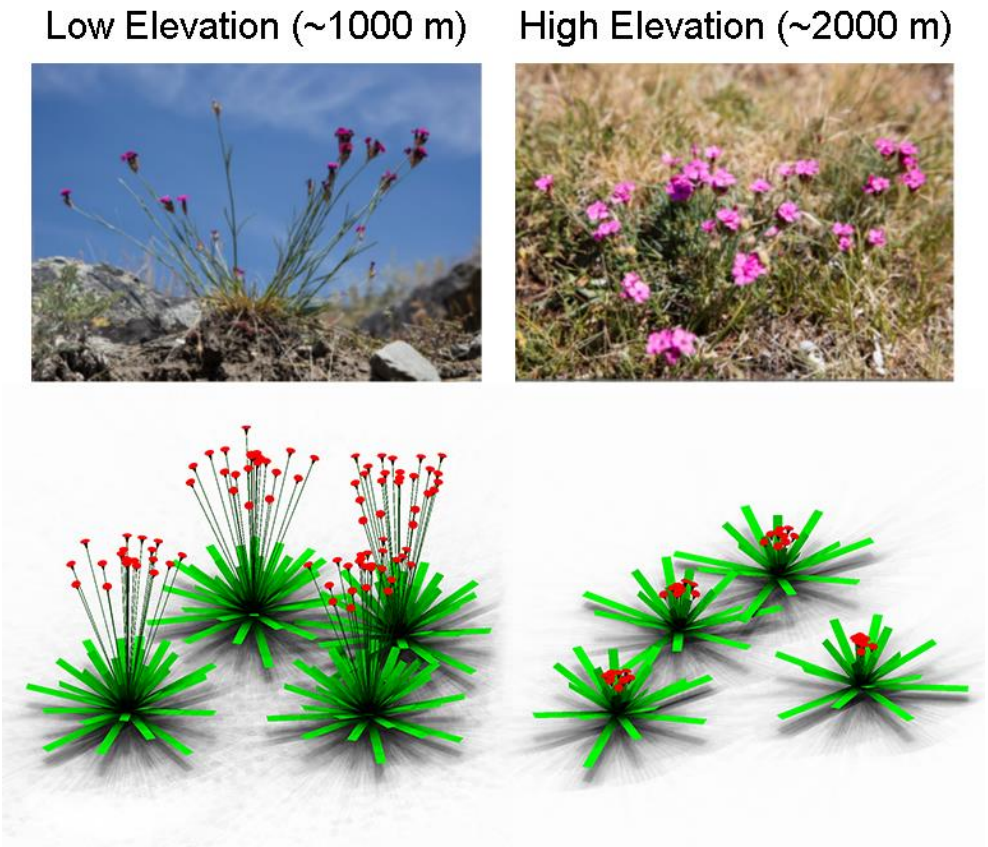

Figure 1. Ecotypes of *Dianthus carthusianorum* growing in high and low elevation populations (top), and the model outcome of selection by conditions that simulate the low and high elevation habitats (bottom).

The model was able to recreate the phenotypes of the two ecotypes of *D. carthusianorum* (Figure 1), suggesting that the simulated selection pressures give rise to the trade-offs in functional traits that define these phenotypes. The results suggest that the trait differences between the high and low elevation ecotypes are the result of interacting mechanisms and selection pressures, with pollination playing a central role. For example, low pollinator densities and strong competition for pollination in high plant densities selected for the increased stalk length that characterises the low elevation ecotype. Additionally, these drivers also selected for increased lignin contents to increase the stalks length:biomass ratio, which in turn selected for a higher base temperature to avoid the frost events that the plants were now more susceptible to due to their increased lignin contents. These results illustrate how multiple interacting mechanisms and selection pressures can shape plant form and function, and can form the basis for a mechanistic understanding of a species' range limits and how these limits might respond to a changing environment.

References

Alexander JM, Diez JM, Hart SP, Levine JM. 2016. When climate reshuffles competitors: a call for experimental macroecology. *Trends in Ecology & Evolution* 31(11): 831-841.

Bornhofen S, Barot S, Lattaud C. 2011. The evolution of CSR life-history strategies in a plant model with explicit physiology and architecture. *Ecological Modelling* 222(1): 1-10.

Halbritter AH, Fior S, Keller I, Billeter R, Edwards PJ, Holderegger R, Karrenberg S, Pluess AR, Widmer A, Alexander JM. 2018. Trait differentiation and adaptation of plants along elevation gradients. *Journal of Evolutionary Biology* 31(6): 784-800.

Yoshinaka K, Nagashima H, Yanagita Y, Hikosaka K. 2018. The role of biomass allocation between lamina and petioles in a game of light competition in a dense stand of an annual plant. *Annals of Botany* 121(5): 1055-1064.

A functional-structural model of tomato simulates increased fruit yields by far-red illumination through higher carbohydrate source and sinks

Pieter de Visser, Anja Dieleman

Wageningen University & Research, Business unit Greenhouse Horticulture, Wageningen, The Netherlands

For correspondence: pieter.devisser@wur.nl

Keywords: ray tracer, photomorphogenesis, carbohydrates, LED illumination, greenhouses, FSPM

Introduction

Functional-structural plant models (FSPM) are an ideal tool to predict crop responses to LED lighting, since FSPM possess 3D functionality to simulate spatial processes with regards to light and plant growth (Godin et al., 2007; De Visser et al, 2014). The 3D features will help in exploring the best illumination strategy with regards to optimal light capture by the crop, given a specific plant structure and specific emission patterns of the lamps. The plant model incorporates photosynthetic potential, that is known to decrease at lower leaf layers. In addition, photomorphogenic changes and photosynthetic acclimation at leaf level may occur and such environmental responses have been shown an FSPM is able to address. A special case of photomorphogenesis is the plant's response to light that is far-red enriched since this causes a strong shade avoidance response (SAR) comprising a significant change in plant structure by increased internode length, apart from other acclimations like leaf length and pigment changes (Dieleman et al., 2019). In this paper the application of FSPM to an illuminated tomato crop is established by calibration of the model on light measurements and crop growth for one growing season, given a LED illumination with red/blue with or without far-red light. Subsequently, the model is validated for two trials, under comparable illumination strategies. The model is used to evaluate the yield increments at the spectra of LED light. Further applications of far-red illumination are explored by simulation of various scenario's.

Materials and Methods

Greenhouse experiments were conducted to examine the response of a number of tomato cultivars to various types of LED illumination. In these trials, the position of the lamps (inter lighting versus top lighting) and the spectral composition (addition of far red light) were altered. All experiments took place at the research facility of Wageningen University & Research in Bleiswijk (52.01 N, 4.31 E), The Netherlands. A total of four experiments were used to study crop response, of which two were used for calibration of crop response to red-blue (R/B) or far-red light, and the other two to validate these modeled responses. Each treatment was conducted in a Venlo-type greenhouse compartment of 144 m^2 having 5 double rows of 50 single-stemmed or 25 double-stemmed plants, bordered by two single rows of 25 plants. The modelling platform used was GroIMP, enabling 3D simulation of plant growth and light distribution (Kniemeyer, 2008). Plant architecture as developing over time was modelled as a series of static 3D representations according to 3-monthly architectural measurements. A spectral ray tracer consisting of an inverted path tracer was used to simulate the 3D light distribution, its absorption, reflection and transmission in the 3D scene (Fig.1)(details in Henke and Buck-Sorlin, 2017). The modelled photosynthesis at leaf level was based on the Farquhar equation (Farquhar et al., 1980) and was made spectrally dependent using an action spectrum specifically measured on tomato. The demand for assimilates was calculated by summing growth and maintenance costs of all plant organs as present in the crop according to weekly registrations of leaf number and size, plant height and truss numbers. Calibration of model parameters involved light absorption, photosynthesis and assimilate partitioning to the organs, as well as photomorphogenetic and photosynthetic response to the additional far-red light. For validation the model output was compared to observed light gradients in the canopy, plant biomass and fruit yield. The model was then used to model alternative set-ups of illumination by modifying light spectrum, lighting duration and lamp positions.

Results and Discussion

The light gradient in the empty greenhouse compartment was modelled in close resemblance to the measurements for the combination of top and interlighting without natural daylight and for natural light solely. The light gradient including the full-grown crop at default R/B illumination without sunlight was modelled best when leaf geometry was simplified to five leaflets per composite leaf. The model on gross photosynthesis was correctly calibrated. Results showed a good match between calculated carbohydrate production from simulated light interception and photosynthesis, and measured carbohydrate sinks, ranging from 15 to 28 g carbohydrates per m^2 ground area per day. At far-red illumination, plant structure was different relative to the control treatment, by more elongation in the first weeks of growth, leading to taller plants with occasionally smaller leaves. Photosynthetic capacity of leaves was increased in the trials where far-red was added to PAR. These architectural and photosynthetic changes were incorporated in the FSPM and resulted in a modelled higher light interception and growth of the crop in the first weeks of the trial, followed by a decrease at smaller leaf size, until the end of the trial, for the far-red illuminated crop relative to the control. When the whole season of artificial lighting was simulated, the total carbohydrate production was higher for the far-red illuminated crop relative to the control. This result was in agreement with the observed differences in fruit yield. The response of internode elongation and fruit growth to far-red perceived by the organs was compared to the relationships reported in Kahlen and Stützel (2011) for cucumber. The observed relationship was cultivar-dependent and may allow scenario studies on far-red illumination of specific cultivars. The observed positive effect on sink strength of fruits was evaluated. These yield-increasing effects of far-red were further explored by scenario modelling with the aim to reduce electricity consumption for lighting. The ideal scenario consisted of a combination of temporal use of far-red light replacing partially the PAR light from lamps and a far-red light sensitive cultivar.

Conclusion

The extensive data on biomass and plant architecture of the different experiments allowed a realistic simulation of spatial light distribution, photosynthesis, carbohydrate supply and fruit yield of LED-illuminated tomato crops. Simulation of 3D light distribution of different colors of LED light is essential to predict the crop's response to different types of LED illumination.

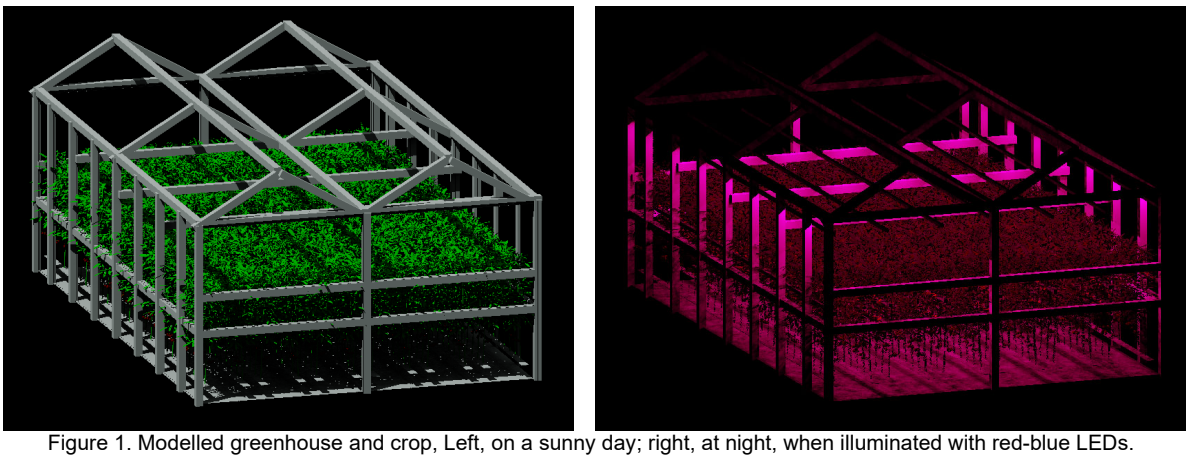

Figure 1. Modelled greenhouse and crop, Left, on a sunny day; right, at night, when illuminated with red-blue LEDs.

References

De Visser et al., 2014, *Front. Plant Sci.,* doi: 10.3389/fpls.2014.00048
Dieleman et al., 2019, *Front. Plant Sci*., doi: 10.3389/fpls.2019.00839
Farquhar et al., 1980. *Planta 149, 78–90*
Henke and Buck-Sorlin, 2017, *Computing and Informatics 36 (6),* doi:10.4149/cai_2017_6_1492
Godin and Sinoquet, 2005, *New Phytologist* 166, 705-708.
Kahlen and Stützel, 2011, *New Phytologist* 190, 697-708.
Kniemeyer, 2008, PhD thesis, BTU Cottbus, http://opus.kobv.de/btu/volltexte/2009/593/

Mechanistic simulation of competition for light and nitrogen in strip intercrops

Jochem B. Evers[1], Wopke van der Werf[1], Tjeerd J. Stomph[1], Jorad de Vries[2], Lammert Bastiaans[1], Niels P.R. Anten[1]

[1] *Centre for Crop Systems Analysis, Wageningen University and Research, Wageningen, the Netherlands*
[2] *ETH Zürich, Institute for Integrative Biology, Zürich, Switzerland*

For correspondence: jochem.evers@wur.nl

Keywords: Niche differentiation, crop mixtures, 3D modelling, virtual plants

Introduction

In strip intercrops, two crop species are grown in alternating strips of varying row number. Such intercrops contribute to various ecosystem services, including high production and efficient use of resources (Brooker *et al.* 2015). A large body of literature exists on the ecological and physiological mechanisms that underlie the increased performance of intercrops over sole crops (Bedoussac *et al.* 2015). To complement experimental and meta-analysis studies on the mechanisms underlying intercrop performance, we proposed functional-structural plant (FSP) modelling (Evers *et al.* 2019), since FSP modelling is ideally geared towards capturing the spatially and temporally heterogeneous canopy structure typical for strip intercrops. FSP models capture interspecific above- and belowground plant-plant interactions, that contribute to the high performance and resource use efficiency of intercrops. We argued FSP models can help 1) identifying plant traits that optimize the complementarity between species needed for high production and efficiency and 2) optimizing the configuration of the intercrop setup in terms of strip widths and distances between rows and plants. Here we present an implementation of the FSP modelling approach proposed in Evers *et al.* (2019). The objective of this work was to demonstrate how behaviour of crop plants in strip intercrops, responding to competition for light and nutrients, can be the result emerging from simulating plants growing in strip intercrop designs. To illustrate the approach, we simulated the effect of root angle for intercrop performance as an example of a plant trait, and the effects of different strip widths (number of rows per strip) as an example of different intercrop setups.

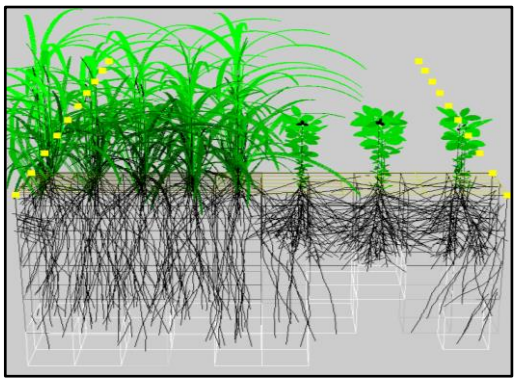

Fig. 1: Field slice of an intercrop of wheat and soybean in the wide root angle simulation.

Methods

To address the objectives we used an FSP shoot model (Evers and Bastiaans 2016) expanded with root growth and nutrient uptake. In the model, the production of new organs (leaves, internodes, roots) on a stem is controlled by temperature. Growth of those organs over time is the result of supply of and demand for assimilates. Assimilate supply follows from photosynthesis by green tissues as a function of leaf light capture, leaf nitrogen content and temperature. Assimilate demand is generated by organ sink strength controlled by organ age and temperature. The leaf nitrogen content driving photosynthesis is the result of nitrogen uptake by the roots and distribution over the leaves following the light gradient in the canopy. Thus, when simulating plants growing together in a stand, plant production is the result of competition with neighbouring plants for light and nitrogen.

To assess the importance of root angle for intercrop performance, we simulated generic wheat and soybean sole crops and strip intercrops composed of five-row wheat strips and three-row soybean strips at identical sowing times (fig. 1). To assess the effect of different strip widths, we simulated wheat and maize sole crops and strip intercrops at increasing row

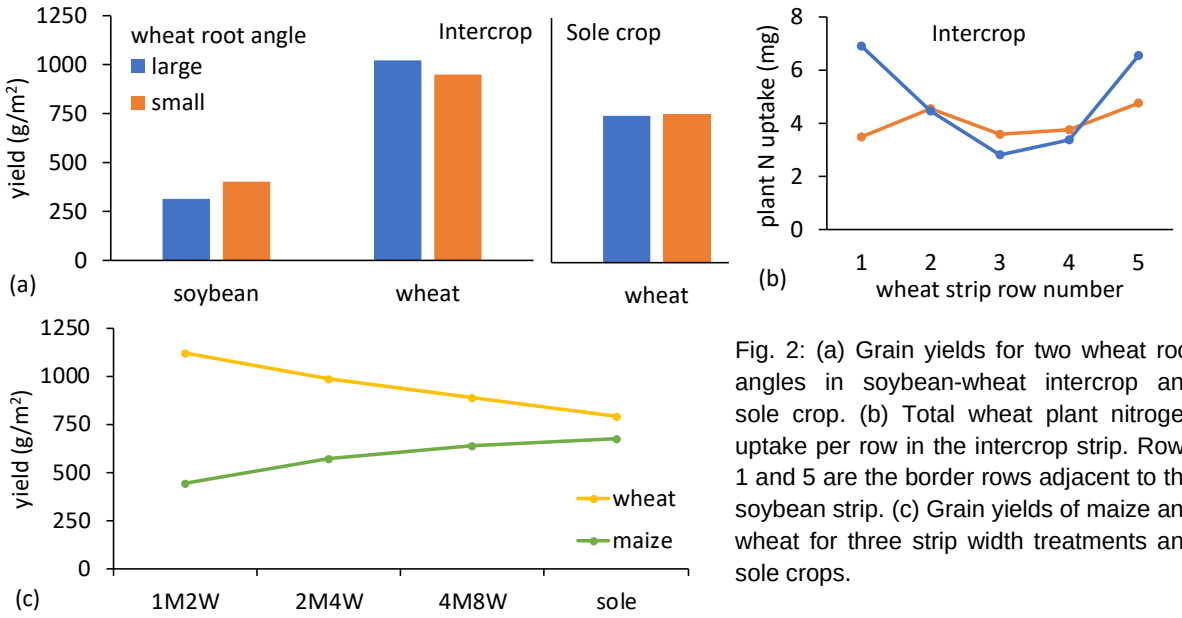

Fig. 2: (a) Grain yields for two wheat root angles in soybean-wheat intercrop and sole crop. (b) Total wheat plant nitrogen uptake per row in the intercrop strip. Rows 1 and 5 are the border rows adjacent to the soybean strip. (c) Grain yields of maize and wheat for three strip width treatments and sole crops.

numbers per strip: one to four for maize (1M, 2M, 4M) and two to eight for wheat (2W, 4W, 8W). Maize was sown 40 days after wheat. In all cases agriculturally sensible population densities were used, and in intercrops both species occupied half of the field area (50/50 designs). Field edge effects were minimized by cloning the simulated scene 100 times. Start soil N was 750 mmol/l, and legume N fixation was not considered. Radiation and temperature were set to Dutch conditions (52° N). Modelling platform was GroIMP v1.5.

Results

Wheat yield per unit of wheat area was higher in intercrop with soybean than in sole crop (fig. 2a) with either root angle. A large root angle gave higher yield than a small root angle in intercrops, whereas there was no difference between angles in sole crops. Soybean performed worse next to wheat with wider root systems. The main contributors to the high wheat yield with large root angles were the border row plants which took up much more nitrogen (fig. 2b) due to easier access to the soil in the soybean strip (seen in fig. 1). As consequence, border cereal plants produced more leaf area and intercepted more light than the inner rows (not shown). Maize-wheat intercropping improved overall system land use efficiency by 4% for all strip widths. Narrower strips (more border rows) resulted in improved wheat yield but decreased maize yield (fig. 2c), mainly due to border row N-uptake and light capture (not shown).

Discussion

These preliminary simulations clearly illustrate the sensibility of selecting genotypes with traits optimized for intercrop performance, as in sole crop root angles did not make a difference. Further tests on different traits should allow to identify promising trait combinations or even whole phenotypes that maximize production and efficiency of intercrops. For intercrops with late sown species like maize, narrow strips mainly benefit the early species at the expanse of the later sown one, which could be improved with varieties showing a high capacity to compensate for heavy competition during the vegetative phase.

Acknowledgements

We thank Elena Pelech and Shuangwei Li for providing soybean parameters. We acknowledge funding from the EU Horizon2020 Programme ReMIX (grant n°727217).

References

Bedoussac et al., 2015, *Agron Sust Dev* 35: 911–935, doi: 10.1007/s13593-014-0277-7
Brooker et al, 2015, *New Phytol* 206: 107–117, doi: 10.1111/nph.13132
Evers and Bastiaans, 2016, *J Plant Res* 129: 339–351, doi: 10.1007/s10265-016-0807-2
Evers et al, 2019, *J Exp Bot* 70: 2381–2388, doi: 10.1093/jxb/ery288

MTG as a standard representation of plants in FSPMs

Christophe Pradal[1,2], Christophe Godin[3]

[1] *CIRAD, UMR AGAP & inria, Zenith, Montpellier, France*
[2] *AGAP, Univ Montpellier, CIRAD, INRAE, Institut Agro, Montpellier, France*
[3] *Laboratoire Reproduction et Développement des Plantes, University of Lyon, ENS de Lyon, UCB Lyon 1, CNRS, INRAE, Inria, F-69342 Lyon, France*

For correspondence: christophe.pradal@cirad.fr

Keywords: plant architecture, multiscale data structure, graph traversal, simulation, modularity

Introduction

Two decades ago, a mathematical formalism was introduced to represent the complexity of plant branching structures at different scales with a unified approach. Using Multiscale Tree Graph (MTG), it was possible to capture the topology and the geometry of a multitude of plant species at different scales in a precise manner. However, the use of this formalism was initially dedicated to quantitative acquisition and analysis of plant branching systems. Its use in mechanistic models of plant growth has progressively emerged in various works to support multiscale modeling. In this paper, we review how the MTG formalism has been applied to models of plant development and extend it to comply fully with the requirements of Functional-Structural Plant Models (FSPM) at different scales.

Methods

Formalizing plant structure representation – To represent branching, different mathematical formalisms have been proposed such as Axial Tree (Prusinkiewicz et Lindenmeyer, 90), MTG (Godin and Caraglio, 1998), which define plant multiscale topological structures as a serie of nested tree graph, and more recently a structure-of-scales (Ong and Kurth, 2012) that, inspired from MTGs, models the scales as a partially ordered sets and allows to manage an extensive range of scales. Here we review how MTGs can be embedded in the context of FSPMs. This includes the possibility to grow MTG using developmental rules expressed for instance in the formalism of L-systems, and to encode the dynamic structure at different developmental stages as a time-series. We also discuss new extensions such as the possibility to manipulate continuous representations of plant properties at different scales.

Generic algorithms - Various algorithms have been designed to manipulate MTGs in a generic manner. We defined multiscale traversal (basipetal or acropetal) and user-defined visitors to model flows through plant structure at different scales, interaction with the environment as well as 3D visualization. Other algorithms are provided such as scale insertion or removal (see Figure), or a merge operator that concatenates several MTGs.
Universal coding of plants - MTGs correspond to computational data structures that can be described as simple bracketed strings. This notation is generic and provides simple means to describe any plant architecture as a universal string of characters. For Multiscale Axial Tree, a restricted family of MTGs, this notation corresponds to the lstring notation in the context of L-Systems (Boudon et al. 2012). This coding strategy has also been extended to encode dynamic multiscale structures.

Results and Discussion

In this section, we illustrate how the formalism of MTGs can be used in different FSPM applications. These applications concern acquisition and reconstruction, transport, interaction with the environment as well as simulation of plant growth.
Mapping real plants to MTG - MTG can be built either: i) from a textual description of a

plant structure provided manually or automatically using digitizing techniques, ii) from root phenotyping pipelines using the RSML format, and iii) from LIDAR or image shoot phenotyping methods available in OpenAlea.

Modelling multiscale transport - One important application of FSPM is the simulation of resource transport between plant components inside the plant architecture. Here, we use multiscale traversal algorithms to solve the flow of resources or hormones. Our approach is computationally efficient in memory and time, and has been applied to model shoot and root hydraulic architecture (Albasha et al., 2019), as well as source/sink carbon allocation at different scales (Reyes et al., 2019).

Interaction with the environment - Plant environment is usually represented as a separated spatial data structure (eg. 1D layers, grid of voxels, octree). This spatial structure models the geometric neighborhood of each plant entity. A mapping between these two structures is maintained to allow information transfer between the spatial and the topological structures. For example, the radiative balance or water uptake in a soil is computed using the spatial structure while the results are back-projected on the topological one.
Simulation of growth - The MTG formalism is the central data structure of the OpenAlea platform. Connexions with several FSPM simulation frameworks (GroIMP, L-Py or LIGNUM) have been developed by using the MTG data-structure as a unifying representation of plants. MTG growth can also be carried out in a procedural, data-driven manner, by interpolating different stages to form a temporal MTG, like in the ADEL model.

Conclusion

The MTG formalism has been extended to model and simulate FSPM at different scales. A package is available in OpenAlea with full documentation (https://mtg.readthedocs.io). Web tutorials are implemented using Jupyter Notebooks and are saved as interactive and reproducible documents with specific MTG and 3D widgets (see https://bit.ly/2QaYgVJ).

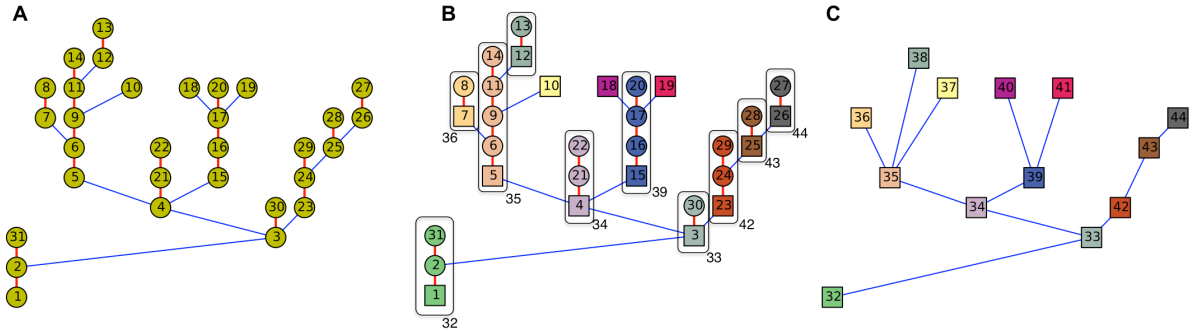

Figure: Automatic visualisation of an MTG at two different scales: A) The MTG is drawn as a tree at the lowest internode scale. Edges are drawn in red (successor) and blue (ramification). B) Automatic insertion of an axis scale. First vertex of each axis is marked to build a quotiented tree (square node). C) The same MTG drawn at the axis scale.

References

Albasha et al., 2019, https://doi.org/10.1093/insilicoplants/diz007
Godin and Caraglio, 1998, https://doi.org/10.1006/jtbi.1997.0561
Ong et al., 2014, https://doi.org/10.1093/aob/mcu155
Prusinkiewicz and Lindenmayer; 1990, https://doi.org/10.1007/978-1-4613-8476-2
Reyes et al., 2019, https://doi.org/10.1093/aob/mcz122

Development of a Quantitative Comparison Tool for Plant Models

Olivier Pieters[1,2], Tom De Swaef[2], Francis wyffels[1]

[1] *IDLab-AIRO -- Ghent University -- imec, Belgium*
[2] *Plant Unit, Research Institute for Agriculture, Fisheries and Food, Belgium*

For correspondence: olivier.pieters@ugent.be

Keywords: model comparison, reservoir computing, machine learning, virtual plant, benchmark

Over the past three decades, plant modelling has become a major research domain. Robust, validated models allow to study the effect of plant treatments on plant development in virtual conditions, providing novel insights and enabling users to optimise field conditions more effectively. Because of this success, a large amount of models has been developed at different scales of detail, from organ level functional-structural plant models (FSPMs) to field-scale crop models. This difference in structure and purpose, offers different optimisations and trade-offs. quantitative-plant.org/model provides an overview of the wide range of available models. However, selecting the right model for a specific purpose is not easy.

Comparing plant models often relies on intricate knowledge of the model, and sometimes experiments. For example, (Feng et al, 2014) compared an empirical crop model with an FSPM. They used detailed knowledge of the models and field trials to compare both models. This significantly obstructs similar studies, due to time and cost requirements involved with learning the inner workings of a model and executing field experiments. To the best of our knowledge, easy to use, quantitative, and model-independent measures are lacking. We propose to build upon (Dambre et al., 2012) and use the reservoir computing (RC) framework to enable fast, quantitative estimates of model performance with a common set of benchmark tasks. The goal of these tasks is to assess the non-linear and memory modelling capabilities of the model through a set of increasingly difficult tasks.

RC is a computational framework related to recurrent neural networks. It is well suited for temporal and sequential data. The input is mapped into a high-dimensional space whose current state is a function of the current input and the previous state of the network. A linear readout of the current network state is used to assess the target task (a benchmark in our case). This structure gives rise to memory due to recursive connections, and non-linearity. The mathematical formulation is included below in the case of discrete time, but is extendable to continuous time. A visual representation is depicted in Figure 1.

$$\boldsymbol{s}_t = f(\mathbf{W}\,\boldsymbol{s}_{t-1}) + \mathbf{A}\,\boldsymbol{x}_t$$
$$\boldsymbol{y}_t = \mathbf{B}\,\boldsymbol{s} + \boldsymbol{b}_0$$

Vectors $\boldsymbol{x}$, $\boldsymbol{s}$ and $\boldsymbol{y}$ represent the input(s), current state and benchmark target(s) of the network at time point t respectively. $\boldsymbol{x}$ and $\boldsymbol{y}$ are reduced to scalars if there is just one input variable and output target, respectively. The output task is computed using a linear combination of network states, represented by **B**. **W** represents the interconnectivity of the network, and how much each state influences the other states in the next time point. $f(\cdot)$ is a non-linear function that is often implemented by means of a tanh or sigmoid that is applied element-wise. Compared to conventional recurrent neural networks, training a reservoir is much simpler. The interconnectivity of the network **W** and input mapping **A** are randomly initialised and kept fixed. Only the linear mapping **B** from the network's state to the output target is optimised. This reduces the optimisation to a linear regression problem, which is well studied.

The RC framework is very general and can be extended to various physical media. For instance, in compliant robots RC is used to outsource part of the control tasks to the physical body (Caluwaerts et al., 2012). Applicability of the RC framework requires two properties: fading memory and non-linearity (Fernando and Sojakka, 2003). These are clearly satisfied

by plants, and their modelling counterparts. Models rely heavily on differential equations, whose solutions are generally not linear, and time-dependent.

This analogy between general RC and plant model-based RC is depicted in Figure 1. A wide range of biotic and abiotic factors form the input of the model, while the reservoir is the plant model itself whose state is observed using the dynamic output variables such as dry matter content, photosynthesis and stomatal conductance. These are combined to compute the benchmark tasks. These benchmark tasks are usually mathematical functions that have to be computed that are non-linear time-dependent transformations of the input signals.

Similar to, (Nakajima et al., 2015), the selected set of tasks should assess the non-linear and temporal modelling capabilities of plant models. This provides further insight into the physiological processes involved in learning and anticipating future events within plants.

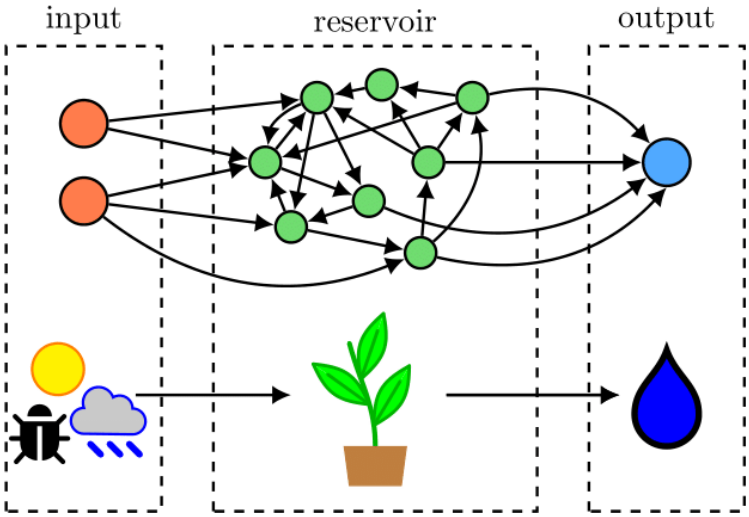

Figure 1 Reservoir computing setup (top) applied to plant models (bottom). The orange, green and blue nodes represent the input ($\boldsymbol{x}$), state ($\boldsymbol{s}$) and output ($\boldsymbol{y}$) of the reservoir respectively. The edges represent the interdependence between nodes (**A**, **B**, and **W**). This is readily applied to the modelling setup we consider here, where the input is the input of the plant model, the reservoir is the plant model itself whose state is observed using the outputs to estimate one of the benchmark tasks.

To conclude, we propose to consider plant models as simulated implementations of reservoirs. From their outputs, a set of user defined benchmark tasks can be calculated. An easy comparison of plant models is then possible by means of these benchmark tasks, providing information about non-linearity, and memory. Since the aim of plant models is the accurate simulation of plants, this can be a stepping-stone for the application of RC to plants, leading to a new framework to explain plant behaviour.

References

Nakajima et al., 2015, *Scientific Reports* 5, 10487, doi: 10.1038/srep10487
Fernando and Sojakka, 2003, *Springer Berlin* 588-597, doi: 10.1007/978-3-540-39432-7_63
Caluwaerts et al., 2012, *Artificial Life* 19:35-36, doi: 10.1162/ARTL_a_00080
Feng et al, 2014, *European Journal of Agronomy* 53:16-17 doi: 10.1016/j.eja.2013.11.005
Dambre et al., 2012, *Scientific Reports* 2:1-7 doi: 10.1038/srep00514

The plant water pump: why water flows uphill of water potential gradients in a root hydraulic anatomy model

Valentin Couvreur[1] and Xavier Draye[1]

[1] *Earth and Life Institute – Agronomy, University of Louvain, Louvain-la-Neuve, Belgium*

For correspondence: valentin.couvreur@uclouvain.be

Keywords: Hydraulics, composite, osmolite, plasmodesmata, aquaporin

Guttation is the exudation of xylem sap from vascular plant leaves. This process is particularly interesting because in its configuration root water uptake occurs against the hydrostatic pressure driving force. Hence, it emphasizes the contribution of another driving force that lifts water in plants: the osmotic potential gradient.

The current paradigm of root water uptake explains that, due to the endodermal apoplastic barrier, water flows across root radius from the same principles as through selective membranes: driven by the total water potential gradient. This theory relies on the idea that during guttation, osmolites loaded in xylem vessels decrease xylem total water potential, making it more negative than the total soil water potential, and generating water inflow by osmosis as in an osmometer.

However, this theory fails at explaining experiments in which guttation occurs without sufficient solute loading in root xylem of maize (Enns et al., 1998; Enns et al., 2000) and arrowleaf saltbush (Bai et al., 2007) among others; studies concluding that experimental observations “could not be explained with the current theories in plant physiology”. Such flow rates towards combined increasing pressure potentials and increasing osmotic potentials between separate apoplastic compartments would necessitate an effective root radial conductivity that is negative; a mind bender.

What piece of hydraulic network would make it possible for water to flow against the total water potential driving force?

We implemented Steudle’s composite water transport model in the explicit root cross-section anatomical hydraulic network MECHA (Couvreur et al., 2018). All apoplastic, transmembrane and symplastic pathways are interconnected in the network. The results show that while root radial conductivity is particularly sensitive to cell membrane permeability, the combination of conductive plasmodesmata and increased dilution of protoplast osmotic potentials inwards is a key to explain root water flow towards increasing total potentials. A triple cell theory is suggested as new paradigm of root radial flow.

References

Bai X-F, Zhu J-J, Zhang P, Wang Y-H, Yang L-Q, Zhang L (2007) Na+ and Water Uptake in Relation to the Radial Reflection Coefficient of Root in Arrowleaf Saltbush Under Salt Stress. *Journal of Integrative Plant Biology* 49: 1334-1340

Couvreur V, Faget M, Lobet G, Javaux M, Chaumont F, Draye X (2018) Going with the Flow: Multiscale Insights into the Composite Nature of Water Transport in Roots. *Plant Physiology* 178: 1689-1703

Enns LC, Canny MJ, McCully ME (2000) An investigation of the role of solutes in the xylem sap and in the xylem parenchyma as the source of root pressure. *Protoplasma* 211: 183-197

Enns LC, McCully ME, Canny MJ (1998) Solute concentrations in xylem sap along vessels of maize primary roots at high root pressure. *J. Exp. Bot.* 49: 1539-1544

A bidirectional interface between BwinPro and GroIMP

Tim Oberländer[1], Winfried Kurth[1]

[1] *Department of Ecoinformatics, Biometrics and Forest Growth, Georg-August Universität Göttingen*

For correspondence: tim.oberlaender@stud.uni-goettingen.de

Keywords: GroIMP, BwinPro, *FSPM*, stand-simulation

Introduction

This project provides a way to transfer data between the software platforms BwinPro (Nagel, 2006) and GroIMP (Kniemeyer, 2008), i.e., between a forest stand simulation platform and an FSPM platform. BwinPro and GroIMP are tools used for similar topics and each of them has its advantages on the scale of spatial resolution for which it was designed. So it is useful to have a simple and customizable way to transfer data between them.

BwinPro is a stand simulation software developed by the North-West German Forest Research Station (NW-FVA). It is mainly designed for analyzing, simulating and evaluating forest stands. Therefore the program can read in existing stand data as well as generate random stands. It can generate reports, e.g., about the growth or the wood volume in simulation periods of five years. BwinPro implements calculations for all major tree species in North-West Germany.

GroIMP (Growth Grammar-related Interactive Modelling Platform) is a software for algorithmic 3D modeling, especially used for plants. GroIMP uses parallel graph grammars, generalizing the well-known Lindenmayer systems, to simulate the growth and ontogenetic development of plants, including trees, at organ level. This is realized by the programming language XL, which is an extension of Java. Conditioned by the plugin-based program structure, GroIMP offers a lot of additional features like geometry objects (e.g., NURBS surfaces), a raytracer for light calculations, a solver package for differential equations and several renderers. The data interface developed in our project was also realized as a plugin of GroIMP.

The tree model

This project is working with a basic tree vector, which can be customized in an advanced usage of our interface. This vector includes the position of the tree, its height, its diameter at breast height, its crown diameter, its crown base, the code for its species, an identification code for the species according to the NW-FVA standards, and its age. This 9-dimensional vector includes all data needed to generate a simplified tree in GroIMP as well as to generate all other data needed in BwinPro.

BwinPro to GroIMP

Due to the fact that TreeGross XML, the file format of BwinPro, is mainly a normal XML file, it is quite simple to import the data to GroIMP. In the final version of our interface it is only needed to open the .xml file like any other file. The basic configuration creates two types of trees, conifers and deciduous trees. They are presented by a cylinder (for the trunk) and either a cone or a sphere (for the crown). It is also possible to customize the tree models and the imported parameters.

The imported trees can be filtered based on BwinPro parameters, for example, only alive trees or trees older than 5 years can be selected. Based on the design of the generated XL code it is simple to change the tree module (GroIMP object) based on the species.

GroIMP to BwinPro

As a consequence of the highly diverse ways to design trees in GroIMP, it is more complicated to read data out of a model which was implemented there. Yet GroIMP comes with a collection of analysis tools. So it was a logical decision to create the export function directly in XL.

Another challenge was that GroIMP stores all data in one huge graph. Therefore it is not always trivial to detect the representation of a single tree within this graph. To solve this, the project uses so called TreePointer modules as objects in XL. A TreePointer module has to be initialized right before each tree, it includes the calculation for the 9 basic tree parameters, and also presents the opportunity to add calculations for the other BwinPro-parameters or to set fixed values for them.

Since XL is based on Java, the xml writer is also implemented directly in GroIMP.

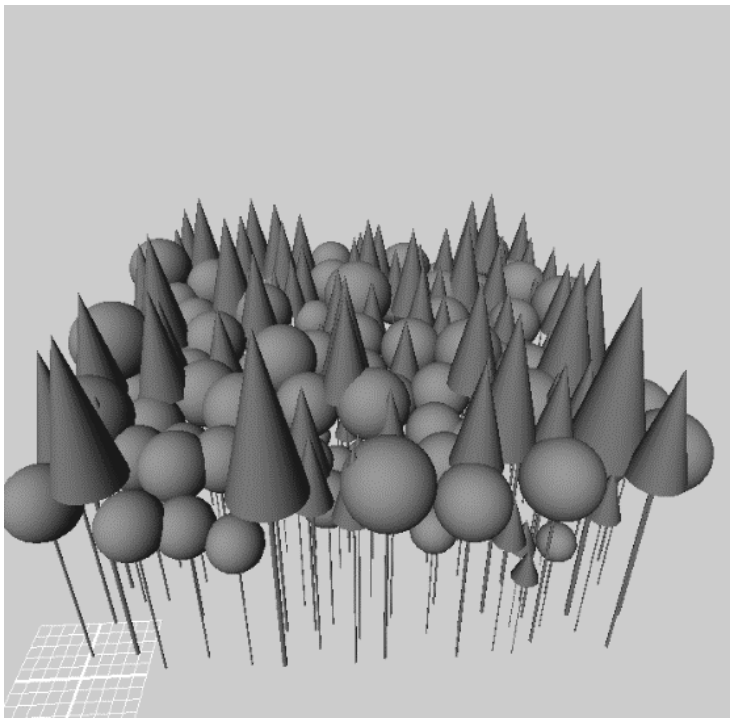

Figure: A stand imported from BwinPro into GroIMP.

Summary

In conclusion the tool which emerged from the project is working in both ways quite well and can hopefully be an advantage for users of both involved software platforms.

References

Nagel, J. 2011. *Forest Simulator BWINPro 7.6 – English Manual – Version April 2011.* [Online]. Available at: http://www.nw-fva.de/?id=194#524. [Accessed: 2020, March 12]

Kniemeyer, *Design and implementation of a graph grammar based language for functional-structural plant modelling*. Diss. Univ. Cottbus, Germany, 2008.

CPlantBox, a whole plant modelling framework for the simulation of water and carbon related processes (flows and growth).

Xiao-Ran Zhou[1], Andrea Schnepf[1], Jan Vanderborght[1], Daniel Leitner[2], André Lacointe[3], Harry Vereecken[1], Guillaume Lobet[1]

1: Agrosphäre (IBG-3), Forschungszentrum Jülich GmbH, Jülich, Germany

2: Simulationswerkstatt, Humboldtstraße 40, 4020 Linz, Austria

3: INRA, UMR 547 PIAF, F-63100 Clermont-Ferrand, France

For correspondence: g.lobet@fz-juelich.de

Keywords: carbon, water, *in silico*, modelling, pressure

The interaction between carbon and flows within the vasculature is at the center of most growth and developmental processes. Understanding how these fluxes influence each other, and how they respond to heterogeneous environmental conditions, is important to answer diverse questions in agricultural and natural ecosystem sciences. However, due to the high complexity of the plant-environment system, specific tools are needed to perform such quantitative analyses.

Here we present CPlantBox (Zhou et al. 2020), a whole plant modelling framework based on the root system model CRootBox (Schnepf et al. 2018). CPlantbox is capable of simulating the growth and development of a variety of plant architectures (root and shoot). In addition, the flexibility of CPlantBox enables its coupling with external modeling tools. Here, we connected the model to an existing mechanistic model of water and carbon flows in the plant, PiafMunch (Lacointe and Minchin 2008). This coupling allows to generate a dynamic feedback between the water uptake, carbon flow and the plant growth and development (fig. 1).

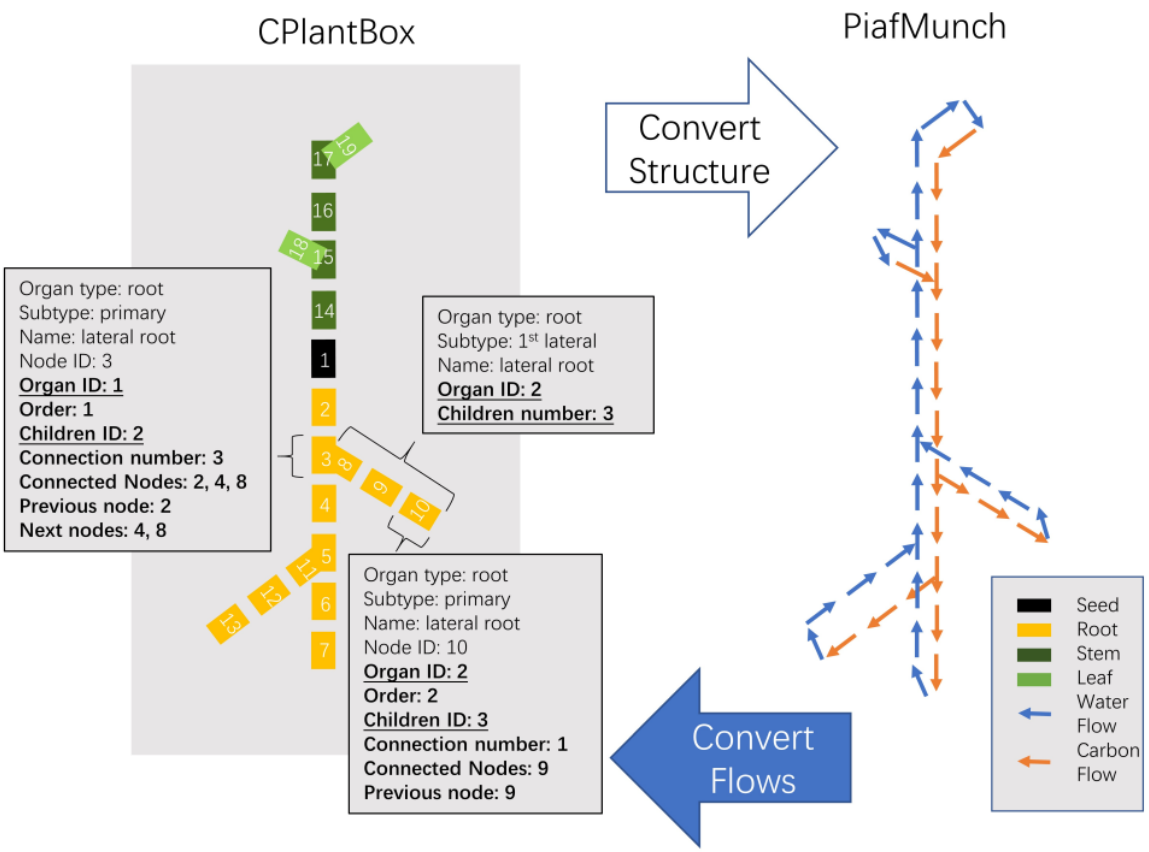

Figure 1. How carbon-feedback-growth is achieved through a couple of CPlantBox and PiafMunch.

The usefulness of the CPlantBox modelling framework is exemplified in several case studies. Firstly, we illustrate the range of plant structures that can be simulated using CPlantBox. We simulated the impacts of heterogeneous environments on carbon and water flows. Finally, we show how such heterogeneous flows generate different architectural patterns.

The CPlantBox modelling framework is open-source, highly accessible and flexible. Its aim is to provide a quantitative framework for the understanding of plant-environment interaction.

References

Lacointe A, Minchin PEH. **2008**. Modelling phloem and xylem transport within a complex architecture. *Functional plant biology: FPB* **35**: 772–780.

Schnepf A, Leitner D, Landl M, *et al.* 2018. CRootBox: a structural–functional modelling framework for root systems. *Annals of botany* **121**: 1033–1053.

Zhou X-R, Schnepf A, Vanderborght J, *et al.* 2020. CPlantBox, a whole-plant modelling framework for the simulation of water- and carbon-related processes. *in silico Plants* **2**.

OpenSimRoot: Software for root architectural models.

Johannes A. Postma[1*], Ernst D. Schäfer[2], Christopher K. Black[3], Christian W. Kuppe[1]

[1] *Insititute for Plant Sciences (IBG2), Forschungszentrum Jülich, Jülich, Germany*
[2] *Centre for Mathematical Medicine and Biology, School of Mathematical Sciences, University of Nottingham, Nottingham, NG7 2RD, UK*
[3] *Department of Plant Science, The Pennsylvania State University, University Park, PA, USA.*

**For correspondence: j.postma@fz-juelich.de*

Keywords: FPSM, plant nutrition, plant hydrology

Introduction: To study the relation between root phenotype and water and nutrient uptake, we developed OpenSimRoot, an open source code base for constructing root architectural models. The aim was to have a flexible code that could represent many architectures, to simulate carbon, nutrient and water flows and utilization. We aimed at constructing a flexible platform using standardized utilities that would allow modular coupling of different differential equations, re-definition of the way state variables are simulated, and robust numerical solving.

Methods: OpenSimRoot was implemented in C++, taking advantage of inheritance in order to have a plug-in like modular behavior for simulating different components. At the highest level it defines a system as a tree-data-structure of minimodels, each minimodel representing a state variable. These minimodels are treated as a system of ordinary differential equations (ODEs) and are solved using predictor-corrector methods (variously implemented). Model coupling is implemented through data requests that loop through the API to other “minimodels”. Different subsystems are allowed to have varying time steps, but all time steps are synchronized at given intervals. Data exchange is achieved through interpolation.
Instantiation of the model is based on an XML formatted input file. The XML allows the user to define different models, ranging from simple coupled ODE systems, like a double mass-spring system to test the coupling algorithm, to FSPMs. The XML allows users to define parameters as varying in time and space, with or without stochastic behavior. Models are defined as tree-data-structures of state variables, each of which can be either directly linked to a parameter, a build-in function class (algebraic or ODE), or an equation provided in the XML. The repository contains example (demo) inputs for, among others, Lotka-Volterra model, a simple crop model, a 3D Richards Equation solver and FSPMs parameterized for various crops. Model output is request driven and maybe in the form of various tables and VTK formats for visualization of both the soil domain and the simulated root system.

Results: Testing the code demonstrated that OpenSimRoot can accurately solve coupled equation systems and various benchmarks described in the recent Benchmarking paper for root architectural models (Schnepf et al., 2020). Scientifically, OpenSimRoot, as well as its non-open-source predecessor SimRoot, have contributed to numerous scientific papers, and various predictions of relations between nutrient uptake and root traits have been confirmed by genotypic contrast studies.

Conclusion: FSPMs combine differential equations (ordinary as well as partial) with algebraic formulation. They typically contain stochastic elements, and discrete events such

as the formation of new organs. This presents great challenges for the implementation, and for finding numerically stable and accurate solutions. OpenSimRoot provides a flexible solution that, thus far, seems to perform well on various benchmarks. The XML model definitions are flexible, different “minimodels” can be specified for state variables, but thereby must also be comprehensive and can be challenging to new users. An additional layer of abstraction may be a useful future development. Although theoretically the number of plants and plant species is unlimited, the current implementation is memory intensive, and thereby limits the simulated root length to the several km range.

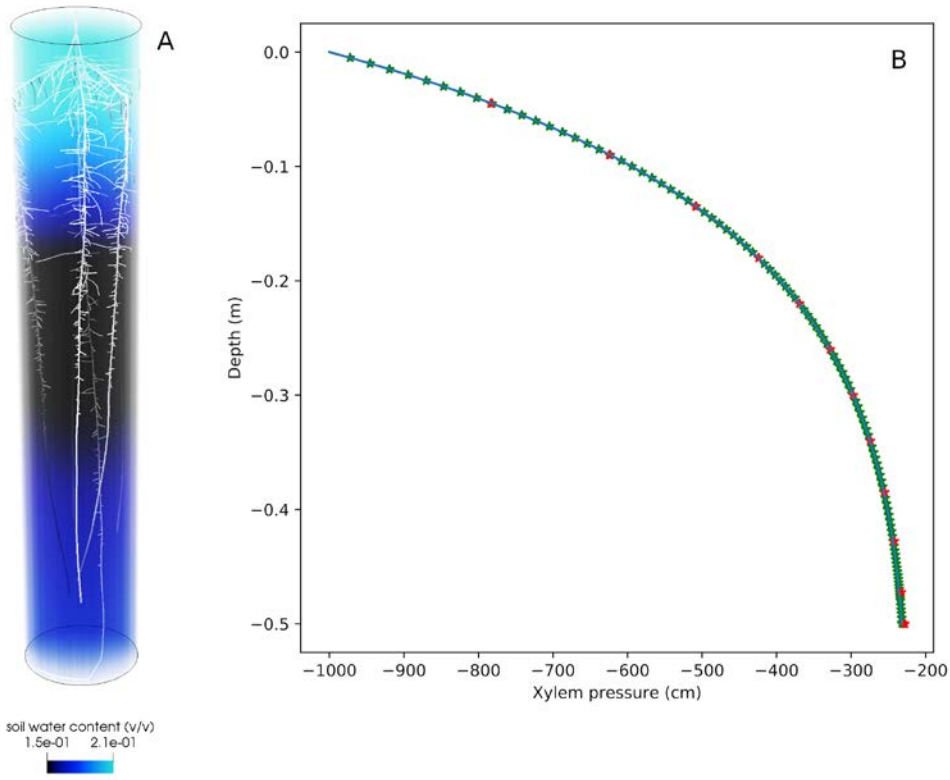

Figure: A) Rendering of simulation of root system growing in a cylindrical pipe. Pseudo colors show simulated soil water content. B) Output of Benchmark 3.1 in Schnepf et al. (2020), which test the xylem pressure in a single vertical root. Blue line analytical solution, green and red dots simulation results for fine and coarse discretized roots.

References

Postma et al., 2017, N*ew Phytologist* 215, doi: 10.1111/nph.14641
Schnepf et al., 2020, Frontiers in Plant sciences, doi: 10.3389/fpls.2020.00316

Co-simulation with OpenAlea and GroIMP for cross-platform functional-structural plant modelling

Qinqin Long[1], Christophe Pradal[2,3], Winfried Kurth[1]

[1] *Department Ecoinformatics, Biometrics and Forest Growth, Georg-August-Universität Göttingen, Göttingen, Germany*
[2] *AGAP, Univ Montpellier, CIRAD, INRAE, Institut Agro, Montpellier, France*
[3] *CIRAD, UMR AGAP, and inria, Univ Montpellier, Montpellier, France*

For correspondence: wk@informatik.uni-goettingen.de

Keywords: component-based, model connection, data exchange, interfacing, interoperability

Introduction

Within the FSPM community, different teams of researchers have specialized on different processes. Thus there is an increasing wish to re-use the diverse simulation packages which were already created but which are usually implemented within different software environments, often not directly compatible with each other. The OpenAlea platform (Pradal et al., 2008) was developed as an environment to connect and reuse components with specific functionality in a scientific workflow environment. However, not all widely-used FSPM-related tools are already available from OpenAlea. In our work, we created an interface between OpenAlea and the FSPM platform GroIMP (Kniemeyer, 2008). The latter contains some dedicated tools, among them a simulator for light distribution and interception, based on stochastic path tracing. This radiation model is interesting due to its accuracy, its spectral capabilities and because it is already used in different applications.
To demonstrate the technical usability of our interface, we took an established simulator for the growth and structural development of apple trees, MAppleT (Costes et al., 2008), which is already accessible from OpenAlea but which does not include a radiation model on its own. By exporting the generated tree structures from MAppleT via OpenAlea to GroIMP, we were able to employ GroIMP's light model on them and to reimport the structures with added information on "absorbed light" at phytomer level. Within OpenAlea, photosynthesis was then calculated and tentatively assumed effects on organ sizes could be visualized.
Our conceptual contributions are a generic web architecture and the bidirectional matching between two different multiscale formalisms for topology and geometry in FSPMs.

OpenAlea

OpenAlea emphasizes modularity and reuse by using a central data structure, the MTG (Godin and Caraglio, 1998). This enables indirect communication between the components that are integrated in the platform, using a blackboard architecture. It captures the multiscale organization of plant canopies, particularly its topology. Various properties can also be stored at the different scales. MTG vertices are topological elements that represent modular parts of a plant (e.g., axis, phytomer, organ). The neighborhood of each element is stored in the MTG as well as its associated properties. Geometrical elements are stored separately in an external scene graph for efficiency but are available from a property of the MTG.

GroIMP

In GroIMP, a scene, including virtual plants, is represented as a rooted graph which can be an MTG in the sense of Godin and Caraglio (1998). At the same time, it has the semantics of a scene graph (a well-known data model in computer graphics). In contrast to the MTG in OpenAlea, it contains all information about the scene including geometry. Its nodes can represent geometrical objects (e.g., standing for plant organs), light sources, spatial transformations (e.g., rotations), or they are abstract nodes used purely for replacement purposes during development. The development of scenes, including plants, is modelled by parallel

graph rewriting: Rules are applied by substituting in every timestep all instances of graphs which occur as left-hand side of a rule by the corresponding right-hand side. L-systems, operating on strings, can be subsumed as special cases under this formalism.

The Interface

Although the data models of OpenAlea and GroIMP were both derived from the same mathematical concept, the implemented data structures of both platforms differ in several aspects. To bridge the gap between them, a data extractor from OpenAlea to GroIMP has first to combine the topological (MTG) with the geometrical information and to build a scene graph where the global positional information of each object is split into the transformation matrices of its predecessors (in the graph) and of itself. Furthermore, the scale information, represented by an indexing of nodes in OpenAlea, must be evaluated to build decomposition edges between all node pairs where a direct "is-part-of" relationship shall exist in the GroIMP graph. An extractor for the reverse data flow, from GroIMP to OpenAlea, faces another problem: since the GroIMP graph can contain cycles in the general case, a spanning tree has first to be derived within each scale level to be able to form a valid MTG on OpenAlea. Our graph model for data exchange is a canonical data model that makes the interoperability infrastructure independent from any specific FSPMs. It is a rooted, directed graph with typed nodes and thus more generic than an MTG. Technically, our connecting software tool consists of a client-side interface on top of OpenAlea and a server-side interface on top of GroIMP. An XML based data exchange format called XEG specified from the generic data exchange graph model is provided for the integration. Details are given by Long (2019).

Results and Discussion

In a case study, we have applied our interface to provide an integration of the MAppleT model (Costes et al., 2008), that simulates apple tree growth and development based on stochastics and biomechanics and which is accessible via OpenAlea, with a light interception model based on stochastic pathtracing implemented within GroIMP. The objective was to get a bi-platform FSPM that simulates growth by taking local light interception into account.
The workflow is as follows: Through the client-side interface the MTG generated by MAppleT is translated to an XEG graph, which is then packed to a message for transmission to the light interception model which resides remotely (on GroIMP). Through the server-side interface, the message is received, unpacked and translated into a GroIMP graph, forming the input of the light interception model. Then, update rules are applied which change a property "absorbed light" of nodes representing geometrical objects, according to the raytracing results. Through the server-side interface, the result is translated to a data frame in XEG packed to be sent back to OpenAlea (respectively, MAppleT) to complete the cross-platform simulation. Through the client-side interface, the data is unpacked and translated to OpenAlea as an MTG. Here, as growth in MAppleT is originally not based on light, we have as a first attempt applied an ad-hoc computation of biomass based directly on the intercepted light. The growth of an apple fruit then depends on the new biomass and thus on the light values from GroIMP. Botanically, this scenario is certainly not realistic since it disregards any translocation of assimilates, but it proves technical usability of the interface.

Acknowledgements

Parts of this work were funded by DFG and ANR in the joint project "Multiscale functional-structural plant modelling at the example of apple trees", DFG grant number KU 847/11-1.

References

Costes et al., 2008, *Functional Plant Biology*, 35:936-950.
Godin and Caraglio, 1998, *J. Theor. Biol.* 191:1-46.
Kniemeyer, 2008, Ph.D. thesis, University of Technology at Cottbus.
Long, 2019, Ph.D. thesis, University of Göttingen.
Pradal et al., 2008, *Functional Plant Biology*, 35:751-760.

Toward Virtual Modelling Environments using Notebooks for Phenotyping and Simulation of Plant Development.

Frédéric Boudon[1,2], Jan Vaillant[3,4], Christophe Pradal[1,2]

[1] *CIRAD, UMR AGAP, F-34398 Montpellier, France.*
[2] *AGAP, Univ Montpellier, CIRAD, INRAE, Institut Agro, Montpellier, France*
[3] *CIRAD, UPR HortSys, F-97455 Saint-Pierre, Réunion, France.*
[4] *HortSys, Univ Montpellier, CIRAD, Montpellier, France*

For correspondence: frederic.boudon@cirad.fr

Keywords: Jupyter Notebooks, Phenotyping, Simulation, FSPM, Virtual Research Environment

Introduction - Functional-Structural Plant Models give new opportunities to understand plant growth and interaction with their environment. In the last decade, dedicated modelling platforms allowed the creation of a multitude of models, built upon series of dedicated tools for the representation, acquisition, analysis and simulation of plant growth and functioning. Such integrative platforms usually relied on software modules built using multiple computer languages or formalisms. While some efforts have been made for the distribution of these tools over multiple operating systems, the resulting models were usually poorly documented and organized. Models were either created as scripts or scientific workflows. The visual representation of workflows gives an overview of the modelled processes. However, their reuse by non-experts was usually limited to the modification of parameters. Reproducibility was also limited due to deployment and installation complexity on new computers with different configurations. Until recently, no cross-platform packaging suite was robust enough to manage modules built with multiple languages. In a new initiative to alleviate these problems, we explored, in the context of the OpenAlea platform (Pradal et al., 2008), the use of the Jupyter framework (Kluyver et al., 2016) to create virtual research environments for plant modelling.

Material and Methods – Our approach is based on Jupyter Notebooks, an increasingly popular web-based interactive computational application. Notebooks allow to formalize modelling scenarios as “computational narrative” (Perkel, 2018) by combining code with clear documentation based on the markdown language that includes illustration and mathematical formula rendering capability. Users can customize the narratives by editing cells of code and execute these cells in any order to refine operations. Notebooks can combine different modelling languages such as Python, R or Julia. Jupyter, combined with web deployment services such as Binder or Google Colaboratory, allow users to manipulate modelling narratives within web browsers while executing them on the cloud. To ease cloud deployment, OpenAlea packages are built and distributed from the Conda management system over multiple platforms. This allows building deployable virtual environments from docker images. Continuous integration services, based on Travis-CI and AppVeyor, deliver new releases on code update after automatic compilation and tests. Jupyter Notebooks have been extended to allow interaction with FSPMs. Using this approach, computational narratives for plant modelling can be formalized as notebooks and can be re-executed with an up-to-date virtual research environment by the community.

Results - Illustration of this approach will be presented on two modelling pipelines. First, we developed a software pipeline to characterize apple tree architecture from point clouds

acquired using terrestrial laser scanner. For this, architectural traits of each tree were extracted from their scan and their heritability was then assessed. This example illustrates standard pipelines where analyses are combined and applied on a large dataset. Scalability can be achieved using distributed computation on the cloud (Heidsieck et al., 2019).

For the second illustration, we integrate L-Py, a L-systems simulation package, into Jupyter Notebooks. By providing specific widgets, different steps of the simulation can be computed and the resulting 3D structures and associated properties can be iteratively visualized and analysed. 3D visualization of complex vegetal structures through client-server protocol was an important challenge. We developed optimized methods that minimize the size of data to exchange and allow interactive visualization of complex scenes. During the design stage, interaction and responsiveness are of main importance when exploring model parameters space. For this, graphical controls are generated within notebooks to allow tuning of parameters. A use case will be presented on the simulation of a mango tree over several growing cycles.

Discussion and Conclusion - Our aim was to provide tools to deliver models as notebooks to improve reproducibility and dissemination of FSPM. Documented and interactive notebooks provide interesting didactic tools to teach or test different types of FSPMs. Good code practices are however necessary to generate appropriate notebooks (Rule et al., 2019). Database of models start being constituted (https://openalea.rtfd.io/en/latest/tutorials). Such an approach can provide a standard for model documentation published with scientific papers to enhance scientific reproducibility.

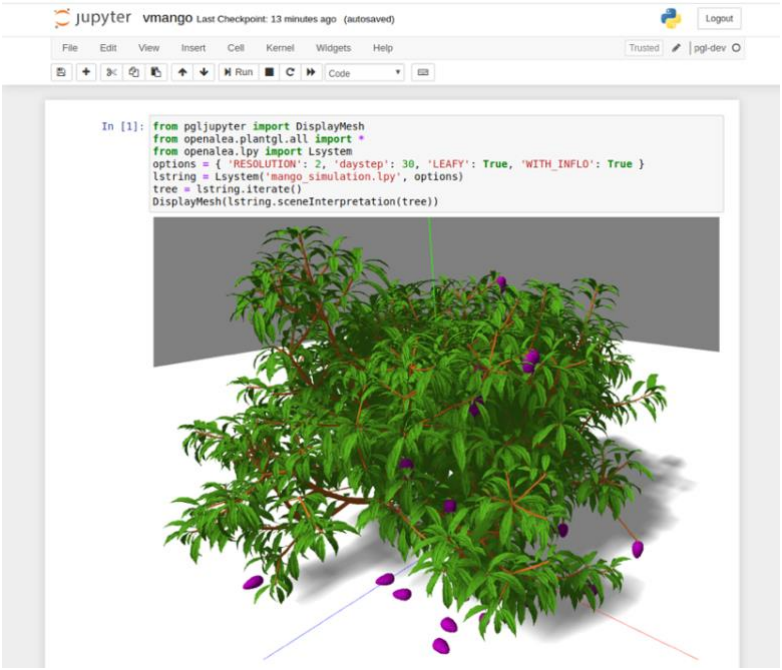

Figure: A notebook presenting a 3D view of a simulation of a mango tree after two growing cycles.

References

Heidsieck et al. 2019. *Dexa*. doi: 10.1007/978-3-030-27618-8_33
Kluyver et al., 2016, *Positioning and Power in Academic Publishing: Players, Agents and Agendas* 87-90, doi: 10.3233/978-1-61499-649-1-87
Perkel, 2018, *Nature* 563, 145-146 doi: 10.1038/d41586-018-07196-1
Pradal et al., 2008, *Functional Plant Biology 35(10),* 751-760, doi: 10.1071/FP08084
Rule et al., 2019, PLoS Computational Biology 15(7). doi: 10.1371/journal.pcbi.1007007

Digitool: A tool for analyzing 3D plant architecture

Dany Moualeu-Ngangué[1],Magnus Adler[1], Yi-Chen Pao[1], San Schwe Myint[1], Andreas Fricke[1], Tsu-Wei Chen[1], Hartmut Stützel[2]

[1] *Institute of Horticultural Production Systems, Leibniz Universität Hannover, Hannover, Germany*

For correspondence: moualeu@gem.uni-hannover.de

Keywords: 3D architecture, virtual plant, leaf angle, plant geometry

Introduction

Morphogenesis of plants is a determinant of the response to different biotic and abiotic factors as well as for the growth and productivity. In order to capture a plant's adaptability and response to different environmental conditions, information about its three-dimensional (3D) architecture is required. Functional–structural plant models (FSPMs) need organ and plant level architectural information (Renton *et al.*, 2005). In the last decade, several methods were developed for efficient phenotyping of plant architecture. Those methods usually led to the production of massive data that needed to be analyzed using sophisticated algorithms, making trait capture time-consuming.

Digitool, a tool for assessing plant 3D architectural information was developed to facilitate rapid assessment of both morphological and architectural traits of single plants, isolated or in a canopy. This computer program is facilitates extraction and calculation of architectural information from 3D coordinates of individual points for calculating organ level traits such as leaf inclination angle, leaf area, leaf and petiole orientation, internode length, petiole inclination angle, petiole length and plant traits such as phyllotaxis and plant height. Digitool can be applied to a broad range of plant species and geometrical complexities for creating 3D models of plants.

Implementation

Digitool is a Java based application that uses the 3D coordinates gathered by Polhemus 3Space Fastrak Digitizer to extract data about plants (angles, lengths, leaf areas, etc.) and to create 3D models of plants. The digitizer is composed of a transmitter, which emits an electromagnetic field, and a receiver. The digitizer measures the receivers' position within that electromagnetic field and records the 3D coordinates. This allows the user to gather the coordinates of individual points and assign them to certain parts of the measured plant (leaves, fruits, stem or petiole) to calculate various properties of the measured plant organ or whole plant. Rules for processing the collected data can be defined by the user in a XML configuration file. In the XML file, all rules are defined to construct shapes, point connections, projection, areas, lengths, angle, special colour, etc. In this file, all single traits of interest can be defined depending on the geometry of the plants and the digitizing points chosen.

The data gathered by the digitizer is simultaneously used to create a 3D model of the plant while several output files can be generated:

- A text file containing an ID, parent module and the coordinates of all measured points for each part of the plant
- An optional .pov file containing a 3D model of the plant which can be opened with programs such as PovRay or PoseRay.
- An optional excel file summarising information on the properties of each single plant organ such as internodes, leaves, fruits, flowers etc.

Angle and area calculation

To calculate each angle, there is a need to perform a projection of the points on the horizontal plan (x-y plan) and determine the angle between the x-y-plan and a vector or a triangle. For example, for calculating the leaf azimuth angle, the coordinates of the leaf base, and tips are required. Let $P_b(X_b, Y_b, Z_b)$ and $P_t(X_t, Y_t, Z_t)$ be these two coordinates obtained from the digitizer. A projection of the vector $\overrightarrow{P_bP_t}$ on the x-y-plane is $\overrightarrow{P_{bt}}$ defined by $\overrightarrow{P_{bt}}(X_{bt}, Y_{bt}, 0) = \overrightarrow{P_{bt}}(X_t - X_b, X_t - Y_b, 0)$. The value can be normalized by dividing the coordinates by the distance length of the vector

$\overrightarrow{P_{btN}}(x_{bt}, y_{bt}, 0) = \overrightarrow{P_{btN}}\left(\frac{X_{bt}}{\sqrt{X_{bt}^2+Y_{bt}^2}}, \frac{Y_{bt}}{\sqrt{X_{bt}^2+Y_{bt}^2}}, 0\right)$ and the azimuth angle can be derived as

$$azimuth = \frac{180}{\pi} * \begin{cases} 2\pi - \cos^{-1}(-y_{bt}), if\ x_{bt} > 0 \\ \cos^{-1}(-x_{bt}), \quad if\ x_{bt} < 0 \\ \pi, \quad if\ x_{bt} = 0\ and\ y_{bt} > 0 \\ 0, \quad otherwise \end{cases}$$

In a comparable way, different angles of the plant organs are calculated using the 3D coordinates.

Area of single leaves are calculated as the sum of areas of triangles made of 3D coordinates of different points defined by the user to shape the leaves.

Result

Digitool was successfully used to reconstruct the 3D architectures of different plant species such as tomato, cucumber, wheat and barley. The results showed that it is possible to derive estimates of leaf area and different leaf angles from the triangulated 3D points obtained from the Digitool, which fits well with destructive measurements, measurements with the ruler or other 3D reconstruction methods.

Using cucumber as model plant, an accuracy of up to 90% was achieved in the estimation of the leaf area between Digitool and destructivemeasurements. While comparing the leaf area estimated by Digitool and the leaf area estimated using 3D reconstruction from photos (photogrammetry), an accuracy of 90% was reached for leaf angles and 80% for leaf area. Similar accuracy values were also obtained for tomato. Therefore, it can be concluded that an efficient plant phenotyping can be obtained using Digitool. Further applications of Digitool include the investigation of long-term morphological and architectural responses of plants (Kahlen and Stützel, 2007).

References

Renton M, Hanan J, Burrage K. 2005. *The New Phytologist* 166: 845–857. doi:10.1111/j.1469-8137.2005.01330.x.

Kahlen K, Stützel H. 2007. *J. Amer. Soc. Hort. Sci.* 132: 439–446. doi:10.21273/JASHS.132.4.439.

Yggdrasil – The Crops in Silico project's open-source Python package for connecting computational models across programming languages

Meagan Lang[1]

[1] *National Center for Supercomputing Applications, University of Illinois at Urbana Champaign, Urbana, IL, USA*

For correspondence: langmm@illinois.edu

Keywords: software, model integration, *in silico*, framework

Introduction

Thanks to advances in functional plant modeling at all scales, scientists have the opportunity to connect models developed to capture different scales/processes and build even more complex representations of the underlying biological systems. Such integrated networks of models can provide insights into how different components and/or scales interact to create emergent behavior that is not captured by the isolated, individual. However, technical barriers (e.g. programming language, data types/formats) can make it difficult for scientists to connect models developed by different groups for different objectives. The yggdrasil Python package aims to make it easier by providing user-friendly tools for lowering these barriers.

Materials and Methods

yggdrasil (Lang, 2019) is an open-source Python package that can be installed on Mac, Linux, and Windows operating systems using pip, conda, or from source. Although written in Python, users do not need to know how to program in Python in order to use yggdrasil; users only need to understand the language that their model is written in. yggdrasil currently supports models written in Python, R, C, C++, and Matlab; work to support models written in Fortran is in progress and planned for completion by Summer 2020. yggdrasil runs models in parallel and coordinates asynchronous communication between the models via five different communication mechanisms. In addition to handling transformation between data types and supporting a wide variety of data formats (e.g. csv, pickle, mat, obj, ply, json, yaml), yggdrasil also handles automatic unit transformation.

The yggdrasil package aims to be as user-friendly as possible. Information about the models and the connections between the models is passed to yggdrasil using human readable specification files that can be written manually or composed using a graphical user interface (GUI). To allow yggdrasil to connect to a model, users can write explicit wrappers in the language of their model using send and receive calls provided by an yggdrasil interface to process model inputs and outputs. Alternatively, they can allow yggdrasil to generate a wrapper based on a provided function.

Results and Discussion

yggdrasil was developed for the Crops in Silico project (Marshall-Colon et al., 2017) to connect computational plant models at different scales ranging from the genetic level to the canopy. During Phase 1, yggdrasil was used to connect five sets of model pairs including integrating a genetic regulatory network, protein translation model, C3 e-photosynthesis model, and micro-meteorological model (Kannan et al., 2019). This integration provided new insights into the response of photosynthesis in soybeans under elevated CO_2.

During Phase 2 (see figure), Crops in Silico aims to integrate and connect three new models, integrate an updated ray tracer for improved efficiency, and finalize/publish results from the other connections made during Phase 1. Phase 2 of the Crops in Silico project will also include integrating models at two new scales: the field and ecosystem. Throughout Phase 1 and the beginning of Phase 2, the Crops in Silico project has learned several lessons about integrating across scales, particularly that modular models are more flexible and more easily connected than components of larger modeling systems which are often difficult to extract. If model

writers desire models to be reused by other scientists, they should consider breaking larger models into smaller components that can be more easily adapted for other applications.

Conclusion

The yggdrasil package allows scientists to connect models written in different programming languages in order to capture the behavior of complex systems including emergent properties that are not captured by the models in isolation. In doing so, scientists can make new discoveries, form new collaborations, encourage publication of modular open-source model software, and benefit from an exchange of models produced by the community.

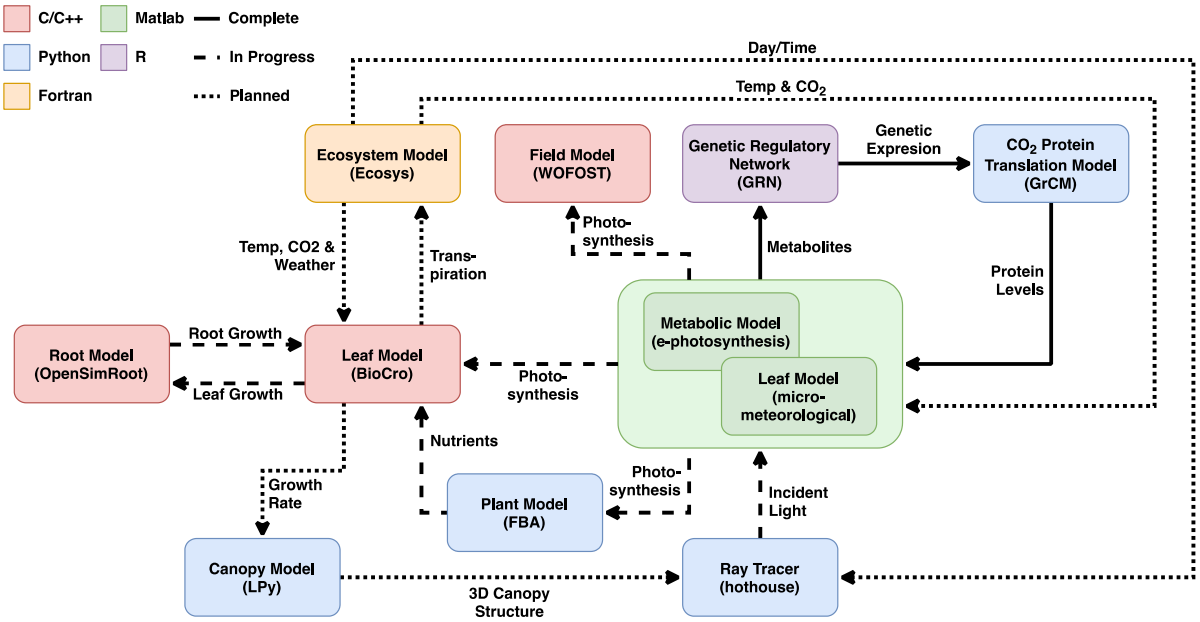

Figure: Network of model connection completed, in progress, and planned for completion during Phase 2 of the Crops in Silico project

References

Kannan et al., 2019, *in silico Plants* 1, doi: 10.1093/insilicoplants/diz008
Lang, 2019, *in silico Plants* 1, doi: 10.1093/insilicoplants/diz001
Marshall-Colon et al., 2017, *Frontiers in Plant Science* 8, 786.

A framework for modelling the transport of water and carbohydrates in apple trees – simulation of a coupled phloem/xylem system

Alex Tavkhelidze[1], Gerhard Buck-Sorlin[2], Winfried Kurth[1]

[1] *Abteilung Ökoinformatik, Biometrie und Waldwachstum, Georg-August-Universität Göttingen, Göttingen, Germany*
[2] *IRHS, INRAE, AGROCAMPUS OUEST, Université d'Angers, SFR 4207 QUASAV, 42 rue Georges Morel, 49071 Beaucouzé cedex, France*

For correspondence: aleksi.tavkhelidze@uni-goettingen.de

Keywords: Functional–structural plant modelling, simulation, phloem and xylem flow, differential equation, GroIMP

Numerous studies show evidence for semipermeable transfer between two vascular tissues, xylem and phloem, which essentially represent the conduit infrastructure in woody plants. However, only few approaches exist for the modelling of sap fluxes in plants that accomodate this selective inter-connection (Höltta et al., 2006; Lacointe and Minchin, 2008; Seleznyova and Hanan, 2018).

This study aims at providing a framework for functional-structural modelling of sap flow in apple trees within the complex environment of coupled conducting systems of xylem and phloem. The best-supported theoretical bases, governing the transport of water and solutes, are considered, namely the Münch (a.k.a. the pressure flow) Hypothesis for phloem translocation and the Cohesion Theory for xylem water uptake. Currently the model operates only on static plant architectures.

We used the platform GroIMP to host our modelling framework (see Fig.1 on the next page), and coupled it with the solver CVODE that provides numerically stable methods for solving both stiff and non-stiff differential equations of water and solute flows. This solver is based on SUNDIALS, a C package of numerical integrators, which is supported (Java-wrapped) within GroIMP. With the CVODE solver incorporated, our modelling framework gained the flexibility of enhancing its structural complexity (such as introducing temporal and spatial/structural scales) without any loss of numerical stability, thus assuring the accuracy of simulation outcomes within our modelling framework.

The framework presented in Merklein et al. (2018) was taken as the departure point for this study. We enhanced the initial environment:

- by introducing a dynamical composite sun/sky model (thus separating direct and diffuse radiation components for more realism) coupled with the radiance distributions of the CIE Standard General Skies,
- by completing the set of major components for computing the total water potential.

We find it particularly worth mentioning that the incorporated sun/sky model is not tailored for the specific modelling environment of apple trees and therefore could be used for any suitable modelling framework that needs to accommodate the realistic simulation of direct and diffuse radiations using any of 15 CIE standard skies (overcast, intermediate, clear).

Two types of (nested) scenarios are considered and respective simulations are carried out in the enhanced environment of our modelling framework:

- different environmental conditions (typical seasonal and diurnal variations as well as stress scenarios based on irradiance intensity, air temperature and drought stress);
- various branch/tree architectures and source-sink ratios.

Future Work (in progress)

Along with further refinements to the modelling framework, we are constantly working on:

- obtaining more apple tree-specific measurement data for the purpose of better parameterization of model equations and subsequent validation of the model;
- reducing time and computational resources for solving initial-value problems of differential equations that will result in faster and longer-term simulations of water and solute flow at no tradeoff in the existing complexity level, thus allowing further enhancements of the framework (such as by moving from static to dynamic tree architectures).

We also aim to conduct comparative analyses of our modelling framework with some of the existing models of coupled phloem/xylem transport, briefly mentioned in the introductory section.

Acknowledgements

Authors wish to thank various people for their contribution to this project: Johannes Merklein and Qinqin Long for their valuable technical support on this project; Christoph Lehrenfeld for his extensive advisory work in theoretical aspects concerning numerical methods and stability issues for the entire system of differential equations; Evelyne Costes and Benoît Pallas for providing the data files of multiscale-architectured apple trees, produced within the MAppleT model (Costes et al., 2008).

Prerequisites of this study were developed in the DFG/ANR funded project "Multiscale functional-structural plant modelling at the example of apple trees", grant number KU 847/11-1.

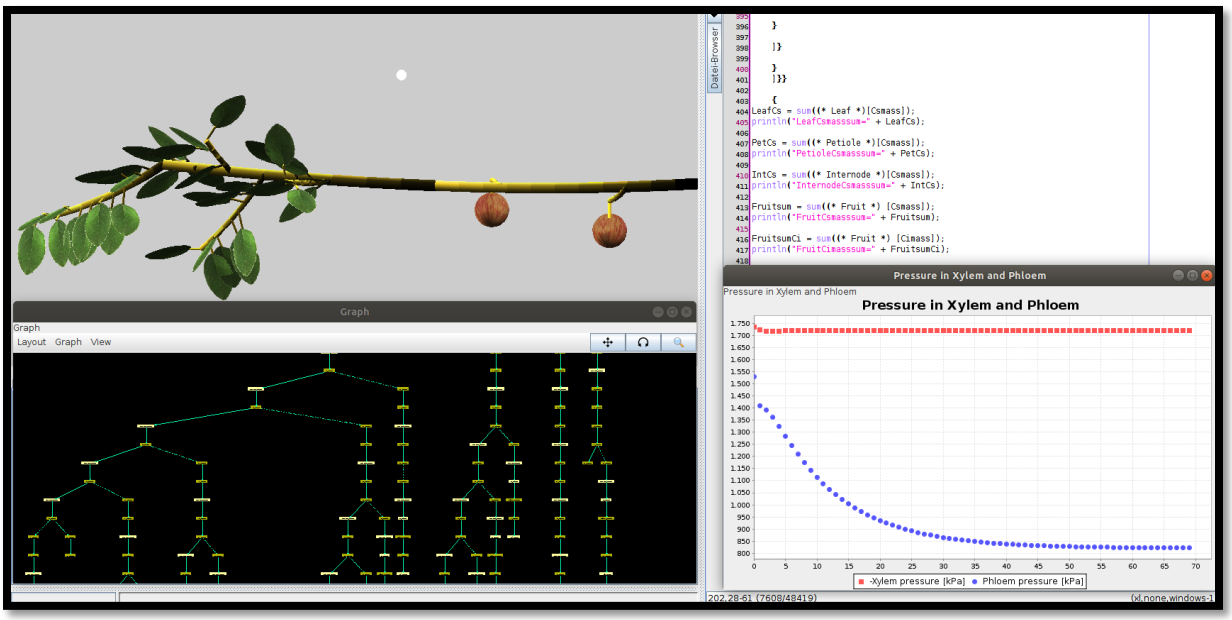

Figure 1: Working environment of the modelling framework in GroIMP

References

Costes et al., 2008, *Functional Plant Biology* 35 (10): 936, doi: 10.1071/FP08081
Hölttä et al., 2006, *Trees* 20 (1): 67–78, doi: 10.1007/s00468-005-0014-6
Lacointe and Minchin, 2008, *Functional Plant Biology* v. 35 (9–10): 772–80, doi: 10.1071/FP08085
Merklein et al., 2018, *6th International Symposium on Plant Growth Modeling, Simulation, Visualization and Applications (PMA)*, 50–55, doi: 10.1109/PMA.2018.8611561
Seleznyova and Hanan, 2018, *Annals of Botany* 121 (5): 991–1003, doi: 10.1093/aob/mcx204

Developing a functional-structural plant model for cocoa to explore pruning-shade interactions

Ambra Tosto[1,2], Pieter A. Zuidema[2], Niels P.R. Anten[1], Jochem B. Evers[1]

[1] Wageningen University, Centre for Crop System Analysis, Wageningen, the Netherlands
[2] Wageningen University, Forest Ecology and Forest Management group, Wageningen, the Netherlands

*For correspondence :*Ambra.tosto@wur.nl

Introduction

The increasing cocoa demand and the climate-induced reduction of suitable growing area call for measures to increase productivity of cocoa cropping systems. Currently, realized yields are typically about 20% of potential yield due to low fertilizer input, pest and decease incidence and poor maintenance practice (Zuidema et al., 2005).

Pruning is an essential practice to increase efficacy of fertilization and pest control, reduce fungal infections and realize optimal light distribution within cocoa crowns. However, recommended pruning practice lacks scientific support, and the interaction between pruning effects and shade levels is poorly understood (van Vliet & Giller 2017). Pruning impacts tree functioning and tree architecture through changes in resource allocation and branching patterns (Ferree & Schupp, 2003), this depending greatly on the plant light environment (Anten et al., 2003). Detailed information on cocoa branching pattern in response to different pruning cuts are missing. To be effective, pruning practice must therefore be tailored to the shade level of the cropping system.

Pruning and shade responses define the 3D structure of cocoa trees, but are also defined by that structure. Experimental trials on pruning-shading interactions are constrained by the longevity and size of cocoa trees. “In silico” pruning experiments within functional structural plant (FSP) models offer a powerful and flexible way to evaluate pruning effects. FSP models dynamically simulate the development of plant 3D architecture as a result of physiological process, responses to light environment and interventions such as pruning (Evers et al ,2018).

Our aim is to develop an FSP model of cocoa to assess the effects of pruning practices on cocoa architecture and canopy photosynthesis at different shade levels. Here we present results from branching pattern calibration based on a pruning trial on two years old cocoa plant in Ivory Coast.

Materials and Methods

Our cocoa model simulates growth and development of cocoa architecture. Architectural and developmental characteristics specific to cocoa plants were included, such as the dimorphism of orthotropic and plagiotropic branches, crown layer formation (jorquetting) and intermittent leaf production driven by thermal time (flushing) (fig. 1).

Light interception is calculated at leaf level, driving leaf photosynthesis. In the FSP model, plant growth is an emergent property of source-sink driven allocation of assimilates. Different levels of homogeneous and heterogenous shade can be simulated.
Branching pattern is simulated assigning to axillary buds probability to break according to their position in the branch.

Removal of branches, or portions of branches, modify the probability of break of dormant buds, resulting in emergent branching patterns. Probability of bud break in presence /absence of a pruning intervention will be estimated from an ongoing pruning experiment on two year old plants, in Ivory coast.

In the experiment we applied at random six pruning treatments including a control. Treatments consisted in the removal of branch tips , the removal of a portion containing the 33% or 66% of branch buds and the removal of one or two entire branches. Pruning were applied to first order branches only. Before cut and after the first cycle of leaf production, total number of bud, number and position of secondary branches as well as secondary branch length and diameter were measured.

Figure 1 Orthotropic and Plagiotropic phases

Conclusion

The cocoa FSPM could serve as a tool to address relevant issues in cocoa production, such as optimal shading, pruning practice, planting design. In addition it could be used for screening promising trial options and for ideotyping plant structure for breeding purposes. The 3D visual output make the model a potential communication tool for academic and non-academic audience.

References

Anten et al. (2003).*Ecology*, 84(11), 2905–2918.

Ferree & Schupp in: *Apples: Botany, Production and Uses*, 2003, D.C. Ferree and I.J. Warrington, 363–388. doi: 10.1079/9780851995922.0000

van Vliet & Giller (2017). Adv Agron, 141,185–270, doi: 10.1016/bs.agron.2016.10.017

Evers et al., (2018), Ann. Bot. 121 767-772, doi: 10.1093/aob/mcy050.

Zuidema et al. (2005). Agric Syst 84,195–225. doi:10.1016/j.agsy.2004.06.015

A 3D model of *Rhizophora mangle* L. saplings based on digitization and reconstruction of foliage on the modelling platform GroIMP

Faustino Chi[1], Katarína Streit[2], Aleksi Tavkhelidze[1], Winfried Kurth[1]

[1] *University of Göttingen, Department Ecoinformatics, Biometrics and Forest Growth, Büsgenweg 4, 37077 Göttingen, Germany*
[2] *University of Western Australia, School of Biological Sciences, 35 Stirling Highway, 6009, Perth, Western Australia, Australia*

For correspondence: tinochi@gmail.com

Keywords: mangrove, phyllotaxis, refoliate, algorithm, downscaling

Mangroves are an integral component of coastal ecosystems and are unique amongst vegetation communities in that they span the marine and terrestrial environment. In this exposed coastal position, mangroves bear the full brunt of hurricanes and tropical storms which recur frequently in these latitudes (Doyle and Girod 1997; Piou et al. 2006).
We present an above ground 3D model of *Rhizophora mangle* L. (red mangrove) with a focus on phyllotaxis. The model was built with the aid of high-resolution mangrove photos and field notes using the software GroIMP. We tested a digitizing equipment (FASTRAK Polhemus Inc.) in tropical conditions for capturing mangrove architecture. FASTRAK Polhemus has been used extensively as a plant digitizing equipment for temperate plants, e.g., fruit trees including walnut tree (Sinoquet and Rivet, 1997), but as far as we know has not been used in a tropical mangrove environment.
This study provides insight on the 3D modelling of phyllotaxis using red mangrove saplings. Onsite mangrove saplings from Turneffe Atoll, Belize were photographed and digitized. We digitized the above ground architecture of ten red mangrove saplings between 1 and 2.5 m (Fig. 1-A and 1-D). The digitized data was also supplemented with field notes and measurements, and photographic close-ups of the leaf arrangements were taken. The leafy part of the branch was defoliated in order to get an accurate digitized 3D mangrove model. For this study the petiole point of insertion of the lowest leaf or pair of leaves along the branch was carefully digitized before defoliation, this was also done for the upper most leaf or pair of leaves along the branch, this section is described as the leafy part. The GroIMP platform was used to visualize, analyse and clean the field data. For the analysis, an algorithm was developed in GroIMP to recreate the topology of digitized samples. Our library of photos was used as a guidance to develop a phyllotaxis model, particularly those photos with high quality resolution and a visible scale in view proved helpful, for example, targeted photos were taken with a measuring stick clearly visible in the background.
The FASTRAK Polhemus equipment proved to be a reliable 3D digitizing equipment in tropical mangrove forest conditions and was suitable for mangrove sapling digitization. Based on our 3D digitized model, measurements and photographic analysis, we developed a mathematical model to describe the phyllotactic pattern of red mangrove. The red mangrove exhibits bijugate phyllotaxis (Tomlinson, 1986), that is, the pairs of leaves diverge from each other at angles less than 90 degrees. The phyllotaxis model was implemented into our 3D defoliated red mangrove model. Based on our model, the leaves were distributed along the leafy part and rendered with a photorealistic texture, using the GroIMP software (see Fig. 1-C and 1-F). Using the digitized points, we recreated geometry and topology, that is, the correct connections between digitized and visualised segments. Then using the topology, we attached reconstructed leaves to segments, based on the distribution pattern along the leafy part. For example, in the leafy part, the leaves are not all positioned in one location, but distributed along one or more leafy segments, based on the algorithm. The algorithm incorporated a probabilistic approach for the purpose of handling perturbations in phyllotactic patterns, and the refoliation of our 3D model. The realistic “dressing” with leaves of our 3D mangrove model using our algorithm proved successful, retaining a very good fit to the real aggregate data

collected during the field work. We were able to obtain a realistic representation of a red mangrove sapling when compared to our field photos (Fig. 1-A and 1-C, 1-D and 1-F).
GroIMP proved to be a very powerful platform which can be used to implement such algorithms, and with few lines of XL code, 3D models can be refoliated according to a specific phyllotactic pattern. We are in the process of fine tuning the model, for example, to implement a realistic petiole and leaf angles along the branch. We hope to make our algorithm more general and applicable for representing the phyllotaxis of a broader list of mangrove trees and other plants of economic and ecological importance. It is our plan to later use the 3D model as the base for both mechanical bending and growth modelling of above ground mangrove, including its aerial roots.

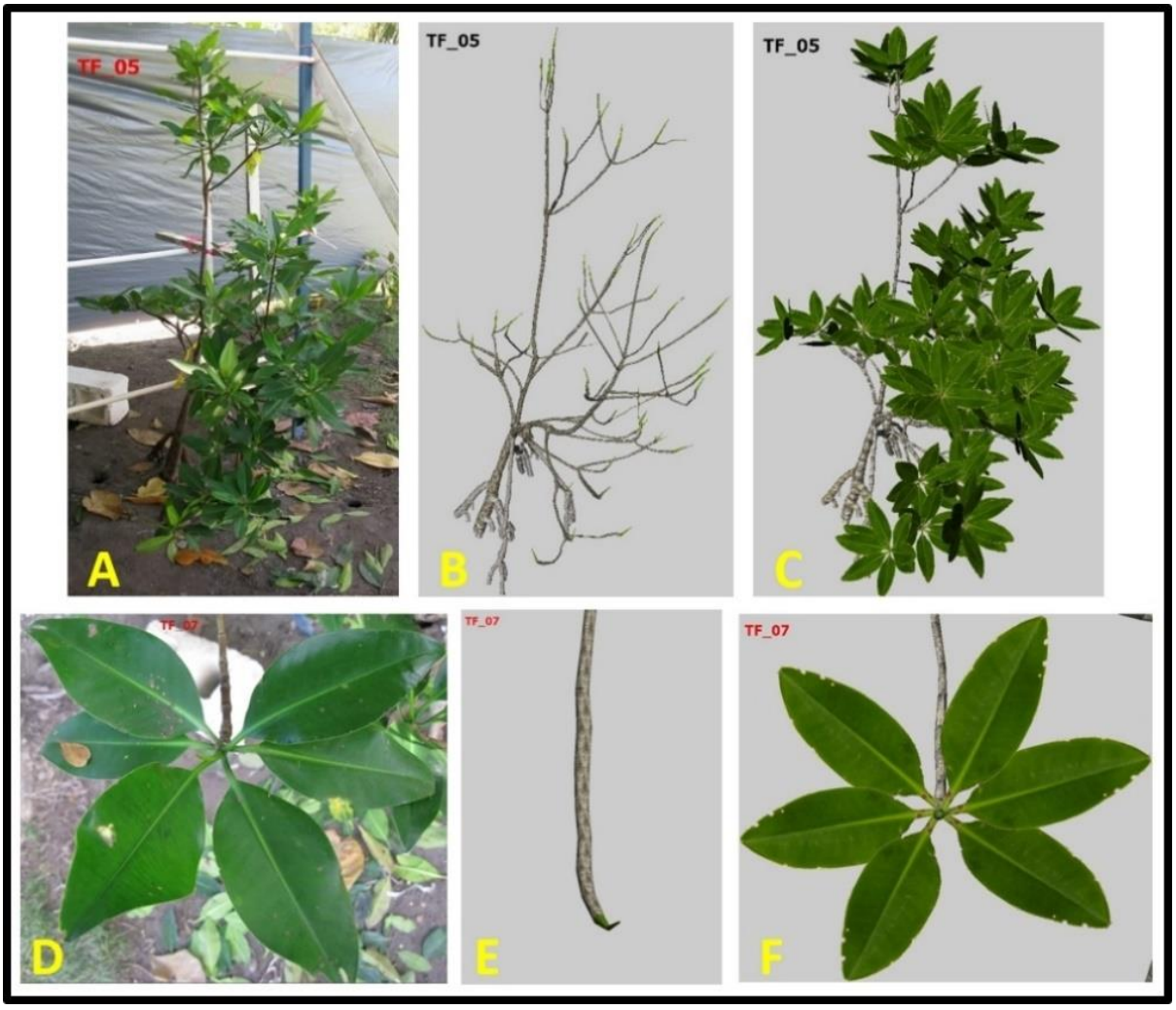

Figure 1: Comparison of mangrove saplings with refoliated mangrove model. A and D: photographs; B, C and E, F: simulation results

References

Doyle and Girod, 1997, In: Diaz and Pulwarty (eds), *Hurricanes*, doi: 10.1007/978-3-642-60672-4_6
Piou et al., 2006, *Biotropica* 38(3):365-374, doi: 10.1111/j.1744-7429.2006.00156.x
Sinoquet and Rivet, 1997, *Trees* 11(5):265-270, doi: 10.1007/s004680050084
Tomlinson, 1986, *The Botany of Mangroves*, Cambridge University Press, doi:10.1017/S0266467400002017

9th International Conference on Functional-Structural Plant Models - Towards Computable Plants

The effect of tree architecture on photosynthetic production in tropical trees

Hannah O'Sullivan[1], Jari Perttunen[2], Risto Sievänen[2], James Rosindell[1], Tania Stathaki[1], Magna Soelma Bessera Moura[3], Jon Lloyd[1]

[1] *Department of Life Sciences, Imperial College London, UK*
[2] *Natural Resources Institute Finland, Helsinki, Finland*
[3] *Brazilian Agricultural Research Corporation, Brasilia, Brazil*

For correspondence: h.osullivan18@imperial.ac.uk

- **Keywords:** Functional-structural plant modelling, intraspecific variation, community ecology, Caatinga.

Introduction

Recent studies have indicated that intraspecific trait variation (ITV), rather than interspecific variation, may provide a better explanation of key questions in plant community ecology (Violle et al., 2007). However, the relative roles of intraspecific variation and interspecific variation in shaping local trait diversity, remain poorly understood. Whilst global databases lend themselves nicely to interspecific meta-analyses, these databases often lack the resolution necessary for tackling studies of local-scale ITV. Collecting data for such studies may be challenging; destructive methods are usually implemented in data collection which hinders the future collection of key trait values such as growth or phenology. Advancements in the fields of biology, computer science and mathematics have led to the development of Functional-Structural Plant Models (FSPMs). In FSPMs, plant structure is explicitly represented in as a network of elementary units (Sievänen et al., 2014). This differentiation of biological organisation in the model structure provides the perfect paradigm for plant trait research.

The efficiency of individual level photosynthetic production is arguably one of the key functional traits dictating plant competitive ability. Investigating the underlying mechanisms for variation in this trait are key to understanding individual plant performance and its subsequent role in community structure. Previous studies have shown that plant architecture can strongly affect light distribution in the canopy as well as photosynthesis, but associated community-level impacts are yet to be explored (Sarlikioti et al., 2011). Here we will evaluate the competitive ability of individual trees by applying a trait-based approach to the FSPM, LIGNUM. We will use terrestrial laser scans (TLS) to refine the model for a semi-arid tropical plant community and couple 3D models with 10 years of meteorological field-sampled data in order to simulate photosynthetic production. The flexibility of this approach allows us to create a 'virtual laboratory' for testing the role of ITV in a tropical plant community whilst using field-sampled data to maintain a high level of realism in the model.

Materials and Methods

In this study, the FSPM LIGNUM is used as a platform for simulating optimal photosynthetic productivity across different crown architectures for Caatinga trees (Perttunen et al., 1998). Basic branching architecture is derived from architectural models outlined in Hallé (1977). From these branching models, a virtual population of static trees are defined using L-systems and parameterised TLS scans from Petrolina, Brazil. The architecture of each

individual tree will differ slightly, in order to generate phenotypic variation within the population. The distribution of photon flux in the whole sky is implemented by means of the Firmament submodel (Perttunen et al. 1998), integrating a decade of field-measured meteorological data from Petrolina. A biochemically-derived photosynthesis submodel is implemented in addition to nested time steps for simulating photosynthetic production for each tree. Once 3D models are constructed, a number of key architectural traits will be extracted for each tree. We will then analyse their variation and coordination within and between species at the same locality.

Results and Discussion

In this study, we will investigate effect of individual architectural traits and their impact on photosynthetic production. In the context of climate change, it is particularly pertinent to have a thorough understanding of photosynthetic production in order to predict individual plant responses. We will present in detail the implementation of a semi-arid tropical environment as it has not yet been implemented in the existing literature. Many FSPM studies are based on terrestrial plant species but here we propose a framework for integrating the LIGNUM model with a tropical environment using nested timesteps to capture a higher resolution of meteorological change. The application of a trait-based approach to FSPMs is a novel method with the potential to yield a number of interesting ecological lines of enquiry in future research. Here, we focus on the effects of plant structure on one key trait in a specific locality, but the flexibility of this framework can be extended to numerous different plant traits and habitats.

Conclusion

In conclusion, trait variation, both intraspecific and interspecific are important factors in understanding strategies for maximising photosynthetic production. With their multi-level structure, FSPMs are the perfect computational tool for simulating plant functional responses in individuals, communities and ecosystems and we hope that this research will influence a wider use of FSPMs in plant ecology.

References

Violle et al., 2007, *Trends in Ecology and Evolution* 27: 244-252, doi:10.1016/j.tree.2011.11.014
Sievänen et al., 2014*, Annals of Botany* 114: 599–603, doi: 10.1093/aob/mcu175
Sarlikioti et al., 2011, Annals of Botany 108: 1065–1073 doi: 10.1093/aob/mcr221
Perttunen et al., 1998, *Ecological Modelling* 108 189–198, doi: 10.10 16/S03 04-38 00(98) 00028-3
Hallé et al., 1978, Springer-Verlag.

3D Shape Modelling of Apple Vasculature with a Space Colonization Algorithm

Leroi Pols[1], Pieter Verboven[1], Bart Nicolai[1]

[1] Division of MeBioS, Department of Biosystems, KU Leuven, Leuven, Belgium

For correspondence: leroi.pols@kuleuven.be

Keywords: fruit growth, fruit geometry, water transport, X-ray micro CT, parameter estimation

Introduction

During apple fruit growth and development one key process is the uptake of water and minerals into the fruit from the plant stem, which happens through the vascular tissue. The vascular tissue of apple fruit has a distinct shape (MacDaniels, 1940) and forms a network inside the fruit.

To develop fine-grained models of apple fruit growth, we require accurate structural models of the vascular network in apple fruit to capture the differences in water and mineral uptake in different regions of the fruit. The spatial structure of apple vasculature can be obtained through X-ray micro-Computed Tomography (CT) scanning of apple samples. Such methods can be very time-consuming and expensive however. Here, we develop algorithms to generate apple vascular networks at different time-points during apple growth and calibrate the algorithm parameters against vascular networks of apples obtained from image segmentation of such X-ray micro-CT scans.

Materials and Methods

In a previous study (Herremans et al., 2015), X-ray micro-CT was used to obtain 3D scans of whole apple fruit, harvested at different time-points during fruit development. From these scans, spatial data of the vascular networks inside the fruit could be obtained through image segmentation techniques.

The vascular network inside the apple core has a distinct shape (MacDaniels, 1940), from which it branches outwards into the apple cortex region. One method of creating natural branching networks is the space colonization algorithm (Runions et al., 2005, 2007). First, an algorithm was developed to approximate the main cortical bundles of apple fruit. Then, using the main cortical bundles as the starting geometry, the space colonization algorithm is used to generate the rest of the vascular network inside the apple.

The algorithm parameters are calibrated by minimizing a cost-function created to capture the differences between the generated and segmented vascular network. The cost-function compares the length of the networks, the number of branching nodes in the networks, and the radial distribution of branching nodes in the networks.

Results and Discussion

Figure 1 shows an example of a generated vascular network representing an apple 12 weeks after full bloom. The algorithm parameters were estimated by minimizing the cost-function. For a single set of parameters, the algorithm can generate vascular networks that are similar in length and number of branching nodes for each of the 6 time-points for which there are X-ray CT scans. The time-points of the scans are 9, 14, 16, 18, 20, and 22 weeks after full-bloom. The network properties are also accurate for any given time, ranging from 9 to 22 weeks, in between the time-points. Using this algorithm we can compare the effects on the properties of the generated network when adjusting the parameters. The generated network can further be used in numerical simulations of apple growth where we can investigate the effects that the structure of the vascular network has on apple development.

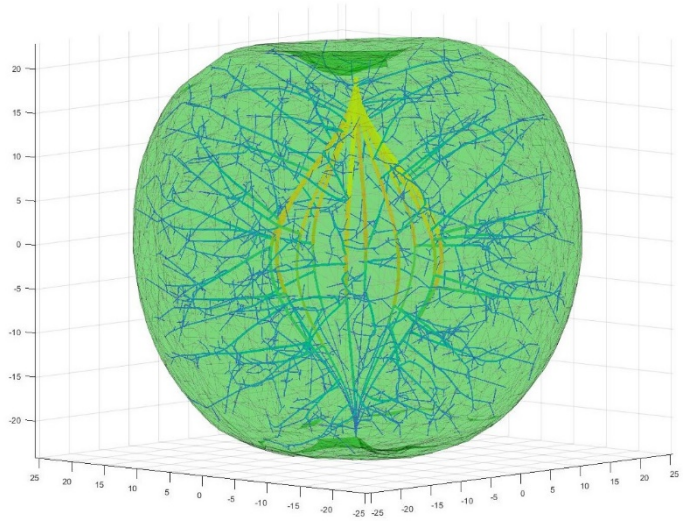

Figure 1: Apple vascular network generated at 12 weeks after full bloom. In the centre are the 10 main cortical bundles entering the apple from the pedicle. From these bundles the vasculature branches off and fills the apple cortex.

Conclusion

Algorithms were developed that can generate an accurate representation of the vascular network of apple fruit at different time-points during fruit development. The properties of the network are similar to that of the segmented networks from the X-ray CT scans at each of the time-points.

References

Herremans, E., Verboven, P., Hertog, M. L. A. T. M., Cantre, D., van Dael, M., De Schryver, T., Van Hoorebeke, L., & Nicolaï, B. M. (2015). Spatial development of transport structures in apple (Malus × domestica Borkh.) fruit. *Frontiers in Plant Science*, *6*(September), 1–14. https://doi.org/10.3389/fpls.2015.00679

MacDaniels, L. H. (1940). *The morphology of the apple and other pome fruits*. Cornell university. Agricultural experiment station.

Runions, A., Fuhrer, M., Lane, B., Federl, P., Rolland-Lagan, A.-G., & Prusinkiewicz, P. (2005). Modeling and visualization of leaf venation patterns. *ACM Transactions on Graphics*, *24*(3), 702. https://doi.org/10.1145/1073204.1073251

Runions, A., Lane, B., & Prusinkiewicz, P. (2007). Modeling trees with a space colonization algorithm. *Natural Phenomena*, 63–70.

Modelling the Guayule plant growth and development with a Functional Structural Plant Model

Authors: Loic Brancheriau[3], Sylvie Sabatier[1,2], Marc Jaeger[1,2], Nicolas Hemery[3], Christ Mougani[1,2], Philippe de Reffye[1,2], Ali Abed Alsater[1,2] and Serge Palu[3]

[1]AMAP, Univ Montpellier, CIRAD, CNRS, INRA, IRD, Montpellier, France
[2]CIRAD, UMR AMAP, F-34398 Montpellier, France
[3]UR BioWooEB, CIRAD, Univ Montpellier, 34398 Montpellier, France

For correspondence: loic.brancheriau@cirad.fr

Keywords: FSPM, Guayule, Natural rubber, GreenLab model, Organ sinks

Introduction

The Guayule (*Parthenium argentatum, Asteraceae*), is a branched shrub native to northern Mexico showing a growing interest in research and agriculture (Ray, 1993). However, few studies have been done on the structure or functioning of the species and the production itineraries in relation to natural rubber production are still to assess. This study aims to propose a first FSPM of the species using the GreenLab model, calibrated with data issued from two varieties in different environmental conditions. The objective is to understand the interaction between the development of Guayule and natural rubber production.

Materials and Methods

Experimental plots were conducted on two varieties (Fig. A), named CL1 (parent USDA 11591 triploid) and CLA1 (parent USDA AZ 101 tetraploid). The CL1 variety has small stem and leaf size compared to the CLA1 variety. These varieties were planted in the field under various environmental conditions related to density (9091 and 62500 plants/ha), and hydric pressure (100%, 66% and 33% of optimal supply).
The measurements carried out to count number of phytomers per module as well as the number of relay axes. We also clustered the total dry weight of leaves and stems per module in order to build the axis organic series (Buis and Barthou, 1984) and to estimate the content of natural rubber from a NIRS analysis (Taurines et al., 2019). The field measurements from the series constituted a target to calibrate the GreenLab model functional parameters such as the organ sink functions (Kang et al, 2018). We chose such a cohort model, since the structure (here the module rank) can be analysed in the biomass production without detailed explicit geometrical computations.

Results and Discussion

Experimental results. The Guayule shows a sympodial development composed of modules with a terminal inflorescence. Its architecture corresponds to the Leeuwenberg's model (F. Hallé *et al.* 1978) producing eight to nine modules per year. The number of internodes within the modules is almost stable regardless of variety and environmental conditions. The architecture of the two varieties CL1 and CLA1 is very similar, including the duration of the functioning of the organs (leaves and inflorescences). In the experiment, the biomass production per module (and thus per plant) was shown to be dependent on both density and water supply, according to the variety. Natural rubber content was found higher on young modules, and the water regime affected the natural rubber content of modules according to the variety (Fig. B).

Modelling results. We have modelled the number of internodes per module with a constant binomial law. The number of relay axis per module was modelled with a damped binomial law, simulating the branching rate decreases on young modules. These laws allowed simulating the plant structure (Fig. C). We then retrieved the organ sinks parameters, fitting the target file, and found significant differences in the leaf sink functions, stronger for the variety CLA1. As a result, the simulation of the functional model allowed the module diameters and the total plant height of the two varieties to be recovered correctly (Fig. D.). We still need to validate the relation between the internode growth and natural rubber production from new field analysis.

Acknowledgement

Authors thank the Agropolis Fondation supporting the “modelling guayule growth as an alternative source of natural rubber” project, referenced as PAI-10605-026.

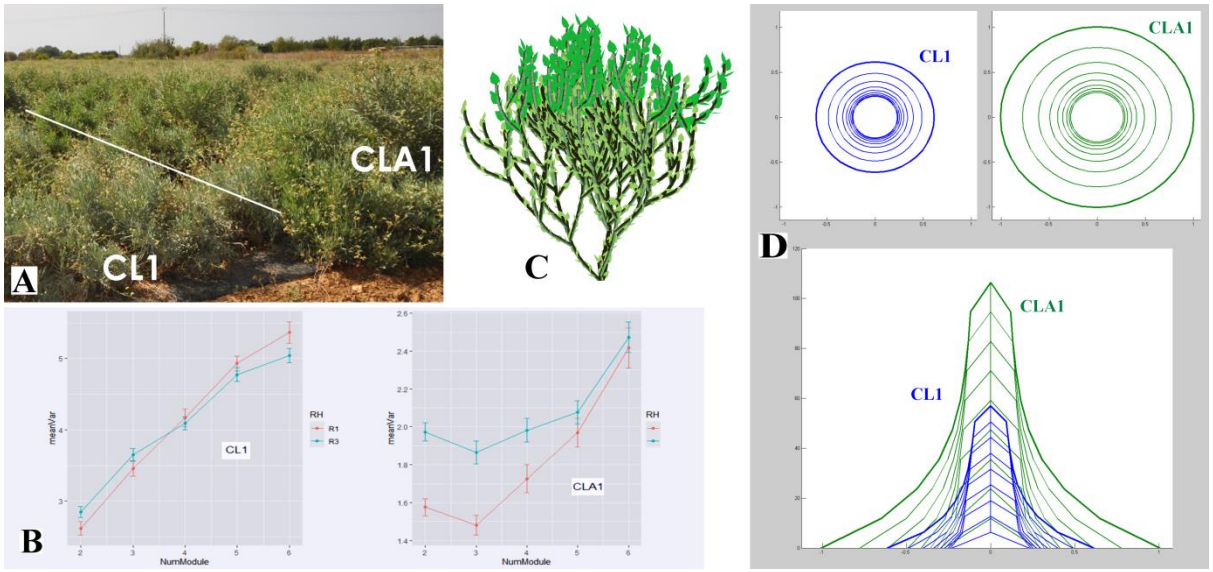

Figure: FSPM Guayule model. A: Field view with CL1 & CLA1 varieties. B: Measured values of the natural rubber content (%) in the optimal (R1) and restricted (R3) irrigation scenarios. C: Simulation of the CL1 structure model. D: Functional structural simulation of primary and secondary module growth on both varieties.

References

Halle, F., Oldeman, R. A. A. and Tomlinson, P. B., .1978. Tropical trees and forests: an architectural analysis. *Springer Verlag*.

Buis, R., and Barthou, H., 1984. Relations dimensionnelles dans une série organique en croissance chez une plante supérieure. *Revue of Biomathematique* 85: 1-19.

Kang, M., Hua, J., Wang, X., de Reffye, P., Jaeger, M., and Akaffou, S., 2018. Estimating Sink Parameters of Stochastic Functional-Structural Plant Models Using Organic Series-Continuous and Rhythmic Development. *Frontiers in Plant Science*, 9, 1688- doi: 10.3389/fpls.2018.01688.

Ray, D.T. 1993. Guayule: A source of natural rubber. p. 338-343. In: J. Janick and J.E. Simon (eds.), *New crops*. Wiley, New York.

Taurines M., Brancheriau L., Palu S., Pioch D., Tardan E., Boutahar N., Sartre P., Meunier F., 2019, Determination of natural rubber and resin content of guayule fresh biomass by near infrared spectroscopy. *Industrial crop & products* 134: 177-184.

Use of process-based system dynamic models to generate biologically aware 3D trees.

Mariano Crimaldi[1], Edoardo Pasolli[1], Francesco Giannino[1]

[1] *Department of Agricultural Sciences, University of Naples "Federico II", Portici (NA), Italy*

For correspondence: mariano.crimaldi@unina.it

Keywords: 3d rendering, virtual plant, biological models, ordinary differential equations

Simulations of plant growth using computers have a long story. Botanists and computer scientists have tried to develop methods to create synthetic alternatives of natural objects for over forty years (Deussen and Lintermann, 2006; Prusinkiewicz and Lindenmayer, 2012). Many scientific areas use these models for scientific purposes. For example, in botany models are useful to assess physiological parameters (Henke et al., 2016). The creation of geometrical plant models helps researchers to visually validate biological process such as the interaction of plants with light and environment. Plants models are also used in ecology to visualize information of deep-lying processes, making scientists aware of "invisible" things happening. Examples are represented by the development of plants in reaction to disease or stress and the plants' grow after pruning (Fabrika et al., 2018). The work presented here has the goal to fill the gap between 3D rendering engine and biological process-based system dynamic models linking the two aspects with a system of ordinary differential equations (ODEs). The link operates in either directions: ODEs system generates the input for 3D engine and the input parameter for the ODEs system is computed in the 3D environment on the other way around (e.g., the amount of light or the quantity of biomass). For example, taking the internode (i.e., the distance between two consecutive nodes in a branch, L [cm]) growth as an exemplificative state variable of the ODE system, the first equation presented in Figure 1 models the growth of the internode *i-th* by a logistic function depending on water resource (W [cm^3/cm^3]) and a species-specific growth factor (g, [$1/d$]). The second system equation presented in Figure 1 defines the availability of water W conditioned by precipitation (R [$1/d$]), transpiration (plant water uptake) function of the total plant biomass (B [kg]) and evaporation where L_{max} ([cm]) is the internode maximum length, r ([$1/d/kg^2$]) is the water uptake rate and I ([$1/d$]) is the evaporation coefficient. During each time step, the ODEs system computes the internode length (L_i) passed as input in 3D engine. The 3D system utilizes the given value as an input parameter of its rendering engine, it also computes the total biomass of the synthetic tree (B), and then returns a new value for the ODE system. The ability of the proposed approach is to integrate time process based mathematical models of biological systems in 3D engines. This can deliver several benefits in the field such as seeing at a glance whether a certain model is related to reality (Yi et al., 2018), modelling future plantation trends for production purposes, evaluate possible interventions, and display results clearly also for end users. Additional studies are in progress in this direction to improve both biological modelling and 3D engine rendering.

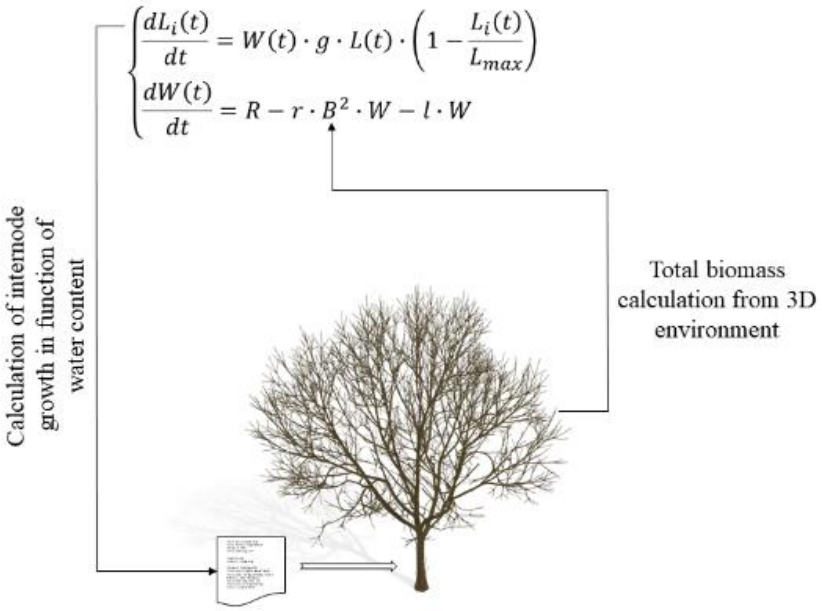

Figure 1: Proposed link between process-based system dynamic models (ODEs) and 3D rendering engines.

References

Deussen and Lintermann, 2006, *Digital design of nature: computer generated plants and organics*, Springer Science & Business Media
Fabrika et al., 2018, Thinning trainer based on forest-growth model, virtual reality and computer-aided virtual environment, *Environmental Modelling & Software,* 100, 11-23
Henke et al., 2016, FSPM-P: towards a general functional-structural plant model for robust and comprehensive model development, *Frontiers of Computer Science,* 10 (6), 1103-17
Prusinkiewicz and Lindenmayer, 2012, *The algorithmic beauty of plants*, Springer Science & Business Media
Yi et al., 2018, Tree growth modelling constrained by growth equations, *Computer Graphics Forum*, 239-53

Comparison of the Light Interception of an Order-based Branching Model of Spruce by Several Simplified Models

Marius Heidenreich[1], Winfried Kurth[1]

[1] *Department of Ecoinformatics, Biometrics and Forest Growth, University of Göttingen, Göttingen, Germany*

For correspondence: m.heidenreich@stud.uni-goettingen.de

Keywords: single tree modelling, radiation, upscaling, growth grammar, L-System

Introduction

Due to increasing interest in understanding forest processes through the usage of models, it is necessary to create and adapt single tree models. The aim is to generate accurate and fast models which can be used for large-scaled modelling without exceedingly high computing capacity. Therefore, this study deals with a structural model of spruce crowns (Kurth, 1999) which is based on L-Systems (Lindenmayer, 1968) and was implemented using the software GROGRA (Kurth, 1994). The goal was to translate the spruce model into the successor software GroIMP (Kniemeyer et al., 2007) and to generate a simplified model which simulates the interception of light with results similar to the complex model and using significantly fewer computing resources.

Materials and Methods

Most of the data comes from a research plot in the Solling (Northern Germany) and was collected from the ground, from a measurement tower, with aerial imagery and with a full harvest of a spruce. Model 1 is the translation of the original model into GroIMP by only adapting some parameters and functions. It is a stochastic model of the crown architecture, with shoot growth and ramification based on the branching order and restricted to a maximum age of 112 years. The model distinguishes between three different tree classes (dominant, medium and suppressed). The time step is one year. The surface of the branches can measure the incoming light, which is simulated by a raytracer; the area of the modelled surface represents the surface of the needles. The following models are derived by simplification from model 1. The principle of model 2 is the generation of the crown as a simple cone with the base radius of the crown, the crown length and the total tree height taken from model 1. Model 3 uses the same growth grammar as model 1 but with a maximal branching order of one and an increasement of the surface of each order-1-branch by the surfaces of the subtended branches of the higher orders. Furthermore, two scaling factors were introduced (*factor_1*, *factor_2*) which are computed through the mean relation of the intercepted light of model 1 and 3 over all tree classes in five year steps (1) and the relation between the light interception at the maximal age of 112 years (2). In model 4, all whorls are generated as slices which have a radius based on the branch lengths of model 1; crown length and tree height are also taken from model 1. The outputs of the four models (light interception values, crown radii) were compared to each other in order to determine the best sort of simplification applied to model 1.

Results and Discussion

The tree parameters, such as the tree height and the crown width at the maximal age, are identical in the original model and model 1. Also, the visual comparison between the two models shows that they give almost equal results. Looking at the simplified models 2 – 4 it is noticeable that the models 2 and 4 have a shorter computation time than model 3. Still all models are much faster than model 1. All models show an increase of the intercepted light per annual step, with the exception of model 4 where the value is decreasing after an age of about 95 years (Figure 1). This clearly shows that model 4 does not describe the intercepted light in the right way in its current state. By comparing the shapes of the curves of the remaining models it becomes clear that model 3 can reproduce the light interception simulated by model 1 in the best way. The shape is quite equal, but the light interception value is significantly (2.833 times) bigger than in model 1 over all years and tree classes. With the use of the scaling *factor_2* (0.278) the curves are almost identical, just in the younger ages there are small differences of the values. Model 3 is, when the scaling factor *factor_2* is taken into account, by far the best simplification of the complex model.

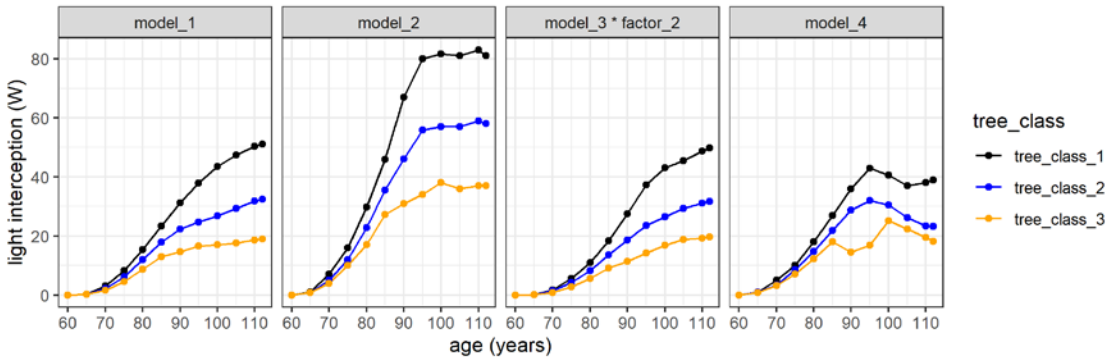

Figure 1: Light interception over time for the complex model (model_1) and the simplified models (model_2, model_3*factor_2, model_4)

Conclusion

Considering the results, model 3 is representing model 1 very well by using the scaling factor. Given the current model versions, model 3 is, in contrast to the others, the only one which can be used as a simplified version of model 1. The computation time is not as short as in the simplified models 2 and 4, but still much shorter than in model 1. Altogether the approach to create a simplified model out of model 1 is achieved by model 3 by increasing the virtual surface of the first order branches by the respective contributions of the higher branching orders. In future applications it might be used for simulating the radiation regime of larger spruce stands.

References

Kniemeyer et al., 2007, "GroIMP as a platform for functional-structural modelling of plants", in: *Functional-Structural Plant Modelling in Crop Production*, Berlin, 43-52, doi: 10.1007/1-4020-6034-3_4
Kurth, 1994, "Growth grammar interpreter Gogra 2.4 - a software tool for the 3-dimensional interpretation of stochastic, sensitive growth grammars in the context of plant modelling", Techn. Rep., Göttingen, doi: 10.1.1.37.968
Kurth and Sloboda, 1997, *Silva Fennica* 31:285-295, doi: 10.1.1.37.6822
Lindenmayer, 1968, Journal *of Theoretical Biology* 18.3:280-299, doi: 10.1016/0022-5193(68)90079-9

Development of a functional-structural plant model of cassava root system during early storage root formation

Nattharat Punyasu[1,3,4], Treenut Saithong[2,3], Jittrawan Thaiprasit[3], Saowalak Kalapanulak[2,3], Tobias Wojciechowski[4],Johannes A. Postma[4]

[1] *Bioinformatics and Systems Biology Program, School of Bioresources and Technology, and School of Information Technology, King Mongkut's University of Technology Thonburi (Bang Khun Thian), Bangkok, Thailand*
[2] *Bioinformatics and Systems Biology Program, School of Bioresources and Technology, King Mongkut's University of Technology Thonburi (Bang Khun Thian), Bangkok, Thailand*
[3] *Center for Agricultural Systems Biology, Systems Biology and Bioinformatics Research Group, Pilot Plant Development and Training Institute, King Mongkut's University of Technology Thonburi (Bang Khun Thian), Bangkok, Thailand*
[4] *Institute for Plant Sciences (IBG2), Forschungszentrum Jülich, Jülich, Germany*

For correspondence: Nattharat.punyasu@mail.kmutt.ac.th

Keywords: Developing storage root, Manihot esculenta, Source-sink carbon allocation

Cassava (*Manihot esculenta*) is a starchy root crop that provides staple food for millions of people in tropical and subtropical regions. Storage root formation is a key mechanism that allows cassava to store a large amount of starch in its roots. Since primary substrate for starch production is transported from source tissues, partitioning and allocation of carbon (C) is one of the major determinants of tuberization and yield production. Source-sink carbon partitioning and allocation are influenced by several environmental factors. However, source-sink carbon partitioning and allocation influenced by environment during growth development remain poorly understood. Here, a functional-structure plant model, OpenSimRoot, was employed to simulate the first three months of cassava growth under irrigation system and to describe dynamic carbon partitioning during initial storage root formation. This study also aimed to represent 3D structure of cassava root systems during storage root initiation phase. An initial set of parameters was collected from cassava KU50 cultivar at 28 to 84 days after planting (DAPs). The experiment was conducted in field experiment at Rayong research field, Thailand. Photosynthesis parameters and canopy characteristics specified to the cultivar were included in the model. Parameters described architecture of cassava root systems were mostly estimated from phenotyping data measured from the same plants. Secondary growth parameters of cassava storage root were estimated from excavated roots. The model successfully simulated growth of cassava roots by fitting well with actual data. The exponential growth phase was predicted to start about 60 DAPs. Simulated 3D structure of root system was approximately to obviously features of cassava root system (Figure 1). The resulting model is expected not only beneficial to the study of dynamic source-sink carbon allocation during root development, but also to the investigation of how environments affect carbon allocation and final root yield. The understanding may provide a guidance for identifying favorable growing conditions towards increase starch production in cassava storage root.

Figure 1. Actual cassava root systems at 84 days after planting (Left) and 3D simulated cassava root system (Right)

Improving the Brazilian silvopastoral system arrangement

Nilson Aparecido Vieira Junior[1], Jochem Evers[1], Murilo dos Santos Vianna[2], Bruno Carneiro e Pedreira[3], Fábio Ricardo Marin[4].

[1] *Centre for Crop Systems Analysis, Wageningen University & Research, Wageningen, Netherlands*
[2] *School of Earth and Environment, University of Leeds, Leeds, United Kingdom*
[3] *Embrapa Agrosilvopastoral, Brazilian Agricultural Research Corporation - Embrapa, Sinop, Brazil*
[4] *Biosystems Engineering Department, University of São Paulo - ESALQ, Piracicaba, Brazil*

For correspondence: nilsonvieirajunior@usp.br

Keywords: Functional-Structural Plant Modeling, Intercropping, *Light competition*, Shading

Introduction

The increase of the global population and lack of available land requires raising yields of the agricultural sector in the coming decades. The silvopastoral system, in which trees and pastures are combined, is an efficient way to intensify animal and crop production. However, the impact on pasture growth caused by the addition of trees is not clear due to a lack of knowledge on the interactions between trees and pasture. Competition for light among species comprising the canopy plays an essential role in such mixed-species system, next to below-ground competition for water and nutrients. Such knowledge could be used to determine the optimal row and arrangements of the trees in silvopastoral systems. Functional-structural plant (FSP) models can be used to quantify and provide substantial information on competition for light in heterogeneous canopies such as silvopastoral systems. Applying the functional-structural plant modelling is possible to aid the planning and arrangement for the silvopastoral systems in Brazil. In this context, the aim of this work is to determine the optimal tree arrangements of the silvopastoral systems in the main livestock producer regions in Brazil.

Materials and Methods

The model is being written in the programming language XL (eXtensible Language), rule-based, and all the routines are implemented in GroIMP v1.5 (Growth Grammar-related Interactive Modelling Platform), a 3D modelling platform (Hemmerling et al., 2008). The tree component will express only the structural aspects, i.e., tree growth will not be simulated. Focusing on solar radiation as the resource under competition within the tree-pasture system, the forage component is being represented only by functional aspects. Therefore, two process-based models, CROPGRO-Perennial Forage (Rymph et al., 2004) and APSIM-*Tropical Pasture* (Brown et al., 2014), will be coupled to the solar radiation simulations composing the FSP model framework. Direct radiation will be simulated using a matrix of 24 sources of directions light, equally distributed at the length of the day, representing the sun trajectory. For the photoperiod simulation, the azimuth will modify the position of each light source azimuth and solar inclination angle, considering the latitude as input. The diffuse radiation will be simulated using 72 light sources that will be randomly distributed in 6 points with 12 light sources each, with different directions (Evers et al., 2010).

The dataset for model calibration and evaluation is composed by three different field experiments in Brazil. Data collected in Sinop, Mato Grosso, Brazil (11°51' S, 55°35' W, 384 m elevation) will be used for the calibration of the model. The structure of trees, we will be calibrated with height (m), diameter at breast height (m) and leaf area index (m) and for pasture production, we will use data of forage accumulation in different distances (4, 7.5 and 15 m) for both the sides (North and South) of between the tree rows collected monthly in the period of June 2015 to May 2017.

Data collected in São Carlos, São Paulo, Brazil (21° 57' S, 47° 50' W, 860 m elevation) for the period of January 2016 to January to 2018 and Ibiporã, Paraná, Brazil (23° 09' S, 51° 01' W, 484 m elevation) for the period of March 2017 to March 2018 will be used to evaluate

the model performance. We will use data of photosynthetically active radiation and shade projection in several distances and for both sides (North and South) between the tree rows. For the tree component, we use height (m), diameter at breast height (m) and leaf area index (m). For pasture production, we will use data of dry matter production in different distances (4, 7.5 and 15 m). We will simulate the interception of light by the trees in different distances between trees rows in distinct silvopastoral systems arrangements and the forage growth. The performance of the model will be evaluated by statistical indexes such as bias, root mean squared error (RMSE), determination index (r^2) and the Willmot index (d) that will be calculated for the average of the simulations.

To simplify the climate data input for the simulations, we will define homogeneous climatic zones for the mains livestock producing regions in Brazil (Van Wart et al., 2013). The simplification of the zones will be achieved through to the homogenization of similar environmental and soil characteristics for the producer regions. The climate data for each climatic zone will be composed of collected data of one location which is representative. Then, the model will be applied to find the best arrangement and species for each homogeneous climatic zone. We will evaluate the mains arrangements adopted for silvopastoral systems in Brazil considering combinations of this factors: (i) trees lines rows of 15 and 30 m; (ii) two orientations (N-S and E-W); (iii) different species and (iv) shading levels, aiming aid the pruning and thinning practices. An animal thermal comfort parameter will be added for keeping the radiation incidence inside the system below to damage levels for the animals.

Perspectives

The area of production of silvopastoral systems is increasing in Brazil, but the adoption of this kind of system still is limited by the lack of knowledge, which results in the resistance of the farmers. Therefore, based on a dataset already collected in different Brazilian regions, this work aims to apply an FSP model to study the distribution of light that occurs in the silvopastoral system, understanding and quantify the shading effect in the forage growth. In this way, the model can be a valuable tool to aid in informed decision making, define the optimal rows and arrangement of the trees, and help design a more efficient system.

The work is under development and preliminary results will be obtained soon. At the conference, we will show the performance of the model and its application for determining the agroclimatic zoning in the main producer regions in Brazil.

Acknowledgements

Acknowledgments to the São Paulo Research Foundation (FAPESP) to funding this research (Projects: 2019/21277-7; 2018/15355-2; 2017/20925-0; 2017/50445-0).

References

Brown et al., 2014, *Environmental Modelling & Software*, 385–398, doi:/10.1016/j.envsoft.2014.09.005
Evers et al., 2010, *Journal of Experimental Botany*, 2203-2216, doi:/10.1093/jxb/erq025
Hemmerling et al., 2008, *Functional Plant Biology*, 739–750, doi:/10.1071/FP08052
Rymph et al., 2004, *Soil Crop Science Socity*, 37-51.
Van Wart et al., 2013, *Field Crops Research*,.34-43, doi:/10.1016/j.fcr.2012.11.018

Modelling maize photosynthesis and light utilization based on 3D maize canopy model

Gu Shenghao[1,2,3], Wang Yongjian[1,2,3], Wen Weiliang[1,2,3], Lu Xianju[1,2,3], Yu Zetao[1,2,3], Guo Xinyu[1,2,3]

[1] *Beijing Research Center for Information Technology in Agriculture, Beijing 100097, China*
[2] *National Engineering Research Center for Information Technology in Agriculture, Beijing 100097, China*
[3] *Beijing Key Laboratory of Digital Plant, Beijing 100097, China*

For correspondence: gu.shenghao@outlook.com

Keywords: phenotyping, 3-D point cloud, leaf angle, radiation use efficiency

Introduction

Crop radiation use efficiency (RUE), one of the major factor in determining yield potential, has been demonstrated to hold great potential to increase yield (Zhu et al., 2010). Optimizing plant architecture is one of the most important selection target when breeding for high RUE and thus for yield improvement (Song, 2013). Rapid development of plant phenotyping techniques empowers modelling canopy photosynthesis with a higher resolution and provides a powerful tool examine the response of canopy photosynthesis and light utilization to 3D architecture.

Materials and Methods

This study built a maize photosynthetic production model 3DMaizeCaP via coupling canopy 3D architecture model, radiative flux distribution model, leaf photosynthesis model and radiation utilization model. In this study, 3 cultivars with different plant architecture, i.e., AD268, JK968 and ZD958, and 2 typical weather conditions, i.e., a sunny day and an overcast day were designed. In order to unravel the responses of canopy photosynthesis rate and radiation use efficiency to cultivar and environment, a simulation study combined with field experiment was performed.

Results and Discussion

The results showed that the maximum photosynthesis rate and dark respiration rate decreased linearly with decreasing leaf rank for AD268, JK968 and ZD958. The distribution of both the maximum photosynthesis rate and dark respiration rate of individual leaves showed a vertical profile from the top to the bottom of the maize canopy. The AD268 had the highest maximum photosynthesis rate and the lowest dark respiration rate among three cultivars. The diurnal course of canopy photosynthesis rate was characterized evidently that canopy photosynthesis rate increased in the morning and reached the maximum value at 12:00 on an overcast day and at 11:00 on a sunny day and then decreased in the afternoon for all cultivars. The maximum canopy photosynthesis rate of AD268 was 21.6 μmol CO_2/(m^2·s) on an overcast day and was 26.5 μmol CO_2/(m^2·s) on a sunny day, which were significantly higher than that of JK968 (20.8 μmol CO_2/(m^2·s) and 24.9 μmol CO_2/(m^2·s)) and of ZD958 (19.6 μmol CO_2/(m^2·s) and 24.4 μmol CO_2/(m^2·s)). The daily net assimilated CO_2 of AD268 was significantly higher than that of ZD958. In comparison with ZD958, the daily net assimilated CO_2 increased by 14.8% and 12.4% on a sunny and an overcast day respectively. The plant architecture of AD268 was significantly different with other cultivars (P<0.05). However, there was no significant difference in the daily intercepted photosynthetic absorbed radiation between cultivars (P>0.8). The leaf at 16th main stem phytomer rank produced the highest daily net assimilated CO_2 among individual leaves at the leaf level. The radiation use efficiency of AD268 was 3.22 g/MJ and 3.03 g/MJ under a sunny and an overcast condition respectively, indicating a 4.5% and a 5.6% increase compared to JK968 and a 7.7% and a 7.8% compared to ZD958. The canopy radiation use efficiency of maize was more sensitive to the initial slope of light

response curve than to the maximum photosynthesis rate (P<0.05).

Conclusion

From the point view of improving canopy radiation use efficiency for maize, designing a maize ideotype that has a more compact plant architecture and higher leaf photosynthetic capacity was suggested for breeding in the future. This study could provide not only an approach for quantitatively estimating canopy photosynthesis rate of maize but also an evaluation basis as well as a phenotyping technique for breeding cultivars with high photosynthetic efficiency.

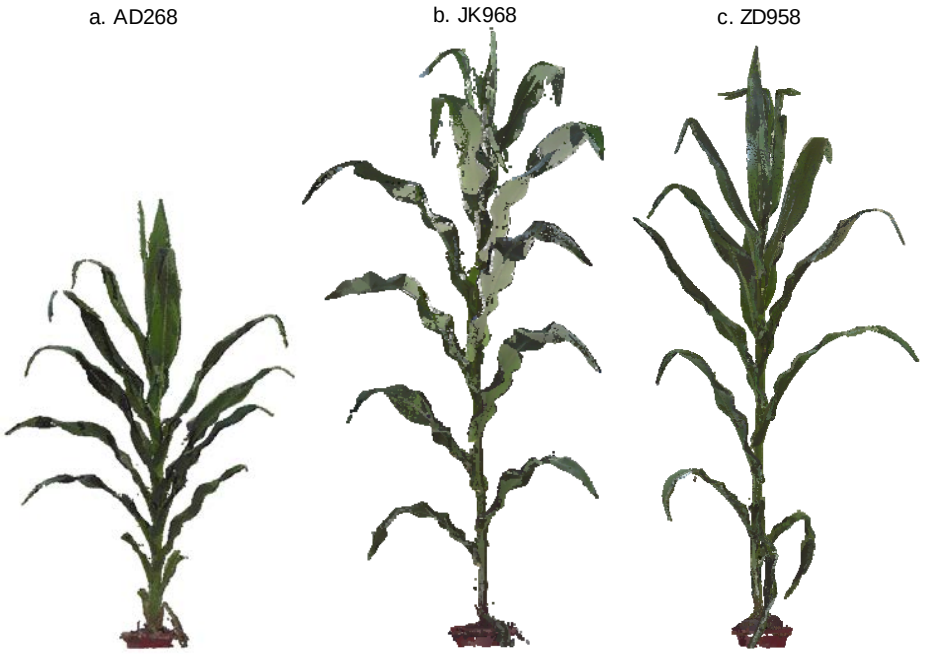

	a. AD268	b. JK968	c. ZD958
Plant height/cm	205.0±6.6	296.3±10.3	285.6±12.4
Leaf number	16	14	16
Rank of ear	15	12	15
Leaf area/m^2	0.95±0.03	0.93±0.06	0.99±0.02
Leaf insertion angle/(°)	70.4±1.2	65.8±0.2	69.9±1.5

Figure: Reconstruction of the individual maize plant using MVS-Pheno (Wu, et al, 2020) for AD268, JK968 and ZD958 during tasseling stage and corresponding architectural parameters

Conclusion

Zhu XG, et al. 2010. *Annu. Rev. Plant Biol.*, 61: 235-61. doi: 10.1146/annurev-arplant-042809-112206

Song Q et al. 2013. *Funct. Plant Biol.*, 40(2): 108-24. doi: 10.1071/FP12056

Wu S, et al. 2020. Plant Phenomics, 2020: 1848437. doi: 10.34133/2020/1848437

Functional-structural modelling of root water uptake based on measured MRI images of root systems

Tobias Selzner[1], Magdalena Landl[1], Andreas Pohlmeier[1], Jan Vanderborght[1], Daniel Leitner[2], Andrea Schnepf[1]

[1] *Institute of Bio-Geosciences (IBG-3, Agrosphere), Forschungszentrum Jülich, Jülich, Germany*
[2] *Simulationswerkstatt, Linz, Austria*

For correspondence: t.selzner@fz-juelich.de

Keywords: mimicking root growth, image-based modelling, non-invasive imaging, virtual repetition, manual reconstruction

The increase in extreme weather events and climate variability combined with a growing world population poses a challenge for global agricultural production and food security. Since drought is one of the most limiting abiotic stress factors for plant growth under rainfed conditions, careful irrigation management will become a key challenge in the future. In order to improve our understanding of the soil-plant-atmosphere-continuum and root water uptake in particular we need to be able to continuously observe roots *in-situ*. Non-invasive imaging techniques, such as magnetic resonance imaging (MRI), are becoming vital tools to investigate interactions of the root system architecture (RSA) with the soil matrix. We performed experiments with lupine plants in two different soil substrates to investigate the influence of RSA on root water uptake. RSA was measured at several times with MRI. These MRI time-lapse images were then manually segmented in order to reconstruct the RSA of the growing root systems and mimic their respective growth. Additional data on root water uptake was gathered by monitoring the soil water content and transpiration rates. We then simulated the experiment by transferring the RSA and the additionally collected data in our root and soil interactions model DuMu^x-ROSI. Hereby we demonstrate possible applications of image-based modelling of root water uptake, such as the investigation of the connection of RSA with water uptake patterns (we define image-based modelling as three-dimensional modelling based on RSA derived from images). At present, the segmentation process is still the bottleneck for image-based modelling approaches. Manual image analysis remains challenging and labour intensive due to the limitations of currently available automated root reconstruction software. Therefore, we are also working on an improved version of the automated method for RSA reconstruction described in Stingaciu et al. 2013.

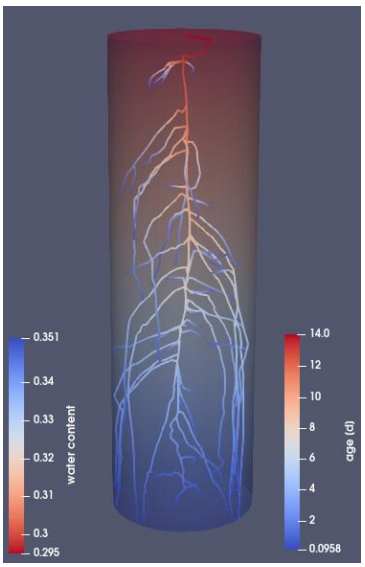

Figure: Virtual replication of a growing root system in a cylindrical container.

References

Stingaciu et al., 2013, *Vadose Zone J.* 12:1-9, doi:10.2136/vzj2012.0019

A Functional-Structural Plant Model of greenhouse-grown cucumber tailored for high-wire production

X. Cornilleau[1], G.H. Buck-Sorlin[1],

[1] IRHS, INRAE, AGROCAMPUS OUEST, Université d'Angers, SFR 4207 QUASAV, 42 rue Georges Morel, 49071 Beaucouzé cedex, France

For correspondence: gerhard.buck-sorlin@agrocampus-ouest.fr

Keywords: source-sink ratio, central carbon pool, LED lighting, GroIMP

Cucumber is a major vegetable crop for growers in the French region Pays de la Loire. It is mainly produced in heated greenhouses, with or without additional lighting using LED lamps. In spite of a long production period, France still imports more than 40 000 tons of cucumber between October and March: there is thus still a need for national production during those particular months. The current challenge is that cucumber plants grown in high-wire production systems can be light deficient in the median zone of the crop. What is more, one of the problems growers are confronted with is to find an optimal additional lighting regime, as reliable information on the response of cucumber to the light spectra emitted by the LED lamps, the light penetration into the canopy, as well as the optimal LAI with respect to photosynthesis, is missing. However, biomass allocation to the fruit may depend on irradiance received by the plant, especially in the long term (Marcelis, 1993). Light quality may also have an impact on internode elongation (Kahlen and Stützel, 2011). Because of that, a better knowledge of the impact of LED characteristics on plant behaviour is required for improving production in this particular horticultural context. Because of its capacity to simulate plant architecture and light penetration in 3D, a Functional-Structural Plant Model (FSPM) adapted for cucumber is a promising tool to predict the impact of LED characteristics on cucumber (Kahlen et al., 2008). The model presented in this paper has been developed for the special case of cucumber for high-wire production systems as used in the vegetable production region of Nantes, France. It takes into account climate data and light conditions to predict at the same time agronomic (fruit harvest, leaf growth) and physiological (transpiration, photosynthesis rate, stomatal conductance) variables. Apart from plants and the greenhouse, all light sources (the sky, the sun and the LED panels) are modeled, with their spatial positions and orientations. At the same time, a light model computes the light intercepted by canopy at an hourly rate, which is necessary for the simulation of physiological phenomena. In the case of photosynthesis, carbon assimilated is supposed to be accumulated by the plant in a central pool; this carbon is then redistributed to each organ, according to its specific relative sink strength (Marcelis et al., 1998). For a given organ type (e.g., fruit), the relative sink strength of one particular organ corresponds to the ratio of the individual potential growth rate (PGR) of the organ to the sum of all PGRs of all organs of the same type. Simulations realized under several climatic and agronomic conditions (e.g., Fig. 1) highlight the impact of LED parametrization on crops. Beyond the light perceived by the canopy, the presence of LEDs results in particular changes in the photosynthetic activity of the plant as well as in the fruit harvest or in the amount of available carbon.

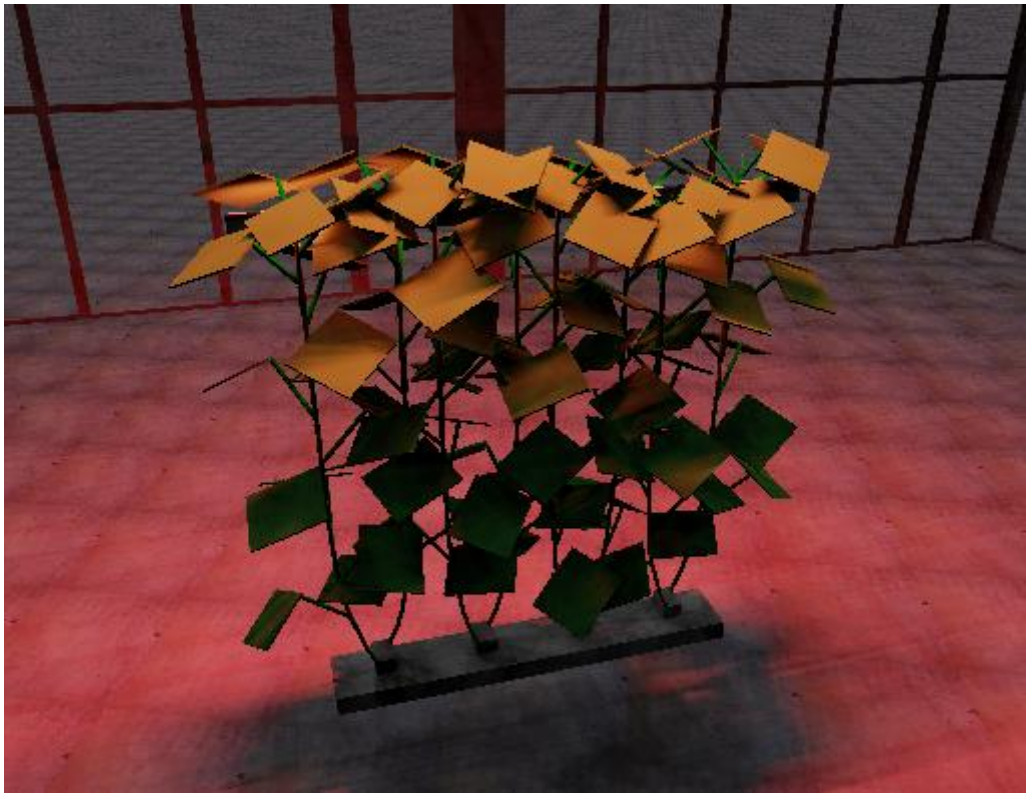

Fig. 1: Simulation of young cucumber crop (age 18 days), exposed to additional LED lighting (Interlighting: panels visible behind tip of canopy; and top lighting: panels not visible), as well as diffuse and direct daylight (climate and sky data for Carquefou, Pays de la Loire, France, 6th January 2019, 10:00 am).

References

Kahlen et al, 2008, Functional Plant Biology, 35(10), 876-884, doi: 10.1071/FP08034

Kahlen and Stützel, 2011, New Phytologist, 190, 697-708, doi: 10.1111/j.1469-8137.2010.03617.x

Marcelis, 1993, Scientia Horticulturae, 54, 123–130, doi: 10.1016/0304-4238(93)90060-4

Marcelis et al, 1998, Scientia Horticulturae, 74:1-2, 83-111, doi: 10.1016/S0304-4238(98)00083-1

New high-throughput methods for leaf area index and height estimation are faster, more precise than and at least as accurate as current methods.

Justin McGrath[1], Matthew Siebers[2], Stephen Long[2], Carl Bernacchi[1]

[1] USDA ARS GCPRU, *Urbana, IL, USA*
[2] Department of Crop Sciences, *University of Illinois, Urbana-Champaign, IL, USA*

For correspondence: jmcgrath@illinois.edu

Keywords: lidar, experimental design, variance

High-throughput phenotyping technology will be a valuable tool for monitoring crop growth, guiding breeding programs and providing data for model development and validation. Numerous technologies are being developed, and researched frequently compare these new methods to established ones. However, the experiments and statistics for these comparisons is often at best inadequate and at worst misleading. For example, the correlation coefficient (r^2) is inappropriate for comparing the quality of two methods, yet it is frequently used to support or discredit a method. Here we present an appropriate experimental design and analysis for comparison of two methods, and use it to validate new high-throughput methods to estimate canopy height and leaf area index using lidar. Compared to established methods, these techniques are unbiased, producing the same mean estimates as established techniques. The method to estimate height is remarkably more precise than the established method, with a variance as small at %5 of the established method in some cases. The new and established methods to estimate leaf area index have similar variability. The new methods are considerably faster, with the ability to measure 1,000 plots in several hours, whereas the established methods would require several work days. The design used here is generally applicable, and adds considerable value to method comparison studies. Thus, we describe the design and avenues of analysis in the hope that it will be useful for the community.

Topological skeleton models of complex jointed tree structures

Qiguan Shu[1], Wilfrid Middleton[1], Mohammad Asrafur Rahman[2], Ferdinand Ludwig[1]

[1] *Professorship for Green Technologies in Landscape Architecture, Technical University of Munich, Munich, Germany*
[2] Chair for *Strategic Landscape Planning and Management, Technical University of Munich, Munich, Germany*

For correspondence: qiguan.shu@tum.de

Keywords: photogrammetry, point cloud, voxel thinning, pipe model theory, living architecture

Introduction

Tree structures grown in natural environment are usually self-similar fractals that can be geometrically described by L-systems. Conversely, tree structures manipulated by humans are complex anastomotic networks without this typical hierarchy between elements. Examples for these structures are the living bridges made from aerial roots of *Ficus elastica* by Khasi and Jaintia communities in India (Ludwig et al., 2019); the tree circus by Axel Erlandson; and Baubotanik constructions like the Plane Tree Cube by Ludwig and Schönle (Ludwig, 2017).

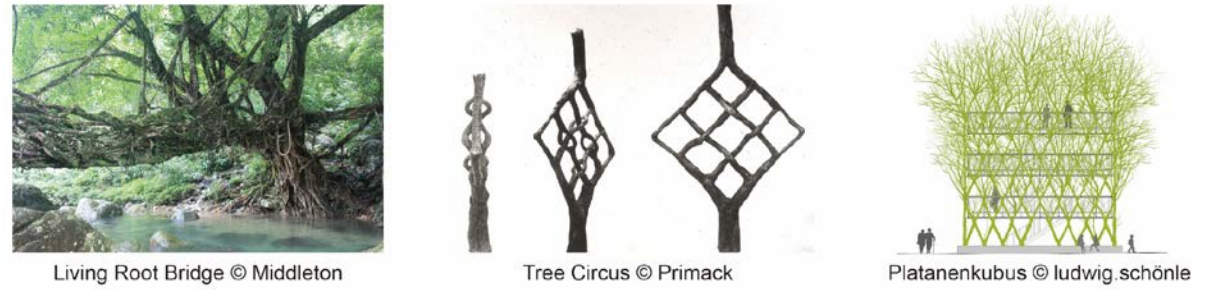

Figure 1: tree branch structures in the form of complex inosculation system

These structures are built with implicit knowledge in understanding and manipulating tree branches. Such manipulations are, however, labor intensive and time consuming. Furthermore, the plants' responses to these manipulations are not well understood, especially in their long-term life cycles. This problem causes high cost and risk in applying the methods of living material manipulation to contemporary architecture and landscape design. Modeling these structures from the real world to the virtual world and analyzing their changes in time are the first steps to study such interactions between humans and plants.

A skeleton model represents the topology and 3D geometry of these structures, allowing physiological and biomechanical processing studies. The questions for developing this model are firstly, how to abstract a topological model out of the tree structure in reality; secondly, how to transfer the topological model to an analytical tool.

Methods and Results

Lidar and photogrammetry surveys are already established methods to capture precise point clouds of on-site tree branches that are thicker than ca. 2 cm in diameter (Middleton et al., 2019). The acquired raw data require pre-treatments such as denoising and initialization. The key procedures for abstracting the topological skeleton are point cloud voxelization; voxel 3D thinning to get a one-voxel-thick voxel chain; and branch segmentation (Figure 2). These abstracted polylines are the pipes that serves both as the vascular passage and as the mechanical support (Shinozaki, Yoda et al. 1964) of the vascular plants. According to this pipe model theory, the distribution of the non−photosynthetic tissues (for girth increase) are correlated with the amount of leaves (the loss of water by transpiration). Furthermore,

the fluid distribution within the branches is calculated as a hydraulic system by Ohm's law and Kirchhoff's circuit laws (Cruiziat, P. et al. 2002). In this way, the girth growth is simulated on the topological branch skeletons by comparing them to 3D electric circuits, where the current flows from the root to the crown. Iterations are taken to allocate a given volume for girth increase to each branch according to their current. So, branches in this network are seen growing in girth at different rates (Figure 3).

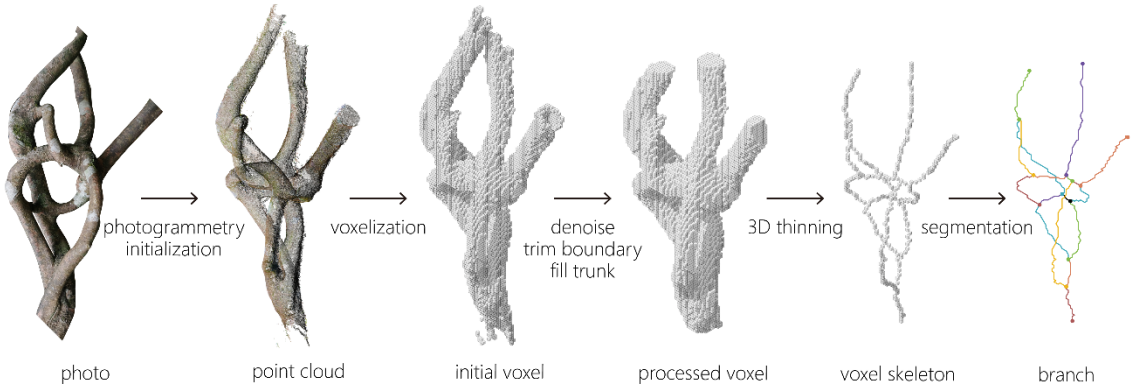

Figure 2: procedures to abstract topological skeleton of tree branches

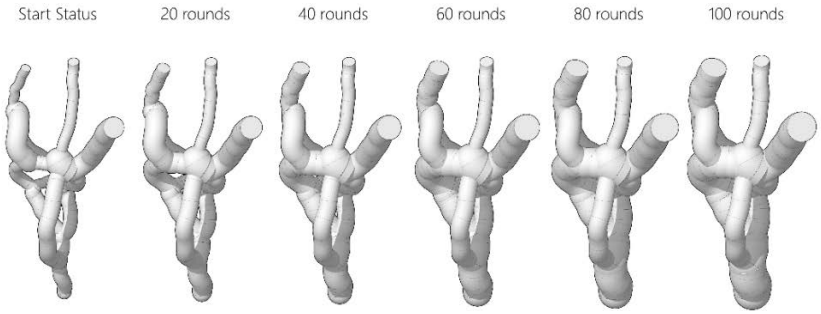

Figure 3: girth growth simulation based on the pipe model and circuit solving methods for the skeleton

Discussion

Our current skeleton abstracting program can only run on a section with ca. 10 connective branch segments due to the limitations in computing power and point cloud quality. Further works are to upscale the automated process for abstracting more complicated structures (i.e. the whole living root bridge). Further analysis applications based on the topological skeleton model should be explored (i.e. simulating the leaf area density distribution based on the branch skeleton). The vision is to transfer the implicit knowledge of manipulating plants into a computable program for robots to perform the works. This will help living structures become sustainable and affordable in architectural practice.

References

Ludwig, Middleton et al., 2019, *Scientific reports, 9(1), 1-11*, doi: 10.1038/s41598-019-48652-w
Ludwig, F., 2017, *In Architecture Today: Landscape, Loft: 170-173.*
Middleton, W., Q. Shu and F. Ludwig, 2019, *International Archives of the Photogrammetry, Remote Sensing & Spatial Information Sciences, Vol. XLII-2/W17, p195-201. 7p.*
Shinozaki, K. et al., 1964, *Japanese Journal of ecology 14(3): 97-105*, doi: 10.18960/seitai.14.3_97
Cruiziat, P. et al., 2002, *Annals of forest science 59: 723-752.*, doi: 10.1051/forest:2002060

Modelling shadow cast by trees using 3D models with artificial leaves

Rafael Bohn Reckziegel[1], Elena Larysch[1], Christopher Morhart[1], Hans-Peter Kahle[1], Thomas Seifert[1]

[1] *Chair of Forest Growth, University of Freiburg, Freiburg im Breisgau, Germany*

For correspondence: rafael.bohn.reckziegel@iww.uni-freiburg.de

Background

Information about availability of spatial and temporal distribution of solar radiation is of high importance for understanding and improving management practices of natural and agricultural ecosystems. Estimations of solar irradiation availability are of particular interest for managing integrated land use systems such as agroforestry systems (AFS). In AFS, woody perennials (i.e. trees) are deliberately grown together with agricultural crops on the same land unit, resulting in a significant interaction of the AFS components with regards to the utilization of water, nutrients and light. Since the supply with radiation energy is equally essential for the growth of trees and crops, estimations of its spatial and temporal variation in different parts of AFS are to be considered for an optimized management. On the one hand, a significant reduction of the light interception for the agricultural crops growing below trees can result in a drastic reduction of crop productivity, especially in case of light-demanding species, and on the other hand, more shade tolerant crop species may even react positively to shading.

Keywords: Shadow model, light projection, LiDAR, agroforestry, *Prunus avium*,

Introduction

Aiming for an improved simulation of the shadow cast by trees in AFS, we use an enhanced approach of a 3D model capable of quantifying tree shading in a high resolution on a temporal as well as on a spatial scale to generate realistic estimations of shade dynamics of trees. Thus, 3D data of wild cherry trees (*Prunus avium*) generated by a terrestrial laser scanner (TLS) serve as basis for a 3D model. Scanning trees in leaf-off conditions increases information about the crown structure but causes the need of adding leaves for plausible simulations of shadows casts during active vegetation period. The enhancement of cylinder models with artificial leaves is the main focus of the presented approach distinguishing this work from others (e.g. Rosskopf et al., 2017).

Materials and Methods

To develop the light model in question, six cherry trees growing in AFS in Southwest German (48°06'26.3"N 7°43'53.6"E, 193 m a.s.l.), were scanned with the TLS Faro Focus 3D S120 in April 2019, under leaf-off conditions. At scanning time, trees had heights ranging between 6 to 9 m and diameters at breast height of 18 to 27 cm. The local climate is temperate and mild with a mean annual air temperature of 11.2 °C and a mean annual precipitation sum of 710 mm for the growing period of the tree (1997-2012).

The TLS- derived point clouds were postprocessed, filtered and cylinder models were computed for each tree using *TreeQSM* (Raumonen et al. 2013).

Detailed information on leaf morphology was gained by sampling 58 branches of 8 randomly selected cherry trees in the summer of 2019. Branches were randomly selected from the crown base until its top in multiple cardinal directions. These were cut, and a subset of 20 branches was photographed with a scale. Leaves were removed from each branch and stored in separate bins. Subsequently, fresh leaves were randomly drawn from the bins and scanned (Microtek ScanMaker 9800XL plus) in a resolution of 600 dpi for estimating leaf area, length and width, using the software *ImageProPlus*. A total number of 630 leaves was randomly

sampled. Based on these findings, size distribution of natural leaves was known, and artificial leaves could be computed for the tree cylinder models.

An algorithm implemented in the open source language R (version 3.5.3) was used to calculate the shadows as described in Rosskopf et al. (2017). Additionally, factual weather data of solar irradiance (until December 2019), obtained from the German Meteorological Service (DWD), was used to quantify the resulting loss of solar radiation energy on the ground.

Results and Discussion

The novelty of this approach is to use 3D data of trees augmented with artificial leaves to compute shadow projections at a high level of temporal and spatial resolution. The model provided single-tree shadow projections in time intervals of 10 min for a raster grid of 10 cm x 10 cm cell size.

Based on our approach, the monthly shadow of six cherry trees was modelled for the entire month of July 2019, since this is the first month of the vegetation period, when the trees have the maximum leaf area. The shadow dynamics throughout the 15th July 2019 is illustrated on Figure 1.

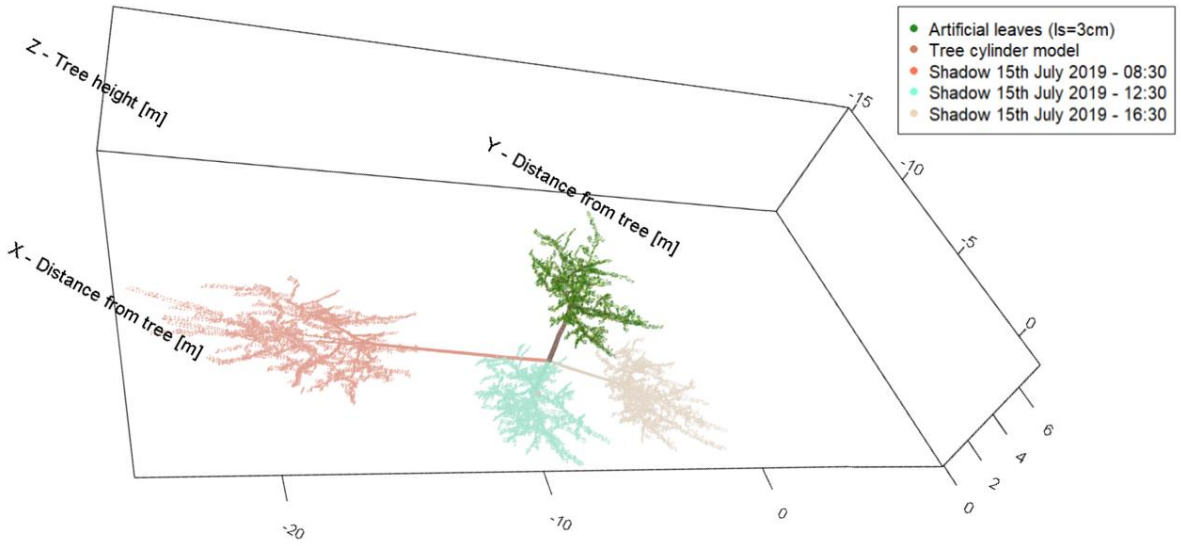

Figure 1: Shadows cast by a cherry tree in the vicinities Eichstetten (48°06'26.3"N 7°43'53.6"E, 193 m a.s.l.).

Conclusion

Using factual climate data from the last season enables us to retrospectively model the radiation regime with leaf-on conditions around trees in a realistic manner. The derived results show the shadow distribution around trees and can help to plan agroforestry systems more efficiently and to optimize their planting design, the best tree-crop combinations, spatial arrangements and management regimes (e.g. tree pruning regimes and tree harvesting).

References

Rosskopf et al. 2017, *Remote Sensing*, *9, 719,* doi: 10.3390/rs9070719
Raumonen et al. 2013, *Remote Sensing*, 5, 491-520, doi:10.3390/rs5020491

Detailed reconstruction of trees from TLS scans for radiative transfer modelling applications

Růžena Janoutová[1], Lucie Homolová[1], Zbyněk Malenovský[2], Jan Novotný[1], Barbora Navrátilová[1]

[1] *Department of Remote Sensing, Global Change Research Institute CAS, Brno, Czech Republic*
[2] *School of Technology, Environments and Design, Discipline of Geography and Spatial Sciences, University of Tasmania, Hobart , Australia*

For correspondence: janoutova.r@czechglobe.cz

Keywords: 3D tree model, TLS, European beech, Norway spruce, White peppermint

Dynamic changes in forest ecosystems caused by climatic changes are being more frequently assessed using remote sensing (RS) based methods which allow extensive monitoring in a relatively short time. Radiative transfer models (RTM) provide a physical link between canopy biochemical and structural properties and canopy reflectance, therefore they are often used to interpret RS data. RTM that are capable implementing detailed 3D objects can precisely simulate interactions between canopy elements and incident light in various parts of the electromagnetic spectra.

In this study we present a method for 3D reconstruction of forest tree species and implementation in 3D canopy RTM Discrete Anisotropic Radiative Transfer model (DART, Gastellu-Etchegorry et al., 2017). We selected three forest species, Norway spruce (*Picea abies)* and European beech (*Fagus sylvatica*) as representatives of European productive forests and White peppermint (*Eucalyptus pulchella*) as a common forest specie in Tasmania. All these species have their specific structural features. European beech represents deciduous forest species. In sense of structural characteristics there are simple shaped leaves of the same age that are distributed typically in spherical leaf angle distribution (LAD). Norway spruce is an evergreen coniferous specie. Compared to broadleaved species the tree structure is more complex and it is challenging to reconstruct it up to the level of single needles. Moreover, the presence of needle shoots with different age requires to separate the shoots in 3D tree model into two different age categories at least. White peppermint is structurally different from common European species. It is a broadleaf, but evergreen specie therefore it is necessary to separate leaves into different age categories. Moreover, it has sparse crown architecture with leaves predominantly distributed according to erectophile LAD.

We design an algorithm for reconstruction of 3D tree model based on terrestrial laser scanning (TLS) data and field measured characteristics as LAD, percentage of current and older needles or leaves etc., which we are not able to derive precisely from TLS data in close forest formation. The tree reconstruction algorithm was primarily designed for Norway spruce (Janoutová et al., 2019) and here it is expanded to broadleaf beech and peppermint trees. The algorithm contains four main steps: i) geometrical transformation of the point cloud to fit site-specific tree dimensions, ii) reconstruction of wooden skeleton from TLS data, iii) distribution of shoot or leaf positions within the tree crown, and iv) separation of the positions into two age categories. The last step is applicable only for spruce and peppermint trees.

The reconstructed 3D models of the tree species were used to build up small forested scenes in the DART model. This contribution summarizes canopy reflectance simulations, its

angular behavior and comparison with spectral signatures extracted from airborne imaging spectroscopy data.

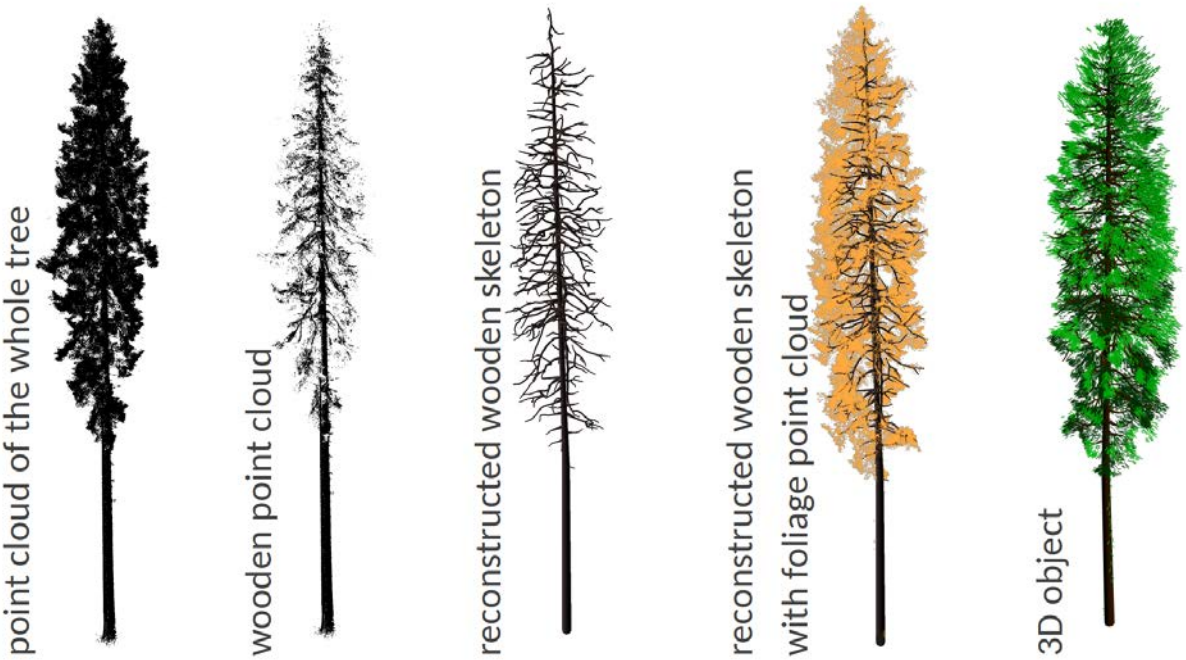

Figure: Illustration of process of 3D spruce model creation from TLS data.

References

Gtellu-Etchegorry et al., 2017, *IEEE J. Sel. Top. Appl. Earth Obs. Remote Sens.*,*10*, 2640–2649, doi: 10.1109/JSTARS.2017.2685528
Janoutová et al., 2019, *Forests* 10(3): 292, doi: 10.3390/f10030292

Characterization of light quantity and quality in agroforestry systems

Willem Coudron *[1,2], Kris Verheyen[2], Pieter De Frenne[2], Bert Reubens[3], Kim Calders[4], Sanne Van Den Berge[2], Tom De Swaef[1]

[1]*ILVO: Plant Sciences Unit, Caritasstraat 39, 9090 Melle, Belgium*
[2]*UGent: Departement environment, Geraardsbergsesteenweg 267, 9090 Gontrode, Belgium*
[3]*ILVO: Plant Sciences Unit, Burg. Van Gansberghelaan, 109 bus 1, 9820 Merelbeke, Belgium*
[4]CAVElab - Computational & Applied Vegetation Ecology, Faculty of Bioscience Engineering, Ghent University, Belgium

For correspondence: Willem.Coudron@ilvo.vlaanderen.be

Keywords: LiDAR, ray-tracing light model, agroforestry

Abstract

Agroforestry is a land use system in which the cultivation of crops or livestock is combined with trees on the same parcel. This cultivation system shows great potential to protect crops from droughts caused by climate change by inducing microclimatic buffer effects. However, present studies about agroforestry systems show large variations in crop yield. More knowledge behind the mechanisms driving crop yield in these systems is required to test the potential of agroforestry systems in drought control. This study presents a methodology to examine the effect of differential light quantity and quality on differential evapotranspiration and crop yield on different places across the field in agroforestry systems bordered with hedgerows and single tree species of different ages.

Terrestrial LiDAR scans from four indicator tree species (*Populus* × *canadensis, Juglans regia*, *Quercus robur*, *Prunus avium*) in leafless condition and from different ages bordering parcels are used. On other parcels, scans will also be taken from hedgerows containing several tree species.

From the point clouds generated by the LiDAR scanner, digital trees will be constructed with TreeQSM, a modelling method that reconstructs quantitative structure models (QSMs) of trees from point clouds (Raumonen et al. 2013). Using the Foliage and Needles Naïve Insertion (FaNNI) algorithm described by Åkerblom et al. (2018) leaves can be added to the tree shape to generate different phenological stages. The QSMs will be integrated in a ray-tracing light model in GroIMP, a 3D crop modelling platform, to quantify the amount of light intercepted by the trees in multiple years (Figure 1). In this light model, based on Spitters et al (1986), the global radiation that falls on the earth's surface can be divided in a diffuse and direct light component. Furthermore, this model allows to differentiate between wavelengths, making it perfectly suitable to study impacts on light quality (van Antwerpen et al. 2011). Validation will be performed with light quantity and quality measurements from the fields. Differences in light interception across tree species and tree ages are studied and the consequences for photosynthesis and transpiration of the crop on multiple distances from the tree are determined.

With the ray-tracing light model, the different number of rays fall on the squares around the virtual tree and thus result in a differential pattern of light intensities. For each of these squares evapotranspiration and photosynthesis can be calculated via the coupled transpiration-photosynthesis model of Tuzet et al. (2003).

This approach can provide more insight in the effect of different agroforestry systems on light quantity and quality for the crop and the subsequent influence on transpiration, photosynthesis and crop yield. This gives us an estimation on how much agroforestry systems buffer against droughts by casting shadows on the field.

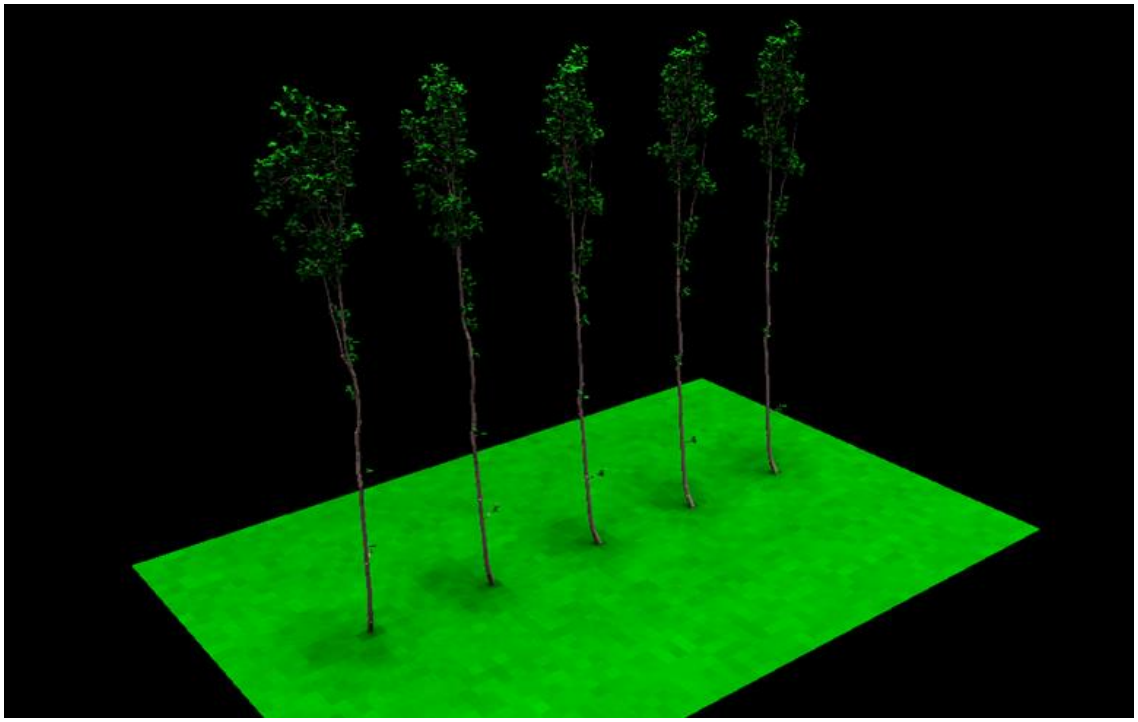

Figure 1: Example of trees constructed based on LiDAR scans integrated in the ray-tracing light model in GroIMP.

References

Åkerblom, M. et al., 2018 Non-Intersecting leaf insertion algorithm for tree structure models. *Interface Focus*, *8*, 20170045.
Raumonen P. et al., 2013, Fast Automatic Precision Tree Models from Terrestrial Laser Scanner Data. Remote Sensing 5(2):491–520.
Tuzet, A. et al., 2003, A coupled model of stomatal conductance, photosynthesis and transpiration. Plant Cell and Environment 26, 1097-1116.
Spitters. C. J. T. et al. (1986). Separating the diffuse and direct component of the global radiation and its implications for modelling canopy photosynthesis. Part I. Components of Incoming radiation. Agric. For. Meteorol. 38: 217-229.
Antwerpen, D. et al (2011). High performance spectral light transport model for agricultural applications. Poster session presented at High Performance Graphics (HPG 2011), . https://edepot.wur.nl/202955

Simulating the red:far-red ratio emitted by individual plants at a local and directional scale.

Arthur Couturier[1], Elzbieta Frak[1], Didier Combes[1], Abraham Escobar-Gutierrez[1]

[1] *INRAE UR4 P3F, CS80006, F-86600 Lusignan, France*

For correspondence: arthur.couturier@inrae.fr

Keywords: *Lolium perenne*, FSPM, directional sensor, perception site

Introduction

Modeling of red:far-red ratio (R:FR) in FSPM is either surface based (i.e nested radiosity, ray tracing) or turbid-medium based (Chelle and Andrieu, 2007). These two types of R:FR modeling methods estimate the light environment all around a specific point, which mimics hemispherical sensors. However, none of these methods mimics the light measurement of directional sensors. Directional sensors are able to detect early R:FR decrease (Ballare, 1987) and reduce the R:FR variations from the sky conditions (Chelle et al., 2007).
Directional sensors with 80° and 40° FOV have been previously tested by Chelle (2007) with the nested radiosity light model from the ADEL-wheat model. However, no further implementation of these directional sensors has been reported.
A new approach of R:FR modeling is proposed in this paper, based on plant architecture "seen" by a sensor at a local scale with directional sensors, and tested in the L-grass model (Verdenal, 2009).

Materials and Methods

R:FR ratio was measured with a 3° FOV sensor directed on Lolium perenne seedlings at 25 distances between 2 cm and 56 cm at multiple growth stages. Seedling's architecture was captured with a 3D laser scanner. A virtual sensor mimicking the directional sensor was simulated with python 3.7, positioned at the same location as the real sensor from the seedling. R:FR is computed by two methods : a) using Caribu (Chelle et al., 2004), b) with the ratio between the leaf area and the non-leaf area within the field of view of the sensor, obtained by dividing the amount of pixels from the plant by the total number of pixel contained in the sensor FOV (plant area pixel ration, PAPR). The results from the two R:FR modelling methods are compared to the measured R:FR using rRMSE.

Results and Discussion

A linear correlation between the measured R:FR ratio and the percentage of plant area within the sensor FOV is observed. The estimated relation between these two variables is described by the following equation:

$$R{:}\,FR = a \times (1 - Plant\ area\ pixel\ ratio) + b$$

Distance seems to have no direct impact on R:FR but has only an impact on PAPR, since the empty area increases with the distance.

A linear relation between R:FR and the LAI has been identified by Ballaré et al. (1987). As such, a linear equation between PAPR and R:FR could be a link to the previously established relationship between LAI and R:FR.
This equation is – for now – based on Lolium perenne and could change for others species, especially dicotyledons, depending on the optical properties of the plant organs.
Computation time is steady between plants because the computation is based on the screen resolution and not on the number of organs. This is very different form surface based and turbid-medium based R:FR modelling approaches which lose performance as the number of

organ increases. However this approaches cannot estimate light environment parameters beside R:FR.
Compared to Caribu, used in previous studies to compute R:FR in FSPM, the predicted R:FR is lower for the area ratio method. However, the plant area ratio method is capped at a R:FR of 1.1, corresponding to a FOV without a plant.

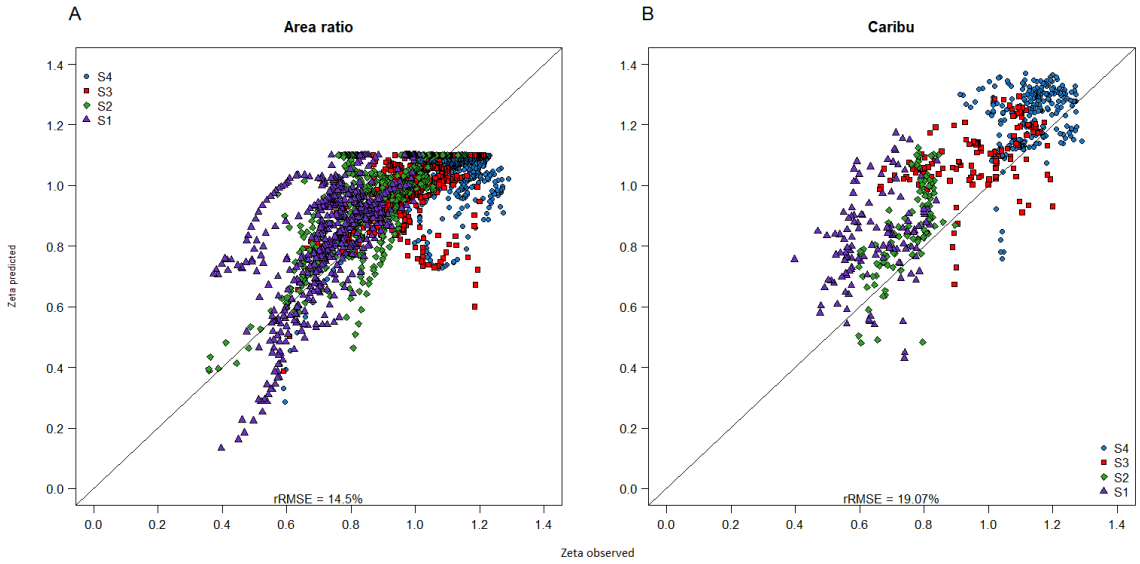

Figure: rRMSE of the two R:FR modeling methods compared to the measured R:FR.

Conclusion

Previous R:FR modelling approaches simulate the global light environment and computes R:FR from this environment. This approach compute R:FR directly from neighbour architecture. The measure of plant area seen from perception sites could combine information from both LAI and optical properties of the considered plant. These biological properties are wrapped into a and b parameters occurring in our equation, biological significance of these parameters need to be addressed.
Measurements have been made on individual plants and the relation between PAPR and R:FR could be different in plants under canopy. Furthermore, only one direction has been considered to evaluate the R:FR perceived by a perception site, but more directional measurements must be done under a plant canopy. Comparison with Caribu shows a better prediction from the PAPR method for the observed conditions, PAPR could be a way to compute R:FR without using a time consuming light model.

References

Chelle et al., 2004, *FSPM04*, link: citeseerx.ist.psu.edu/viewdoc/summary?doi=10.1.1.122.8333
Chelle and Andrieu, 2007, *Frontis,* 22:75–89, link: library.wur.nl/ojs/index.php/frontis/article/view/1373
Ballaré et al., 1987, *Plant, Cell & Environment*, 10:551-557, doi:10.1111/1365-3040.ep11604091
Chelle et al., 2007, *New Phytologist*, 176:223-234, doi:10.1111/j.1469-8137.2007.02161.x
Verdenal, 2009, PhD Thesis. *Université de Poitiers*, link: theses.univ-poitiers.fr/notice/view/3302

Bayesian statistical calibration of parameters in the APSIM-Maize crop model for improved yield prediction

Matteo G. Ziliani*[1], Matthew F. McCabe[1]

[1] *Biological and Environmental Science and Engineering (BESE), King Abdullah University of Science and Technology, WDRC Departement, 23955, Thuwal, Kingdom of Saudi Arabia*

For correspondence: matteo.ziliani@kaust.edu.sa

Keywords: crop growth simulation models, precision faming, APSIM, bayesian calibration

Introduction

One of the application of crop simulation models is to estimate crop yield throughout the growing season. Despite their wide utilization, crop models are often limited by uncertainties in input parameters such as soil condition, planting date and density, fertilization and irrigation management (Zhao et al., 2014). Apart from application in controlled experimental fields, many of these parameters are poorly known, and their uncertainty affects the reliability of models' predictions. A comprehensive calibration of these parameters is therefor needed when the crop model is applied to a new environment or a new cultivar (Confalonieri et al., 2010; Sexton et al., 2014). This study evaluates the use of a Markov Chain Monte Carlo (MCMC) Bayesian approach (Jadoon et al., 2016) to calibrate the Agricultural Production Systems sIMulator (APSIM)-Maize model's cultivar parameters. MCMC calibration was able to accurately simulate LAI, biomass, maize yield and crop height under irrigated and non-irrigated conditions in Nebraska, thereby providing more comprehensive insights into the model and its parameters. In addition, while such approach has mainly been investigated at the regional scale, we propose to calibrate the crop model considering the soil intra-field variability that characterize the agricultural fields. The detection of intra-field biophysical parameters is particularly valuable since it may be employed to infer inefficiency problems at different stages of the season, and hence drive specific and localized management decisions for improving the final crop yield. Also, the use of Bayesian statistical calibration technique supply model developers with a reproducible method for calibrating model parameters while simultaneously quantifying the uncertainty in those parameters values. Keeping APSIM-Maize model up-to-date with new commercially released varieties will also allow crop modelers to investigate the impact of interactions between variety, environment and farm management practices and help advance the understanding and management of agricultural systems in the context of precision agricultural application.

Materials and Methods

We assess the sensitivity of the predicted maize biomass (kg ha^{-2}), LAI (m^2 m^{-2}), yield (kg ha^{-2}) and crop height (cm) to the APSIM-Maize model's input parameters. We used the crop simulations at harvesting time and throughot the season to identify which parameters generated most of the uncertainty in the output values using a Global Sensitivity Index approach (as described in Cannavo, 2012). Bayesian inference through a MCMC algorithm (Jadoon et al., 2016) was then applied to calibrate and assess the uncertainty in the most influential model parameters.

Results and Discussion

Figure 1 shows an example of trajectory for LAI, biomass and crop height as simulated by the APSIM-Maize model against in-situ observation. Multiple parameters have been identified as sensitive to the model output for the studied regions and their values calibrated

against intra-season LAI, biomass and crop height data. The new calibrated parameters provided promising yield prediciton for a subsequent validation datasets.

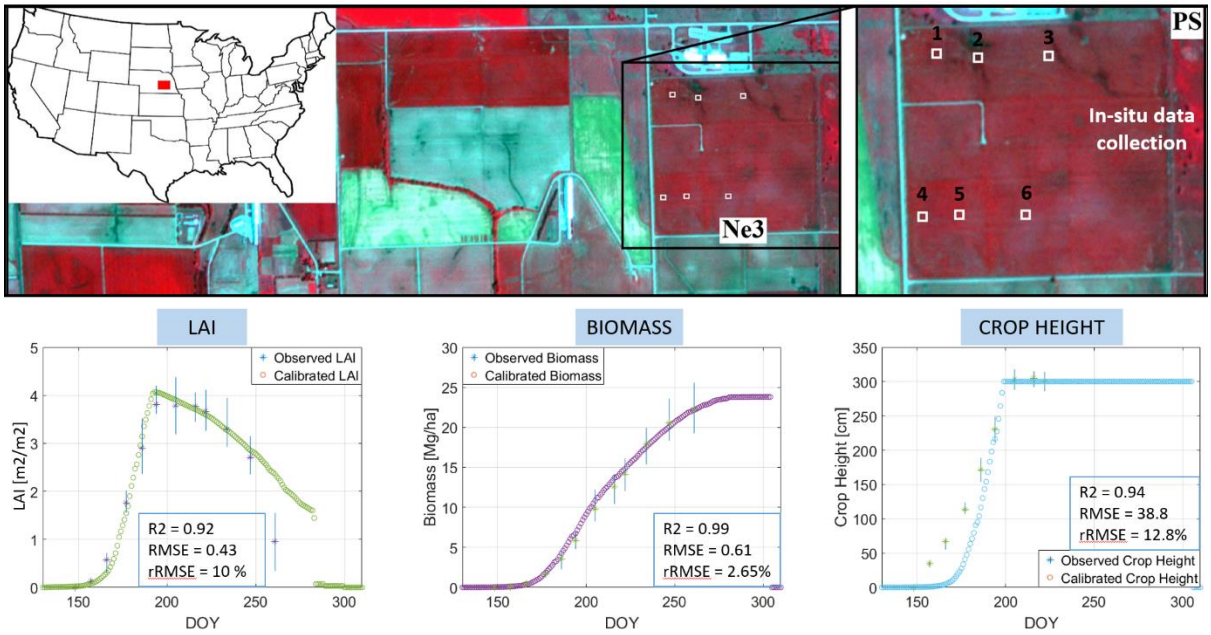

Figure 1: APSIM-Maize calibration results for site 3 in Nebraska for the 2017 season. Comparisons of simulated and field-measured LAI (left), biomass (middle) and crop height (right) are depicted.

References

Zhao, G., Bryan, B. A., & Song, X. (2014). Sensitivity and uncertainty analysis of the APSIM-wheat model: Interactions between cultivar, environmental, and management parameters. *Ecological Modelling*, *279*, 1-11.

Confalonieri, R. (2010). Monte Carlo based sensitivity analysis of two crop simulators and considerations on model balance. *European Journal of Agronomy*, *33*(2), 89-93.

Sexton, J., & Everingham, Y. (2014). Global sensitivity analysis of key parameters in a process-based sugarcane growth model: a Bayesian approach.

Jadoon, K., Altaf, M., McCabe, M., Hoteit, I., Muhammad, N., & Weihermüller, L. (2016). Inferring soil salinity in a drip irrigation system from multi-configuration EMI measurements using adaptive Markov chain Monte Carlo.

Cannavó, F. (2012). Sensitivity analysis for volcanic source modeling quality assessment and model selection. *Computers & geosciences*, *44*, 52-59.

An algorithm to measure root hair response to abiotic stresses in microscopy images

Peter Pietrzyk[1], Chartinun Chutoe[2], Patompong Saengwilai[2], Alexander Bucksch*[1,3,4]

[1] *Department of Plant Biology, University of Georgia, Athens, GA, USA*
[2] *Department of Biology, Faculty of Science, Mahidol University, Thailand*
[3] *Warnell School of Forestry and Natural Resources, University of Georgia, Athens, GA, USA*
[4] *Institute of Bioinformatics, University of Georgia, Athens, GA, USA*

For correspondence: bucksch@uga.edu

Keywords: root hair, phenotyping, machine learning, abiotic stress

Improving nutrient and water uptake in crops is one of the major challenges to sustain a fast-growing population that faces increasingly nutrient limited soils. Root hairs, which are specialized epidermal cells, comprise up to 70% of the total root surface area. Therefore, root hairs are important drivers of nutrient and water uptake from the soil. Microscopy provides a mean to record root hairs as digital images. However, due to their geometry and complex spatial arrangements quantifying root hairs in microscopy images manually remains a bottleneck. This process is often based on a limited manual selection of representative root hairs, which can result in inaccurate estimations of root hair traits and misrepresentation of root hair functions. We present a method to automatically quantify phenotypic traits of all individual root hairs in digital microscopy images. Our method uses a machine learning approach that classifies root hair, parent root and the image background. We define metrics to evaluate segments of root hairs that intersect or form blobs of two or more root hairs. Using combinatorial optimization we can reconstruct individual root hairs by resolving these complexities in a globally optimal way. As a result, we measure the root hair traits, length and straightness, as well as the distribution of these traits in each image. We demonstrate our method on examples of rice, maize and common bean under phosphorus, nitrogen and potassium stress. Results show that our measurements of root hair traits strongly correlate with manually measured validation data in mean and maximum root hair length (Pearson-correlation: both >0.95), as well as in root hair number (Pearson-correlation: 0.84). We expect that our method distinguishes subtle differences between genotypes and treatments on the basis of the extracted traits. We believe our study paves a way towards identifying the genetic control of root hair traits and increased agricultural production. In the future we will use our method to identify intersecting branches and branching points in complete root systems to automatically characterize branching patterns of roots from 2D imaging and 3D point cloud data. The resulting information can be then used to calibrate functional-structural plant models.

Digitizing plants: simultaneous capturing of plant structure and functioning for building a maize FSPM

Selwyn Villers[1,2], Jonas R. Coussement[1], Dirk Inzé[2], Kathy Steppe[1]

[1] *Ghent University, Faculty of Bioscience Engineering, Laboratory of Plant Ecology, 9000 Gent, Belgium*

[2] *Flemish Institute for Biotechnology (VIB), Rijvisschestraat 120, 9052 Zwijnaarde*

Correspondence: Selwyn.Villers@UGent.be

Introduction

Functional-structural plant modeling requires data on plant structure and functioning, which can be a challenge to capture. Technology and automation form a powerful solution for recording this type of data. High-throughput phenotyping platforms are an effective tool to capture plant architecture on a daily basis and additionally provide detailed information on environmental parameters and growth conditions. Plant sensors provide a more continuous stream of information on plant physiology with high temporal resolution and are especially adept at capturing daily patterns. In order to benefit from the advantages of both technologies we can integrate these two systems.

Materials and Methods

Small plant sensors for measuring sap flow, leaf thickness and stem diameter variation can be connected to a single, battery-powered data logger to wirelessly transfer data. This constitutes a compact and mobile system to operate within many phenotyping platforms and move along with plants if necessary (Figure 1). Data on plant structure is recorded with the phenotyping platform on a daily basis and supplemented with climatic information. This system generates information which is stored into a database structure that allows further automated analysis of the data.

Results and Discussion

The combination of technologies enables collection of a high dimensional dataset consisting of phenotypic traits and real-time plant functioning in combination with daily acquired 3D structural information throughout plant development, resulting in a more complete picture of the plant's phenotype and traits (Coppens et al., 2018). In order to navigate and extract the useful information from the data, a well-designed processing pipeline is needed. This is especially the case for structural information of plants which only becomes accessible after digital reconstruction of the plants and processing of the 3D volume. Automation of the data collection shifts the burden from manual collection of the plant structure towards data processing. Although it can be difficult to implement the processing pipeline, once established, a vast amount of high-quality data becomes available. The information gathered in this manner forms an ideal foundation to study the mechanisms that regulate biomass accumulation across different organs, their competition for water at different developmental stages and in response to drought. The measured plant-water relations and associated turgor-driven growth (Coussement et al., 2018) is crucial for simulating the impact of drought in FSPMs.

Conclusions

Technological innovations have enabled us to integrate plant sensors within automated phenotyping, providing real-time information on plant physiology and growth in addition to plant structure. Gathering additional information on the plant water status is necessary for modeling plant growth as driven by turgor pressure, which forms a more realistic mechanism for representing plant growth.

Figure 1: Integrated sensor system on a high-throughput phenotyping platform

References:

Coppens et al., 2017, *Current Opinion in Systems Biology*, *4*, 58-63, doi: 10.1016/j.coisb.2017.07.002.

Coussement et al., 2018 *Annals of botany*, *121*(5), 849-861, doi: 10.1093/aob/mcx144

Simulating the spatial distribution of physiological processes using a reduced functional-structural plant model for wheat

Simon Lauwers[1], Jonas Coussement[1], Sarah Verbeke[1], Veerle De Schepper[2], Kathy Steppe[1]

[1] *Laboratory of Plant Ecology, Ghent Uiversity, Ghent, Belgium*
[2] *BBCC – Innovation Center Ghent, BASF, Ghent, Belgium*

For correspondence: simon.lauwers@UGent.be

Keywords: GroIMP, PROSPECT, Photosynthesis, Stomatal conductance, *Triticum aestivum* L.

Introduction

A static FSPM for wheat was designed, parameterized, calibrated and validated using both morphological and physiological data from two wheat varieties with a different drought tolerance. Model simulations were performed in order to analyze the spatial distribution of physiological parameters throughout the wheat canopy, including light interactions, photosynthesis, stomatal conductance, transpiration and leaf temperature.

Materials and Methods

For both varieties, structural data of eight plants was implemented in the model using the XL-language, as available in GroIMP. All morphological parameters were manually measured, avoiding 3-dimensional or image visualisation. Leaf curvature was approached by a circular arc and leaf shape was approached by using the lamina2Shape model introduced by Dornbusch et al. (2007). Using manual measurements and approximations, measurements were kept to a minimum, allowing rapid data collection. The functional counterpart of the model was divided in two sub-models. First, the PROSPECT-D model (Féret et al., 2017) was used to calculate leaf spectral characteristics based on measured SPAD-values for every leaf. Second, the coupled P-SC-T model (Kim et al., 2003) was introduced combining calculations for photosynthetic rate, stomatal conductance and transpiration. Incoming light was reproduced by combining assimilation lights with a module for diffuse sunlight. Direct sunlight and the greenhouse structure were neglected. Validation was performed by comparing the photosynthetic rate of a container filled with wheat plants to the simulated photosynthetic rate of a virtual container, consisting of numerous copies of eight selected plants, distributed at random. Canopy photosynthetic rate was measured using the canopy photosynthesis and transpiration system (Song et al., 2018).

Results and discussion

The model showed good correspondence between measured and simulated photosynthetic rate. Further refinement should be conducted towards dark respiration, as simulated dark respiration tended to be constant, while measured dark respiration was not. A first application of the FSPM was a comparison of both wheat varieties. Little significant differences were observed between measured parameters in both varieties. Using the FSPM and its sub-models, differences were further clarified. Calibration of the sub-models made it possible to identify important traits affecting photosynthetic rates and stomatal conductance. Using the model, new conclusions could be drawn considering the needed quantity of data. The FSPM was also used to simulate the spatial distribution of different physiological processes in the wheat canopy, including leaf spectral characteristics, photosynthesis, stomatal conductance, transpiration and leaf temperature. Using this information, hypotheses for both cultivars concerning their drought tolerance will be assessed.

Conclusion

A good model validation was obtained, even with simple, manual measurements and direct sunlight neglected. Using both the FSPM and its sub-models, insights could be gathered concerning the effect of different traits on physiological processes and the spatial distribution

of these physiological processes in the wheat canopy. Local sensitivity analysis could be applied to structural, functional and even environmental parameters, to further investigate the effect of changing parameters on each variety. As both measurements and calibration were rather simple, new varieties could be introduced in the FSPM fast and easy. The model will be used to further evaluation of the needed quantity of data.

Acknowledgements
We would like to thank BASF (BBCC- Innovation Center Ghent) for providing us with wheat plants and for their support during the measurements. We would like to thank Selwyn Villers and Jonathan Vermeiren for their contributions to the model.

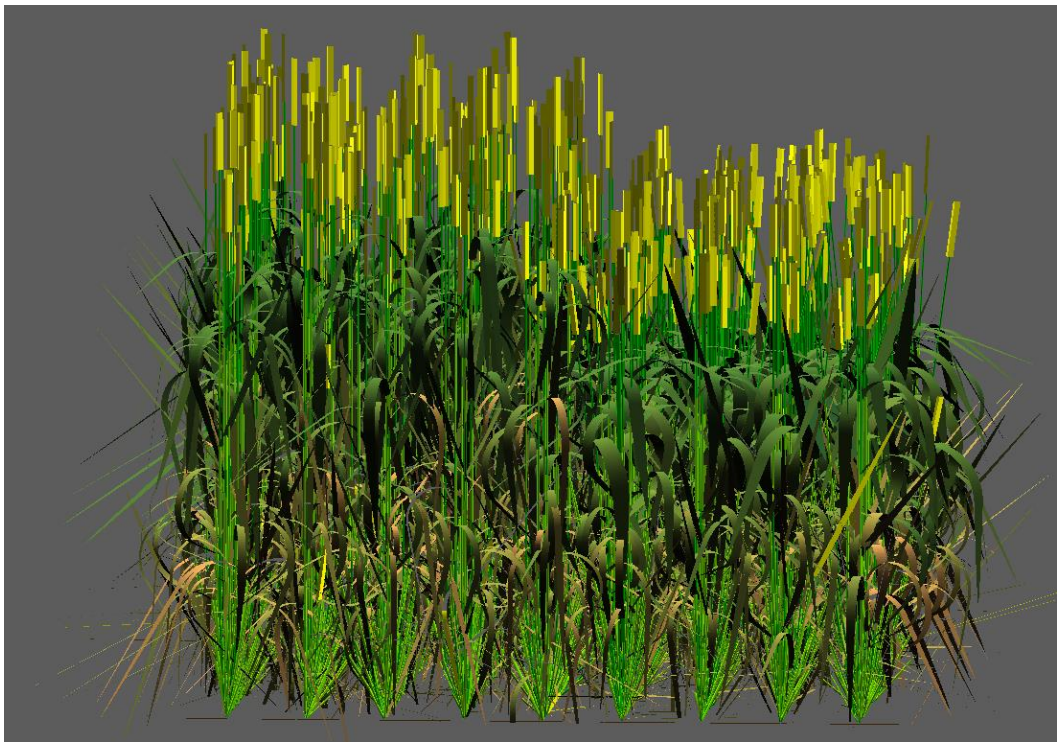

Figure: Visualization of the FSPM for both wheat cultivars

References

Dornbusch et al., 2010, *Comput. Electron. Agr.* 217-224, doi: 10.1016/j.compag.2009.10.009
Féret et al., 2017, *Remote Sens. Environ*. 204-215, doi: 10.1016/j.rse.2017.03.004
Kim et al., 2003, *Ann. Bot.* 771-781, doi: 10.1093/aob/mcg080
Song et al., 2018, *Methods Mol. Biol.* 69-81. doi: 10.1007/978-1-4939-7786-4_4

Modelling the extension of silk and ear of summer maize

Zhiwei Wang, Weiwei Sun, Youhong Song*

School of Agronomy, Anhui Agricultural University, Hefei, China

** For correspondence: uqysong@163.com*

Keywords: *Zea mays*; Silk and Cob; Functional-Structural Plant Modelling; Dynamic Extension

Introduction

Maize is one of the three staple crops and plays an important role in ensuring food security (Ma and Ma, 2017). Maize silk is the organ receiving pollen (Kapu and Cosgrove, 2010). The silking time determined by maize silk extension is the key to determine the drought tolerance during flowering (Araus et al., 2012). The extension drought response of maize silk is one of the important indexes to measure the effect of drought tolerance. Functional-structural plant model for maize has been developed (Fournier et al., 1998; Guo et al., 2006). However, few studies on model dynamic characteristics of silk extension have been conducted in functional-strucutral plant modelling. Therefore, it is necessary to study the extension characteristics of maize silk. In this study, the dynamic extension model of silk at the bottom, middle and top of the ear was established using two local cultivarsi.e. Zhongdan909 (ZD909) and Annong591 (AN591).

Materials and Methods

The experimental field located at Anhui Agricultural University (31°86'N, 117°25'E), Hefei city, Anhui Province, PR China. The seeds were planted on July 17th, 2019 at a density of 66,700 plants /hm^2, with 60 cm row spacing and in rain-fed. The soil type of the experimental field is yellowish brown soil. The other field management measures are the same as general fields.

Microsoft Excel 2010 software was used for data processing and analysis. Origin 2019b 64Bit software was used to draw the dynamic characteristics of silk and ear extension. Then the model "$Y = a + \frac{b}{1+\left(\frac{x}{x0}\right)^p}$" was used to simulate the dynamic extension of silk and ear.

Results and Discussion

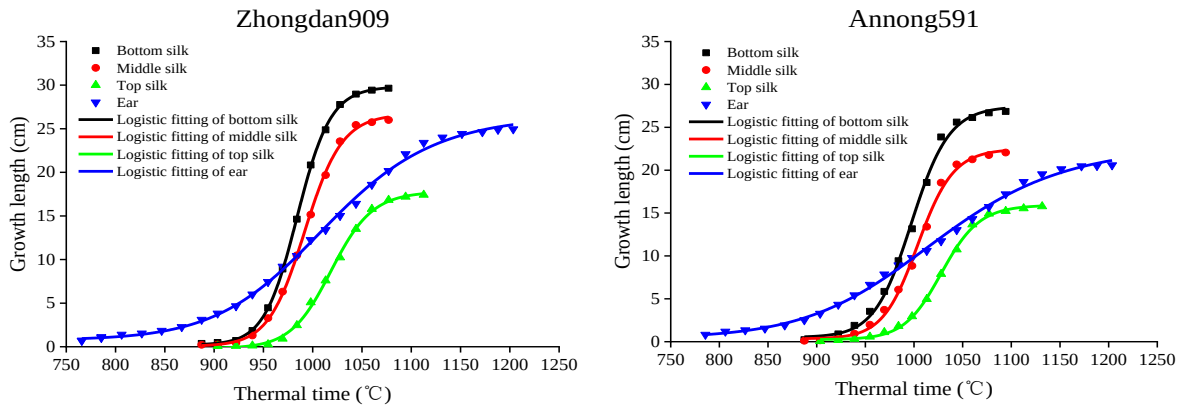

Fig. 1: Dynamic fitting of extension of silk and ear

Silk and ear extension grow slowly at the early stage, and grow rapidly in a linear way before and after the silking stage, after pollination, the extension rate drops obviously (Carvova et al., 2003; Kapu and Cosgrove, 2010). And the extension of silk and ear at different positions

can be modelled by the “S-shaped” growth curve (Fig. 1), which is consistent with Avan (2008). When the ear development rate is about 12%, the silk is visible. The ear development rate is about 50%, silking stage starts, and the development rate of bottom, middle and top silk is about 70%, 60% and 30%. As the ear development rate is about 80%, the bottom and middle silk developed completely and start to abscise, and the top silk developed about 96%.

Tab. 1: The parameters of model of developmental and extension rate and thermal time

Cultivars	Parts	Model	Developmental rate (%)			Extension rate and thermal time				
			Visible	Silking	Abscission	V_m(cm/°C)	V_a(cm/°C)	T_t(°C)	T_r(°C)	T_s(°C)
ZD909	Bottom silk	$y = 29.85 - \frac{29.63}{1+\left(\frac{x}{984.53}\right)^{58.38}}$	0	70.28	100	0.42	0.15	984.0	954.7	1013.1
	Middle silk	$y = 26.70 - \frac{26.63}{1+\left(\frac{x}{992.33}\right)^{52.86}}$	0	58.27	100	0.32	0.13	998.0	969.5	1027.8
	Top silk	$y = 17.79 - \frac{17.97}{1+\left(\frac{x}{1019.10}\right)^{49.14}}$	0	29.19	96.58	0.19	0.08	1027.8	984.0	1043.9
	Ear	$y = 26.56 - \frac{25.78}{1+\left(\frac{x}{1012.57}\right)^{18.11}}$	12.44	49.08	80.81	0.11	0.06	1060.0	938.8	1112.7
AN591	Bottom silk	$y = 27.45 - \frac{26.94}{1+\left(\frac{x}{997.76}\right)^{51.79}}$	0	69.16	100	0.36	0.13	1013.1	969.5	1027.8
	Middle silk	$y = 22.48 - \frac{22.14}{1+\left(\frac{x}{1004.21}\right)^{55.12}}$	0	60.79	100	0.33	0.10	1013.1	984.0	1043.9
	Top silk	$y = 15.92 - \frac{15.68}{1+\left(\frac{x}{1028.55}\right)^{53.14}}$	0	31.45	96.53	0.19	0.07	1027.8	998.0	1060.0
	Ear	$y = 22.85 - \frac{22.44}{1+\left(\frac{x}{1021.43}\right)^{15.23}}$	12.27	51.50	83.53	0.08	0.05	1077.0	938.8	1112.7

The model is established by fitting the data, and the parameters of V_m, V_a, T_t, T_r and T_s were obtained. And the maximum and average extension rate of bottom silk are the largest, and the bottom silk with the shortest thermal time at the maximum extension rate and in slow increase period. And the ear took the least thermal time to reach the rapid increase period (Tab. 1). This study was complete in a relatively optimal watering condition. However, the extension of silks may vary with water conditions. The fittings will have to be tested and adjusted under water limited conditions.

Conclusion

In this study, a logistic model was used to fit the dynamic characteristics of silk and ear extension. This study provided a base in simulating the dynamic characteristics of silk extension and ear extension. These finding will be used in functional-structural maize silk organ development model. Next step, we will study how sucrose metabolism and osmotic potential may drive silk dynamic extension under drought stress for modeling use.

References

Araus et al., 2012, *Frontiers in Plant Physiology* 3: 305, doi:10.3389/fphys.2012.00305

Avan et al,. 2008, *Plant, Cell and Environment* 31:1349-1360, doi:10.1111/j.1365-3040.2008.01839.x
Carvova et al., 2003, *Crop Science* 43(3):914-920, doi:10.2135/cropsci2003.9140
Kapu and Cosgrove, 2010, *Journal of Experimental Botany* 61(14):4097-4107, doi: 10.1093/jxb/erq225
Ma and Ma, 2017, *Science of the Total Environment* 586:1150-1161, doi: 10.1016/j.scitotenv.2017.02.106

A parameter-free system to measure morphological and physiological traits of Arabidopsis rosettes

Suxing Liu[1,2,3], Maria Ortega[1,2,4], Chung-Jui Tsai[1,2,4], Alexander Bucksch*[1,2,3]

[1] *Department of Plant Biology, University of Georgia, Athens, GA, United States*
[2] *Warnell School of Forestry and Natural Resources, University of Georgia, Athens, GA, United States*
[3] *Institute of Bioinformatics, University of Georgia, Athens, GA, United States*
[4] *Department of Genetics, University of Georgia, Athens, GA, United States*

For correspondence: bucksch@uga.edu

Keywords: Computer vision, Time series analysis, Plant development

Abstract

Introduction

Phenotyping is a labour-, time-, and cost-intensive bottleneck in plant functional genomics research (Reynolds, Baret et al. 2019). In particular, plant imaging was identified as the largest challenge to accelerate scientific discovery (Chen, Neumann et al. 2014). Currently, low-cost phenotyping systems are lacking even for the model plant *Arabidopsis thaliana* (Cabrera-Bosquet, Fournier et al. 2016). Because gene discovery and molecular/biochemical characterization are already labour-, time-, and cost-intensive, most investigators cannot afford commercial systems and associated data analytics staff in standard research grants. Commercial imaging systems with proven quality are available in some institutions as core facilities, but access is often restricted to large-scale projects. As a result, plant imaging remains inaccessible for most researchers. Here, we present a low-cost plant phenotyping system complete with open-source software to tackle the bottleneck in plant phenotyping using *Arabidopsis thaliana* as a test case.

Materials and Methods

We developed a complete set of hardware and software tools for time-course monitoring and analysis of the *Arabidopsis thaliana* rosette development, using a top-mount Raspberry Pi RGB camera. We developed a dominant color clustering method to segment the plant from the background and computed 15 traits from the images. Those traits include leaf area, leaf width, leaf curvature, number of leaves and a leaf temperature. A unique feature of our phenotyping system is the ability to estimate leaf temperature by comparing the colour differences between a temperature marker and the leaf surface colour.

Results and Discussion

Our plant phenotyping software is validated on a test panel of eight *Arabidopsis thaliana* genotypes differing in growth, with three replicates per genotype. Experimental results suggest that our software can characterize the development of *Arabidopsis* by tracking the 15 traits over time. The system accurately captured the genotypic differences in growth and rosette development. The leaf surface temperature trait proved to be a reliable proxy to characterize physiological properties of the different genotypes.

Conclusion

Our plant phenotyping software includes a suite of parameter-free algorithms that do not require prior user knowledge to derive the 15 traits from *Arabidopsis* rosette images. The software suite is available as an open source code and executable Singularity container on high-performance-computing systems (https://github.com/Computational-Plant-Science/SMART).

The cost of the presented phenotyping system, including a Raspberry Pi camera, is comparably low, at about $200. Our system is designed to fit standard growth chambers. Thus, our low-cost solution can be readily adopted by most molecular biology labs working with *Arabidopsis thaliana*. The system is currently used in Conviron growth chambers at the University of Georgia to characterize tolerance to heat and cold stress. In collaboration with molecular biologists, we hope to link phenotypes to the molecular mechanisms that underlie plant resilience to abiotic stresses.

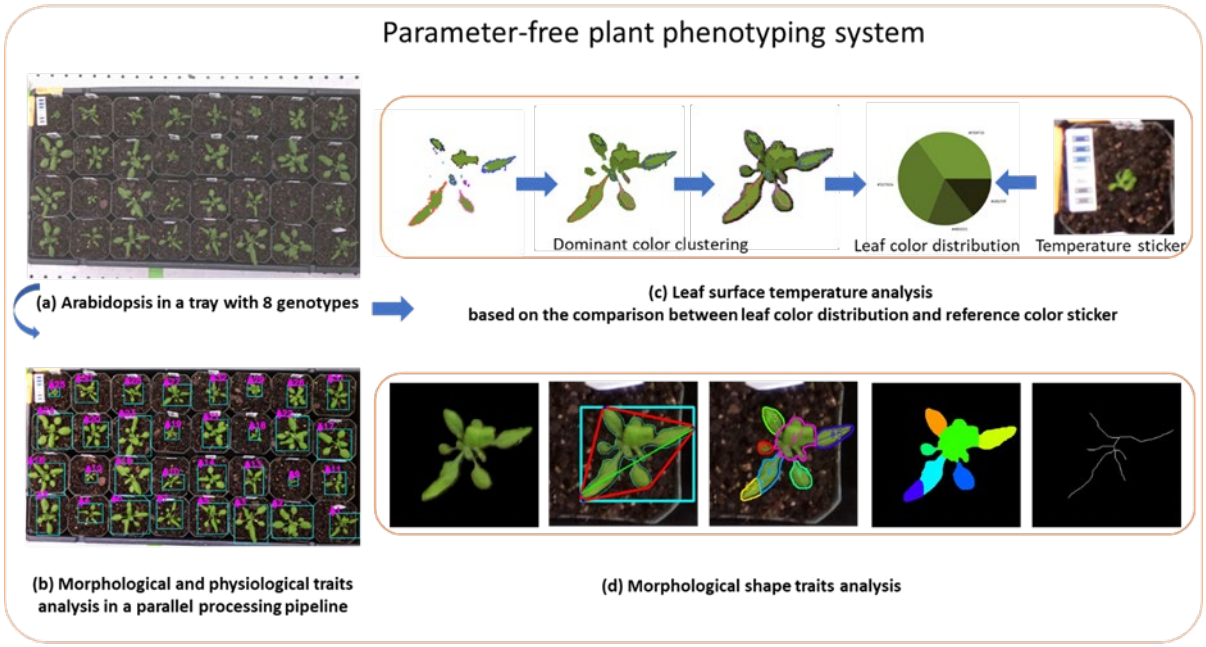

Figure 1: Schematic overview of our plant phenotyping system

Figure 1: Schematic overview of our plant phenotyping system. (a) We captured top-view images using a Raspberry Pi system for trays with eight randomized genotypes. (b) We analysed the morphological and physiological traits using a newly developed parallel processing pipeline. (c) For each individual plant, we computed leaf surface temperature on the basis of the dominant colour clustering. (d) In total, we computed 15 traits of the *Arabidopsis thaliana* rosettes.

References

Reynolds D, Baret F, Welcker C, Bostrom A, Ball J, Cellini F, Lorence A, Chawade A, Khafif M, Noshita K, Mueller-Linow M. What is cost-efficient phenotyping? Optimizing costs for different scenarios. Plant Science. 2019 May 1;282:14-22.

Chen D, Neumann K, Friedel S, Kilian B, Chen M, Altmann T, Klukas C. Dissecting the phenotypic components of crop plant growth and drought responses based on high-throughput image analysis. The Plant Cell. 2014 Dec 1;26(12):4636-55.

Cabrera-Bosquet L, Fournier C, Brichet N, Welcker C, Suard B, Tardieu F. High-throughput estimation of incident light, light interception and radiation-use efficiency of thousands of plants in a phenotyping platform. New Phytologist. 2016 Oct;212(1):269-81.

DIRT/3D: 3D phenotyping system for maize architecture in the field

Suxing Liu[1,2,3], Carlos Sherard Barrow[4], Molly Hanlon[5], Jonathan P. Lynch[5], Alexander Bucksch[*1,2,3]

[1] *Department of Plant Biology, University of Georgia, Athens, GA, United States*
[2] *Warnell School of Forestry and Natural Resources, University of Georgia, Athens, GA, United States*
[3] *Institute of Bioinformatics, University of Georgia, Athens, GA, United States*
[4] *Instrumentation Shop, University of Georgia, Athens, GA, United States*
[5] *Department of Plant Science, Penn State University, State College, PA, United States*

For correspondence: bucksch@uga.edu

Keywords: root phenotyping, automatic measurement

Abstract

Introduction
The development of crops with deeper roots holds substantial promise to improve water uptake and nitrogen capture, sequester carbon from the atmosphere, and increase soil organic fertility. A major bottleneck has been the difficulty of phenotyping root architecture in the field in a high-throughput manner. These challenges demand efforts across a range of disciplines, from mathematics over computer science to plant biology and applied fields like plant breeding and agronomy (Bucksch, Atta-Boateng et al. 2017, Bucksch, Das et al. 2017).

Materials and Methods
We developed an image-based 3D root phenotyping platform (DIRT/3D) which can measure 16 root crown architectural traits of mature maize plants in the field (Figure 1).
We designed a 3D root scanner to capture images for 3D reconstruction of the root. The 3D root scanner utilizes ten industrial cameras mounted on a rotating curved frame (Figure 1(b)) to capture images from all sides of the maize root. Scanning of one maize root completes in five minutes. After obtaining the image data, we reconstruct a 3D point cloud of the root system. By analyzing thin level sets of the 3D point cloud, DIRT/3D computed all 16 root traits behind multiple layers of occlusions. Representative traits include whorl distance, and the number, angle, and diameters of crown and brace roots.
DIRT/3D also tracks every individual root within the root system, starting from the stem down to the emerging lateral in the excavated root crown. Each individually tracked root enables the measurement of numbers, angles, and diameters at the individual root level and the computation of a root topologic structure.

Results and Discussion
DIRT/3D was validated on a test panel of 12 contrasting maize genotypes with 100 samples. These 12 genotypes include six inbred lines (B101, B112, DKIB014, LH123HT, Pa762, PHZ51) and six hybrid lines (DKPB80 x 3IIH6, H96 x 3IIH6, LH59 x PHG29, Pa762 x 3IIH6, PHG50 x PHG47, PHZ51 x LH59) and represent the extremes of dense vs. sparse, large vs. small, and maximum and minimum number of whorls selected from a full diversity panel.
We observed a coefficient of determination of r^2>0.84 for key root architecture traits. The 16 traits and a newly introduced 3D whole root descriptor were able to distinguish all genotypes uniquely with high broad sense heritability H^2_{mean}> 0.7. Further research will focus on the details of the photogrammetric calibration of the 3D root scanner, which will allow for thinner cross-section slices during level set extraction.

Conclusion

Unlike many root phenotyping methods developed under lab conditions, DIRT/3D measures maize roots grown under field conditions. DIRT/3D is a step towards automated quantification of highly occluded maize root systems in the field. It supports breeders and root biologists alike in their research to improve carbon sequestration and food security in the face of the adverse effects of climate change.

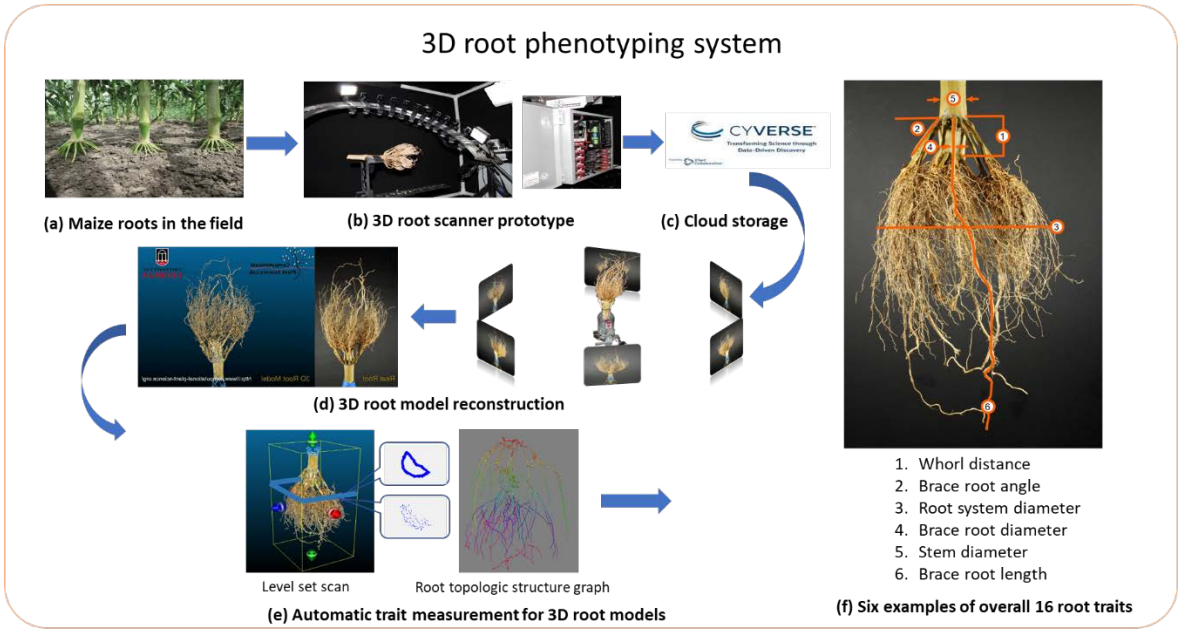

Figure 1: Schematic overview of our DIRT/3D system .

Figure 1: Schematic overview of our DIRT/3D system. The 3D root scanner (b) fits roots grown in the field (a) and excavated with the Shovelomics protocol. The scanner with ten synchronized industrial cameras mounted on a curved frame acquire about 2000 images of the root. The images are directly transferred and stored at Cyverse Data Store (c). The 3D reconstruction principle computed with DIRT/3D's structure-from-motion software (d) and the resulting 3D root model (e). Overall, the analysis software calculates 16 root traits from the 3D point cloud of the root system. The image in (f) shows examples for the trait classes angle, diameter, and length. All developed software methods are open source and executable as a Singularity container on high-performance-computing systems.

References

Bucksch A, Atta-Boateng A, Azihou AF, Battogtokh D, Baumgartner A, Binder BM, Braybrook SA, Chang C, Coneva V, DeWitt TJ, Fletcher AG. Morphological plant modeling: unleashing geometric and topological potential within the plant sciences. Frontiers in plant science. 2017 Jun 9;8:900.

Bucksch A, Das A, Schneider H, Merchant N, Weitz JS. Overcoming the law of the hidden in cyberinfrastructures. Trends in plant science. 2017 Feb 1;22(2):117-23.

Proteomics integrated with metabolomics reveals the systems reprograming in wheat inoculated with native bacteria and arbuscular mycorrhizal (AM) fungi

Radheshyam Yadav[1] & Ramakrishna Wusirika[1]
[1]Central University of Punjab, city campus Mansa road, Bathinda, India 151001

For correspondence: Radheshyam.yadav@cup.ac.in

Keywords: PGPB, wheat, nutrient reservoir proteins, grain metabolites

Plant Growth Promoting Bacteria (PGPB) and Arbuscular Mycorrhizal (AM) fungi are vital components of nearly all agroecosystems and a potentially sustainable alternative to optimize crop yield and productivity. Most of the PGPB-AM fungi-plant interaction studies provide useful insights but mostly at the physiological level without a comprehensive study of participating proteins and metabolites. Accordingly, the current study is aimed at elucidating the proteomic and metabolomic responses in durum wheat (*Triticum aestivum*) triggered by native-PGPB, CP4 (*Bacillus subtilis*) alone and in combination with AM fungi under field conditions.

Global proteome analysis of wheat grain reveals that a total of 66 proteins with at least 1.5-fold expression change ($p < 0.05$) that were differentially expressed in response to native PGPB alone and in combination with AM fungi (CP4 and/or AM fungi) compared to the control. Identified common differentially expressed proteins were distributed in different biological process, molecular functions and cellular component based on gene ontology. Proteins related to ion-transport, metabolic pathway, protein synthesis and defense responsive, were significantly enhanced in treated plants. Most of the commonly up-regulated proteins were involved in carbohydrate metabolism, nutrient reservoir activity, cellular homeostasis and embryonic development, which implied that both energy generation and the production of amino acids were enhanced thereby, ensuring an adequate supply of amino acids for the synthesis of new proteins in wheat seedlings to promote plant growth and productivity. Similarly, our metabolomics results showed that deferentially expressed metabolites ($p < 0.05$) between PGPB and AM fungi treated plants were mainly carbohydrates, nucleic acids, fatty acids, amino acids and N-compounds. Highest number of proteins and metabolites were identified in plants treated with CP4 in combination with AM fungi compared to the PGPB and AM fungi individually, indicating that combined inoculation of native PGPB and AM fungi modulates protein and metabolites in the wheat grains and root leading to enhanced plant growth, productivity and nutrient uptake in edible part of the grain.

Taken together, these results suggest that native PGPB, *B. subtilis* in combination with AM fungi may promote crop productivity, grain yield and nutrient uptake compared to the control under field. The ability of PGPB to modulate interconnected biochemical pathways could be exploited to increase crop productivity under field conditions.

Virtual pruning in cocoa: assessing the potential of a 3D cocoa model as communication tool for training purposes

Ambra Tosto[1,2], Faustina Obeng Adomaa [3], Urcil Kenfack Essougong [3,4], Pieter A. Zuidema [,2] Jochem B. Evers[1], Niels P.R. Anten[1]

[1] Wageningen University, Centre for Crop System Analysis, Wageningen, the Netherlands

[2] Wageningen University, Forest Ecology and Forest Management group, Wageningen, the Netherlands

[3] Wageningen University, Knowledge, Technology and Innovation group, Wageningen, the Netherlands

[4] Wageningen University, Plant Production Systems group, Wageningen, the Netherlands

For correspondence: ambra.tosto@wur.nl

Keywords: workshop, virtual plants, tropical perennial, Theobroma cacao, Ghana.

Introduction

Pruning, the manipulation of trees for production purposes, consists in a complex set of decisions that differ from tree to tree and with the experience of the person that is carrying out the activity (Ferree and Schupp, 2003). This hampers the formulation of precise sets of rules that can be easily communicated and used in training. Thus, it is essential that cocoa value chain actors understand the impact that pruning actions have on the tree functioning and the repercussions for the future development and production of the plant. In cocoa cultivation pruning is considered as a fundamental part of good agronomical practices but recommendations are rather general and not specific for farm conditions such as shaded and unshaded environment. Farmers' practices encompass varying degrees of adoption and adaptation emanating from a combination of knowledge on the general recommended practices and their situated knowledge on specific farm conditions. The outputs/outcomes of these are varied and largely uncertain.

Functional structural plant (FSP) models are spatially explicit simulations of plant growth and development at individual plant level resulting from the feedback between environmental factors/management practices, physiological processes and plant architecture (Evers et al. 2018). A FSP model of cocoa has been developed that allows for virtual pruning interventions, a wide range of planting designs and different shade conditions.

The visual 3D outputs of FSP models (fig.1) possess the potential to make them effective communication tools for non-academic purposes. Especially in the case of pruning where the outcomes of current practices are varied and largely uncertain and are suitable for visualisation. This potential however has not been so far explored.

We explore the potential of our cocoa FSP model output as a communication tool for training purpose engaging in a discussion with professionals with long experience in the field of cocoa. We aim to critically evaluate the model output, discuss current pruning recommendations and understand whether and how this tool could be further developed and used as a training tool.

Material and Methods

We will organize a one-day workshop in Accra, Ghana, with various professionals from the cocoa sectors, such as agronomist, extension officers and field officers. The participants will fill in a pre-workshop survey on current pruning recommendations, what factors are considered in providing these recommendations and the uniformity or lack thereof in such recommendations. During the workshop, the modelling approach will be explained and video outputs of various pruning practices scenarios, i.e. heavy and light pruning in shaded and unshaded systems, pruning impact at different planting density and pruning for the formation of single or double layered canopy will be presented. Participants will then break out into groups to discuss and evaluate the outputs adherence with their reality and potential to

serve as communication tools during training. Feedback will be collected from the participants through a short survey after the workshop.

Results

We expect feedback from participants on their perception of the model output's adherence to reality and inputs on what could make the tool more accessible, user friendly and effective for communication purpose regarding pruning. Most importantly, we will receive feedback from professionals working in the cocoa sector on the potential of using this FSP model as a communication tool in training of cocoa pruning.

Conclusion

We anticipate that the feedback from the participants will be used as base for a possible critical revision of cocoa model, as well as a good first step to exploring FSP modelling potential as an effective tool to communicate the impact of different pruning scenarios and outputs. This can be particularly relevant in a context like pruning in cocoa where the oxymoron of general recommendations in specific contexts results in varying adapted practices and largely uncertain outcomes.

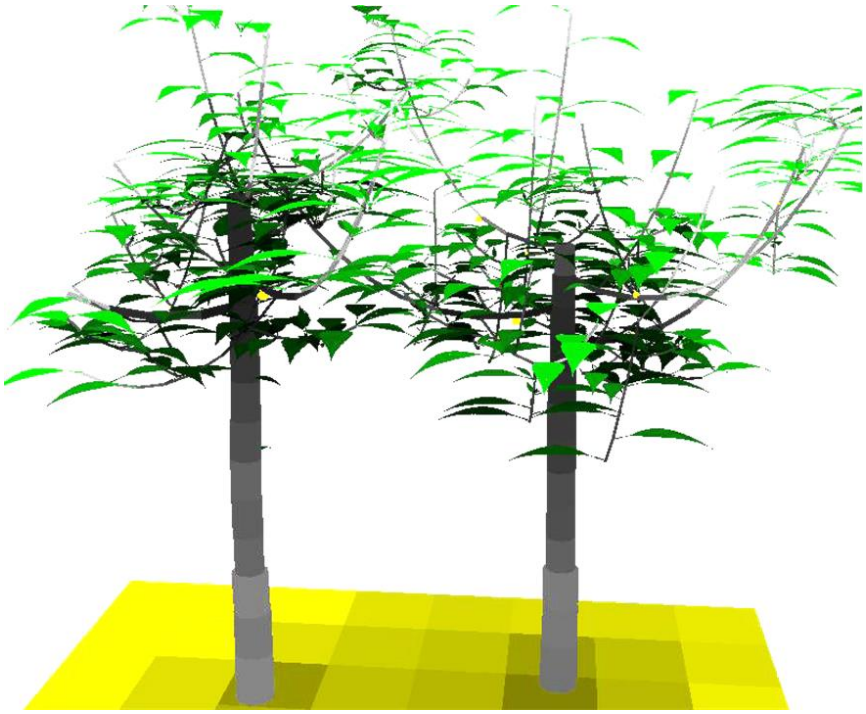

Fig. 1 Example of visual model output

References

Ferree & Schupp in: *Apples: Botany, Production and Uses*, 2003, D.C. Ferree and I.J. Warrington, 363–388 doi: 10.1079/9780851995922.0000

Evers et al., 2018, Ann. Bot. 121 767-772, doi: 10.1093/aob/mcy050

Exploratory analysis of bud fate frequency of Tonda di Giffoni cultivar (*Corylus avellana* L., 1753) in own-rooted and grafted plants.

Francesca Grisafi, Daniela Farinelli, Sergio Tombesi

For correspondence: francesca.grisafi1@unicatt.it

Keywords: Hazelnut, grafting, plant architecture, modeling, bud fate.

Introduction

One of the most expensive horticultural cares in Hazelnut (*Corylus avellana* L.) orchards, is sucker removal. To reduce crop management costs, it is possible to graft hazelnut scion on non-suckering rootstock (Tombesi, 1985; Botta and Valentini, 2018). This work aimed to compare own-rooted 'Tonda di Giffoni' plants with plants grafted on *C.colurna* L. to determine the effect of grafting on *C. colurna* L. on shoot architecture.

Materials and Methods

The study was performed in January 2020 in an experimental hazelnut (*Corylus avellana* L.) orchard planted in September 2014 and located near Perugia Italy. The evaluation was performed on 1-year-old shoots representative of four length categories: "Very long" shoots (more than 40cm), "Long" shoots (between 20cm and 40cm), "Medium" shoots (between 5cm and 20cm) and "Short" shoots (less than 5cm). Each node was analyzed considering the number of buds per node (1 for single buds, 2 for multiple buds (from 2 buds per node to 7 buds per node) and the bud fate: Catkin, Vegetative, Mixed, Blind (Costes and Guédon, 2002; Negrón *et al.*, 2013; Prats-Llinàs *et al.*, 2019).

Results and Discussion

Shoot mean length ranged from 9 to 11 nodes and it was higher in grafted shoots. Grafted trees had less mixed buds in Very Long and Long shoots, while there was no difference in shorter shoots. Production efficiency was higher in own-rooted trees (37%) than grafted ones (31%). The number of vegetative buds and catkins was the same among grafted and own-rooted plants in all length categories, while blind buds were significantly more in grafted plants. Overall, zones with a high frequency of single buds were alternated to zones with a high frequency of multiple buds, describing a single-multiple buds' pattern.

In Very long, Long and Medium shoots, the first zone had a high frequency of blind buds; the second zone had a high frequency of vegetative buds; the third zone had a high frequency of mixed buds. The fourth exists only for Long and Very Long and it was defined by vegetative buds, as well as the fifth zone, present only in the longest category, was described by vegetative and catkin buds.

Own-rooted plants followed the same pattern. In all the length category, the first zone was characterized by high frequencies of vegetative buds, while the second zone by mixed buds. The third zone was present only in Very Long and Long shoots and had a high density of vegetative buds. The fourth zone existed only in Long shoots with a high frequency of catkins.

Conclusion

This analysis suggests that in both, grafted and own-rooted plants, the same zone pattern is repeated for all the categories. Own-rooted trees had fewer blind zones and the mixed zone is composed of more nodes than in the grafted trees. This could suggest a higher yield efficiency in own-rooted plants.

References

Botta, R. and Valentini, N. (2018) 'Il nocciolo. Progettazione e coltivazione del corileto'.

Costes, E. and Guédon, Y. (2002) 'Modelling branching patterns on 1-year-old trunks of six apple cultivars', *Annals of Botany*. Oxford University Press, 89(5), pp. 513–524.

Negrón, C. *et al.* (2013) 'Systematic analysis of branching patterns of three almond cultivars

with different tree architectures', *Journal of the American Society for Horticultural Science*, 138(6), pp. 407–415.

Prats-Llinàs, M. T. *et al.* (2019) 'Long proleptic and sylleptic shoots in peach (Prunus persica L. Batsch) trees have similar, predetermined, maximum numbers of nodes and bud fate patterns', *Annals of botany*. NLM (Medline), 123(6), pp. 993–1004.

Tombesi, A. (1985) 'Il nocciolo: manuale pratico'.

Phenotypic spectrum: quantifying diversity of root architectures within genotypes on the example common bean (*Phaselous vulgaris L*)

Limeng Xie[1], James Burridge[2], Nicolas Klepp[3], John Miller[3], Jonathan P. Lynch[2], Alexander Bucksch*[1,4,5]

[1] *Department of Plant Biology, University of Georgia, Athens, USA*
[2] *Department of Plant Science, Penn State University, University Park, USA*
[3]*Department of Computer Science, University of Georgia, Athens, USA*
[4]*Warnell School of Forestry and Natural Resources, University of Georgia, Athens, USA*
[5] *Institute of Bioinformatics, University of Georgia, Athens, USA*

For correspondence: bucksch@uga.edu

Keywords: shape descriptor, clustering, within-genotype population

Root architecture, the temporal and spatial distribution of roots, is important for the uptake of water and nutrients. The divergent growth of roots at various classes, developmental patterns, and neighboring roots interactions can result in extensively diversified root architectures, even within the same genotype. Yet, such root architecture diversity within genotypes is largely ignored due to various reasons, of which a lack of computational tools is the most prominent. Here, we propose a shape descriptor, named *DS-curves* (the rate of root width changes by rooting depth), to summarize the architecture of a single root. Using DS curves as a core, we developed a new computing pipeline that combines Kmeans++ clustering, outlier filtering, and evaluation processes to classify root architectures into similar root architecture types. Subsequently, we apply this pipeline to analyze a large image dataset, which includes the roots of the three common bean *(Phaselous vulgaris)* genotypes DOR364 (n=874), SEQ7 (n=983) and L88_57 (n=2037) in well-watered and water-stress environments. The imaging data was collected at the Apache Root Biology Center (Willcox, Arizona) during the years 2015 and 2016 using the DIRT imaging protocol. Our first results suggest that each genotype exhibits five distinguishable root architecture types in each environment, and year. Moreover, DOR364, SEQ7, and L88_57 show consensus architecture types across years and environments, which might suggest that these architecture types might be heritable. We also observed that the ratio of root architecture types for each genotype varies among environments, which links a preference for specific architecture types to certain environments. Interestingly, the aboveground biomass does not differ significantly between root architecture types. We hypothesize that this biomass homogeneity arises from a strategy of the plant to optimize water and nutrient uptake on the population level. Based on our findings, we introduce the “Phenotypic Spectrum” as a new concept to describe the phenomenon that a single genotype can display several distinct root architecture types within or among environments. For future work, we will also investigate the effects of specific genetic or environmental causes on the variations within the phenotypic spectrum.

Book of Abstracts

References

Balduzzi, M. *et al.*, 2017, *Front. Plant Sci* 8:117, doi: 0.3389/fpls.2017.00117 Bucksch et al., 2014, *Plant Physiol.* 166: 470–486, doi: 10.1104/pp.114.243519 Das, A. *et al.* 2015, *Plant Methods.* 11: 1–12, doi: 10.1186/s13007-015-0093-3

Estimation of extinction coefficients and light interception in 3D Arabic coffee trees under water deficit

Miroslava Rakocevic[1], Ricardo Antônio Almeida Pazianotto[2], Fabio Takeshi Matsunaga[3], Eliemar Campostrini[1], Rafael Vasconcelos Ribeiro[4], Romain Barillot[5], Didier Combes[5]

[1] *Department of Plant Physiology, Northern Rio de Janeiro State University, Campos dos Goytacazes-RJ, Brazil*
[2] *Department of Statistics, Embrapa Meio Ambiente, Jaguariúna-SP, Brazil*
[3] *Department of Computation, Faculty of Industry - SENAI, Londrina-PR, Brazil*
[4] *Department of Plant Biology, IB/UNICAMP, Campinas-SP, Brazil*
[5] *INRAE, UR P3F, F-86600 Lusignan, France*

For correspondence: mima.rakocevic61@gmail.br

Keywords: *Coffea arabica*, LAI, PAI.

Introduction

Quantifying the fate of photosynthetic active radiation (PAR) passing through the tree canopy, is vital for understanding the physiological responses of plants to environment and environmental constrains, such as water deficit. Canopy extinction coefficient (*k*) is a key indicator of the interception efficiency of light penetrating through a canopy. The *k* is determined by the direction of incoming solar beams (Monsi and Saeki, 1953), defined as: $k(\theta_s, \varphi_s) = G(\theta_s, \varphi_s)/\cos(\theta_s)$, where θ_s and φ_s are zenith and azimuthal angles of beam direction, and $G(\theta_s, \varphi_s)$ is the mean projection of unit leaf area on the plane perpendicular to beam direction. Different models have been developed to compute the G-function by approximating foliage orientation probability distribution based on geometric objects (Campbell, 1990). *k* could also be roughly estimated by approximation to Beer-Lambert law ($k_e = -\ln(I_h / I_o) / (LAI\sqrt{a_p})$, where I_0 is PAR above the canopy, I_h is the PAR at the depth *h* of the plant canopy, LAI is the cumulative leaf area index to depth *h*, a_p is the coefficient of leaf light absorption.

As leaf and branch structures are modified with plant age (Niinemets, 2010), the quantitative description of the canopy geometric is complicated by its spatial and temporal variability, besides being changed by abiotic stresses. Aiming at estimation of light interception based on light penetration measurements or computing solar and scattering directions defined for coffee trees, 3D mock-ups of Arabic coffee were used, considering five phenological stages during the first two years of production under two water regimes.

Materials and Methods

Arabica coffee trees (accession 'E083') were followed in five phenological stages relative to berry production, during the first two years of production under the drip irrigation (IRR) and rainfed (NI) conditions. Virtual 3D coffee trees were obtained by plant coding and reconstructions (see Rakocevic et al. at this book of abstracts). The 'vgx' files provided from 3D reconstructions were posteriorly explored in 'R' to calculate the distribution of leaf inclinations, LAI for five phenological stages and ANOVA for age and water effects on k_{scatt}.

We used the procedure of Unigarro et al. (2016) to estimate parameter x (Campbell, 1990) from 3D coffee mock-ups, assuming the angular distribution of leaf area in a canopy on the surface is like a prolate or oblate spheroid. By assuming that all elements of the canopy were randomly distributed, *k* in G-function for coffee trees was estimated for direct beams ($k_{dir} = (x + \tan^2\theta_s)^{1/2}/(x + 1.774\,(x + 1.182)^{-0.733})$) and for scattering light ($k_{scatt} = k_{dir}\,(1-\delta)^{0.5}$), where δ is the light scattering coefficient, which is assumed to be 0.2. The continuous measurements of irradiance were performed by sensors positioned above the canopy and at the ground level. The average value of irradiance for each phenological stage and reconstructed tree was

expressed in MJ day^{-1}. The light interception was estimated at daily scale idealizing the light distribution over the plant canopy to Beer-Lambert law, permitting the calculation of k_e and probability of light interception. The a_p was assumed 0.85.

Results and Discussion

The k_{dir} varied from 0.54 to 0.72, k_{scatt} from 0.49 to 0.64, and k_e from 0.52 to 0.98. The variation in k_{scatt} over five stages in the first two years of production revealed it was more impacted by plant age than by water stress (Table 1). The highest k_{scatt} values were found at the stage of expansion of leaf area and fruits in both production years, decreasing with plant age and fruit maturation. During the expansion of leaf area and fruits, k_{scatt} was higher in NI than in IRR plants in the wet period of 2012-2013, which was probably more related to intensive leaf area expansion than to water deficit. The light interception probability based on k_{dir} and k_{scatt} was related to LAI, where lower LAI corresponded to NI plants and higher to IRR ones (Figure 1A). The comparison of light interception probability based on LAI estimated from 3D mock-ups including k_{scatt} or k_e calculated from collected irradiance data showed accurate fits (Figure 1B). Generally, lower light interception values were observed in NI than in IRR plants (Figure 1B), due to lower LAI (Figure 1A) and more erected leaves (see Rakocevic et al. at this book).

Table 1. Means ± s.e. of k_{scatt} in five stages during the first two Arabic coffee production years: expansion of leaf area and fruits, summer 2011-2012, FE-11-12; fruit ripening 2012, FM-12; fruit harvesting 2012, FH-12; expansion of leaf area and fruits, summer 2012-2013, FE-12-13; fruit harvesting 2013, FH-13. The plants were irrigated (IRR) or cultivated under rainfed condition (NI).

Stage	FE-11-12	FM-12	FH-12	FE-12-13	FH-13
IRR	0.624 ± 0.004 aA	0.519 ± 0.004 cA	0.514 ± 0.004 cdA	0.571± 0.007 bB	0.498 ± 0.002 dA
NI	0.631 ± 0.003 aA	0.521 ± 0.004 bA	0.521 ± 0.002 bA	0.638 ± 0.003 aA	0.495 ± 0.005 cA

The lower-case letters indicate differences between phenophases, while the upper-case indicate differences between two water regimes.

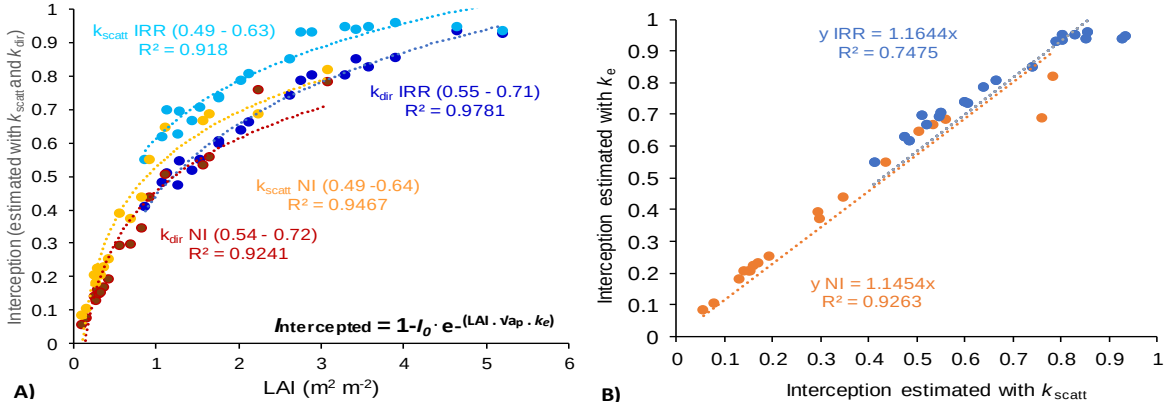

Figure 1: **A)** Light interception probability of coffee plants calculated using k_{dir}, k_{scatt} and LAI estimated from 3D mock-ups. **B)** Comparison of light interception probability using k_{scatt} from G-function and k_e calculated from collected irradiance data, for irrigated (IRR, light and dark blue) or not-irrigated (NI, red and orange) plants.

Conclusion

The effect of ontogenic development of the structure on the k_{scatt} was higher than the effect the water stress. k_{scatt} was higher in NI than in IRR plants only during the expansion of leaf area and fruits, in the wet period of 2012-2013, probably more related to intensive leaf area expansion than to water deficit. Generally lower light interception was observed in NI than in IRR plants, due to lower LAI formed under water deficit.

References

Campbell, 1990, *Agr. Forest Meteorol*. 49 (3): 173–176, https://doi.org/10.1016/0168-1923(90)90030-A
Monsi and Saeki, 1953, *Jpn. J. Bot*. 14: 22–52.
Niinemets, 2010, *Ecol. Res.* 25(4): 693–714, doi 10.1007/s11284-010-0712-4
Unigarro et al., 2016, *Acta Agron*. 65(4): 383-389, http://dx.doi.org/10.15446/acag.v65n4.51899

Structural acclimations of 3D coffee plants to water deficit

Miroslava Rakocevic[1], Ricardo Antônio Almeida Pazianotto[2], Fabio Takeshi Matsunaga[3], Eliemar Campostrini[1], Rafael Vasconcelos Ribeiro[4]

[1] *Department of Plant Physiology, Northern Rio de Janeiro State University, Campos dos Goytacazes-RJ, Brazil*
[2] *Department of Statistics, Embrapa Meio Ambiente, Jaguariúna-SP, Brazil*
[3] *Department of Computation, Faculty of Industry - SENAI, Londrina-PR, Brazil*
[4] *Department of Plant Biology, IB/UNICAMP, Campinas-SP, Brazil*

For correspondence: mima.rakocevic61@gmail.br

Keywords: *Coffea arabica*, inclination angle, LAI, PAI.

Introduction

Water deficit is a limiting factor affecting various aspects of coffee morphology and production (Costa et al., 2019). The leaf area index (LAI) reduction is considered a defence against drought and its reduction is a consequence of decreases in individual leaf size and leaf number, followed by more intensive leaf senescence and leaf abscission (Costa et al., 2019; Rakocevic and Matsunaga, 2018). In a long term, coffee plants exposed to multiple drought cycles can develop a differential acclimation that promotes defence mechanisms, allowing them to be kept in an 'alert state' to successfully cope with further drought events (Menezes-Silva et al., 2017).

Our hypothesis was that multiple drought cycles can modify the coffee tree architecture, as an adaptative response to decrease drought impacts with plant aging. It was aimed to estimate leaf inclination (α), individual leaf area (ILA), LAI and plant area index (PAI) of an Ethiopian accession of Arabic coffee ('E083'), considering some phenological stages during the first two years of production, using 3D models of plants.

Materials and Methods

Coffee plants were grown in the field conditions of Londrina-PR (Brazil), under two water regimes: drip irrigation system (IRR) and rainfed conditions (NI, multiple drought cycles). Plants were evaluated in five phenological stages relative to berry production: **1**) expansion of leaf area and green fruits during long days, end of December 2011 - beginning of January 2012 (FE-11-12); **2**) fruit ripening of first production, at the beginning of short days April/May 2012 (FM-12); **3**) harvesting of the first production in July/August 2012 during short days (FH-12); **4**) expansion of leaf area and green fruits during long days, December 2012 beginning of January 2013, (FE-12-13); and **5**) harvesting of the second production, June/July 2013 (FH-13). The virtual plant coding and 3D reconstructions were performed with platform OpenAlea (Pradal et al., 2008) and software Cafe3D (Matsunaga et al., 2016). Posteriorly, the α, ILA, LAI and PAI were calculated using statistical functions from 'R' programming language, from the resulted 3D reconstructions exported files, called 'vgx' files. Over the coffee trees, many leaves were angulated at α <0°. The α values were transformed into absolute values (0-90°), in order to calculate the average lamina inclination.

Results and Discussion

Coffee plants cultivated under two water regimes showed one general tendency of plagiophile inclination, with the average α varying from 40 to 55° (Figure 1A). The leaves of plants that were exposed to different periods of drought (NI) presented higher α per plant than the IRR ones, except for the FM-12 stage. We observed that many leaves inside the canopy of IRR plants were partially or completely shaded, inducing more plagiophile inclinations. In NI treatment plants had more erectophile leaves than in IRR, which can be considered as one structural acclimation to water deficit, reducing radiation loading and water lost.

The ILA increased from FE-11-12 to FH-13 stages (Figure 1A). In IRR plants, the mean ILA increased from 18.9 to 29.5 cm^2, while it varied from 15.2 to 27.7 cm^2 in NI treatment. In the first year of production, from FE-11-12 until fruit collection in 2012, the differentiation of ILA was

significant between IRR and NI plants, however, in the beginning of the second productive year, in the FE-2012-13 stage, the mean leaf size was similar between water treatments and again differed in FH-13, when the leaves of plants under IRR were bigger than that those under NI. The increase in average ILA could be related to the increase in the number of leaves of higher branching orders (3rd and 4th), which were shaded, reaching significantly higher size than 2nd order leaves exposed to full light (analyses not shown, see illustration of mock-ups - Figure 1C).Non-irrigated plants formed a much lower LAI and PAI than IRR ones (Figure 1B). The temporal variation of LAI and PAI revealed that irrigated plants were favored when compared to NI ones. The LAI of NI plants did not grow significantly during the first year of production, but significantly increased reaching the FE-2012-13 stage. The variability in responses increased with plant age, inducing lower P-values relative to ILA (Figure 1A), PAI and LAI (Figure 1B).

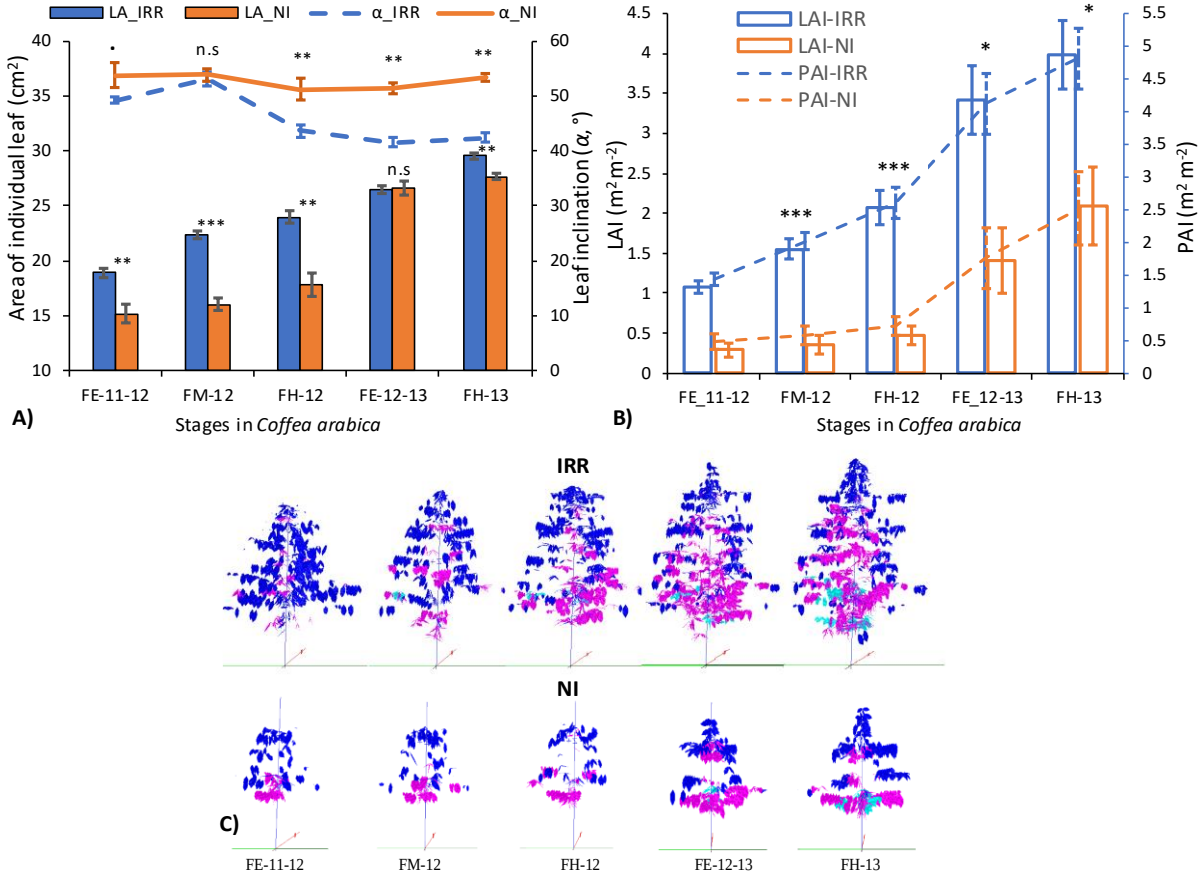

Figure 1. Structural characteristics in *Coffea arabica* plants grown under irrigation (IRR) and rainfed (NI) conditions. **A)** Average individual leaf area (cm^2) and leaf inclination (α, °), **B)** LAI and PAI ($m^2\ m^{-2}$), **C)** Mock-ups of plants differing orders of branching (dark-blue: 2nd order, pink: 3rd order, light-blue: 4th order) in five phenological stages during the first two years of production.

Conclusion

The greater leaf angle in NI than in IRR plants can be considered as one structural acclimation to water deficit. In long term, the ILA, LAI and PAI were reduced under water deficit, but water deficit impacts decreased with age of coffee trees, as the adaptative responses developed after multiple drought cycles.

References

Costa et al., 2019, *Acta Sci. Agron*., 41:e42703, doi: 10.4025/actasciagron.v41i1.42703
Matsunaga et al., 2016, *SpringerPlus*, 5: 2075, https://doi.org/10.1186/s40064-016-3762-4
Menezes-Silva et al., 2017, *J. Exp. Bot.*, 68(15):4309–4322, doi: 10.1093/jxb/erx211
Pradal et al., 2008, *Graph Models.*, 71:1-21, doi: 10.1016/j.gmod.2008.10.001
Rakocevic and Matsunaga, 2018, *Ann Bot*. 122:117–131, doi: 10.1093/aob/mcy042

Understanding the impact of the aerial architecture on the performance of wheat cultivar mixtures

Emmanuelle Blanc[1], Jérôme Enjalbert[1], Christian Fournier[2], Christophe Pradal[3,4], Christophe Lecarpentier[1], Pierre Barbillon[5]

[1] *Université Paris-Saclay, INRAE, CNRS, AgroParisTech, GQE - Le Moulon, 91190, Gif-sur-Yvette, France*
[2] *LEPSE, Univ Montpellier, INRAE, Institut Agro, UMR LEPSE, Montpellier, France*
[3] *CIRAD, UMR AGAP & inria, Zenith, Montpellier, France*
[4] *AGAP, Univ Montpellier, CIRAD, INRAE, Institut Agro, Montpellier, France*
[5] *Université Paris-Saclay, AgroParisTech, INRAE, UMR MIA-Paris, 75005, Paris, France*

For correspondence: emmanuelle.blanc@inrae.fr

Keywords: plant-plant interactions, competition for light, tillering, plasticity, agroecology

Introduction

Increasing the within-field diversity through varietal mixtures is a key leverage for agroecology, as it could buffer environmental stochasticity, and improve the resilience of low-input cropping systems (Reiss and Drinkwater, 2017). However, many questions are raised by the complex interactions occurring in such variety mixtures, ranging from synergy to competition. Wheat mixtures are a good model to study plant-to-plant interactions, as wheat is a strategic crop worldwide. Moreover, the use of wheat mixtures by French farmers has increased sharply in recent years, leading to a growing need for practical rules on how to design and manage such populations. Nevertheless, few studies have focused on reasoning the genetic composition of these mixtures in order to optimize complementarity and competition between genotypes. In particular, how differences in traits of the aerial architecture can improve light interception and yield has been poorly studied, while mixing varieties with contrasted architectures has even been discouraged (Borg et al., 2018) to avoid competition but discarding any potential beneficial role of such functional diversity.
As individual-based models, functional structural plant models (FSPM) are particularly adapted to study the interactions taking place in these heterogeneous populations, and they offer an alternative to the complexity of experimental studies, due to high number of combinations of wheat cultivars that can be evaluated. Here, we used the WALTer FSPM to simulate varietal associations and try to better understand how differences between cultivars in key traits of the aerial architecture influence mixture performance.

Materials and Methods

WALTer (Lecarpentier et al., 2019) is an FSPM, implemented in OpenAlea, that simulates the development of wheat fields from sowing to maturity with a daily time step. The development of vegetative organs follows descriptive rules adapted from the ADEL-wheat model (Evers et al., 2007). The model simulates the plasticity of tillering in response to competition for light based on three simple rules: (i) tillers are emitted following a thermal time schedule and a fixed probability of emergence, (ii) the emission of tillers stops due to an early neighbour perception and (iii) tillers that don't intercept enough light due to shading regress.
Using WALTer, we simulated binary mixtures (50% of each variety) differing in height (H), leaf surface (L), leaf insertion angle (A) and tillering capability (T). For each of these traits, the mean value of the trait in the mixture and the difference of the trait between the 2 varieties in mixture varied. Using a sensitivity analysis approach, we identified the traits that

had the most impact on the mean number of ears produced per plant (Num_{ears}) and on the fraction of intercepted photosynthetically active radiation (fiPAR).

Results and Discussion

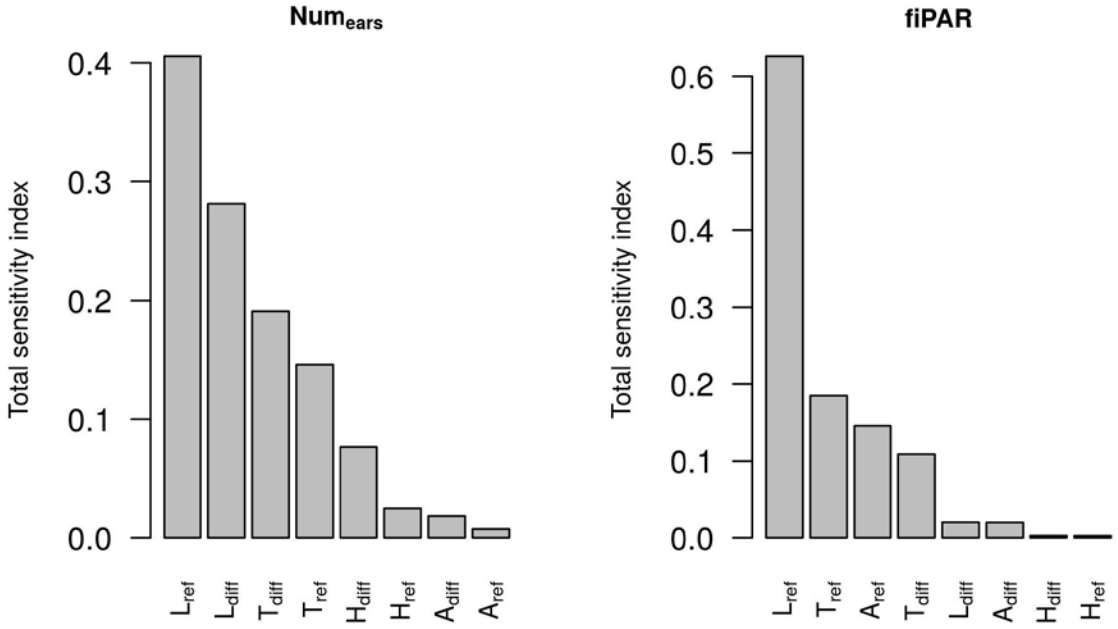

Figure 1: Total sensitivity indices for Num_{ears} (left) and fiPAR (right). Ref denotes the mean value of the trait in the mixture and diff denotes the difference of the trait between the 2 varieties.

The leaf dimensions and the tillering capability had an important influence on the mean numbers of ears produced per plant (Num_{ears}) and on the fiPAR in the simulated fields. For the tillering capability, both the mean value of the trait and the difference between the two varieties had an important impact on Num_{ears} and fiPAR. The mean dimensions of the leaves in mixture (L_{ref}) explained the major part of the variance of both outputs, but the difference of leaf dimensions between varieties (L_{diff}) only had a limited impact on fiPAR, while it had a great influence on Num_{ears}. The mean leaf insertion angle in the mixture (A_{ref}) was the least important factor explaining the variance of Num_{ears}, but it accounted for almost 15% of the fiPAR total variance.

Conclusion

Using the WALTer FSPM, we were able to isolate the effect of some key architectural traits on indicators of mixture performance. Our results highlight the importance of the leaf dimensions and tillering capability in the development of wheat cultivar associations. Interestingly, if mean trait values of mixtures drive their light interception performance, the number of ears produced is much more depending on trait variances, due to the shade response of tillering dynamics. This study thus improves our understanding of the interactions taking place in variety mixtures and represents a step towards the identification of practical rules for the design of mixtures.

References

Borg et al., 2018, Field Crops Research 221, 298-313, doi: 10.1016/j.fcr.2017.09.006
Evers et al., 2007, Ecological Modelling, 200(3–4), 308–320, doi: 10.1016/j.ecolmodel.2006.07.042
Lecarpentier et al., 2019, Annals of botany, 123(6), 961-975, doi: 10.1093/aob/mcy226
Reiss and Drinkwater, 2017, Ecological applications, 28(1), 62-77, doi: 10.1002/eap.1629

Impact of intraspecific trait variance on interspecific competition: a theoretical case study using the Virtual Grassland model

Béatrice Wolff [1], Bernadette Julier [1], Gaëtan Louarn[1]

[1] *INRAE, UR 004 P3F, route de Saintes, F86600 Lusignan, France*

For correspondence: gaetan.louarn@inra.fr

Keywords: grasslands, intraspecific variability, individual-based model, competition, stability

Increasing intra-specific genetic variability has been identified as a potential factor stabilizing yield and botanic composition in grasslands. However, little is known about the mechanisms by which such diversity might promote stability. Virtual Grassland (Louarn and Faverjon, 2018) is an individual-based model available on the Openalea platform that simulates plant-plant competition for resources (light, water, nutrients). This model has already been assessed for contrasting legume-based binary mixtures. However, the parameters of each species were considered as for an « average plant » and did not reflected the intraspecific diversity actually present in grassland species populations (Louarn et al., 2020). The present study proposes to test the impact of incorporating trait variance through a Gaussian distribution of parameter values, and to test its effects for a major parameter involved in light competition (i.e. internode length). The range of trait variability was calibrated for two species from nursery experiments on isolated plants of alfalfa and red clover. A series of virtual binary competition experiments was then simulated following a de Wit replacement design to analyse the potential impact of average trait value differences, trait variance and species proportion on the outcome of competition in terms of yield and deviation of species proportion. The results showed that the impact of a greater trait variance on mixture stability depended on the range of variability tested with respect to average trait difference between the species, and thus from the degree of overlap between trait values from the two species. This more precise characterization of interaction traits in grassland species should facilitate the identification of selection criteria for the creation of new varieties adapted to mixture conditions.

References

Louarn, G., & Faverjon, L. (2018). Annals of Botany, 121(5), 875-896., doi: 10.1093/aob/mcx154

Louarn, G., Barillot, R., Combes, D., & Escobar-Gutiérrez, A. (2020). Annals of Botany., doi: 10.1093/aob/mcaa014

WHEAMM: a functional-structural model to study plant growth and interactions with neighbors in wheat variety mixtures

Meije Gawinowski[1,2], Jérôme Enjalbert[1], Paul-Henry Cournède[2*], Timothée Flutre[1*]

[1] Université Paris-Saclay, INRAE, CNRS, AgroParisTech, *GQE - Le Moulon, 91190, Gif-sur-Yvette, France*
[2] Université Paris-Saclay, *CentraleSupélec, Lab MICS, 91190, Gif-sur-Yvette, France*
[*] Contributed equally

For correspondence: meije.gawinowski@inrae.fr

Keywords: tillering, light interception, competition, performance

Introduction

In the context of the agroecological transition, crop diversification at different levels is seen as a means to decrease chemical inputs and increase yield stability. For wheat, variety mixtures are identified as a promising lever (Borg et al. 2018). Even though this cultivation technique has an important potential, the lack of practical rules for the assembly of varieties is detrimental to its development. Plant models combined with field experiments can be very useful to explore by simulation the processes underlying complementarity and competition. Many plant models already simulate wheat growth effectively but few of them take plant interactions into account. We will present WHEAMM (Wheat Model for Mixtures) designed to account for competition for light and its impact on tillering as the main interaction factor in order to evaluate mixture performance in terms of yield.

Modeling Concept

Tillering dynamics are decomposed in three stages (emission, plateau and regression of tillers), but most wheat models do not model the regression of tillers or only with stochastic processes. One exception is WALTer (Lecarpentier et al., 2019) that was created to understand the key mechanisms affecting light interception efficiency in wheat variety mixtures and simulate accurately tillering dynamics (Figure 1). However, it does model neither biomass production nor allocation between organs. We hence conceive WHEAMM to represent tillering dynamics similarly to WALTer, but with a methodology adapted to source-sink models.

WHEAMM is based on the GREENLAB functional-structural model, combining organogenesis, biomass production and allocation. A GREENLAB model was designed for wheat (Kang et al., 2008) but it was created for homogeneous populations without interaction between plants. A method of surface projection was however conceived to model plant competition for light for other GREENLAB models (Cournède et al., 2008). WHEAMM will hence be a combination of the GREENLAB wheat model with this projection method to simulate competition for light. Moreover, compared to the earlier version of GREENLAB-wheat, regression will be modeled using biomass allocation rules to prioritize tillers by age (Larue et al., 2019). Tillering dynamics simulated with this method will be compared with WALTer tillering dynamics.

Experiments for data collection and parameter estimation

In order to estimate WHEAMM parameters, a field experiment is currently conducted in the frame of the PerfoMix project. At Le Moulon (Gif-sur-Yvette, France), two different mixtures

of four varieties differing for height and earliness were sown on October 30, 2019, at density 160 plants/m² with two replicates for each mixture, and another replicate at density 250 plants/m². Corresponding pure stands were also sown at density 160 plants/m². Measures of height, number of tillers and biomass (several destructive measures on plants in pure stands and a few on plants in mixed stands) were made at regular time steps. At harvest the same records were made on all the remaining plants, as well as measures of yield components (ears per plant, kernels per ear, thousand kernel weight). The first year of the experiment will be presented, along with preliminary parameter estimates for tillering dynamics and trophic competition obtained in the Bayesian paradigm using a hybrid Metropolis-Hastings-Gibbs algorithm dedicated to non-linear hierarchical models. Once the model is parameterized, we expect simulations of contrasted mixtures of varieties to allow us to identify the least and most productive ones, hence suggesting which ones to experiment in the field before designing assembly rules.

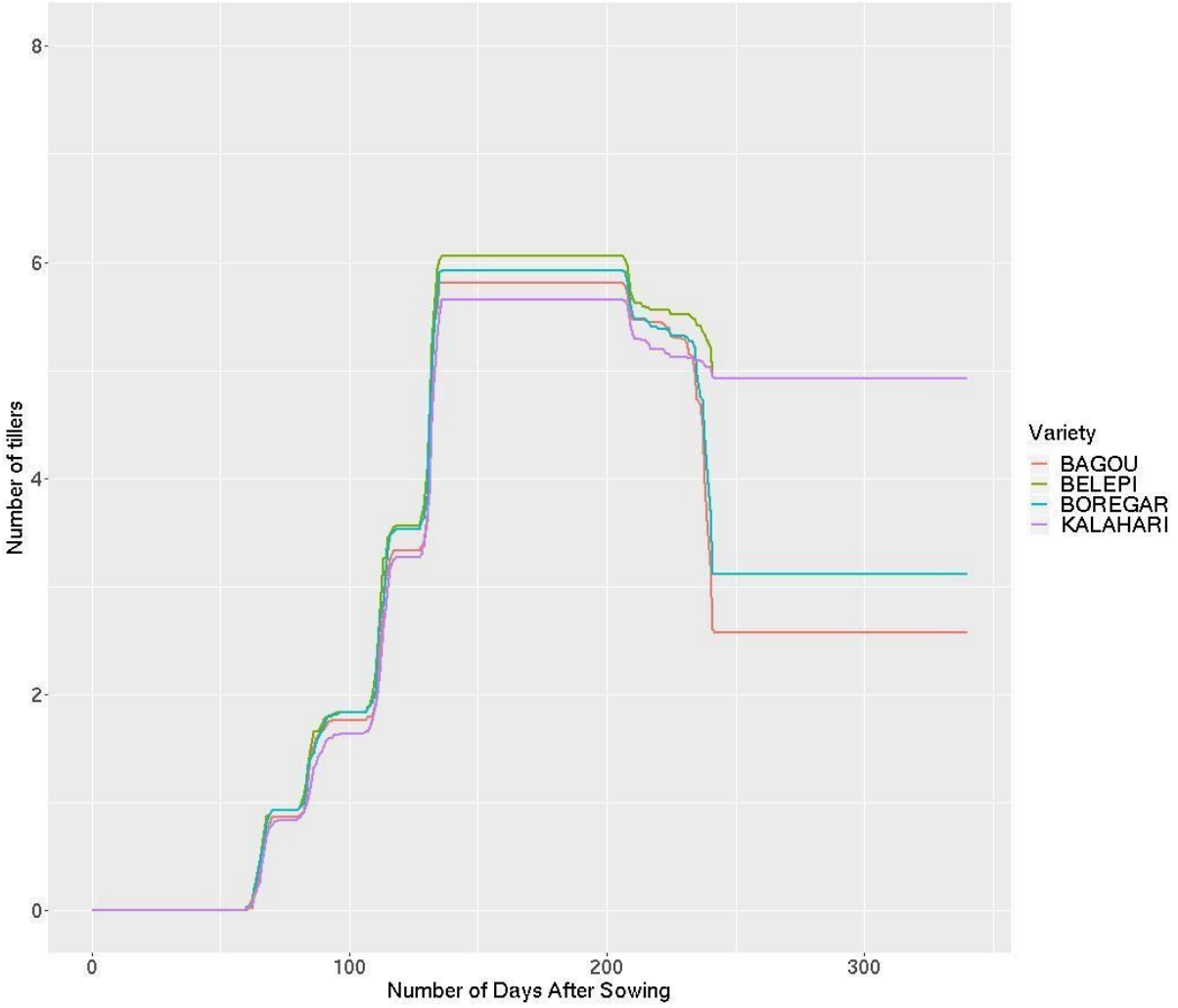

Figure 1: Tillering dynamics in a four-way mixture as simulated by WALTer. Simulations were made on a plot of 264 plants and the number of tillers was averaged over all plants per genotype at each time step. Simulations were made for a climatic sequence averaged over 10 years in different locations in France.

References

Borg et al., 2018. *Field Crops Research*, 121, doi: 10.1016/j.fcr.2017.09.006
Cournède et al., 2008. *Annals of botany*, 101:8, doi: 10.1093/aob/mcm272
Kang et al., 2008. *Annals of Botany*, 101, doi: 10.1007/1-4020-6034-3_6
Larue et al., 2019. Annals of Botany , 124:4, doi: 10.1093/aob/mcz038 Lecarpentier el al., 2019. Annals of botany , 123:6, doi: 10.1093/aob/mcy226

Modelling shade cast by rows of trees using 3D models based on terrestrial laser scanning data

Rafael Bohn Reckziegel[1], Jonathan P Sheppard[1], Christopher Morhart[1], Ben du Toit[2], Hans-Peter Kahle[1]

[1] *Chair of Forest Growth, University of Freiburg, Freiburg im Breisgau, Germany*
[2] *Department of Forest and Wood Science, Stellenbosch University, Stellenbosch, South Africa*

For correspondence: rafael.bohn.reckziegel@iww.uni-freiburg.de

Keywords: shadow model, LiDAR, agroforestry, windbreak, *Alnus cordata*

Introduction

The establishment and utilization of trees within an agricultural setting has both traditional roots and modern-cutting-edge applications for increased benefits in terms of productivity and other ecosystem services. In order to understand the functioning and interplay between trees and crops within agroforestry systems (AFS), it is important to investigate the interactions of the AFS components with regard to the utilization of water, nutrients and light. The availability of incoming solar radiation, while considering its temporal and spatial distribution is largely dependent on the spatial and functional structures that are present in the field. This issue is of high significance in AFS, and understanding such interactions is essential to improve, effectively plan and manage these integrated land-use systems. Targeting an enhanced simulation of the shade cast by trees within AFS, we apply a tested approach that utilises a 3D model capable of quantifying tree shading at a high temporal and spatial resolution. This procedure allows for the modelling of the shade dynamics in the vicinity of single trees as well as groups of trees, such as in windbreaks.

Here, the use of this technique on windbreaks consisting of multiple aligned alder trees (*Alnus cordata*) is presented in a southern African context. The application of an approach modelling the shade cast by windbreaks, distinguishes the current work from others.

Materials and Methods

The study site utilised alder trees planted in rows as windbreaks, surrounding various berry species (*Rubus* spp.) within a fruit farm near Stellenbosch, South Africa (33°54.4'S 18°56.7°E; 404 m a.s.l.). The study site experiences a Mediterranean climate (rainy winters and dry summers) with mean maximum and minimum annual air temperatures of 22.3 and 12.5 ˚C respectively. The study site boasts a mean annual precipitation sum of approximately 934 mm, with an average of 80 rain days (≥1 mm) per year. With respect to crop production, water limitation is an issue in summers.

The windbreaks were scanned with the RIEGL VZ 2000i, a terrestrial laser scanner (TLS) in September 2019, under leaf-off conditions to reduce occlusion of the tree crown and to increase the accuracy of scanning. At the time of scanning, the target trees had heights ranging between 4 and 16 m, a diameter at breast height of between 7 to 26 cm and were 15 to 20 years old. Trees were located in rows with a spacing of approximately one metre between trees.

Point clouds derived from TLS were postprocessed, filtered, and downsampled. Single-tree point clouds were manually segmented and cylinder models were computed using *TreeQSM* (Raumonen et al. 2013). Number of cylinders was reduced to a maximum of 3000 cylinders per tree model, as a means of reducing required computational effort in the shadow simulations. Finally, cylinder models of single trees were combined with neighbouring trees, representing actual spatial arrangement in the field.

An enhanced version of the algorithm developed by Rosskopf et al. (2017), implemented in the free software environment R (version 3.5.3), was used to calculate the shade cast using the derived cylinder models. Solar irradiance data for September 2019 (Stellenbosch University, 2020) was utilised to quantify the resultant deficit of solar radiation energy on the ground due to the shading effect of the trees.

Results and Discussion

The chosen approach allows the utilisation of 3D point cloud data of groups of windbreak trees to compute shade cast projections at a high level of temporal and spatial resolution in southern African landscapes. The derived model provides tree shade cast projections of multiple trees in 10 minutes time intervals for a raster grid with a cell size of 10 cm x 10 cm. Leaves were not incorporated in the modelling at this stage due to their inherent complexity and increase in processing time; this represents a future goal in the modelling of shade for multiple trees.

Based on our approach, the monthly shade cast by four sample windbreaks was modelled for the entire month of September 2019. The shade cast by one windbreak section consisting of five alder trees, for a 10 minutes interval, is shown in Figure 1.

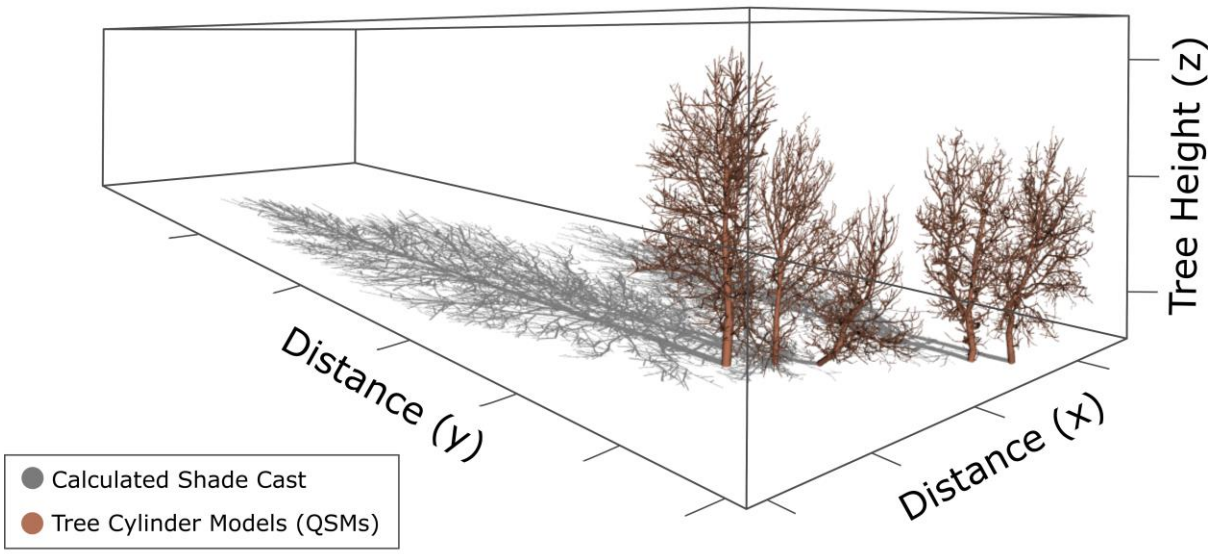

Figure 1: Computed shade cast for a ten minutes interval of a windbreak section consisting of five alder trees near Stellenbosch, South Africa (33°54.4'S 18°56.7°E; 404 m a.s.l.).

Conclusion

The use of 3D point cloud data coupled with actual solar irradiance data provides the possibility to accurately and effectively model the shade cast by groups of trees. This approach allows land managers to effectively plan their operations by either managing windbreak dimensions to minimise shading effects or to plant shade tolerant species in highly shaded areas of the field.

References

Rosskopf et al. 2017, *Remote Sensing*, *9, 719,* doi: 10.3390/rs9070719
Raumonen et al. 2013, *Remote Sensing*, 5, 491-520, doi:10.3390/rs5020491
Stellenbosch University, 2020. Stellenbosch Weather – Sonbesie station [Online] http://weather.sun.ac.za/ [accessed 1 April 2020]

Efficient stochastic Functional Structural sympodial Shrubs Modelling based on structural hierarchy. Application to Guayule

Marc Jaeger [1,2], Sylvie Sabatier [1,2], Philippe de Reffye [1,2], Ali Abed Alsater [1,2], Loic Brancheriau [3]

[1]AMAP, Univ Montpellier, CIRAD, CNRS, INRA, IRD, Montpellier, France
[2]CIRAD, UMR AMAP, F-34398 Montpellier, France
[3]UR BioWooEB, CIRAD, Univ Montpellier, 34398 Montpellier, France

For correspondence: marc.jaeger@cirad.fr

Keywords: FSPM, Organ cohorts, GreenLab model, metaphytomers, Guayule

Introduction

Functional structural modelling of shrubs, especially aromatic plants, confronts with a fine consideration of their structures, often complex and with many reiterations, especially for sympodial plants. The models and their simulations are therefore complex and costly to use for the selection and definition of crop routes. Here we propose alternative solutions suitable for sympodial plants that do not show neoformations, by reducing the structural complexity to that of a monocaul plant.

Material and methods

The conceptual framework used is that of GreenLab, in its most extensive formalism, applicable in particular to the stochastic modelling of rhythmically growing trees (Wang et al., 2012). In our case, sympodial plants erect axes composed of modules. First, in the absence of neoformations, the succession of phytomers per module is replaced by a meta-phytomer (Jaeger et al. 2016), each module materializing a development cycle. We extend this work to the functional properties that inherit from those of the phytomers: we substitute the binomial probabilities at the phytomer scale by distributions reflecting mean and variance at the module scale. In a second step, we linearize the representation of the structure as follows: we represent an axis of theoretical development including the succession of meta-phytomers, from the initial module (unique, it is the oldest) to the last (the youngest). This representation is thus similar to that of a monocaul plant, except that we substitute a cohort of meta-phytomers instead of each phytomer. Under these conditions, we can use a simple version of the model dedicated to single-stemmed plants, StemGL (Ribeyre et al. 2018), after taking into account several phytomers per age along the trunk, with particular impact on the distribution of secondary growth biomass. The approach is applied to the Guayule, a plant of increasing interest for latex production (Snoeck et al., 2015).

Results and discussion

In our application on the Guayule, stochastic structures were generated by the explicit phytomer approach and the meta-phytomer approach where we show that the number of organs generated is reduced by a factor close to $(N\text{-}1)\cdot b^a$ where N represents the mean number of phytomers per module, b the mean branching factor and a the age.
Similarly, the linearization of the structure allows a substantial reduction of time (by a factor of 7 for age 4 and up to more than 1000 for age 8) while obtaining the same biomass distributions in simulation and the same values in the estimation of the model functional structural parameters. The lack of geometric instantiation is open to discussion. In our implementation

under StemGL, the visualization of simulated plants is based on functional representation [Jaeger et al. 2018]. It does not take into account geometrical features such as height, but allows the materialization of biomass variations and the number of meta-phytomers per cohort (C and D in the figure).

Conclusion

An approach well adapted to a context requiring numerous simulations and experiments. The gain in complexity brought is major and becomes the only possible alternative for important ages (the complexity remaining linear in age and not polynomial). It is exploitable on stochastic models and on a large number of species showing sympodial growth, with a single physiological age.

Acknowledgement

Authors thank the Agropolis Fondation supporting the “modelling guayule growth as an alternative source of natural rubber” project, referenced as PAI-10605-026.

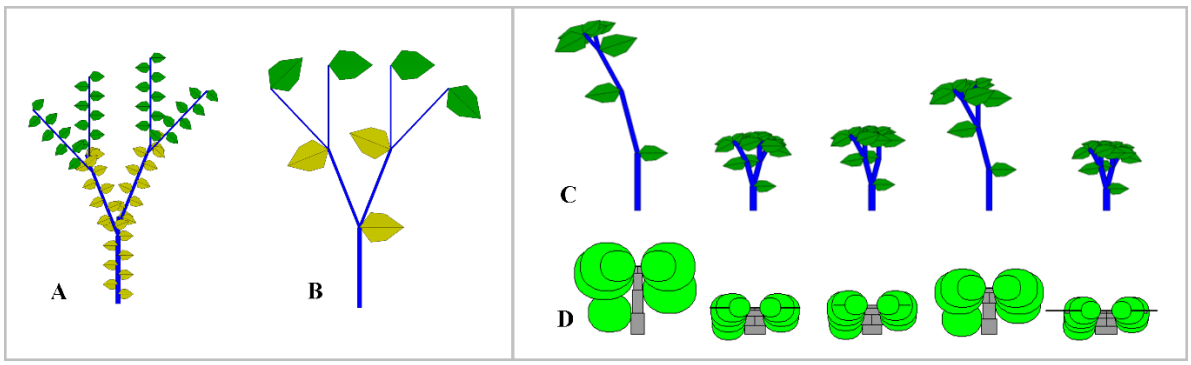

Figure: Reducing geometrical and topological complexity in FSPM illustrated on the Guayule. A: An explicit structural model simulation at age 3. B: the same structure simulation with meta-phytomers. C and D: Five instantiations of a functional structural stochastic simulation hold on the guayule at age 5 with meta-phytomers; the upper row simulates explicitly the plant geometry and topology, while the lower row performs the simulation without geometrical computations.

References

Wang, F., Letort, V., Lu, Q., Bai, X., Guo, Y., De Reffye, P., & Li, B. 2012. A functional and structural Mongolian scots pine (Pinus sylvestris var. mongolica) model integrating architecture, biomass and effects of precipitation. *PloS one*, 7(8)

Snoeck, D., Chapuset, T., García, J., Sfeir, N., Palu, S., 2015. Feasibility of a guayule commodity chain in the Mediterranean region. *Industrial Crops and Products,* 75, 159–164

Jaeger, M., Taugourdeau, O., de Reffye, P., 2016. Efficient structure development operators, application to mature tree structure simulations. Poster. *FSPMA 2016 -Functional-Structural Plant Growth Modeling, Simulation,Visualization and Applications*, 07-11/11/2016, Qingdao, China.

Ribeyre, F., Jaeger, M., Ribeyre, A., & de Reffye, P., 2018. StemGL, a FSPM tool dedicated to crop plants model calibration in the single stem case. *IEEE Proceedings of PMA’18*, Nov 2018, Hefei, China, 33-38

Jaeger, M., Sabatier, S., Borianne, P., de Reffye, P., Letort, V., Gang, Y., Zhang, X.-P. Kang, M.-Z., 2018. Data visualization for vegetal landscapes: Building 3D representations of organ biomass compartments. How plant production could constrain 3D lollypop-like representations. *IEEE Proceedings of PMA’18*, Nov 2018, Hefei, China. 85-93

Light exchanges in discrete directions as an alternative to raytracing and radiosity

Rémi Vezy[1], Raphaël Perez[2], François Grand[1], Jean Dauzat[1]

[1] *CIRAD, UMR AMAP, F-34398 Montpellier, France.*
AMAP, Univ Montpellier, CIRAD, CNRS, INRAE, IRD, Montpellier, France
[2] *CIRAD, UMR AGAP, F-34398 Montpellier, France.*
AGAP, Univ Montpellier, CIRAD, INRAE, Montpellier SupAgro, Montpellier, France

For correspondence: remi.vezy@cirad.fr

Keywords: ARCHIMED, light interception, scattering, photosynthesis, FSPM

Introduction

Light modelling at the scale of organs is essential to account accurately for the complex interactions between biophysical processes such as photosynthesis, stomatal conductance and energy balance. Yet, the calculation of radiative exchanges at fine scales is computationally-intensive and it remains a hindrance to a widespread use of FSPMs despite advances in light modelling using either radiosity (Chelle and Andrieu, 1998) or raytracing (Bailey, 2018). This study shows that simplifications based on the discretization of radiative fluxes allow processing radiative exchanges in a natural environment while maintaining good accuracy on the simulation of biophysical processes such as carbon assimilation.

Material and Methods

The present study is based on biophysical simulations performed using the ARCHIMED model. Incident radiation is depicted as a set of specular fluxes (i.e. parallel rays) in discrete directions using the sun direction for direct radiation and predefined “turtle” directions for the diffuse radiation. The “turtle” directions are obtained by splitting the sky hemisphere into sectors of equal solid angle (Dauzat et al, 2001). Optionally, direct radiation can be distributed in neighboring "turtle" sectors (turtle only). For each direction, the scene is projected on an image plane and the interception of incident light is deduced from rasterized pixel projections. Additionally, Z-Buffering gives the overlay of scene objects and, in this regard, pixels can be viewed as rays traced from outside down to the ground level. Light scattering can thus be processed similarly to raytracing. In the case of Lambertian objects, we further assume that all rays scattered by an object carry the same energy whatever the “turtle” direction. Net assimilation (*An*) is calculated with Farquhar’s model (Farquhar et al. 1980), stomatal conductance with Medlyn’s model (Medlyn et al. 2011) and the leaf temperature is found by solving the energy balance of the system.

Simulations are run on a dense three-dimensional scene including two palms (*Elaeis guineensis*) with the following configuration: latitude= 15°, Day of year 71, time steps of 30mn, clearness index *Kt*= 0.5. A “toricity” option is used to generate a virtually infinite canopy. The number of “turtle” directions is set to 6, 16, 46 or 136. The sun position is either integrated into the turtle or separately computed. The pixel density ranges from 341 to 6821 pixels m^{-2}. The reference outputs are obtained with the highest number of directions and pixels.

- *Scene metrics: plot= 15.9m*9.2m, meshes= 24 863, triangles= 571 934, LAI= 3.2, leaflets= 24 493*

Results and Discussions

Figure 1 (left) illustrates the effect of the number of discrete light directions on the estimation of biophysical processes in comparison with the reference of 136 directions. Sampling the sun direction provides best results since direct radiation largely contributes to the PAR irradiance, the energy load of leaflets and, finally, their assimilation. Bias remain low when the sun direction is not sampled except when the number of “turtle” directions is decreased to six. The

dispersion of residuals remains quite limited for 46 directions, meaning that reliable values can be obtained at leaflet scale for such configuration.

Figure 1 (right) shows that a low pixel density (682 pixels m^{-2}, i.e. 50 000 pixels) is sufficient to get a relatively unbiased estimation of carbon assimilation at plot level, but a higher density is necessary to get reliable estimation at leaflet scale.

Figure 1: Evaluation of the error induced by a reduction in number of directions (Left), or a reduction of the number of pixels (Right) for the intercepted photosynthetically active radiation (PAR), absorbed energy (PAR + near infrared) and net carbon assimilation (An) at the leaflet scale for a palm plot. Values are presented relative to the reference simulation shown as the first value on left, i.e. 136 directions on the left plot (500 000 pixels), 1000 pixels on the right (46 directions, turtle only). Red color is used for a simulation with a precise computation of the sun position, and blue for an integration of the sun position in the turtle.

The reference configuration in the left pane of Fig. 1 generates 68.5M rays for each time step and, since several hits are recorded per ray (6 on average) this generates about 5 sub-rays that are used for the calculation of light scattering.

Running the complete simulation with the reference configuration from the right pane of Fig. 1 lasts ~3.4 min for each time step[1] (23M rays). This time can be decreased to only 2 seconds per step by storing partial scene illumination for each direction, but this preliminary step can be time-consuming, mainly during the multiple scattering for the PAR and NIR ranges. A considerable shortening is expected by treating light exchanges using directional form factors between pairs of objects instead of propagating scattered light by individual rays.

Conclusion

Using discrete ordinates allows performing accurate and unbiased simulations of light interception. Biases arise when decreasing the number of directions but with limited consequences on carbon assimilation. Larger biases occur when pixel density is too low to sample correctly individual leaflets. A configuration with 46 turtle directions for depicting both direct and diffuse radiation and a pixel density of 682 pixels m^{-2} allows fast computations while providing sufficient information to get precise light budget at fine scales.

References

Bailey, 2018, *Ecological Modelling*. 368:233-245, doi: 10.1016/j.ecolmodel.2017.11.022.

Chelle and Andrieu, 1998, *Ecological Modelling* 111:75-91, doi: 10.1016/S0304-3800(98)00100-8

Dauzat et al., 2001, Agric. & Forest Met. 109(2)143-160, doi: 10.1016/S0168-1923(01)00236-2

Farquhar et al., 1980, *Planta*. 149:78-90, doi: 10.1007/BF00386231

Medlyn et al., 2011, *Global Change Biology*. 17:2134-2144, doi: 10.1111/j.1365-2486.2010.02375.x

[1] Tests on a computer with 6 cores, Intel Xeon W2133 3.60 GHz, RAM 32Go.

Author Index

Adler, Magnus 101
Almeida Pazianotto, Ricardo Antônio 160, 162
Alméras, Tancrède 13
Alsater, Ali Abed 115, 171
Altartouri, Bara 65
Andrieu, Bruno 22, 32, 38
Anten, Niels P.R. 34, 84, 107, 155
Aparecido Vieira Junior, Nilson 123
Aper, Jonas 63
Bahr, Christopher 18, 76
Bailey, Brian N. 6
Balasus, Jens 49
Barbillon, Pierre 164
Barczi, Jean-Francois 14
Baril, Mickaël 70
Barillot, Romain 22, 32, 38, 43, 68, 160
Barrow, Carlos Sherard 152
Begum, Fareeda 51
Belhassine, Fares 16
Bernacchi, Carl 130
Bertheloot, Jessica 78
Bidhendi, Amir J 65
Black, Christopher K. 95
Blanc, Emmanuelle 164
Bodner, Gernot 2
Bohn Reckziegel, Rafael 133, 169
Borianne, Philippe 70
Borne, Frédéric 70
Borra-Serrano, Irene 63
Boudon, Frédéric 36, 47, 78, 99
Brancheriau, Loïc 36, 115, 171
Bucksch, Alexander 143, 150, 152, 159
Buck-Sorlin, G.H. 105, 128
Burridge, James 159
Cabrera-Bosquet, Llorenç 57
Calders, Kim 137
Caliman, Jean-Pierre 36
Campostrini, Eliemar 160, 162
Caraglio, Yves 14
Carneiro e Pedreira, Bruno 123
Chai, Honghong 24
Chambon, Camille 32
Chen, Tsu-Wei 101
Chi, Faustino 109
Chitwood, Daniel H. 5
Chopard, Jérôme 16
Chutoe, Chartinun 143
Cieslak, Mikolaj 59
Combes, Didier 43, 139, 160
Cornilleau, X. 128
Costes, Evelyne 11, 16, 47
Cournède, Paul-Henry 167
Coussement, Jonas R. 26, 144, 146
Couturier, Arthur 139

Couvreur, Valentin....57, 72, 90
Crimaldi, Mariano....117
Dauzat, Jean....36, 173
De Frenne, Pieter....137
de Haldat, Alexandre....14
de Reffye, Philippe....115, 171
De Schepper, Veerle....146
De Swaef, Tom....38, 63, 68, 88, 137
de Visser, Pieter....82
de Vries, Jorad....80, 84
Dieleman, Anja....82
dos Santos Vianna, Murilo....123
Draye, Xavier....57, 90
du Toit, Ben....169
Duan, Tao....53
Durand, Jean-Louis....38, 43, 68
Enjalbert, Jérôme....164, 167
Escobar Gutiérrez, Abraham....43, 139
Evers, Jochem B.....10, 28, 34, 41, 84, 107, 123, 155
Farinelli, Daniela....157
Ferraro, Pascal....59
Fior, Simone....80
Fleming, Andrew....40
Flemisch, Bernd....20
Flutre, Timothée....167
Fournier, Christian....32, 55, 164
Frak, Elzbieta....139
Fricke, Andreas....101
Friedel, Matthias....18, 76
Fumey, Damien....16
Gangapersad, Shiv....40
Gaudio, Noémie....8
Gauthier, Marion....22, 32, 38
Gawinowski, Meije....167
Geitmann, Anja....65
Giannino, Francesco....117
Godin, Christophe....30, 78, 86
Grand, François....36, 173
Grisafi, Francesca....157
Gu, Shenghao....125
Guo, Xinyu....125
Guo, Yan....24, 41, 53
Hanlon, Molly....152
Hegemann, Tim....49
Heidenreich, Marius....119
Hemery, Nicolas....115
Henke, Michael....28, 51
Hétroy-Wheeler, Franck....30
Heymans, Adrien....72
Holsteens, Kristof....66
Holzapfel, Bruno....51
Homolová, Lucie....135
Hu , Pengcheng....53
Huysmans, Marlies....66
Inzé, Dirk....26, 144
Iwasaki, Hideo....61

Iwata, Hiroyoshi....61
Jaeger, Marc....70, 115, 171
Jake, Alexander....80
Janoutová, Růžena....135
Jones, Bryn....40
Julier, Bernadette....166
Kadirkamanathan, Visakan....40
Kahle, Hans-Peter....133, 169
Kahlen, Katrin....18, 76
Kalapanulak, Saowalak....121
Kenfack Essougong, Urcil....155
Khan, Nazifa....59
Khare, Deepanshu....2
Kirié, Shiryu....61
Klepp, Nicolas....159
Koch, Timo....20
Kuppe, Christian W.....95
Kurth, Winfried....45, 91, 97, 105, 109, 119
Lacointe, André....93
Lammert, Bastiaans....84
Landl, Magdalena....127
Lang, Meagan....103
Larysch, Elena....133
Launay, Marie....8
Lauwers, Simon....146
Lecarpentier, Christophe....74, 164
Ledroit, L.....78
Leitner, Daniel....20, 93, 127
Li, Baoguo....41
Li, Shuangwei....41
Liu, Fusang....53
Liu, Suxing....150, 152
Lloyd, Jon....111
Lobet, Guillaume....2, 57, 72, 93
Long, Qinqin....97
Long, Stephen....130
Lootens, Peter....63
Louarn, Gaëtan....166
Ludwig, Ferdinand....131
Lynch, Jonathan P....152, 159
Ma, Yuntao....24, 41
Malenovský, Zbyněk....135
Marcelis, Leo F.M.....34
Marin, Fábio Ricardo....123
Matsunaga, Fabio Takeshi....160, 162
McCabe, Matthew F.....141
McGrath, Justin....130
McQuillan, Ian....59
Meunier, Félicien....72
Middleton, Wilfrid....131
Miller, John....159
Mirande, Katia....30
Morhart, Christopher....133, 169
Moualeu-Ngangué, Dany....101
Mougani, Christ....115
Moura, Magna Soelma Bessera....111

Muller, Bertrand....57
Myint, San Schwe....101
Nagao, Yuichi....70
Navrátilová, Barbora....135
Nelissen, Hilde....26
Nicolai, Bart....66, 113
Nicolini, Eric....14
Noshita, Koji....61
Novotný, Jan....135
O'Sullivan, Hannah....111
Obeng Adomaa, Faustina....155
Oberländer, Tim....91
Ortega, Maria....150
Pagès, Loïc....22, 74
Pallas, Benoît....16, 47
Palsson, Aksel....80
Palu, Serge....115
Pao, Yi-Chen....101
Parkin, Isobel....59
Pasolli, Edoardo....117
Perez, Raphaël....36, 173
Perez-Garcia, M.-D.....78
Perttunen, Jari....111
Pieters, Olivier....88
Pietrzyk, Peter....143
Plazas Cebrián, Andrea....45
Pohlmeier, Andreas....127
Pols, Leroi....113
Postma, Johannes A.....95, 121
Pradal, Christophe....16, 22, 32, 55, 57, 61, 86, 97, 99, 164
Prusinkiewicz, Przemyslaw....59
Punyasu, Nattharat....121
Quoc Khanh, Tran....49
Raharjo, Doni Artanto....36
Rahman, Mohammad Asrafur....131
Rakocevic, Miroslava....160, 162
Rees, Frédéric....22
Renton, Michael....28
Reubens, Bert....137
Rey, Hervé....14, 70
Ribeiro, Rafael Vasconcelos....160, 162
Richard-Molard, Céline....74
Robinson, Steve....59
Roldán-Ruiz, Isabel....38, 63
Rosindell, James....111
Rossouw, Gerhard....51
Rouet, Simon....43
Sabatier, Sylvie....115, 171
Saengwilai, Patompong....143
Saint Cast, Clément....57
Saithong, Treenut....121
Sakr, S.....78
Salagovic, Jakub....66
Saleem, Aamir....63
Schäfer, Ernst D.....95
Schmidt, Dominik....18, 76

Schneider, Anne....32, 78
Schnepf, Andrea....2, 20, 93, 127
Seifert, Thomas....133
Seleznyova, Alla N....51
Selzner, Tobias....127
Shao, Jinwang....24
Shao, Ke....24
Sheppard, Jonathan P....169
Shu, Qiguan....131
Siebers, Matthew....130
Sievänen, Risto....111
Simon, Artzet....47, 55
Song, Youhong....148
Soolanayakanahally, Raju....59
Stathaki, Tania....111
Steppe, Kathy....1, 26, 144, 146
Stiehm, Christoph B.....45
Stomph, Tjeerd J.....84
Streit, Katarína....28, 109
Stützel, Hartmut....101
Sui, Yang....24
Sun, Weiwei....148
Tardieu, François....55, 57
Tavkhelidze, Aleksi....105, 109
Thaiprasit, Jittrawan....121
Tombesi, Sergio....157
Tosto, Ambra....107, 155
Tsai, Chung-Jui....150
Vaillant, Jan....99
Van de Poel, Bram....66
Van Den Berge, Sanne....137
van der Werf, Wopke....41, 84
van Westreenen, Arian....34
Vanderborght, Jan....2, 20, 93, 127
Verbeke, Sarah....146
Verboven, Pieter....66, 113
Vereecken, Harry....2, 20, 93
Verheyen, Kris....137
Verlinden, Bert....66
Vezy, Rémi....36, 173
Viennois, Gaëlle....70
Villers, Selwyn....26, 144
Wang, Ruili....24
Wang, Zhiwei....148
Weiliang, Wen....125
Widmer, Alex....80
Willem, Coudron....137
Wojciechowski, Tobias....121
Wolff, Béatrice....166
Wusirika, Ramakrishn……154
Wyffels, Francis....88
Xianju, Lu....125
Xie, Limeng....159
Yadav, Radheshyam....154
Yongjian, Wang....125
Yu, Chao....24

Zetao, Yu.....125
Zhang, Ningyi.....34
Zheng, Bangyou.....53
Zhou, Xiaoran.....2
Zhou, Xiao-Ran.....93
Zhu, Binglin.....53
Zhu, Junqi.....41, 51
Ziliani, Matteo G.....141
Zuidema, Pieter A.....107, 155